

# Use of Physiologically Based Pharmacokinetic Models to Quantify the Impact of Human Age and Interindividual Differences in Physiology and Biochemistry Pertinent to Risk

## Final Report

Cooperative Agreement  
CR828047010

John C. Lipscomb, Ph.D., DABT  
U.S. Environmental Protection Agency  
Office of Research and Development  
National Center for Environmental Assessment  
26 W. Martin Luther King Drive, MS-190  
Cincinnati, OH 45268  
Tel 513/ 569-7217  
lipscomb.john@epa.gov

Gregory L. Kedderis, Ph.D.  
Independent Consultant  
1803 Jones Ferry Road  
Chapel Hill, NC 27516  
Tel 919/ 942-3921  
GKedderis@msn.com

## **NOTICE**

The U.S. Environmental Protection Agency through its Office of Research and Development funded and managed the research described here under cooperative agreement CR828047010 to Gregory L. Kedderis, Ph.D. It has been subjected to the Agency's peer and administrative review and has been approved for publication as an EPA document. Mention of trade names or commercial products does not constitute endorsement or recommendation for use.

## TABLE OF CONTENTS

	<u>Page</u>
TABLE OF CONTENTS.....	iii
LIST OF TABLES.....	vii
LIST OF FIGURES .....	x
EXECUTIVE SUMMARY .....	xii
1. INCORPORATING HUMAN INTERINDIVIDUAL BIOTRANSFORMATION VARIANCE IN HEALTH RISK ASSESSMENT .....	1-1
ABSTRACT.....	1-1
INTRODUCTION .....	1-2
DEFINITION OF THE PROBLEM.....	1-7
OBJECTIVE .....	1-8
APPROACH.....	1-9
REQUIRED CONDITIONS.....	1-12
APPLICABILITY.....	1-12
CONCLUSIONS.....	1-13
REFERENCES .....	1-14
2. HOW DIFFERENCES IN ENZYME EXPRESSION CAN TRANSLATE INTO PHARMACOKINETIC VARIANCE AND SUSCEPTIBILITY TO TOXICITY .....	2-1
ABSTRACT.....	2-1
BACKGROUND .....	2-2
TOXICITY AND ASSESSMENT .....	2-2
METABOLISM AND PHARMACOKINETICS IN RISK ASSESSMENT.....	2-3
USING ENZYME KINETIC DATA TO ESTIMATE PHARMACOKINETIC VARIANCE .....	2-6
IMPACT OF STUDY DESIGN .....	2-10
SUMMARY AND CONCLUSIONS .....	2-11
REFERENCES .....	2-11
3. APPLICATION OF <i>IN VITRO</i> BIOTRANSFORMATION DATA AND PHARMACOKINETIC MODELING TO RISK ASSESSMENT.....	3-1
ABSTRACT.....	3-1
TOXICOLOGY AND HUMAN HEALTH RISK ASSESSMENT.....	3-2
PHYSIOLOGICALLY BASED PHARMACOKINETIC MODELS .....	3-4
EXTRAPOLATION OF <i>IN VITRO</i> DATA TO HUMANS.....	3-5
INCORPORATION OF PHARMACOKINETICS INTO RISK ASSESSMENTS.....	3-9
REFERENCES .....	3-13

## TABLE OF CONTENTS cont.

		<u>Page</u>
4.	THE IMPACT OF CYTOCHROME P450 2E1-DEPENDENT METABOLIC VARIANCE ON A RISK-RELEVANT PHARMACOKINETIC OUTCOME IN HUMANS .....	4-1
	ABSTRACT .....	4-1
	INTRODUCTION .....	4-2
	METHODS .....	4-7
	Human Samples and Quantification of CYP Proteins .....	4-8
	Distribution of CYP2E1 to Human Hepatic MSP .....	4-8
	Estimation of Proteins in Intact Liver .....	4-9
	CYP2E1-Dependent Oxidation of TCE.....	4-10
	Statistical Analysis.....	4-10
	Combination of Data Sets .....	4-14
	PBPK Model .....	4-15
	RESULTS .....	4-16
	Distribution of CYP2E1 to Human Hepatic MSP .....	4-16
	Distribution of CYP2E1 to Intact Human Liver .....	4-16
	<i>In vitro</i> Metabolic Rate Constant ( $V_{max}$ ) .....	4-18
	Determining the Metabolic Capacity of Intact Tissue and Extrapolation of Units.....	4-19
	PBPK Model Predictions .....	4-20
	DISCUSSION .....	4-20
	SUMMARY AND CONCLUSIONS .....	4-28
	REFERENCES .....	4-30
	APPENDIX: MATLAB Code to Generate AxD .....	4-45
5.	PHARMACOKINETIC ANALYSIS TO SUPPORT AN INHALATION RfC FOR CHLOROFORM .....	5-1
	BACKGROUND .....	5-1
	Purpose.....	5-2
	Objective.....	5-2
	RISK ASSESSMENT APPLICATION.....	5-2
	SCOPE AND LIMITATIONS.....	5-4
	APPROACH .....	5-5
	APPLICATION OF PHYSIOLOGICALLY BASED PHARMACOKINETIC MODELING.....	5-11

## TABLE OF CONTENTS cont.

	<u>Page</u>
METHODS: PBPK MODEL STRUCTURE AND PARAMETERS .....	5-14
Model Structure .....	5-14
Partition Coefficient Derivation.....	5-14
Mice .....	5-15
Adult Rats .....	5-15
Adult Humans .....	5-17
Children.....	5-18
Parameter Values .....	5-18
METABOLIC VARIABILITY .....	5-24
Simulated Exposure Conditions.....	5-27
RESULTS .....	5-34
Derivation of the Rodent NOAEL Values .....	5-34
Model Response.....	5-41
Chloroform Model Verification.....	5-42
Comparison to Mouse and Rat Pharmacokinetic Data .....	5-45
Model Sensitivity .....	5-49
Comparisons to Human Pharmacokinetic Data .....	5-55
Choice of Values for Km .....	5-58
Human Equivalent Concentration.....	5-61
Human Variability .....	5-62
Deriving CM <sub>24</sub> at Which to Determine Human Variability.....	5-62
Human Variability: Metabolic Capacity and Age .....	5-62
Human Variability: Hepatic Blood Flow .....	5-62
Human Variability: Blood:Air PC Value.....	5-65
Combined Variability in the Adult .....	5-65
Obesity in Adult Males .....	5-68
Summary of Results.....	5-68
DISCUSSION .....	5-69
CONCLUSIONS.....	5-80
REFERENCES .....	5-82
APPENDIX A: COMPUTER CODE FOR THE CHLOROFORM PBPK MODEL .....	5-86
APPENDIX B: DERIVATION OF CHLOROFORM PARTITION COEFFICIENTS.....	5-89

**TABLE OF CONTENTS cont.**

	<u>Page</u>
APPENDIX C: VARIABILITY OF HEPATIC BLOOD FLOW IN ADULT HUMANS.....	5-102
APPENDIX D: EXTRAPOLATION OF <i>IN VITRO</i> DERIVED CHLOROFORM METABOLIC RATE CONSTANTS AND VARIABILITY FOR PBPK MODELING.....	5-113

## LIST OF TABLES

<u>No.</u>	<u>Title</u>	<u>Page</u>
2-1	Effect of a 10-Fold Induction of $V_{max}$ on Hepatic Clearance over a Four-Log Increase in Substrate Delivery .....	2-14
3-1	Variance in Human Hepatic CYP2E1-Dependent TCE Oxidative Capacity and the Amount of TCE Oxidized .....	3-16
4-1	Identification of Data Sets and Parameters for Statistical Evaluation .....	4-35
4-2	Liver Enzyme Data .....	4-36
4-3	CYP2E1 Content and TCE Metabolic Activity Used to Produce Data Set 3, Describing Parameter D .....	4-38
4-4	Distributions of TCE Metabolism Rate Constant, Microsomal Protein and CYP2E1 Content of Adult Human Liver .....	4-39
4-5	Effect of Human Hepatic CYP2E1 Activity Distribution on the Bioactivation of TCE Following an Inhalation and Oral Exposure.....	4-39
5-1	Adult Rat Blood:Air and Tissue:Air Partition Coefficient Values .....	5-16
5-2	Adult Rat Tissue:Blood Partition Coefficient Values Derived from Paired Tissues .....	5-16
5-3	Adult Human Blood:Air Partition Coefficient Values.....	5-17
5-4	Tissue:Blood Partition Coefficient Values for Adult Humans .....	5-17
5-5	Tissue:Air PC Values in PND 10 Rat Pups .....	5-19
5-6	Tissue:Blood PC Values Used for Children PBPK Model.....	5-19
5-7	Age and Species Dependent Model Parameter Values.....	5-20
5-8	Parameters and Selected Percentile Values for the Fraction of Cardiac Output as Hepatic Blood Flow .....	5-21
5-9	Distribution of Chloroform Metabolic Rate Constants in Adults and Children.....	5-26
5-10	Derivation of $V_{max}C$ Values for Inclusion in PBPK Modeling for Adults, Children and Rats.....	5-28

**LIST OF TABLES cont.**

<u>No.</u>	<u>Title</u>	<u>Page</u>
5-11	Exposure Conditions, Relative Liver Weight and Hepatocyte Labeling Index from Constan et al. (2002) .....	5-35
5-12	Exposure Conditions and Endpoints Examined in Rodent Inhalation Bioassays.....	5-37
5-13	Endpoints and Response Levels Identified in Rodent Inhalation Bioassays .....	5-38
5-14	Chloroform Metabolized in Liver in Mice, Rats and General Adult (Male) Humans .....	5-43
5-15	Results from Open Chamber Metabolism Studies in Rats and Mice.....	5-48
5-16	Results from Studies with Male Humans.....	5-59
5-17	Results from Studies with Female Humans .....	5-59
5-18	Derivation of the Human Equivalent Concentration from Liver Effects Observed in Mice and Rats.....	5-61
5-19	The Impact of CYP2E1-Dependent Metabolic Parameters on Chloroform Metabolism Among Selected Segments of the Human Population .....	5-64
5-20	Effect of Variance in Hepatic Blood Flow on Chloroform Metabolism Among Adult Humans .....	5-66
B-1	Rat and Human Blood:Air and Tissue:Blood Partition Coefficient Values as Reported in Corley et al. (1990).....	5-90
B-2	Fractional Fat and Water Content of Adult Human Tissues.....	5-92
B-3	Blood:Air and Tissue:Air Partition Coefficient Values Derived from Studies with Rat Tissues .....	5-93
B-4	Tissue:Blood Partition Coefficient Values Derived from Studies with Rat Tissues .....	5-94
B-5	Blood:Air Partition Coefficient Values Derived from Studies with Adult Human Blood.....	5-94
B-6	Tissue:Blood Partition Coefficient Values Derived by Combining Mean Human B:A PC Values with Individual Rat T:A PC Values.....	5-95

## LIST OF TABLES cont.

<u>No.</u>	<u>Title</u>	<u>Page</u>
B-7	Predictions of Human Blood:Air and Tissue:Blood Partition Coefficient Values.....	5-95
B-8	Human Tissue:Air and Tissue:Blood Partition Coefficient Values Based on Adjusted Predictions of Tissue:Air PC Values .....	5-96
B-9	Comparison of B:A and T:B PC Values for Mature Individuals.....	5-96
B-10	Fractional Fat and Water Content of Children's Tissues .....	5-98
B-11	Predicted T:A PC Values in Humans.....	5-98
B-12	Child-Specific Blood:Air and Tissue:Blood PC Values .....	5-98
B-13	Adult-Specific Blood:Air and Tissue:Blood PC Values.....	5-99
B-14	Blood:Air and Tissue:Blood PC Values in PND 10 Rat Pups.....	5-100
C-1	Hepatic Blood Flow and Fraction of CO as HBF, Estimated from Data of Ceasar et al. (1961).....	5-105
C-2	Hepatic Blood Flow and Fraction of CO as HBF Estimated from Data of Wiegand et al. (1960).....	5-106
C-3	Hepatic Blood Flow and Fraction of CO as HBF, as Reported by Feruglio et al. (1964), "Before" Condition .....	5-107
C-4	Hepatic Blood Flow and Fraction of CO as HBF, Derived from HBF and Patient Characteristics Presented by Reemtsma et al. (1960).....	5-108
C-5	Hepatic Blood Flow and CO Data which Served as the Basis for Results Presented in Iijima et al. (2001) .....	5-109
C-6	Hepatic Blood Flow and CO Data which Served as the Basis for Results Presented in Sakka et al. (2001) .....	5-110
C-7	Parameters and Selected Percentile Values for the Fraction of Cardiac Output as Hepatic Blood Flow .....	5-111
D-1	Information Used to Extrapolate <i>in vitro</i> Derived Vmax Value to the Intact Liver.....	5-115
D-2	Donor Demographic Information for 10 Child Organ Donors .....	5-116
D-3	Determination of Cytochrome P450 Enzyme in Liver Tissue of 10 Child Organ Donors.....	5-117
D-4	Distribution of CYP2E1 to Adults and Children .....	5-118

## LIST OF FIGURES

<u>No.</u>	<u>Title</u>	<u>Page</u>
1-1	Isolation of Microsomal Protein from the Intact Liver .....	1-16
1-2	Relationship Between Intact Liver, Microsomal Protein and Some CYP Forms .....	1-17
1-3	Extrapolation and Incorporation of <i>in vitro</i> Derived Metabolic Rates in PBPK Modeling .....	1-18
2-1	Pharmacokinetics and the Risk Assessment Paradigm.....	2-15
2-2	The Relationship Between Km Value and Substrate Concentration .....	2-16
2-3	The Relationship Between Substrate Delivery, Metabolic Capacity and the Amount of Metabolite Formed.....	2-17
2-4	The Impact of Substrate Delivery and Metabolic Capacity on the Formation of Metabolites in Liver .....	2-18
3-1	The <i>in vitro/in vivo</i> Parallelogram Approach.....	3-17
3-2	Use of a PBPK Model to Interpret the Risk Significance of Differences in Metabolic Capacity .....	3-18
4-1	Application of PBPK Modeling to Link External Dose with Concentration of Toxicant in Target Organs .....	4-40
4-2	Relationship Between Liver, Microsomal Protein and Some CYP Forms .....	4-41
4-3	Correlation Between mg MSP/gram and pmol CYP2E1/mg MSP .....	4-42
4-4	Classification Tree Model for the Distribuiotn of A = pmol CYP2E1/gram Liver .....	4-43
4-5	Extrapolation and Incorporation of <i>in vitro</i> Derived Metabolic Rates in PBPK Modeling .....	4-44
5-1	A Conceptual Presentation of the Application of TK Information and the TK Approach to Human Health Risk Assessment.....	5-3
5-2	Subdivision of Uncertainty Factors into Toxicokinetic and Toxicodynamic Components .....	5-8

**LIST OF FIGURES cont.**

<u>No.</u>	<u>Title</u>	<u>Page</u>
5-3	Application of PBPK Modeling to Extrapolate Internal Dosimetry Between Species .....	5-9
5-4	Five Compartment PBPK Model .....	5-10
5-5	Achieving Steady State in Liver Tissue.....	5-29
5-6	Relationship Between Exposure Concentration and $CM_{24}$ in Rats, Mice and Humans at Steady State .....	5-31
5-7	Derivation of the Human Equivalent Concentration .....	5-32
5-8	Relationship Between the Blood:air Partition Coefficient for CF and $CM_{24}$ ....	5-51
5-9	Relationship Between Hepatic Blood Flow and $CM_{24}$ for CF.....	5-52
5-10a	Relationship Between the Maximal Rate of CF Metabolism and $CM_{24}$ .....	5-53
5-10b	Expanded Scale Showing the Relationship Between the Maximal Rate of CF Metabolism and $CM_{24}$ .....	5-54
5-11a	Relationship Between the Michaelis Constant for CF Metabolism and $CM_{24}$ .....	5-56
5-11b	Expanded Scale of the Relationship Between the Michaelis Constant for CF Metabolism and $CM_{24}$ .....	5-57
5-12	Application of Toxicokinetic Analysis to Address Animal-to-Human and Human Interindividual Differences for Chloroform Metabolism and Risk Assessment.....	5-67

## EXECUTIVE SUMMARY

Outbred species, like humans, are more diverse than the animal species routinely used for testing and research. This diversity often complicates the extrapolation of animal findings to and among humans; lack of understanding of the impact of that diversity on tissue dosimetry and response confounds the level of certainty we place on default measures of human variability used in risk assessment. The uncertainty factors governing animal to human extrapolation (UFA) and human interindividual extrapolation (UFH) have recently begun to be addressed by information which can inform their subsequent division into their respective toxicokinetics (TK) and toxicodynamics (TD) components. This is explicit in the RfC methodology, where TK information is used to develop the human equivalent concentration, effectively reducing the TK component of UFA to 1. Specific and advanced risk assessments have used pharmacokinetic models and information, often physiologically based pharmacokinetic (PBPK) models and predictions, to inform the ascription of values for UFA and UFH.

This report is intended to communicate a framework developed for the extrapolation and integration of *in vitro*-derived measures of chemical metabolism, including those that define human interindividual variability. It presents instruction on the most useful measures of chemical metabolism constants and guides the proper interpretation of differences in enzyme content, so that risk assessors who summarize these types of data for inclusion in human health risk assessment make optimal use of the available information. Likewise, the demonstration of the approach and data requirements will guide the construction of laboratory research protocols which result in the development of data optimally relevant to informing the true nature of human variability. Finally, this approach is communicated through instruction and demonstration of the

approach and framework; it is useful to those who develop and evaluate PBPK models intended to address human variability for risk assessment application.

Chapters 1-3 represent generally-applicable works already published, Chapter 4 represents work specific to cytochrome P450 2E1 (CYP2E1) using trichloroethylene as an example and accepted for publication, and Chapter 5 represents the original presentation of results describing variance in the CYP2E1-mediated metabolism of chloroform.

Most of the past measures of human variability conducted to evaluate susceptibility have not been conducted under the proper guidance; faulty interpretations based on unstated and untenable assumptions fuel inaccurate evaluations of variability, susceptibility and risk. While banks of liver preparations have been available for more than a decade, they have been exploited to ascertain measures of human interindividual variability, expressed per unit of isolated subcellular fraction without regard to measuring variability at the level of the intact tissue. This has resulted in inaccuracies in estimations of variability, and their well-intentioned inclusion in evaluations of susceptibility. With regard to chemical-metabolizing enzymes, there are two fundamental errors in this approach: (1) the variability of the enzyme is not expressed at the level of the intact tissue, disregarding the impact of the isolation procedure, and (2) enzyme variability is assumed to represent variability in chemical metabolism. This second error disregards the dependency of metabolism on substrate (chemical) availability; it disregards the anatomic, physiologic and biochemical constraints which govern transport of the chemical from air or ingested material into the bloodstream, and its ultimate diffusion from blood into liver tissue.

This report contains tutorial materials, data quality objectives and guidance (Chapters 1-3) as well as case study investigations (Chapters 4 and 5) which address the development, evaluation and integration of laboratory-derived data aimed at quantifying human interindividual variability for application in human health risk assessment. The integrating framework is that of

physiologically based pharmacokinetic modeling, a procedure popularized two decades ago.

This framework allows the application of appropriate constraints of the intact body on chemical absorption, distribution, metabolism and elimination.

The case studies developed for two important water contaminant chemicals, trichloroethylene and chloroform. These case studies comprise data which are chemical-specific, enzyme-specific, and general in nature. Chemical-specific data include measured or predicted measures of chemical partitioning into blood and solid tissues, and metabolic rate constants. In each case study, cytochrome P450 2E1 (CYP2E1) is the enzyme responsible for metabolism; in each case study metabolism is a fundamental requirement for toxicity – the metabolite is toxic. Enzyme-specific data include those which characterize the distribution of CYP2E1 to the intact liver, including age-dependent differences in humans. These data were developed from the analysis of intact liver tissue samples obtained from human organ donors. Measures of enzyme content of the liver, and age-dependent differences will be applicable to the many environmental toxicants metabolized by CYP2E1. This investigation does not include an evaluation of genetic polymorphisms, as no polymorphisms in the CYP2E1 gene have been linked to changes in the expression or activity of this enzyme. Data generally applicable in PBPK modeling in humans, regardless of chemical, are those which characterize the distribution of hepatic blood flow. This analysis of hepatic blood flow variability is noteworthy in that hepatic blood flow often limits the metabolism of solvents. This analysis is the first of its kind, and is based on the collection of peer-reviewed data from the open literature, as well as individual data sets collected from respective authors. While the case studies have addressed chemicals for which metabolism represents a bioactivation step, the data on enzyme variability are equally applicable when metabolism of the contaminant represents a detoxication step.

These results demonstrate the successful application of this approach to guide the collection, interpretation compilation and evaluation of risk-relevant pharmacokinetic data. Data on human biochemical and physiologic variability have been incorporated into PBPK models for adults and children which were designed to assess human interindividual differences in the production of a PK outcome linked with risk. While both examples have involved chemicals whose metabolism is limited by hepatic blood flow; both examples have produced data which allow us to dispel certain events or co-exposures as modifiers of risk, from the standpoint that they change the level of CYP2E1 expression. From these results, it is clear that interindividual differences in the content of the CYP2E1 enzyme can now be quantified, and the data are useful in investigations of additional environmental contaminants that are also metabolized by CYP2E1, including benzene, bromobenzene, styrene, the trihalomethanes drinking water disinfection byproducts and several low molecular weight halogenated solvents.

# 1. INCORPORATING HUMAN INTERINDIVIDUAL BIOTRANSFORMATION VARIANCE IN HEALTH RISK ASSESSMENT

## ABSTRACT

The protection of sensitive individuals within a population dictates that measures other than central tendencies be employed to estimate risk. The refinement of human health risk assessments for chemicals metabolized by the liver to reflect data on human variability can be accomplished through 1) the characterization of enzyme expression in large banks of human liver samples, 2) the employment of appropriate techniques for the quantification and extrapolation of metabolic rates derived *in vitro*, and 3) the judicious application of physiologically based pharmacokinetic (PBPK) modeling. While *in vitro* measurements of specific biochemical reactions from multiple human samples can yield qualitatively valuable data on human variance, such measures must be put into the perspective of the intact human to yield the most valuable predictions of metabolic differences among humans. For quantitative metabolism data to be the most valuable in risk assessment, they must be tied to human anatomy and physiology, and the impact of their variance evaluated under real exposure scenarios. For chemicals metabolized in the liver, the concentration of parent chemical in the liver represents the substrate concentration in the Michaelis-Menten description of metabolism. Metabolic constants derived *in vitro* may be extrapolated to the intact liver, when appropriate conditions are met. Metabolic capacity ( $V_{\max}$ ; the maximal rate of the reaction) can be scaled directly to the concentration of enzyme (or enzyme fraction) contained in the liver. Several environmental, genetic and lifestyle factors can influence the concentration of cytochrome P450 forms (CYP) in the liver by affecting either 1) the extent to which the CYP forms are expressed in the endoplasmic reticulum of the cell (isolated as the microsomal fraction from tissue homogenates),

or 2) the expression of microsomal protein in intact liver tissue. Biochemically sound measures of the hepatic distribution of xenobiotic metabolizing enzymes among humans, based on expression of the enzymes within microsomal protein and the distribution of microsomal protein among intact livers, can be combined with metabolic constants derived *in vitro* to generate values consistent with those employed in PBPK models. When completed, the distribution (and bounds) of  $V_{\max}$  values can be estimated and included in PBPK models. Exercising such models under plausible exposure scenarios will demonstrate the extent to which human interindividual enzyme variance can influence parameters (i.e., the detoxication of a toxic chemical through metabolism) that may influence risk. In this article, we describe a methodology and conditions which must exist for such an approach to be successful.

## **INTRODUCTION**

The establishment of safe exposure limits for chemicals is a primary concern for individuals exposed in their occupations, through the environment, or the through the consumption of sustenance or medication. Several different federal agencies (e.g., National Institute for Occupational Safety and Health, US Environmental Protection Agency, US Food and Drug Administration) are charged with developing safe exposure guidelines for xenobiotics (chemicals and drugs). Often, these xenobiotics are encountered through more than one exposure scenario. An industrial chemical may become an environmental pollutant, and a therapeutic agent (either human or animal) may find its way into the environment and the food chain. Thus, the uniform recognition of some fundamental underlying concepts and their consistent application to identify and protect sensitive individuals seem to be in order.

In the US EPA's methodology to ascribe Reference Dose (RfD) values to environmentally-occurring contaminants, adequate information from studies with test animals

are used to determine human doses deemed to be without increased probability of risk when encountered continuously over a lifetime. Uncertainty factors (UF) are employed to adjust Lowest-Observed-Adverse-Effect Level (LOAEL) or No-Observed-Adverse-Effect Level (NOAEL) values determined in animal (or human) studies to doses (concentrations) deemed to be without significant human health risk. Within the US EPA, specific attention has been focused on the dissection of metabolic differences from the general UF in risk assessments by dividing the UF used in the derivation of RfD values into their constituent pharmacokinetic (PK) and pharmacodynamic (PD) components. This division follows similar earlier advances in the establishment of safe exposure limits set for inhaled substances. Although the genetic similarity among humans is remarkable (when compared to differences between humans and animals), the degree of human interindividual variance in key biochemical machinery produces differences in xenobiotic distribution and sensitivity to toxic insult among humans. Small differences in the genetic code can result in lower or higher expression of certain genes, resulting in lower or higher expression of coded enzymes or in the expression of enzymes whose function is compromised compared to the normal expression. Genetic polymorphisms can exist in unencoded genetic domains (introns) or in coded domains (exons); the latter are responsible for the transcription of a compromised protein. Some polymorphisms are responsible for allelic expression, where the number of alleles expressed is quantitatively related to the enzyme content, and thus to enzyme activity. Other polymorphisms may exist that alter the three-dimensional structure of an enzyme without altering the degree to which the enzyme is expressed. These alterations may affect how an enzyme interacts with substrate molecules, thus potentially altering substrate specificity, substrate affinity, and maximal activity.

Factors beyond genetic polymorphisms may also be responsible for human interindividual differences in chemical metabolism. Dietary factors, including types and quantity of food, control the expression of some forms of cytochrome P450 (CYP). Lifestyle factors such as cigarette smoking, stress, and alcohol consumption may alter the expression of CYP forms. Health conditions such as diabetes and obesity may alter the expression of CYP forms, and the expression of some members of other enzyme families (i.e, UDP glucuronyl transferase, glutathione S-transferase) are themselves recognized as markers of disease processes. Immortalized cell lines used for *in vitro* studies express different levels of some enzymes compared to the corresponding normal cells. These differences in enzyme expression and activity *in vivo* can alter the circulating levels and tissue distribution of xenobiotics and their metabolites. Thus, differences in the expression of xenobiotic-metabolizing enzymes can have an appreciable impact on risk relevant PK outcomes (i.e., rate of degradation of a toxic parent compound, rate of formation of a toxic metabolite, tissue concentrations of a toxic metabolite, etc.). Not all PK outcomes may quantitatively correlate to risk (i.e, circulating levels of a compound whose bioactivated metabolite formed in target tissues produces toxicity). However, studies on the variance in expression of hepatic (and extrahepatic) drug metabolizing enzymes will be useful when the risk relevant PK outcome is dependent on their activity and/or expression.

Factors other than the expression of an enzyme may also lead to changes in metabolic parameters which can influence risk. Drug-drug interactions based on either enzyme inhibition due to competition between two xenobiotics for a single enzyme or xenobiotic-dependent induction are well recognized and serve as the basis for therapeutic contraindications. Sometimes, the balance between the content of two or more enzymes determines toxicity. For

example, bioactivated CYP-derived metabolites of acetaminophen are detoxicated by GST-catalyzed conjugation. Increases in CYP activity or decreases in conjugating activity will increase the level of acetaminophen toxicity.

The extent to which differences in enzyme expression and activity (two different measures) predispose individuals to the toxic effects of xenobiotics is worthy of study, given the increasing degree to which toxicity and PK information are becoming available. The relationships between xenobiotics (environmental contaminants or therapeutic agents) and the enzymes responsible for their metabolism, and between xenobiotic metabolites and toxicity are critical factors in determining susceptibility. Individuals who allelically express low (or no) levels of CYP2D6 are at increased risk for toxicity (adverse drug reaction) due to the accumulation of some commonly employed therapeutic compounds. Likewise, individuals who over-express an enzyme which bioactivates a non-toxic parent compound to bioactive (toxic) metabolites may, to some degree, be protected from the toxic response.

The CYP enzymes are studied most often and with the highest degree of certainty *in vitro*. The preparation of metabolically active tissue fractions for *in vitro* investigations necessarily involves their removal from surrounding tissue, and often requires an artificial increase in their relative concentration, usually produced via ultracentrifugation (Figure 1-1). The variance in the content of CYP enzymes in the metabolically active subcellular fraction isolated from human liver has been evaluated in several key publications (Iyer and Sinz, 1999; Shimada et al., 1994; Snawder and Lipscomb, 2000; see Figure 1-2). In the absence of data describing the microsomal protein (MSP) content of liver, however, these evaluations of metabolic rates and enzyme expression in MSP isolated (literally, in isolation) from the intact liver provide data which are of limited value in determining the expression of microsomally-

contained enzymes in the intact liver or metabolic rates representative of the intact liver sufficient for inclusion in PK models.

Most CYP enzymes follow saturable Michaelis-Menten kinetics:

$$v = V_{\max} * [S] / (K_m + [S]) \quad (1-1)$$

where  $v$  is the initial velocity (rate;  $d[S]/dt$ ) of the reaction,  $V_{\max}$  is the maximal rate of the reaction,  $[S]$  is the substrate concentration, and  $K_m$  is the Michaelis constant. Equation (1-1) indicates that the initial velocity of the reaction increases hyperbolically as a function of the substrate concentration. The  $V_{\max}$  is a horizontal tangent to the zero-order (saturated) portion of the curve, while the tangent to the initial linear (first-order) portion of the curve at low substrate concentrations is the initial rate of the reaction,  $V/K$  ( $V_{\max}/K_m$ ). The  $K_m$  is the substrate concentration that gives one-half  $V_{\max}$ . Thus, at the low tissue concentrations attained after occupational or environmental exposures to chemicals, the  $V/K$  (reflected by the  $K_m$ ) is more important than the  $V_{\max}$  in describing the kinetics of the reaction. In situations such as bolus exposures to chemicals or drugs,  $V_{\max}$  can be more important. For rapidly metabolized chemicals, the slowest overall step in disposition is not biotransformation but rather delivery of the substrate to the liver via hepatic blood flow. In many exposure scenarios involving rapidly metabolized chemicals, differences in CYP activity due to genetics or induction do not result in differences in metabolic activation because of the overall limitation of blood flow delivery of the chemical to the liver (Kedderis, 1997).

PBPK modeling offers an opportunity to study the impact of differences in enzyme expression on both risk relevant and other PK outcomes in humans. When PK models are constructed to include metabolic rates (and rate constants) derived *in vitro*, several extrapolations are necessary, not the least of which is the extrapolation of enzyme content. PBPK models

include the apparent  $V_{max}$  expressed as mg/hr/kg body mass, while typical *in vitro* studies express  $V_{mac}$  in terms of nmoles product formed/minute/mg microsomal protein. Accurate extrapolation requires initially that enzyme content be expressed per unit intact liver (i.e., pmoles CYP2E1/gram liver), and the extrapolation has usually included a numerical estimation of the MSP content of liver (i.e, 50 mg MSP/gram liver). Measures of the MSP content of the intact liver have been inferred or developed in several PBPK studies in which rates of metabolism derived *in vitro* have been extrapolated to the *in vivo* setting (Lipscomb et al., 1998; Reitz et al., 1996).

This manuscript identifies the types of data required, communicates an approach, describes the limitations of the approach and proposes the applicability of the approach to estimate the human interindividual PK variance of outcomes which are relevant to risk and which may signify susceptibility to chemical injury.

## **DEFINITION OF THE PROBLEM**

The wealth of information being generated from genomic and proteomic investigations places more and more opportunities for refinement within the grasp of risk assessors. These results allow investigators to more correctly identify the fraction of the population which differs from the norm for enzyme expression, and to gather data on the degree to which enzyme content and/or activity varies among the population under investigation for risk. For example, advances in US EPA's inclusion of specific mechanistic, biochemical and PK modeling techniques in risk assessments encourages the development of methods to incorporate emerging data that can be used to quantify differences in enzyme expression. Because metabolism and PK are components of chemical exposure that have been specifically linked with risk, we were compelled to develop

and communicate methods to include these new data sets in risk assessments. Several key concepts defining the problem are given below.

- Environmental human health protection guidelines are designed to limit exposure to chemicals producing adverse effects in tissues, organs or organ systems.
- Newer risk assessment methods used to ascertain “safe” doses include specific mechanistic and biochemical information.
- Attention is given to the absorption, distribution, metabolism and elimination of a chemical.
- US EPA has been encouraged to develop risk assessment approaches that reduce uncertainty in the extrapolation of results from animals to humans and within the human species in order to protect sensitive humans.
- *In vitro* measurements of human enzyme activity toward a toxicant can yield qualitatively and quantitatively valuable data on human variance.
- PBPK models can be used to investigate the extent to which human interindividual enzyme variance can influence parameters (i.e., the detoxication of a toxic parent chemical through metabolism) that may influence risk.

## **OBJECTIVE**

In order to refine human health risk assessments for chemicals metabolized by the liver to reflect data on human interindividual metabolic and PK variance, the objective of this report is to communicate a method developed to 1) extrapolate measures of enzyme activity derived *in vitro* that capture human interindividual variance, and 2) demonstrate the applicability of the data and approach for risk assessment purposes. This report communicates a means by which new information on the variance of enzyme expression may be linked with PBPK modeling to estimate the degree of human interindividual variance with respect to a risk-relevant PK outcome.

## APPROACH

Extrapolation of metabolic rates derived *in vitro* from the subcellular preparations (i.e., cytosolic protein or MSP) to the intact liver requires two sets of data. The first set is the liver (or pertinent extrahepatic tissue) content of the enzyme (e.g., pmoles CYP2E1/gram liver). This may be empirically derived by quantitatively recovering liver homogenate protein (i.e., pmoles CYP2E1/mg homogenate protein) and assessing the homogenate protein's content of the enzyme. This is seldom done. Another approach to determining the liver's content of the enzyme involves the application of information presently available which describes the MSP's content of enzymes. However, this approach requires the generation of an additional data set: that describing the liver's content of MSP (i.e., mg MSP/gram liver). This measurement is rarely reported in metabolism studies, regardless of the subcellular fraction investigated. In instances where the individual enzyme responsible for metabolism has been identified and data on its distribution (and variance) have been determined in the corresponding subcellular fraction (e.g., pmoles CYP2E1/mg MSP), data can be included to quantify the variance of enzyme expression within the subcellular fraction as well as the variance in the distribution of the subcellular fraction to the intact liver. The liver content of an enzyme (Figure 1-3, panel C) can thus be determined by combining separate data sets describing the MSP content of the liver (panel A) and the CYP content of MSP (panel B). Because the objective of this initial step is to develop a measurement of the amount of enzyme present per gram liver tissue, a direct measurement of this parameter may also be obtained from the quantification of the enzyme directly in liver homogenate protein, although this has not been demonstrated. When estimating variance of the summed measurements, it is important to characterize and capture adequate measures of the variance within each individual data set.

The second required data set is that which describes the metabolic rate expressed per unit pertinent enzyme (i.e., CYP2E1; Equation 1-2; Figure 1-3, panel D) or per unit subcellular protein (i.e., mg MSP; see Equation 1-3). This measurement is typically available as a point estimate, although it can be measured as a distribution when adequate data are available. Data describing the metabolic rate may be available as a turnover number, the quantity of substrate metabolized per unit time per unit of enzyme. This measurement may be developed from purified enzymes or from genetically expressed enzymes. In exceptional cases, variance about this measurement may be characterized and that variance also captured in the extrapolation procedure. Ideally, the turnover number should be independent of preparation as long as each enzyme is genetically identical. However, some human CYPs exhibit genetic variance that affects their catalytic activity. Additionally, CYP and other xenobiotic metabolizing enzymes are membrane bound and interact with other proteins and lipids in ways that affect their catalytic activity. These lipids and other cellular constituents, which are present in human tissue preparations, are not present in genetically expressed systems. The potential instability of some purified enzymes must also be considered.

$$\frac{(\text{product formed/min/pmol CYP}) * (\text{pmol CYP/mg MSP})}{(\text{mg MSP/gram liver})} = \text{product formed/min/gram liver} \quad (1-2)$$

$$(\text{product formed/min/mg MSP}) * (\text{mg MSP/gram liver}) = \text{product formed/minute/gram liver} \quad (1-3)$$

Equation 1-2 would be best suited when *in vitro* metabolic rates are expressed per unit of the CYP form demonstrated to be responsible, and the data are deemed sufficient to represent the variance of the MSP content of human liver. Because of the demonstrated variance of CYP forms within the isolated MSP and because of the content of endoplasmic reticulum (which contains the microsomal enzymes) may vary among humans, Equation 1-2 seems to better

capture the variance of the expression of CYP enzyme expression in the intact liver. However, Equation 1-3 is perhaps most widely applicable at present, given that *in vitro* metabolic rates (and rate constants) are most commonly expressed per unit subcellular protein. Both equations demonstrate the need for data describing the content of microsomal protein in intact liver.

The mathematical combination of individual data sets describing 1) enzyme activity, 2) enzyme content of MSP, and 3) MSP content of the intact liver must be undertaken through statistically defensible procedures. When data sets are demonstrated (or assumed) to be independent and the observations are lognormally distributed within the sets, the statistical method of moments (addition of errors) can be combined to produce the overall distribution. In this method, the critical information is the geometric mean and geometric standard deviation of the distributions. Most publications describing the variance of enzyme activity and enzyme expression are devoid of descriptions of distribution and the measurements necessary to facilitate this recombination of data. The recombination of these data sets will produce a distribution, whose parameters can be used to identify metabolic rates at specifically identified points in the resultant distributions in the population (i.e., those representing the 5<sup>th</sup> and 95<sup>th</sup> percentiles of the distribution).

Most PBPK models are constructed assuming that all metabolism occurs in the liver, and the metabolic rate constants (apparent  $V_{max}$ ) are expressed as mg substrate metabolized/hr/kg body weight. Therefore the *in vitro* rate constants must be converted to those units. This is accomplished by correcting for molecular weight, time, the fractional composition of the body mass accounted for by liver (approximately 2.6% in humans), and body weight. The PBPK models can be expanded to incorporate additional information on extrahepatic metabolism or protein binding as this information becomes available.

## REQUIRED CONDITIONS

Several conditions must first be met for this strategy to be successful:

- Information must exist to identify the target organ (and should identify the target cells in that organ), the mechanism of toxic action, and the metabolic species responsible for toxicity (parent compound or metabolite). For example, available information may identify the parent chemical and its concentration in the brain as responsible for the noted nervous system toxicity.
- When a metabolite is responsible for toxicity, the identity of the metabolite must be known and enzyme(s) responsible for its formation must be identified. For example, the epoxide metabolite formed by CYP1A2-catalyzed oxidation may be responsible for toxicity.
- The kinetic mechanism of metabolism should be known. Most CYP enzymes follow Michaelis-Menten saturation kinetics. Ideally, information on metabolic rate should be expressed per unit enzyme. For example, the  $V_{max}$  is most suitable when expressed as product formed/time/pmol CYP2E1.
- Data quantifying the expression and variance of the enzyme in the intact liver tissue should be available. Sometimes information exists quantifying metabolic rate per unit of individual enzyme, and those data may be best employed when other information is available describing their expression in MSP (Snawder and Lipscomb, 2000). Most often, metabolic rates are expressed as product per unit subcellular fraction (i.e., product formed per mg MSP), and so the distribution of the pertinent subcellular fraction (and not the expression of the individual enzymes) to the liver is required. Equation 1-3 represents this condition. Regardless, not only should the variance be known, but also the type of distribution. The relationships between the individual data sets must be known to enable the most valid statistical recombination of the sets.
- An adequately characterized PBPK model must be available for adaptation.

## APPLICABILITY

With the availability of large banks of well-characterized subcellular fractions (mainly hepatic MSP) derived from the livers of human organ donors comes the opportunity to determine several measures of human interindividual biochemical variance. Although several investigations have failed to identify a consistent inverse relationship between post mortem cold-clamp time and microsomal enzyme activity, the assumption that the activity of these enzymes *in vitro* represents their activity *in vivo* must be applied. From these samples, we can measure

interindividual differences in enzyme activity and differences in enzyme content in isolated MSP. The *in vitro* metabolism of several CYP2E1 substrates, such as furan (Kedderis et al., 1993; Kedderis and Held, 1996), perchloroethylene (Rietz et al., 1996), and trichloroethylene (Lipscomb et al., 1998) have been successfully extrapolated to the *in vivo* setting through application of adequately developed and validated PBPK models. The additional validation of the extrapolation procedure for metabolic activity based on enzyme recovery data is important. This demonstrates the applicability of the methodology to determine the interindividual variance of risk-relevant PK outcomes (i.e., the amount of metabolite formed in the liver for a bioactivated hepatotoxicant) for xenobiotics to which humans cannot be safely exposed for the generation of experimental data. It is anticipated that toxicological data can be generated in test species *in vivo* and *in vitro* to determine the metabolic species responsible for toxicity, the PK of the xenobiotic and metabolite(s), and the identity of the enzyme responsible for metabolism. With this information, an adequate test animal-based PBPK model can be extrapolated to humans, using human tissue partition coefficients and the appropriate physiological parameters. Data on human enzyme recovery could be used to develop appropriate bounds on the distribution of metabolic activity for evaluation with the PBPK model.

## CONCLUSIONS

1. Human interindividual PK variance is important both for chemicals with adequate human PK data and for those chemicals to which humans cannot be experimentally exposed.
2. The described approach makes maximal use of data on the variance of enzyme content in the intact liver and enzyme specific activities derived *in vitro* with samples prepared from human organ donors.
3. The statistical combination of multiple data sets can be performed using widely accepted statistical methods.
4. This methodology can be employed to quantify the human interindividual variance of risk-relevant PK outcomes, when sufficient data are available to identify underlying fundamental

conditions such as the toxicologically-active metabolic species, the target organ for toxicity, the enzyme responsible for its formation/degradation, and the distribution of that enzyme to the intact liver.

5. Additional studies to characterize the distribution of MSP in intact liver in humans, in test animal species, and across developmental stages will benefit future efforts.

## REFERENCES

- Iyer, K.R. and M.W. Sinz. 1999. Characterization of phase I and phase II hepatic drug metabolism activities in a panel of human liver preparations. *Chem. Biol. Interact.* 118:151-169.
- Kedderis, G.L. 1997. Extrapolation of *in vitro* enzyme induction data to humans *in vivo*. *Chem. Biol. Interact.* 107:109-121.
- Kedderis, G.L. and S.D. Held. 1996. Prediction of furan pharmacokinetics from hepatocyte studies: Comparison of bioactivation and hepatic dosimetry in rats, mice, and humans. *Toxicol. Appl. Pharmacol.* 140:124-130.
- Kedderis, G.L., M.A. Carfagna, S.D. Held, R. Batra, J.E. Murphy and M.L. Gargas. 1993. Kinetic analysis of furan biotransformation by F-344 rats *in vivo* and *in vitro*. *Toxicol. Appl. Pharmacol.* 123:274-282.
- Lipscomb, J.C., J.W. Fisher, P.D. Confer and J.Z. Byczkowski. 1998. *In vitro* to *in vivo* extrapolation for trichloroethylene metabolism in humans. *Toxicol. Appl. Pharmacol.* 152:376-387.
- Reitz, R.H., M.L. Gargas, A.L. Mendrala and A.M. Schumann. 1996. *In vivo* and *in vitro* studies of perchloroethylene metabolism for physiologically based pharmacokinetic modeling in rats, mice and humans. *Toxicol. Appl. Pharmacol.* 136:289-306.
- Shimada, T., H. Yamazaki, M. Mimura, Y. Inui and F.P. Guengerich. 1994. Interindividual variations in human liver cytochrome P450 enzymes involved in the oxidation of drugs, carcinogens and toxic chemicals: Studies with liver microsomes of 30 Japanese and 30 Caucasians. *J. Pharmacol. Expt. Ther.* 270:414-423.
- Snawder, J.E. and J.C. Lipscomb. 2000. Interindividual variance of cytochrome P450 forms in human hepatic microsomes: Correlation of individual forms with xenobiotic metabolism and implications in risk assessment. *Reg. Toxicol. Pharmacol.* 32:200-209.

**NOTICE:** The authors appreciate the constructive comments received from Dr Harlal

Choudhury. The views expressed in this paper (NCEA-C-0963J) are those of the individual

authors and do not necessarily reflect the views and policies of the US Environmental Protection

Agency (EPA). This paper has been reviewed in accordance with EPA's peer and administrative review policies and approved for presentation and publication. This manuscript was published in *Science of the Total Environment* as part of the proceedings of the Spring Conference on Toxicology, held April 2001, in Fairborn, Ohio. Lipscomb, J.C. and Kedderis, G.L. 2002. Incorporating human interindividual biotransformation variance in health risk assessment. *Sci. Total Environ.* 288:13-21.

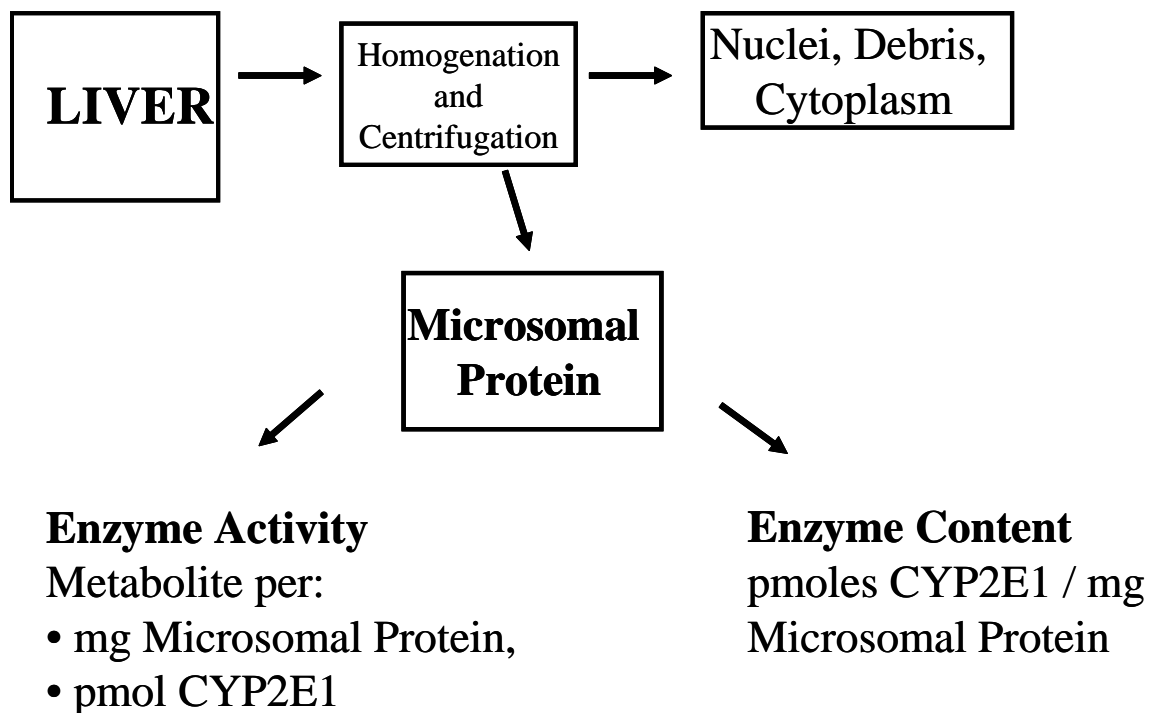


FIGURE 1-1

Isolation of Microsomal Protein from the Intact Liver. In this procedure, intact tissue is homogenized and subjected to an initial centrifugation which results in the sedimentation of cellular debris, mitochondria and nuclei. A subsequent higher speed centrifugation results in sedimentation of microsomal protein, the fraction enriched for the content of endoplasmic reticulum and associated enzymes. The supernatant of this high-speed centrifugation contains proteins distributed to the cytoplasm of the cell. A resuspension of the pelleted microsomal protein is performed in limited volume to retain as much of the concentrating effect as possible.

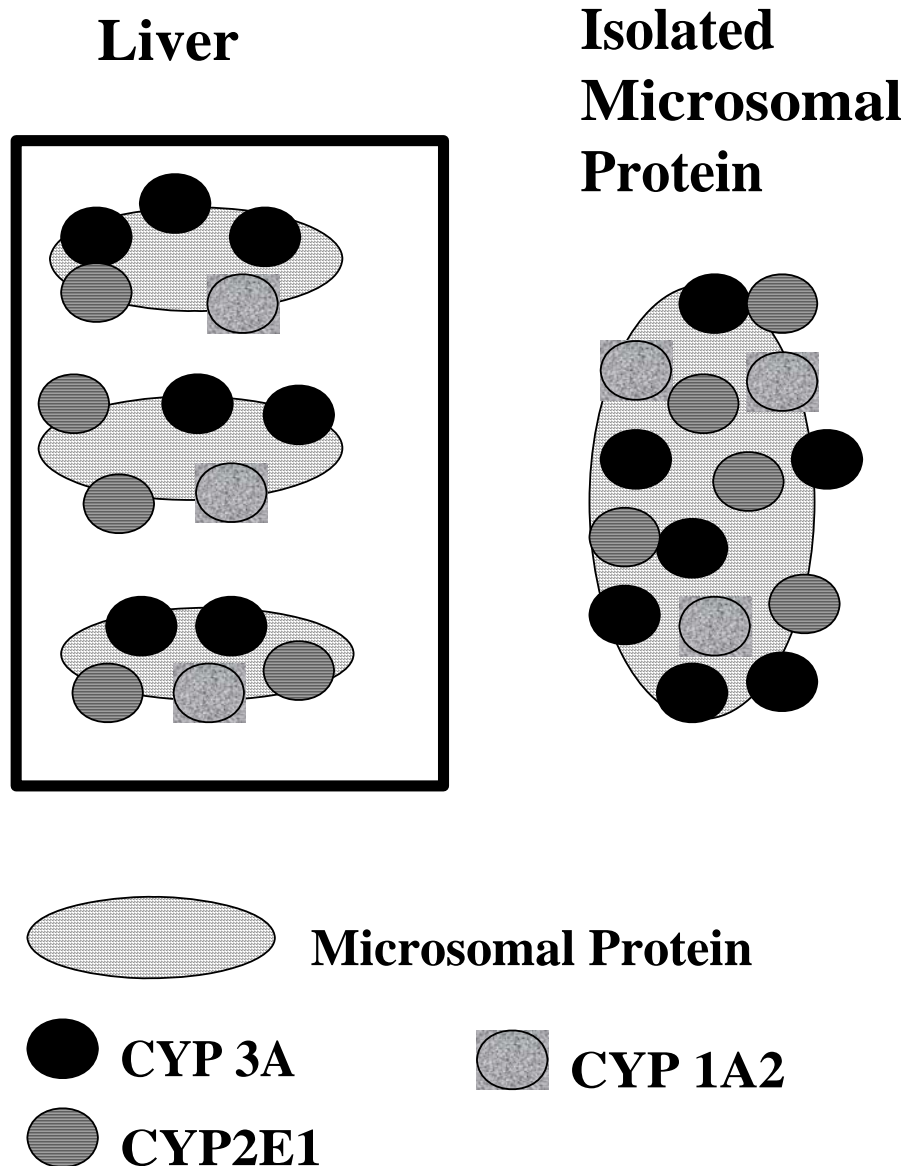


FIGURE 1-2

Relationship Between Intact Liver, Microsomal Protein and Some CYP Forms. The isolation of microsomal protein from intact liver via homogenation of tissue and differential centrifugation results in a 100,000 x g pellet which is enriched for endoplasmic reticulum content. The enrichment results in an artificial increase in the concentration of biological components associated with the endoplasmic reticulum. This isolation produces a fraction (microsomes; MSP) which is subjected to *in vitro* investigations of metabolic activity and enzyme content. However, a quantitative relationship to the intact liver is not possible without further information on the distribution of microsomal protein to the intact liver.

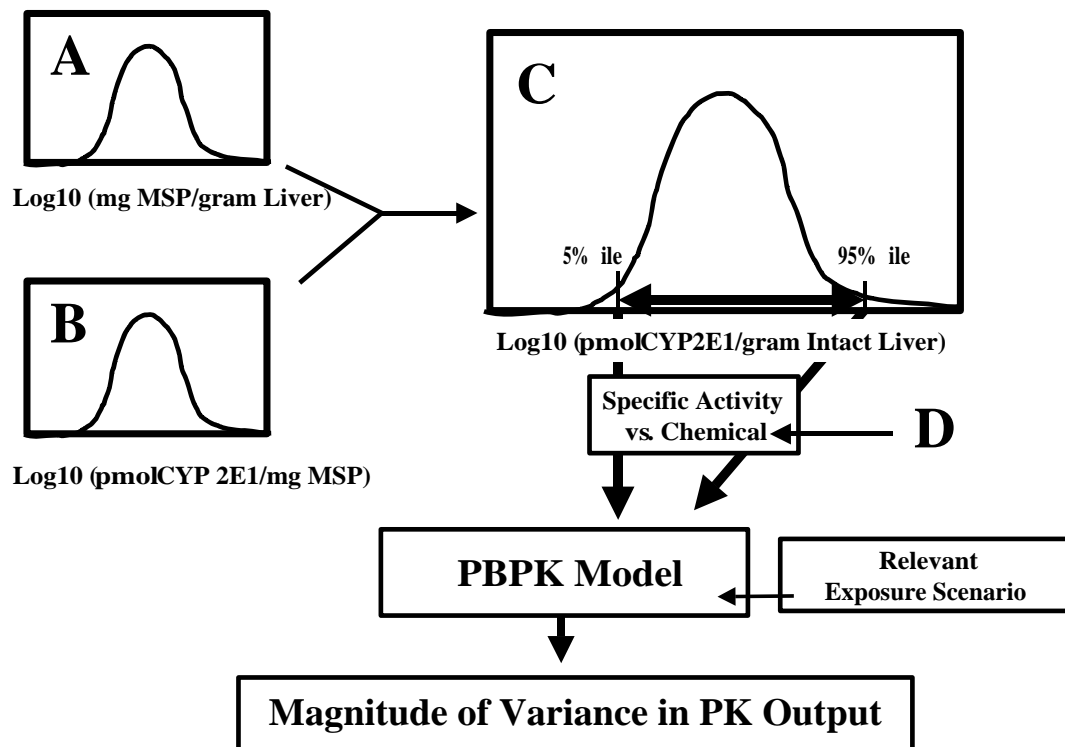


FIGURE 1-3

Extrapolation and Incorporation of *In Vitro* Derived Metabolic Rates in PBPK Modeling. This figure depicts the framework for deriving appropriate *in vitro* measures and their extrapolation into a PBPK model. Basically, the metabolic rate should be expressed per unit of responsible enzyme, and the distribution of that enzyme to the intact liver must be known. Because CYP2E1 and many other enzymes are expressed solely in the endoplasmic reticulum or MSP of the cell, this figure depicts the distribution of MSP to the intact liver (panel A). Secondly, the distribution of CYP2E1 within the MSP derived from liver tissue of human organ donors is depicted (panel B). By statistically combining these two (independent) data sets (see Equation (2)), an estimate of the CYP2E1 content of intact liver can be produced (panel C). Consistent with estimating the variance surrounding 90% of the population, we chose to represent the 5<sup>th</sup> and 95<sup>th</sup> percentiles of this distribution for evaluation. The enzyme activity representing the 5<sup>th</sup> and 95<sup>th</sup> percentiles for enzyme content can be determined by multiplying the content (pmoles CYP2E1/gram liver) by the specific activity of CYP2E1 toward a selectively metabolized substrate, and then correcting for molecular weight, time and fractional body weight attributed to the liver (2.6% or 26 grams liver/kg body mass). Panel D demonstrates the specific activity (turnover number) of the enzyme for the xenobiotic substrate as a point estimate, but a distribution for that value might also be obtained and employed to capture additional biochemical variance. These extrapolated upper and lower bound metabolic rates, when corrected to those expressed as mg/hr/kg body weight, can then be incorporated in a human PBPK model. The model should be exercised to simulate the exposure under relevant conditions. Models may behave differently, and the impact of the variance in enzyme content and activity may be different under different exposure conditions.

## **2. HOW DIFFERENCES IN ENZYME EXPRESSION CAN TRANSLATE INTO PHARMACOKINETIC VARIANCE AND SUSCEPTIBILITY TO TOXICITY**

### **ABSTRACT**

Advances in risk assessment methodologies invite the consideration of more pharmacokinetic, pharmacodynamic and biochemical information than ever before. When toxicity data are adequate, the identification of enzymes responsible for detoxication or bioactivation invite their consideration in risk assessment. Consideration should be given not only to the ontogeny of enzyme expression, but to other biochemical factors such as tissue lipid content and changes in relative organ size and blood flow during development. Dogma that enzyme alterations result in alterations of risk requires reexamination. Sometimes these do alter risk, even though the enzymes form toxicologically active metabolites. Knowledge that a given enzyme is responsible for metabolism of an environmental contaminant often stimulates the search for and use of information on its variance in expression and/or activity. Separate data on enzyme expression (content) and enzymatic activity can be useful in human health risk assessment, but requires the application of physiologic constraints, which can vary with age. Without these constraints, data from otherwise well-conducted studies have fueled incomplete and misleading conclusions. This manuscript uses the generic example of variance in xenobiotic metabolizing enzymes to make some points on the proper conduct and interpretation of *in vitro* findings pertinent to risk and susceptibility, such as findings inferred from studies of genetic polymorphisms. This information must be integrated in the context of the intact animal and/or intact human. The technique of physiologically based pharmacokinetic modeling offers a platform upon which to integrate findings from disparate areas of biochemical research, while maintaining the constraints of the intact body.

## **BACKGROUND**

Biological variability is a key component of risk, serving as the basis for differences in susceptibility between species, and among adult members of the human species and between adults and children. Continued advances in risk assessment methodologies should capture the refinements in our understanding of biological variability underlying differential susceptibility to effects. Not all biological or biochemical differences modulate risk, and a critical task is to discern which biochemical differences do and which do not contribute to susceptibility by linking them with key causal events. Logically, the next step in the process is to evaluate those which do alter risk and determine the basis for their contribution. Although biological variability can relate to either pharmacokinetic (PK) or pharmacodynamic (PD) processes, the present manuscript attempts to address variance in drug metabolizing enzymes, whether differences in their expression relate to developmental, genetic or other factors, and the determination of their contribution to risk through PK alterations. Of paramount importance is the availability of xenobiotic substrate to the liver, and consideration of first-order metabolism. None of these findings should be taken out of the context of the intact body:

*Structure without function is a corpse, function without structure is a ghost; in vitro findings unbounded by in vivo constraints are conjecture.*

## **TOXICITY AND RISK ASSESSMENT**

The availability of advanced information on human genetics and proteomics, as well as the increasing level of detail about toxic mechanisms, invites the inclusion of more technical information in human health risk assessments. Risk assessments should be advanced to include relevant data interpreted under appropriate constraints. In the absence of full considerations of human anatomy, physiology and biochemistry, this can lead to some mischaracterizations. Risk

assessors, and those developing advanced toxicokinetic and toxicodynamic information should bear in mind that the ultimate location where genetic variance and human biochemical individuality, regardless of developmental stage, impacts human health risk is the juxtaposition of the toxic molecular species and the biochemical target. This interaction may be at a specific site such as a receptor (Nesaretnam et al., 1996) or an individual protein (Soldin et al., 2001), or it may result from the development of a non-specific condition, such as oxidative stress (Umemura et al., 1998).

The derivation of human exposure limits often includes extrapolation of doses at identified response levels in animal studies to corresponding doses in the general human population and the further consideration of sensitive humans, requiring a second extrapolation of the dose in the general human population to that in sensitive individuals. The uncertainty factors governing these two extrapolations ( $UF_A$  and  $UF_H$ , respectively) have been further divided into pharmacokinetic (PK) and pharmacodynamic (PD) components (IPCS, 2001; US EPA, 1994). These components have different importance in the risk assessment paradigm (Figure 2-1). While both are involved in the dose-response evaluation phase, only PK is involved in exposure assessment, which is best developed to describe the internal (target tissue) dose rather than the concentration of agent in an environmental contact medium.

## **METABOLISM AND PHARMACOKINETICS IN RISK ASSESSMENT**

Recently, the default uncertainty values have begun to be replaced with chemical-specific uncertainty factors in the derivation of reference doses (RfD) (Smallwood et al., 2001; Murray and Andersen, 2001). This requires toxicity information sufficient to identify the chemical species (e.g., parent or metabolite, which metabolite) responsible for toxicity and the target organ or tissue.

Genetic polymorphisms and the impact of enzyme variance between individuals and among age groups should be evaluated in a chemical-specific manner. When differences in enzyme activity are risk-relevant, some preliminary consideration should be given to the potential impact of variance on the ultimate risk. A hypothetical case where a chemical is either 95% or 99% metabolized provides a useful example. When metabolism results in bioactivation, the risk resides in the formation of the metabolite and the significance of that difference ( $0.99/0.95 = 1.04$ -fold) in the toxicologically active species is rather small. However, when metabolism represents a detoxication step, the risk is from the parent chemical, not the metabolite, and the difference [ $(1 - 0.95) / (1 - 0.99) = 5$ -fold] becomes appreciable.

Consideration of enzyme kinetics, especially reactions governed by first-order kinetics, becomes critical in considering whether differences in enzyme content and/or activity can be important mediators of susceptibility. The parameters governing first-order reactions are  $V_{max}$  (the theoretical maximal initial rate of the reaction) and  $K_m$  (the substrate concentration necessary to drive the reaction at one-half maximal velocity). These constants are unique for each reaction; even reactions for different substrates which are catalyzed by the same enzyme; the constants are readily measurable for most substrates. Their characterization is complicated by the choice of *in vivo* test system (selection of test species and dosing conditions) choice of *in vitro* test system (subcellular fraction or isolated hepatocytes derived from animals or humans) and method of detection employed to quantify metabolism (appearance of product or disappearance of parent compound). Under the conditions used to characterize metabolism,  $V_{max}$  and  $K_m$  are representative of “quantity” and “quality”, respectively.  $V_{max}$  is directly dependent on the concentration of the enzyme in the test system.  $K_m$ , on the other hand, includes the affinity of the substrate for the enzyme (and vice-versa), and reflects the ability of

the enzyme to catalyze the reaction at lower substrate concentrations. Thus, observed changes in the  $V_{max}$  for one reaction may be generalizable to the metabolism of other substrates for the same enzyme, while the generalizability of changes in  $K_m$  is complicated by chemical-specific characteristics and, for the many lipophilic environmental contaminants, by age-dependent differences in tissue lipid content. The relationship between substrate concentration (*in vivo*, and for risk assessment purposes, this is best represented by the concentration in target tissues),  $V_{max}$  and  $K_m$  is demonstrated in the Michaelis-Menten rate equation (Equation 2-1).

$$\text{Rate} = (V_{max} * [s]) / (K_m + [s]) \quad (2-1)$$

Saturation of metabolism (when substrate is not limiting to the reaction rate) is not frequent in environmentally-encountered toxicants, only seldom observed in occupational exposure, but is frequently observed in experimental studies with research animals. When the concentration of the enzyme in metabolically active tissues varies, the metabolism of the substrate is related to the amount of enzyme present (note that physiological restrictions of the delivery of the substrate to the enzyme have an important, sometimes limiting, effect on metabolism *in vivo*, this is discussed later). Thus, under conditions where substrate delivery is not limiting, rates of metabolism are directly proportionate to the amount of enzyme present ( $V_{max}$ ). However, the rate of metabolism is not proportionately related to the  $K_m$  value; results in Figure 2-2 demonstrate that when substrate is present at concentrations far above the  $K_m$  value, that metabolic rates are not particularly sensitive to changes in  $K_m$  values. Thus, alterations of  $K_m$  and  $V_{max}$  values have different effects on metabolic rates, dependent on the ratio of substrate concentration to  $K_m$  value. Figure 2-2 demonstrate the effect of 10-fold increases and 10-fold decreases in  $K_m$  and  $V_{max}$  on metabolic rates when substrate is present below, at and above the  $K_m$ . Here, metabolic rates are proportionate to  $V_{max}$  across the entire range of substrate

concentrations. Changes like these are typical of enzyme induction – a term used to indicate an *in vivo* up-regulation of enzyme content. In contrast, 10-fold changes in  $K_m$  only produce changes in metabolic rate roughly proportionate to the change in  $K_m$  value at substrate concentrations 100-fold lower than the  $K_m$  value. A change in  $K_m$  value results in only moderate changes in metabolic rate when substrate is present at concentrations much higher than the  $K_m$  value. These results plainly demonstrate 1) the need to determine whether alterations in metabolic rate are due to changes in the quantity of protein (enzyme) present (directly related to  $V_{max}$ ), or due to changes in the qualitative nature of the enzyme (directly related to  $K_m$ ), and 2) the need to ascertain the substrate concentration relative to the  $K_m$  value. The predictive value of *in vivo* findings relating polymorphisms (qualitative or quantitative changes) and quantitative age-dependent changes in enzyme content of drug metabolizing enzymes to metabolic rates can only be fully appreciated when the metabolic rates are related to 1) the concentration of substrate attained *in vivo*, and 2) the  $K_m$  for the reaction. An additional note of caution should be applied to address the developmental pattern of drug metabolizing enzymes, especially so when multiple enzymes may contribute to the metabolism of a given xenobiotic. Several data sets have demonstrated the contribution of several P450 forms to the oxidation of trichloroethylene; these forms have appreciably different affinities ( $K_m$  values) and different developmental patterns of expression.

## **USING ENZYME KINETIC DATA TO ESTIMATE PHARMACOKINETIC VARIANCE**

The basis of differences in tissue concentrations of toxicants typically brings to mind differences in the partitioning of the chemical from blood to tissue or differences in metabolism. Removal of the xenobiotic from circulating blood reduces tissue concentrations, and the effect of the xenobiotic, whether beneficial or toxic, on the biological system. For therapeutics, the

concentration in blood (or plasma) is typically the target of predictions, as this fluid is available for analysis during clinical and preclinical trials. The effect of interest is related to blood (plasma) concentrations. These conditions differ from those in chemical risk assessment, in which concentrations of toxic agent in, most often, non-blood target tissue are the object of investigation. Under these two disparate conditions, different measures of clearance are justified. To estimate the impact of variance in enzyme content and activity, the best approach is to employ the aid of a physiologically based pharmacokinetic (PBPK) model (Lipscomb and Kedderis, 2002). For extrapolation and inclusion in the model, the variance in enzyme content should be statistically quantified (see Snawder and Lipscomb, 2000) and information on the variance in catalytic activity (Michaelis-Menten kinetic parameters) should be available (see Lipscomb et al., 1997).

Intrinsic clearance ( $CL_{int}$ ) of substrates (Equation 2-2) describes the removal of substances from the circulation and is expressed in units of milliliters cleared per hour. This measure has value in the pharmacokinetic assessment of therapeutics (Houston, 1994) where target tissue concentration is not considered critical, and when the doses are somewhat standardized. However,  $CL_{int}$  does not account for the concentration of the substrate in the metabolically active tissue (Table 2-1).

$$CL_{int} = V_{max}/K_m \quad (2-2)$$

Hepatic clearance ( $CL_{hep}$ ; Equation No. 2-3) of substrates is used to describe the metabolism of substrates in physiologically based pharmacokinetic (PBPK) modeling, and includes a term used to quantify the rate of delivery of the substrate to the liver via hepatic blood flow. Delivery to liver is a function of the concentration of the chemical in the medium which contacts blood, the partitioning of the chemical from the medium into blood, and the partitioning

of the chemical from the blood to the liver (Figure 2-3). These three physiologic components are not considered in the prediction of intrinsic clearance.

$$CL_{\text{hep}} = (V_{\text{max}}/K_m) * Q_{\text{Liver}} / (V_{\text{max}}/K_m) + Q_{\text{Liver}} \quad (2-3)$$

Table 2-1 demonstrates the impact of variances in  $V_{\text{max}}$  and  $K_m$  in the presence of variances in the  $Q_{\text{Liver}}$  term in a hypothetical but plausible example. The results from this example clearly demonstrate the differential applicability of assumptions about the impact of qualitative ( $K_m$ ) and quantitative ( $V_{\text{max}}$ ) differences in xenobiotic metabolizing enzymes relative to exposure conditions. Under the conditions of a lower exposure ( $Q_{\text{Liver}} = 0.005$ ), a 10-fold increase in  $V_{\text{max}}$  (enzyme content) results in virtually no change in  $CL_{\text{hep}}$ . In comparison, this same change in  $V_{\text{max}}$  under the conditions of higher exposure ( $Q_{\text{Liver}} = 50$ ) results in a roughly proportionate difference in  $CL_{\text{hep}}$ . Because of the  $V/K$  term in the equation for Hepatic Clearance, this same effect would be observed for a 10-fold decrease in  $K_m$ , because  $V/K$  would remain the same as that value for a 10-fold increase in  $V_{\text{max}}$ . Note that for this exercise, difference in the  $V/K$  term representing Intrinsic Clearance remains fixed at 10-fold, regardless of substrate delivery. Figure 2-3 demonstrates the importance of substrate delivery via hepatic circulation. Kedderis (1997) treated this concept in more detail, when he demonstrated that the influence of enzyme induction on furan metabolism was dampened significantly by limitations of metabolism imposed by delivery of substrate via blood flow.

The delivery of a substrate to the liver can be rate-limiting in metabolism and is determined by factors including 1) contact of blood with the substrate, 2) the concentration of the substrate in the medium contacting blood, 3) solubility of the substrate in blood, 4) the distribution (partitioning) of the substrate from blood into extrahepatic tissues, 5) the rate of blood flow to liver, 6) the duration that blood remains in contact with the liver, and 7) the

partitioning of the substrate from the blood into liver tissue. The solubility of xenobiotics in blood and solid tissues is a critical factor in pharmacokinetic analyses, and is one for which few children-specific data sets exist. Metabolic capacity of the liver is characterized by the enzyme *content* of the liver and by the *activity* of the enzyme present in the liver. The activity of an enzyme functioning under first order conditions is best described by the Michaelis-Menten Rate equations, integrating substrate concentration,  $V_{max}$  and  $K_m$  values. Figure 2-4 demonstrates three general cases of chemical metabolism. Case A represents a flow-limited scenario, in which the metabolic capacity of the liver is such that it quite efficiently metabolizes the chemical delivered to the liver. Here, increases in the metabolic capacity will have no further effect on the amount of chemical metabolized; increases in the amount of chemical metabolized will only occur under conditions which increase the delivery of the chemical to the liver. Decreases in metabolic capacity may decrease the amount of chemical metabolized, but such a decrease must be rather marked. Case B represents a chemical which is well-metabolized: the amount of chemical delivered to the liver is such that the metabolic capacity of the liver (a function of both enzyme content and activity) is capable of metabolizing the amount of chemical delivered. Increases in metabolic capacity will not increase the amount of chemical metabolized, decreases in metabolic capacity are more likely to result in decreases in the amount of chemical metabolized than in the flow-limited case. Case C represents a poorly-metabolized chemical, in which delivery of the chemical to the liver exceeds the metabolic capacity of the liver; the amount of metabolite formed is dependent on the metabolic capacity of the liver. Increases in metabolic capacity will result in more metabolite formed; decreases in metabolic capacity will reduce the amount of metabolite formed. This figure demonstrates the need to apply physiologic,

anatomic and biochemical constraints as well as relevant exposure conditions to *in vitro* findings of variance in xenobiotic metabolism parameters when determining their relevance to chemical risk.

## **IMPACT OF STUDY DESIGN**

Studies of the impact of differences in enzyme content or activity, including polymorphisms, on risk can be carried out at several levels and, with respect to polymorphisms in xenobiotic metabolizing enzymes, carry the most weight in this order:

1. Characterization of metabolic activity toward the substrate of interest *in vivo*
2. Characterization of metabolic activity toward the substrate of interest *in vitro*
3. Characterization of metabolic activity against a marker substrate *in vivo*
4. Characterization of variance in enzyme expression (qualitative or quantitative)
5. Characterization of metabolic activity against a marker substrate *in vitro*
6. Characterization of changes in mRNA content
7. Characterization of changes in DNA

While changes in DNA are critical underlying events, these changes may occur in different positions, and with different effects. For instance, genetic alterations occurring in non-transcribed portions of the genome (exons) are highly unlikely to have functional significance, while changes in introns are more likely to have a functional effect. Likewise, changes in base sequence may or may not change amino acid sequence. For these reasons, even when changes are observed, but not characterized, in genes coding for xenobiotic-metabolizing enzymes, it is critical to demonstrate their impact on metabolism. Just as xenobiotics can be either detoxicated or bioactivated through metabolism, changes in the genes for these enzymes can increase or decrease their activity. These changes are best evaluated with respect to their impact on enzymatic activity, and that impact should be characterized fully, and with a keen eye to likely exposure conditions for the substrate of interest.

## SUMMARY AND CONCLUSIONS

It is important to remember that, just as metabolism can alter PK, PK can alter metabolism. Factors which increase or decrease the activity of metabolic enzymes can, but do not always, alter tissue dosimetry, which should be the fundamental expression of dose for the dose-response assessment phase of risk assessment. Extrahepatic factors, including age-dependent differences in organ blood flows and tissue lipid content, which alter the delivery of the substrate to the liver can, but do not always, change rates of bioactivation or detoxication. In the consideration of age-related PK differences measured *in vivo*, one must give careful consideration to substrate concentrations attained in the liver, extrahepatic factors and the age-dependent expression of drug metabolizing enzymes. The platform offered by a physiologically based pharmacokinetic model may offer the best mechanism through which to extrapolate *in vitro* findings such as qualitative and quantitative changes in a drug metabolizing enzyme or enzymatic activity to the intact human. These models can be constructed so that other age-dependent extrahepatic factors can be modified to reflect requirements, however there are few data sets available which address tissue partition coefficients in children. When considering interindividual variance in enzyme content and activity as modulators of risk, that consideration should be chemical-specific: metabolic variance in one direction can increase the susceptibility to one chemical while decreasing the susceptibility to another.

## REFERENCES

Houston, J.B. 1994. Utility of *in vitro* drug metabolism data in predicting *in vivo* metabolic clearance. *Biochem. Pharmacol.* 47:1469-1479.

IPCS (International Programme on Chemical Safety of the World Health Organization). 2001. Guidance Document for the Use of Data in Development of Chemical-Specific Adjustment Factors (CSAFs) for Interspecies Differences and Human Variability in Dose/Concentration-Response Assessment. Available at <http://www.ipcsharmonize.org/csaf-intro.html>

Kedderis, G.L. 1997. Extrapolation of *in vitro* enzyme induction data to humans *in vivo*. Chem. Biol. Interact. 107:109-121.

Lipscomb, J.C. and G.L. Kedderis. 2002. Incorporating human interindividual biotransformation variance in health risk assessment. Sci. Total Environ. 288:13-21.

Lipscomb, J.C., C.M. Garrett and J.E. Snawder. 1997. Cytochrome P450-dependent metabolism of trichloroethylene: Interindividual differences in humans. Toxicol. Appl. Pharmacol. 142:311-318.

Lipscomb, J.C., J.W. Fisher, P.D. Confer and J.Z. Byczkowski. 1998. *In vitro* to *in vivo* extrapolation for trichloroethylene metabolism in humans. Toxicol. Appl. Pharmacol. 152:376-387.

Murray, F.J. and M.E. Andersen. 2001. Data-derived uncertainty factors: Boric acid (BA) as an example. Hum. Ecol. Risk Assess. 7:125-138.

Nesaretnam K., D. Corcoran, R.R. Dils and P. Darbre. 1996. 3,4,3',4'-Tetrachlorobiphenyl acts as an estrogen *in vitro* and *in vivo*. Mol. Endocrinol. 10:923-936.

Smallwood, C.L., J. Swartout and J.C. Lipscomb. 2001. Using data to replace default uncertainty factors for boron reference dose. Presented at the annual meeting of the Society for Risk Analysis, Seattle, WA, December.

Snawder, J.E. and J.C. Lipscomb. 2000. Interindividual variance of cytochrome P450 forms in human hepatic microsomes: Correlation of individual forms with xenobiotic metabolism and implications in risk assessment. Reg. Toxicol. Pharmacol. 32:200-209.

Soldin O.P., L.E. Braverman and S.H. Lamm. 2001. Perchlorate clinical pharmacology and human health: A review. Ther. Drug. Monit. 23:316-331.

Umemura T., A. Takagi, K. Sai, R. Hasegawa and Y. Kurokawa. 1998. Oxidative DNA damage and cell proliferation in kidneys of male and female rats during 13-weeks exposure to potassium bromate (KBrO<sub>3</sub>). Arch. Toxicol. 72:264-269.

US EPA (U.S. Environmental Protection Agency). 1994. Methods for Derivation of Inhalation Reference Concentrations and Application of Inhalation Dosimetry. Office of Research and Development, Washington, DC. EPA/600/8-90/066F.

NOTICE: This manuscript (NCEA-C-1348) has been reviewed and cleared for publication in accordance with EPA/ORD policy; the author is grateful to Harlal Choudhury, Jeff Gearhart and Gregory Kedderis for critical comments during manuscript development. The views contained herein are those of the author and not necessarily those of the Agency. This paper contains several key points made during a presentation to the workshop on Biological Variability in Children and Implications for Environmental Risk Assessment: New Perspectives on the Roles of Ethnicity, Race and Gender, held at the University of Maryland, March 2002. It was subsequently published in the Journal of Children's Health: Lipscomb, J.C. 2003. How differences in enzyme expression can translate into pharmacokinetic variance and susceptibility to risk. J. Child. Health 1:189-202.

TABLE 2-1

Effect of a 10-Fold Induction of Vmax on Hepatic Clearance over a Four-Log Increase in Substrate Delivery

Vmax <sup>a</sup>	Q <sub>Liver</sub> <sup>b</sup>	Km <sup>c</sup>	CL <sub>Int</sub> <sup>d</sup>	CL <sub>Hep</sub> <sup>e</sup>	Magnitude of Change in CL <sub>Hep</sub>
5	0.005	10	5	0.00495	
50	0.005	10	0.5	0.004995	1.01
5	0.05	10	5	0.045455	
50	0.05	10	0.5	0.049505	1.09
5	0.5	10	5	0.25	
50	0.5	10	0.5	0.454545	1.82
5	5	10	5	0.454545	
50	5	10	0.5	2.5	5.50
5	50	10	5	0.49505	
50	50	10	0.5	4.545455	9.18

<sup>a</sup> Vmax in units of mg/hour/gram liver

<sup>b</sup> Q<sub>Liver</sub> in units of mg/hr

<sup>c</sup> Km in units of mg substrate/liter blood

<sup>d</sup> Intrinsic Clearance in units of milliliters/hr

<sup>e</sup> Hepatic Clearance in units of milliliters/hr

NOTE: Changes in enzymatic activity, resulting from changes in enzyme content (pmoles of enzyme/gram tissue) and/or the specific activity of the enzyme (pmoles substrate metabolized / time / pmol of enzyme) can alter chemical metabolism, regardless of substrate concentration. However, the effect of changes in Km is dependent on substrate concentration, as demonstrated in Figure 2-2. Similarly, the delivery of substrate to the liver is critical *in vivo*, and represents a somewhat complicated and frequently under appreciated limitation in the extrapolation of *in vitro* findings. The results in Table 2-1 demonstrate the impact of considering substrate delivery *in vivo* (Q<sub>Liver</sub>) and the choice of clearance model (Intrinsic versus Hepatic Clearance) when extrapolating *in vitro* data on chemical metabolism. Intrinsic Clearance (Equation 2-2) does not take into account substrate delivery and predicts a consistent 10-fold change in clearance regardless of substrate delivery, while Hepatic Clearance (Equation 2-3) includes rate of substrate delivery and demonstrates that clearance can be substantially influenced by substrate delivery (see also Figures 2-3 and 2-4).

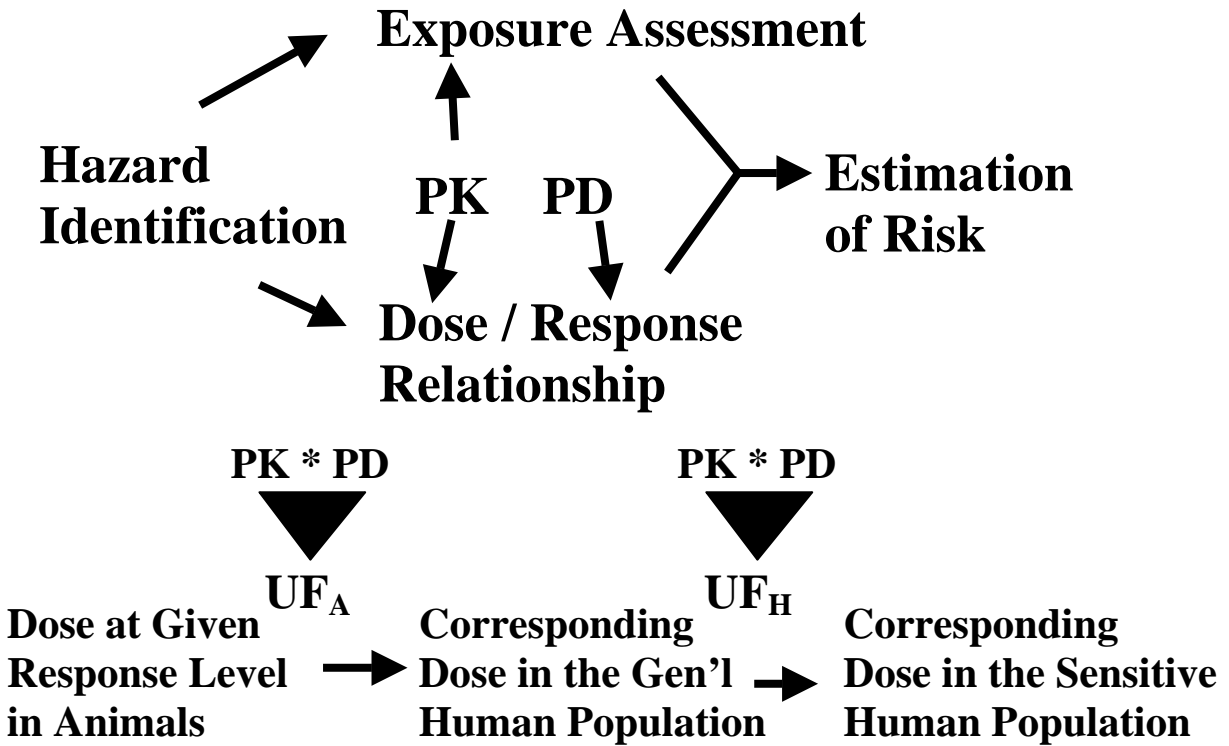


FIGURE 2-1

Pharmacokinetics and the Risk Assessment Paradigm. Both pharmacokinetic (PK) and pharmacodynamic (PD) data are useful in establishing the value for the two ( $UF_A$  - animal-to-human, and  $UF_H$  - human interindividual) uncertainty factors used to extrapolate the dose-response relationship from animals to sensitive humans. PK data are also useful in refining human and animal exposures to reflect tissue dosimetry of the chemical species responsible for the effect (PD).

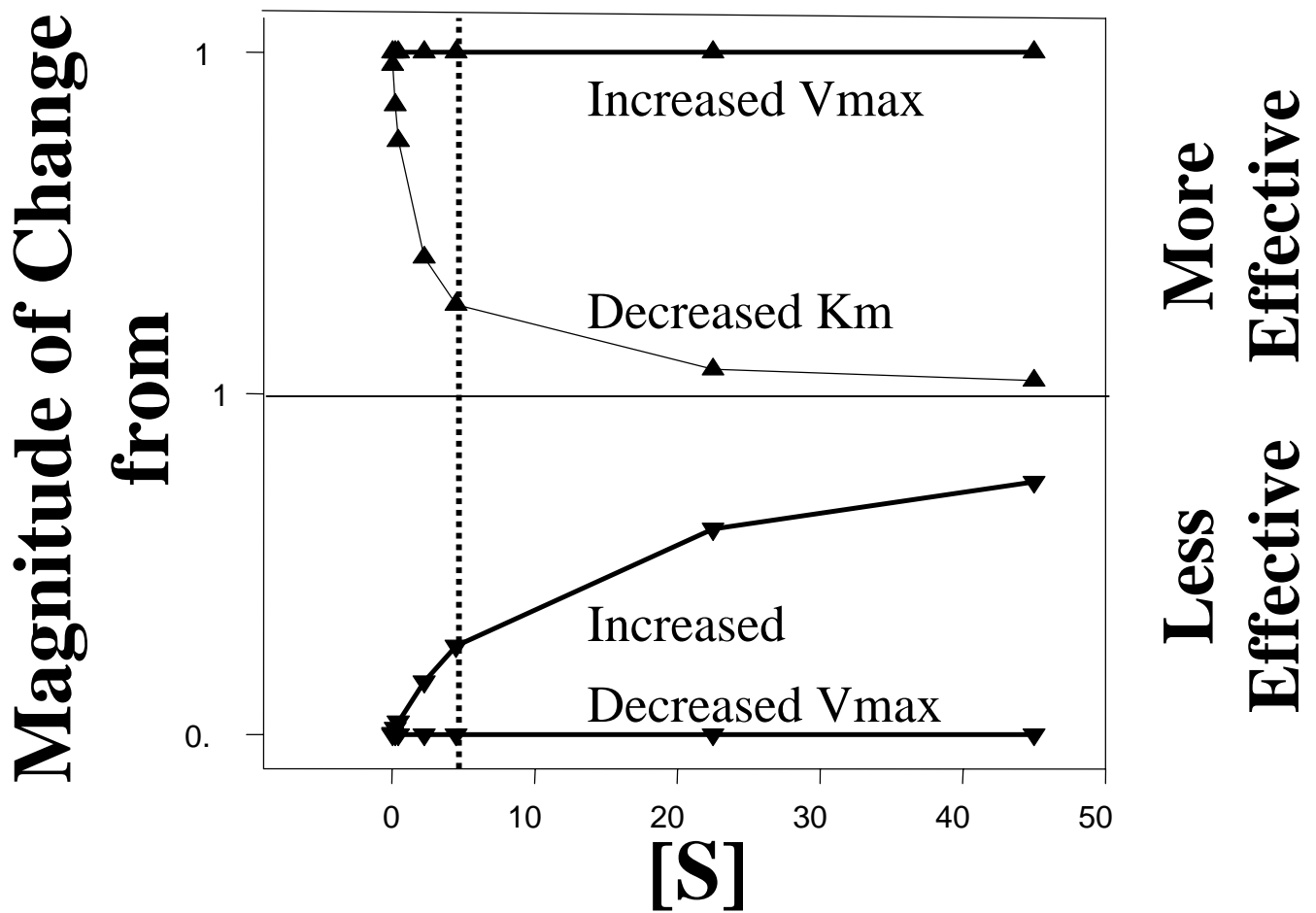


FIGURE 2-2

The Relationship Between  $K_m$  Value and Substrate Concentration. This figure represents the magnitude of change in the rate of the metabolic reaction following 10-fold increases and decreases in  $V_{max}$  and  $K_m$  values, with substrate concentrations from 0.45 to 450  $\mu\text{M}$ . Metabolic rates were predicted by the Michaelis-Menten reaction equation. Basal conditions were:  $K_m = 45 \mu\text{M}$ ;  $[s] = 45 \mu\text{M}$ ,  $V_{max} = 1200 \text{ nmol es/min/mg protein}$ .  $V_{max}$  changes result in proportionate changes in metabolic rate across substrate concentrations, while changes in  $K_m$  do not result in proportionate changes in metabolic rate, especially under saturating substrate concentrations.

**Chemical Availability      Metabolic Capacity      Amount Metabolized**

---

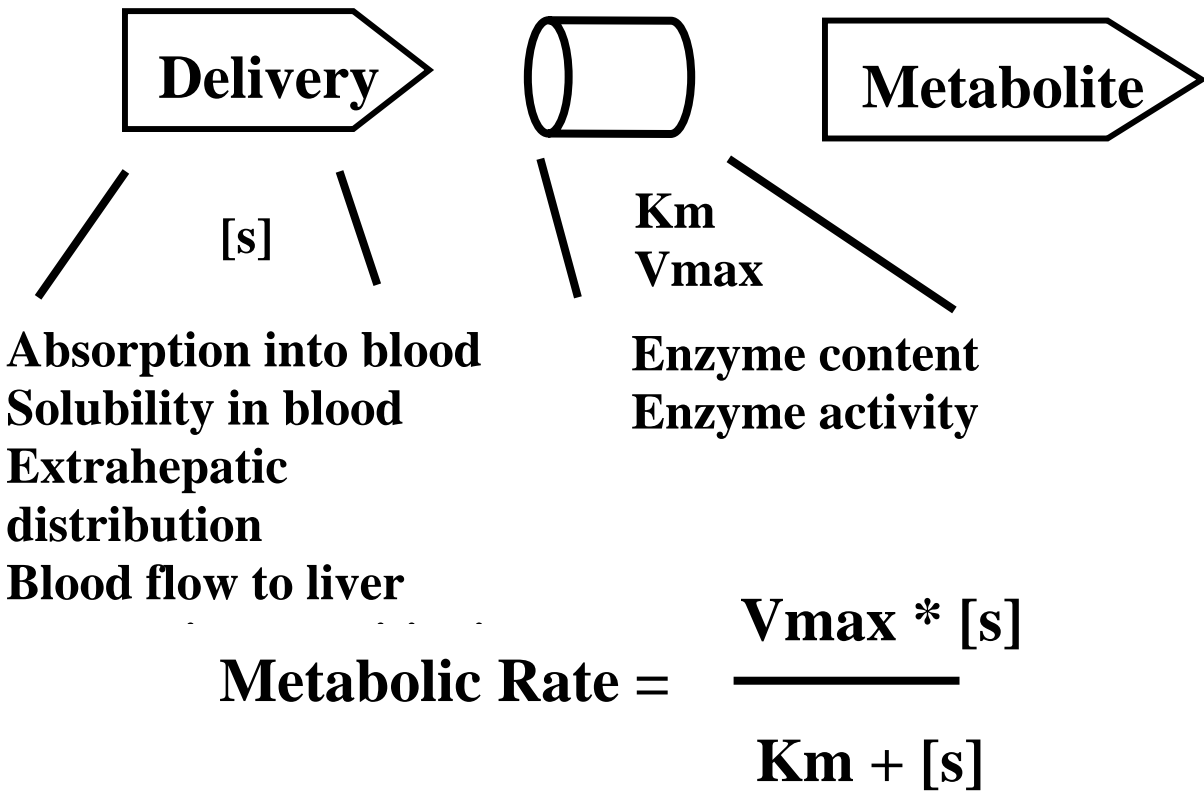


FIGURE 2-3

The Relationship Between Substrate Delivery, Metabolic Capacity and the Amount of Metabolite Formed. The “delivery” term is comprised of the amount of chemical present in the blood, the rate of blood flow to the liver, and the equilibrium attained between blood and liver tissue concentration of the substrate, which can be a function of transit time through the liver; this may be affected by extrahepatic factors such as the fat compartment serving as a “sink” for highly lipophilic xenobiotics. Metabolic Capacity is comprised of the enzyme content of the liver and the activity of the enzyme, dictated by the  $K_m$  and  $V_{\max}$  values of the enzyme for the chemical substrate under investigation.

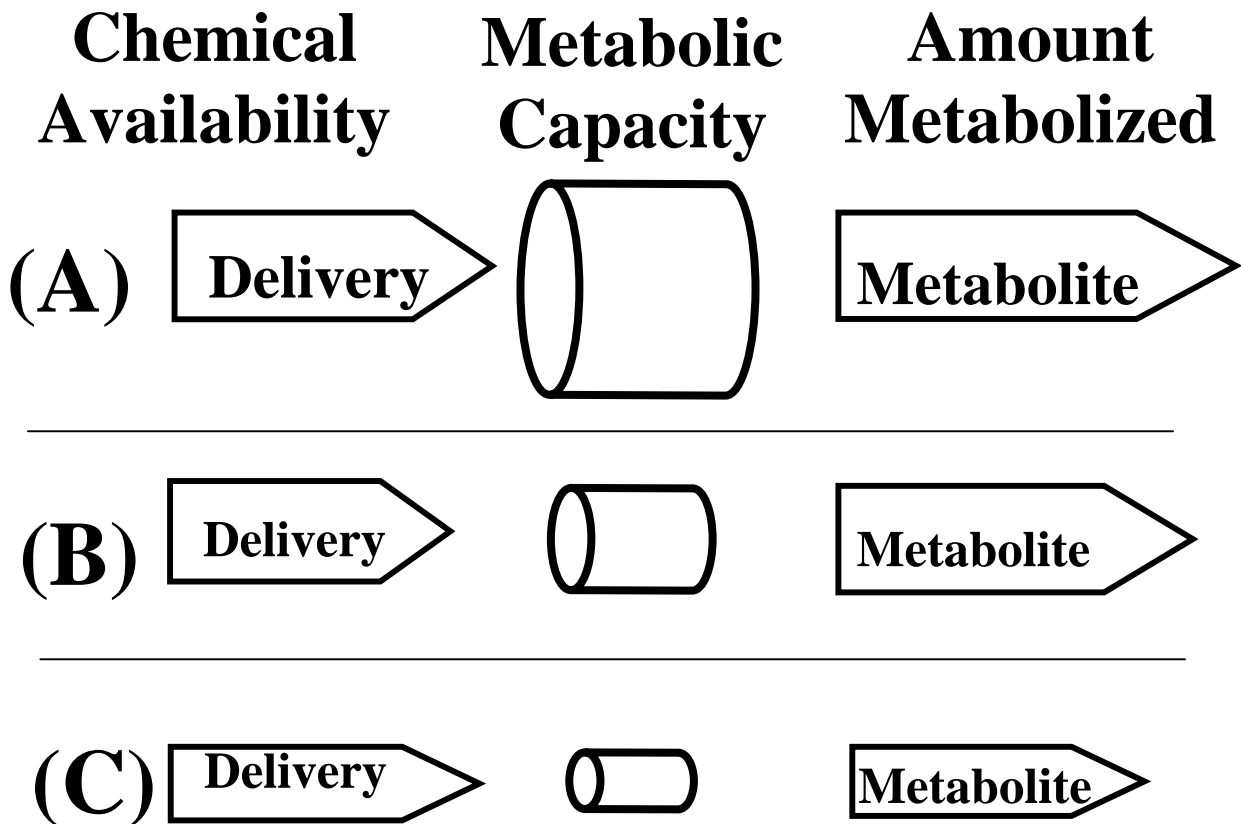


FIGURE 2-4

The Impact of Substrate Delivery and Metabolic Capacity on the Formation of Metabolites in Liver. This figure shows three of the possible cases of this relationship. Panel A demonstrates the metabolism of a flow-limited chemical. Here, the metabolic capacity of the liver is very large relative to the delivery of the substrate. In this condition, increases in enzyme activity (i.e., through induction) will not increase the amount of metabolite formed. Panel B demonstrates the metabolism of a well-metabolized chemical. Here, the metabolic capacity of the liver is sufficient to handle the amount of substrate delivered. Panel C demonstrates the metabolism of a poorly metabolized chemical. Here, the metabolic capacity of the liver is such that it is not sufficient to handle the amount of chemical available. Under this condition, increases in metabolic capacity, due to an increase in  $V_{max}$  and/or a decrease in  $K_m$ , will result in higher amounts of the chemical metabolized. Likewise, a decrease in  $V_{max}$  or an increase in  $K_m$  will result in further reductions of metabolism.

### **3. APPLICATION OF *IN VITRO* BIOTRANSFORMATION DATA AND PHARMACOKINETIC MODELING TO RISK ASSESSMENT**

#### **ABSTRACT**

The adverse biological effects of toxic substances are dependent upon the exposure concentration and the duration of exposure. Pharmacokinetic models can quantitatively relate the external concentration of a toxicant in the environment to the internal dose of the toxicant in the target tissues of an exposed organism. The exposure concentration of a toxic substance is usually not the same as the concentration of the active form of the toxicant that reaches the target tissues following absorption, distribution, and biotransformation of the parent toxicant. Biotransformation modulates the biological activity of chemicals through bioactivation and detoxication pathways. Many toxicants require biotransformation to exert their adverse biological effects. Considerable species differences in biotransformation and other pharmacokinetic processes can make extrapolation of toxicity data from laboratory animals to humans problematic. Additionally, interindividual differences in biotransformation among human populations with diverse genetics and lifestyles can lead to considerable variability in the bioactivation of toxic chemicals. Compartmental pharmacokinetic models of animals and humans are needed to understand the quantitative relationships between chemical exposure and target tissue dose as well as animal to human differences and interindividual differences in human populations. The data-based compartmental pharmacokinetic models widely used in clinical pharmacology have little utility for human health risk assessment because they cannot extrapolate across dose route or species. Physiologically based pharmacokinetic (PBPK) models allow such extrapolations because they are based on anatomy, physiology, and biochemistry. In PBPK models, the compartments represent organs or groups of organs and the flows between

compartments are actual blood flows. The concentration of a toxicant in a target tissue is a function of the solubility of the toxicant in blood and tissues (partition coefficients), blood flow into the tissue, metabolism of the toxicant in the tissue, and blood flow out of the tissue. The appropriate degree of biochemical detail can be added to the PBPK models as needed.

Comparison of model simulations with experimental data provides a means of hypothesis testing and model refinement. *In vitro* biotransformation data from studies with isolated liver cells or subcellular fractions from animals or humans can be extrapolated to the intact organism based upon protein content or cell number. *In vitro* biotransformation studies with human liver preparations can provide quantitative data on human interindividual differences in chemical bioactivation. These *in vitro* data must be integrated into physiological models to understand the true impact of interindividual differences in chemical biotransformation on the target organ bioactivation of chemical contaminants in air and drinking water.

## **TOXICOLOGY AND HUMAN HEALTH RISK ASSESSMENT**

One of the most difficult problems in toxicology and human health risk assessment is the use of appropriate animal models to predict the potential adverse effects of xenobiotic exposures to human beings. Laboratory animals can differ from humans in both the pharmacokinetics and pharmacodynamics of toxicant action. Differences in biochemistry and physiology can lead to differences in the target tissue dose of a toxicant following exposure of animals and humans to the same toxicant concentration. Significant species differences have been observed in the metabolic activation and detoxication of chemical toxicants. Species differences have also been observed in the pharmacodynamics of toxicant action at the cellular and molecular level. It is very difficult to know in advance if the toxic response to a chemical observed in experimental animals is predictive of the response in humans, or if humans would exhibit a toxicity not

expressed in experimental animals. Thus, differences between species can be both qualitative and quantitative in nature. With information on the mode or mechanism of toxicity (a descriptor of the response), appropriate pharmacokinetic information can be collected and used to refine the dose-response assessment so that concentrations of the toxic moiety in the target organ are considered.

In the development of therapeutic compounds and the reassessment of approved drugs and some occupationally important chemicals it is possible to derive pharmacokinetic data in human subjects. These human pharmacokinetic data can readily be compared with those derived from research animals. However, in the case of toxicologically uncharacterized compounds, and compounds already thought to exert toxicity in humans, ethical considerations preclude the exposure of humans. One approach to overcome these difficulties is the use of *in vitro* systems. A general experimental approach is to develop predictive *in vitro* systems using animal tissues and compare the results with those from *in vivo* studies using experimental animals. If the *in vitro* system provides a reasonable prediction of the *in vivo* result (e.g., the kinetics of toxicant bioactivation), then analogous *in vitro* systems can be developed using human tissues. The *in vitro* human data can be integrated into pharmacokinetic models to predict the human target tissue concentrations of toxicants and their metabolites following chemical exposure, along the lines of the classic *in vitro/in vivo* parallelogram approach (Figure 3-1). In this article, we will demonstrate the importance of pharmacokinetics in risk assessment and discuss important experimental considerations for producing useful *in vitro* data, the extrapolation of that data to humans through the use of pharmacokinetic models, and the incorporation of pharmacokinetic information into human health risk assessments.

## **PHYSIOLOGICALLY BASED PHARMACOKINETIC MODELS**

Pharmacokinetic models have utility in toxicology because the adverse biological effects of toxic substances are dependent upon the exposure concentration and the duration of exposure. Pharmacokinetic models can quantitatively relate the external concentration of a toxicant in the environment to the internal dose of the toxicant in the target tissues of an exposed organism. The exposure concentration of a toxic substance is usually not the same as the concentration of the active form of the toxicant that reaches the target tissues following absorption, distribution, and biotransformation of the parent toxicant.

Biotransformation modulates the biological activity of chemicals through bioactivation and detoxication pathways. Many toxicants require biotransformation to exert their adverse biological effects. Considerable species differences in biotransformation and other pharmacokinetic processes can make extrapolation of toxicity data from laboratory animals to humans problematic. Species differences in biotransformation pathways can be qualitative or quantitative. If a species exhibits a metabolic pathway that is not present in another species, that difference is qualitative. If both species possess a given metabolic pathway but differ in the rate or flux through that pathway, the difference is quantitative. Interindividual differences in biotransformation exist within genetically diverse human populations and among segments of the general population that are exposed to enzyme inducing agents through occupations or lifestyles that can alter the expression and/or function of xenobiotic-metabolizing enzymes. Differences in enzyme content and activity can lead to considerable variability in the pharmacokinetics and bioactivation of toxic chemicals. Some enzymes exhibit genetic polymorphisms, leading to the expression of aberrant enzyme forms with reduced activity. Many xenobiotic-metabolizing enzymes are induced by exposure to chemicals in food, air, water, and the environment.

Individual differences in genetics and exposure to inducing agents lead to considerable variability in xenobiotic metabolizing enzymes in human populations.

Compartmental pharmacokinetic models of animals and humans are needed to understand the quantitative relationships between chemical exposure and target tissue dose as well as animal to human differences and interindividual differences in human populations. The data-based compartmental pharmacokinetic models widely used in clinical pharmacology have little utility for human health risk assessment because they cannot extrapolate across dose route or species. Physiologically based pharmacokinetic (PBPK) models allow such extrapolations because they are based on anatomy, physiology, and biochemistry (Clewell and Andersen, 1994). In PBPK models, the compartments represent organs or groups of organs and the flows between compartments are actual blood flows. The concentration of a toxicant in a target tissue is a function of the solubility of the toxicant in blood and tissues (partition coefficients), blood flow into the tissue, metabolism of the toxicant in the tissue, and blood flow out of the tissue. The appropriate degree of biochemical detail can be added to the PBPK models as needed. The goal of PBPK modeling is to define one set of parameters that describe the behavior of a chemical in an animal. Comparison of model simulations with experimental data provides a means of hypothesis testing and model refinement. The predictive power of PBPK models makes them ideally suited for use in human health risk assessments.

### **EXTRAPOLATION OF *IN VITRO* DATA TO HUMANS**

*In vitro* biotransformation data can be extrapolated to intact animals and humans because the overall rate of an enzyme-catalyzed reaction is directly proportional to the total amount of enzyme present in the system. Therefore data generated with subcellular fractions such as microsomes or cytosols can be extrapolated to *in vivo* based on protein content. Studies with

rodent and human liver microsomes have established the quantitative expression of microsomal protein in liver tissue (Houston, 1994; Lipscomb et al., 2002c) and cytochrome P450 enzymes in microsomal protein (Shimada et al., 1994; Snawder and Lipscomb, 2000). Data from intact cellular systems such as hepatocytes can be extrapolated to *in vivo* based on cell number. There are approximately  $130 \times 10^6$  hepatocytes per gram of mammalian liver (Seglen, 1976; Arias et al., 1982). The liver is approximately 2.6% of human body weight (Snyder et al., 1992).

The isolation of intact and metabolically competent hepatocytes provides an excellent model to study biotransformation in an *in vitro* system that most closely resembles the *in vivo* setting. While subcellular fractions such as microsomes enrich the content of associated enzymes, enzymes in isolated hepatocytes retain their physical relationship to the endogenous lipid environment, the natural orientation toward soluble cofactors, and the unperturbed spatial relationship of multienzyme systems such as cytochromes P450 and NADPH-cytochrome P450 reductase. Isolated hepatocytes provide the best intact cellular system to predict chemical pharmacokinetics when used in a nutritive medium such as Williams' Medium E to maintain biochemical homeostasis. The cells synthesize the necessary cofactors and the enzymes are arrayed in membrane and cytoplasmic structures in the same manner as in the intact liver. Although there is some limited mechanical damage to the hepatocytes upon isolation, the cells repair the damage quickly upon incubation. In contrast to freshly isolated hepatocytes, which maintain enzyme functions close to those of the intact liver (Billings et al., 1977), hepatocytes in monolayer culture rapidly decrease expression of many xenobiotic metabolizing enzymes and do not reflect the kinetics of xenobiotic metabolism *in vivo* (Sirica and Pitot, 1980). Immortalized liver cell lines such as Hep G2 cells also have low metabolic capacity and are not appropriate models for predicting chemical pharmacokinetics.

We have previously shown that extrapolation of the kinetic parameters for the bioactivation of the rodent hepatocarcinogen furan from freshly isolated rat hepatocyte suspensions *in vitro* to whole animals *in vivo* accurately predicted the pharmacokinetics (Kedderis et al., 1993). Studies with human liver microsomal protein and isolated hepatocytes have been used to predict the *in vivo* pharmacokinetics of the industrial chemical and common groundwater contaminant trichloroethylene (Lipscomb et al., 1997, 1998). Studies by Houston (1994) showed that rat hepatocytes were more consistent than rat liver microsomes in accurately predicting the intrinsic clearance of 11 therapeutic agents metabolized by various isoforms of cytochromes P450. Isolated rat hepatocytes and rat hepatic microsomes were consistently more accurate in predicting intrinsic clearance than precision cut liver slices (Worboys et al., 1996). Drug concentration gradients within the liver slice do not allow every cell in the slice to participate in metabolism, indicating that this *in vitro* system is not appropriate for estimation of *in vivo* metabolic parameters.

One important factor in extrapolating *in vitro* data to predict *in vivo* pharmacokinetics is knowledge of the actual concentration of the xenobiotic in the cell suspension or incubation from measurement of the partition coefficient. Most xenobiotics are not very water-soluble, and the nominal concentration added is not always the concentration in the medium. Any other kinetically significant component that removes substrate from the system, such as specific protein binding or chemical reactivity, needs to be accounted for in the kinetic description of the *in vitro* system. Care should be taken that volatile chemicals are incubated in sealed flasks and that transfer rates between the vapor phase and aqueous phase are taken into account. This can be accomplished using a simple two-compartment kinetic model of the incubation system (Kedderis et al., 1993).

In order to extrapolate *in vitro* kinetic data to whole animals, the kinetic mechanisms of the enzymes catalyzing the metabolic reactions need to be known (or assumed). Most cytochrome P450-catalyzed reactions are known to follow an ordered sequential mechanism displaying saturable Michaelis-Menten kinetics (Hollenberg, 1992):

$$\text{Rate} = (V_{\max} * [S]) / (K_M + [S]) \quad (3-1)$$

where  $V_{\max}$  is the maximal rate of the reaction at infinite substrate concentration,  $[S]$  is the substrate concentration, and  $K_M$  is the Michaelis constant for the reaction. The Michaelis-Menten Equation 3-1 indicates that the initial velocity of the reaction will increase hyperbolically as a function of substrate concentration. The  $V_{\max}$  is a horizontal tangent to the top (saturated) part of the curve, while the tangent to the initial linear portion of the hyperbolic curve is the initial rate of the reaction,  $V/K$ . The  $V/K$  is the pseudo-first-order rate constant for the reaction at low substrate concentrations. The point where these two tangents intersect corresponds to the  $K_M$  (Northrop, 1983). The  $K_M$  is defined as the substrate concentration that gives one-half the  $V_{\max}$ .

The *in vitro* kinetic data can be incorporated into PBPK models after rearrangement to the appropriate units. The units of the  $V_{\max}$  value need to be expressed relative to body weight rather than per mg protein or cell number. As described above, these relationships have been defined. Values of  $K_M$ , the substrate concentration that gives one-half  $V_{\max}$ , have units of concentration and can be used directly if the solubilities of the chemicals in the *in vitro* system were measured. The PBPK model can be used to simulate a variety of toxicant exposure scenarios, including workplace environment, inhalation exposure, drinking water exposure, exposure in food, or dermal exposure.

## **INCORPORATION OF PHARMACOKINETICS INTO RISK ASSESSMENTS**

The development of PBPK modeling techniques was undertaken to better describe dose in terms of tissue concentrations for use in human health risk assessments for methylene chloride (Andersen et al., 1987). This early work recognized and incorporated species differences in metabolic capacity and a bifurcation in the metabolic pathway for methylene chloride, and represented a significant advance in risk assessment theory and practice. Since that time, several other works have addressed the employment of pharmacokinetic information in risk assessment, including the USEPA's guidance on the derivation of Reference Concentrations (RfC) for inhaled substances (US EPA, 1994). A recent publication by Clewell et al. (2002) breaks down the application of pharmacokinetic investigations into risk assessment into six steps, summarized as follows:

1. Evaluate toxicity information to understand the mode of action for the critical effect in the critical species;
2. Identify or develop a PBPK model parameterized for the test species;
3. Employ the PBPK model to calculate the relevant dose metric for the dose at the required dose level (i.e., BMD or NOAEL);
4. Define the uncertainty factors to be employed to determine the numerical value for the corresponding dose metric in humans;
5. Develop or identify an appropriately parameterized human PBPK model, and employ that model to determine the exposure conditions which result in the value for the dose metric determined in step 4;
6. Consider the dose metrics evaluated, and give priority to the dose metric which provides the most plausible basis for estimating the biologically effective dose in humans; when unclear, select the dose metric which is the most health-protective (conservative).

The incorporation of pharmacokinetics into human health risk assessment is essential for the understanding of species differences in toxicant bioactivation when human risk is extrapolated from animal models and for understanding the impact of interindividual differences

in toxicant bioactivation among humans. Measurement of differences in toxicant bioactivation by human tissue preparations is an important beginning to understanding pharmacokinetic factors that are related to risk, but the *in vitro* data must be integrated into PBPK models to understand the consequences of kinetic variability in the context of the whole organism. Our studies with furan and trichloroethylene illustrate these points.

The accurate prediction of furan pharmacokinetics from kinetic studies with isolated F-344 rat hepatocytes (Kedderis et al., 1993) suggested that kinetic studies with hepatocytes from other species could be used to develop species-specific pharmacokinetic models for furan. Therefore we determined the kinetics of furan bioactivation by cytochrome P450 2E1 (CYP2E1) in hepatocytes from B6C3F1 mice and humans (Kedderis and Held, 1996). The  $K_M$  values for furan oxidation were in the low micromolar range for hepatocytes from all three species. Hepatocytes from male mice oxidized furan at a greater rate than rat or human hepatocytes. Hepatocytes from three different human liver donors oxidized furan at rates equal to or greater than those of rat hepatocytes. Note that these results are not predicted by allometric scaling of the rat or mouse data to humans since allometry predicts slower rates in larger mammals (Mordenti, 1986). This underscores the importance of using human tissue samples to predict the human bioactivation of toxicants. A greater than 2-fold variation in  $V_{max}$  was observed among the three preparations of human hepatocytes (Kedderis and Held, 1996). The human liver preparations exhibiting the highest bioactivation rates were from donors who died in automobile accidents involving alcohol consumption, consistent with the interpretation that the higher  $V_{max}$  values were due to the induction of CYP2E1 by ethanol (Perrot et al., 1989).

The kinetic data from hepatocytes were used to develop PBPK models for furan in rats, mice, and humans (Kedderis and Held, 1996). Simulation of inhalation exposure to 10 ppm

for 4 hours indicated significant species differences in the amount of furan absorbed. The absorbed dose of furan (mg/kg; inhaled minus exhaled divided by body weight) and the integrated exposure of the liver to the toxic metabolite were approximately 3.5-fold and 10-fold greater in rats and mice, respectively, than in humans following the same inhalation exposure. The reason for this species difference is that humans are larger and physiologically slower than mice or rats (Mordenti, 1986). The volatile toxicant furan is metered into the blood stream via the breathing rate and distributed throughout the organism at rates that are a function of body size. Thus the inhalation exposure concentration of a toxicant is clearly not an appropriate measure of the dose to the organism. In the case of furan, comparing the absorbed dose (mg/kg) or the target organ (liver) exposure to the toxic metabolite among species is more appropriate. These concepts should be applied when assessing interspecies differences to inhaled toxicants, particularly when animal data are used to estimate human health risks from chemical exposure.

Simulations with the dosimetry models showed that steady-state blood concentrations of furan were achieved by approximately 1 hour after inhalation exposure to 10 ppm and were similar among species (0.7-0.8  $\mu\text{M}$ ). Comparison of the initial rates of furan oxidation with the rate of hepatic blood flow for rats, mice, and humans indicated that the rate of furan oxidation was approximately 13- to 37-fold higher than the rate of furan delivery to the liver via blood flow (Kedderis and Held, 1996). These results indicate that the bioactivation of furan is limited by hepatic blood flow. Simulations of the liver concentration of the toxic metabolite of furan as a function of the furan exposure concentration indicated that furan bioactivation in humans was limited by hepatic blood flow through at least 300 ppm. The hepatic blood flow limitation in rodents and humans was also evident following oral bolus administration of furan through approximately 2 mg/kg (Kedderis, 1997). One important consequence of the limitation of

bioactivation by hepatic blood flow is that increases in  $V_{\max}$  due to CYP2E1 induction have little or no effect on the amount of the toxic metabolite formed in the liver. Pharmacokinetic analyses of the bioactivation of several other hazardous chemical air pollutants also indicated a hepatic blood flow limitation of bioactivation (Kedderis, 1997).

The hepatotoxicity of trichloroethylene (TCE) is mediated by acid metabolites formed by CYP2E1 oxidation (Bull, 2000), and differences in CYP2E1 expression have been hypothesized to affect susceptibility to liver injury by TCE. Therefore the contribution of variance in CYP2E1 content and activity on the risk of hepatotoxic injury among adult humans was investigated (Lipscomb et al., 2002a,b). New and existing data sets describing the microsomal protein content of human liver (Lipscomb et al., 2002c), the CYP2E1 content of human liver microsomal protein (Snawder and Lipscomb, 2000), and the *in vitro*  $V_{\max}$  for TCE oxidation by humans (Lipscomb et al., 1997) from 60 human liver samples were combined and subjected to statistical analysis. The data were log-normally distributed. Analysis by the method of moments indicated that the 5<sup>th</sup> and 95<sup>th</sup> percentiles of the distribution in human liver (TCE oxidized per minute per gram liver) differed by approximately 6-fold. These values were converted to mg TCE oxidized/hr/kg body mass and incorporated in a human PBPK model for TCE (Allen and Fisher, 1993). Simulations of 8 hour inhalation exposure to 50 ppm (the TLV) and oral exposure to 5  $\mu$ g TCE/L in 2L drinking water (the MCL) showed that the amount of TCE oxidized in the liver differed by 2% or less even though the distribution of metabolic capacity varied 6-fold. The results are presented conceptually in Figure 3-2 and shown in Table 3-1. These results indicate that differences in CYP2E1 enzyme expression among the central 90% of the adult human population account for only approximately 2% of the variance in the risk-relevant pharmacokinetic outcome for TCE-mediated liver injury (amount of TCE oxidized in the liver).

These data indicate that physiological processes such as hepatic blood flow limit the full impact of the differences in CYP2E1 activity toward TCE mediating the formation of toxic metabolites (Lipscomb et al., 2002c). Integration of *in vitro* metabolism information into PBPK models may reduce the uncertainties associated with risk contributions of variance in enzyme expression and the uncertainty factors that represent pharmacokinetic variance. The *in vitro* data must be evaluated in the context of the intact animal. A framework describing this process has been previously published (Lipscomb and Kedderis, 2002).

## REFERENCES

- Allen, B.C. and J.W. Fisher. 1993. Pharmacokinetic modeling of trichloroethylene and trichloroacetic acid in humans. *Risk Anal.* 13(1):71-86.
- Andersen, M.E., H.J. Clewell III, M.L. Gargas, F.A. Smith and R.H. Reitz. 1987. Physiologically based pharmacokinetics and the risk assessment process for methylene chloride. *Toxicol. Appl. Pharmacol.* 87:185-205.
- Arias, I.M., H. Popper, D. Schachter and D.A. Shafritz. 1982. *The Liver: Biology and Pathobiology.* Raven Press, New York, NY.
- Billings, R.E., R.E. McMahon, J. Ashmore and S.R. Wagle. 1977. The metabolism of drugs in isolated rat hepatocytes: A comparison with *in vivo* drug metabolism and drug metabolism in subcellular liver fractions. *Drug Metab. Dispos.* 5:518-526.
- Bull, R.J. 2000. Mode of action of liver tumor induction by trichloroethylene and its metabolites, trichloroacetate and dichloroacetate. *Environ. Health Perspect.* 108(Suppl 2): 241-259
- Clewell, H.J. and M.E. Andersen. 1994. Physiologically-based pharmacokinetic modeling and bioactivation of xenobiotics. *Toxicol. Ind. Health.* 10(1-2):1-24.
- Clewell, H.J., M.E. Anderson and H.A. Barton. 2002. A consistent approach for the application of pharmacokinetic modeling in cancer and noncancer risk assessment. *Environ. Health Perspect.* 110(1):85-93.
- Hollenberg, P.F. 1992. Mechanisms of cytochrome P450 and peroxidase-catalyzed xenobiotic metabolism. *FASEB J.* 6(2):686-694.
- Houston, J.B. 1994. Utility of *in vitro* drug metabolism data in predicting *in vivo* metabolic clearance. *Biochem. Pharmacol.* 47:1469-1479.

- Kedderis, G.L. 1997. Extrapolation of *in vitro* enzyme induction data to humans *in vivo*. *Chem Biol Interact.* 107:109-121.
- Kedderis, G.L. and S.D. Held. 1996. Prediction of furan pharmacokinetics from hepatocyte studies: Comparison of bioactivation and hepatic dosimetry in rats, mice, and humans. *Toxicol. Appl. Pharmacol.* 140:124-130.
- Kedderis, G.L., M.A. Carfagna, S.D. Held, R. Batra, J.E. Murphy and M.L. Gargas. 1993. Kinetic analysis of furan biotransformation by F-344 rats *in vivo* and *in vitro*. *Toxicol. Appl. Pharmacol.* 123:274-282.
- Lipscomb, J.C. and G.L. Kedderis. 2002. Incorporating human interindividual biotransformation variance in health risk assessment. *Sci. Total Environ.* 288:13-21.
- Lipscomb, J.C., C.M. Garrett and J.E. Snawder. 1997. Cytochrome P450-dependent metabolism of trichloroethylene: Interindividual differences in humans. *Toxicol. Appl. Pharmacol.* 142:311-318.
- Lipscomb, J.C., J.W. Fisher, P.D. Confer and J.Z. Byczkowski. 1998. *In vitro* to *in vivo* extrapolation for trichloroethylene metabolism in humans. *Toxicol. Appl. Pharmacol.* 152:376-387.
- Lipscomb, J.C., L.K. Teuschler, J. Swartout and G.L. Kedderis. 2002a. Incorporation of human interindividual enzyme expression and biotransformation variance into human health risk assessments. *Toxicol. Sci.* 66(Supp. 1):154-155.
- Lipscomb J.C., L.K. Teuschler, J.C. Swartout, D. Popken, T. Cox and G.L. Kedderis. 2002b. The impact of cytochrome P450 2E1-dependent metabolic variance on a risk relevant pharmacokinetic outcome in humans. *Risk Anal.* (submitted for publication)
- Lipscomb, J.C., L.K. Teuschler and J.C. Swartout. 2003. Variance of microsomal protein and cytochrome P450 2E1 and 3A forms in adult human liver. *Tox. Mech. Meth.* 13:45-51.
- Mordenti, J. 1986. Man versus beast: Pharmacokinetic scaling in mammals. *J. Pharmacol. Sci.* 75:1028-1040.
- Northrop, D.B. 1983. Fitting enzyme-kinetic data to V/K. *Analyt. Biochem.* 132:457-461.
- Perrot, N., B. Nalpas, C.S. Yang and P.H. Beaune. 1989. Modulation of cytochrome P450 isozymes in human liver by ethanol and drug intake. *Eur. J. Clin. Invest.* 19(6):549-555.
- Seglen, P.O. 1976. Preparation of isolated rat liver cells. *Meth. Cell Biol.* 13:29-83.

Shimada, T., H. Yamazaki, M. Mimura, Y. Inui and F.P. Guengerich. 1994. Interindividual variations in human liver cytochrome P450 enzymes involved in the oxidation of drugs, carcinogens and toxic chemicals: Studies with liver microsomes of 30 Japanese and 30 Caucasians. *J. Pharmacol. Expt. Ther.* 270:414-423.

Sirica, A.E. and H.C. Pitot. 1979. Drug metabolism and effects of carcinogens in cultured hepatic cells. *Pharmacol. Rev.* 31(3):205-228.

Snawder, J.E. and J.C. Lipscomb. 2000. Interindividual variance of cytochrome P450 forms in human hepatic microsomes: Correlation of individual forms with xenobiotic metabolism and implications in risk assessment. *Reg. Toxicol. Pharmacol.* 32:200-209.

Snyder, W.S., M.J. Cook, E.S. Nasset, L.R. Karhausen, G.P. Howells and I.H. Tipton. 1992. Report of the Task Group on Reference Man. Pergamon Press, New York, NY.

US EPA. 1994. Methods for Derivation of Inhalation Reference Concentrations and Application of Inhalation Dosimetry. Office of Research and Development, Washington, DC. EPA/600/8-90/066F.

Worboys, P.D., B. Brennan, A. Bradbury and J.B. Houston. 1996. Metabolite kinetics of ondansetron in rat. Comparison of hepatic microsomes, isolated hepatocytes and liver slices, with *in vivo* disposition. *Xenobiotica.* 26(9):897-907.

**NOTICE:** The views expressed in this paper are those of the individual authors and do not necessarily reflect the views and policies of the US Environmental Protection Agency (EPA).

This manuscript has been reviewed in accordance with EPA/ORD policy and approved for public release. This research was supported in part by US EPA/NCEA cooperative agreement CR828047-01-0. This paper was presented at the Spring Toxicology Conference, April 2002, Cincinnati, Ohio, and published in *Toxicology and Industrial Health*: Kedderis, G.L. and Lipscomb, J.C. 2003. Application of *in vitro* biotransformation data and pharmacokinetic modeling to risk assessment. *Toxicol. Ind. Health.* 17:315-321.

TABLE 3-1		
Variance in Human Hepatic CYP2E1-Dependent TCE Oxidative Capacity and the Amount of TCE Oxidized <sup>a</sup>		
Liver Metabolites (mg/L)		
Oxidation Rate	Inhalation <sup>b</sup>	Oral <sup>c</sup>
5 <sup>th</sup> Percentile (approx. 7 mg/hr/kg)	258.3	5.4
95 <sup>th</sup> Percentile (approx. 40 mg/hr/kg)	264.9	5.5
Magnitude of Difference	2%	2%

<sup>a</sup>Data from Lipscomb et al. (2002a,b)

<sup>b</sup>Simulations of 8 hr exposure to TCE (50 ppm) by a 70 kg male human

<sup>c</sup>Simulations of exposure to TCE in drinking water (5 µg/L; 2 L) over 24 hours by a 70 kg male human

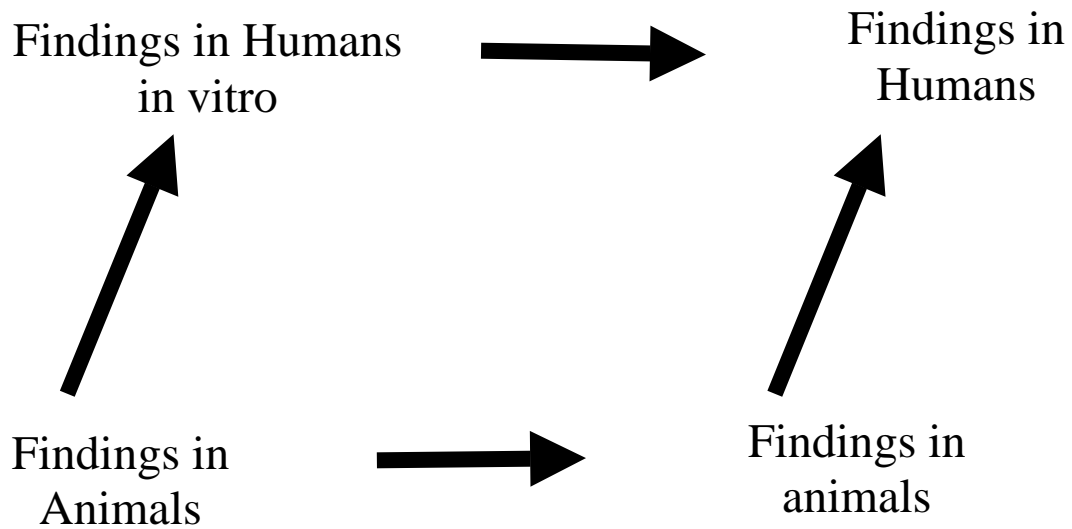


FIGURE 3-1

The *in vitro/in vivo* Parallelogram Approach. In this scheme, data are derived *in vitro* in test animal species and considerations including those imposed by anatomy and physiology are used to extrapolate those findings to the *in vivo* setting in the animal. Likewise, information on the underlying biochemistry for the event are collected from animals and humans *in vitro*, and serve as the basis upon which to modify expectations from *in vitro* studies with animal tissue preparations to predict the results obtained from studies of human tissues *in vitro*. Lessons learned from the *in vitro* to *in vivo* extrapolation within the species and lessons learned from the extrapolation of results from *in vitro* studies across species are combined to better enable the prediction of the *in vivo* consequences in the human.

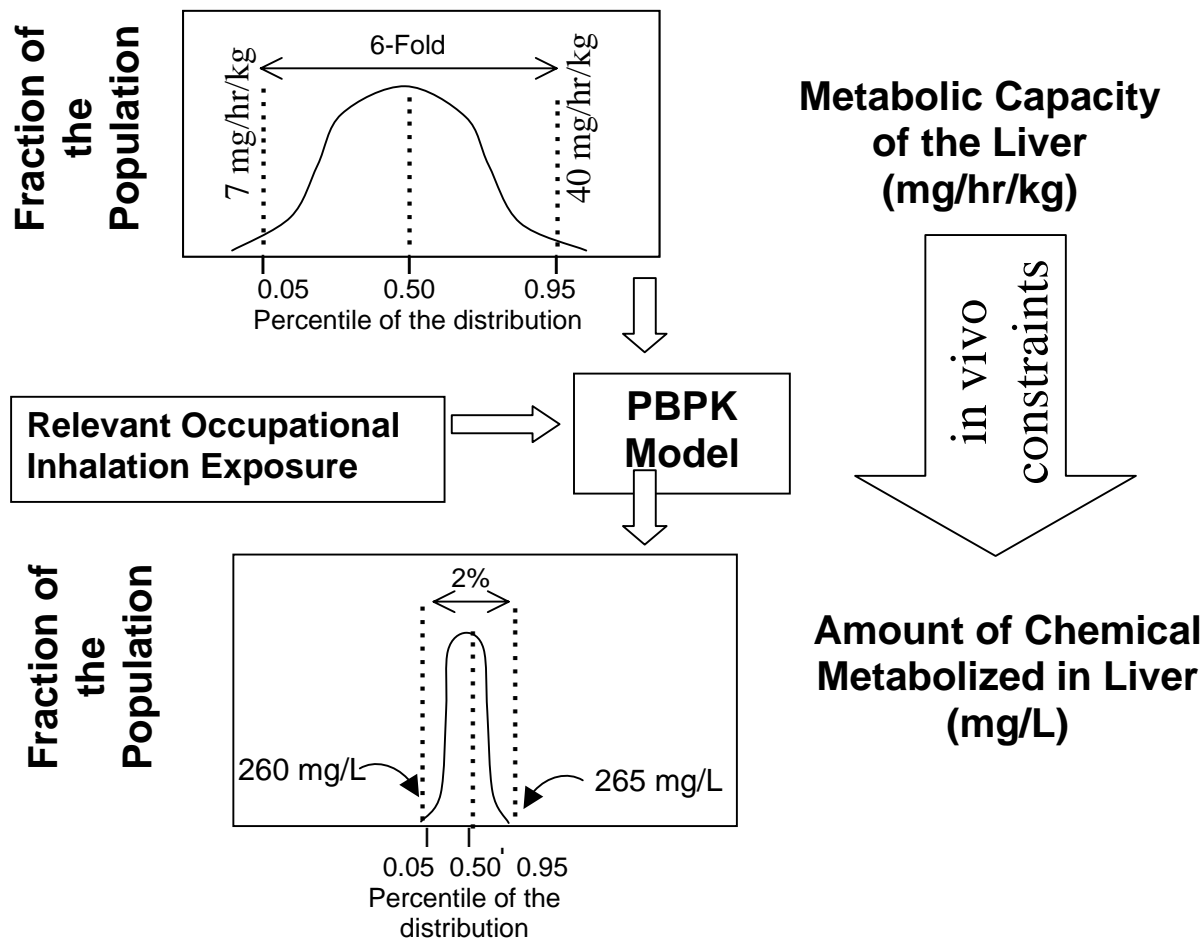


FIGURE 3-2

Use of a PBPK Model to Interpret the Risk Significance of Differences in Metabolic Capacity. This figure demonstrates, for an inhalation exposure, that measured differences of *in vitro* metabolic capacity of the liver, when extrapolated to the *in vivo* condition, do not result in marked differences in the dose-metric for TCE hepatotoxic injury: amount of TCE metabolized in liver. In this experiment, the PBPK model was refined to include  $V_{max}$  values representing those at the 5<sup>th</sup> and 95<sup>th</sup> percentiles of the lognormal distribution and was exercised to simulate the amount of TCE metabolized in the liver under an environmental and an occupational exposure. Results (Table 1) demonstrated that considerations of anatomy, physiology and biochemistry (absorption of TCE into blood, blood flow to the liver, distribution of TCE from blood to liver tissue, and the capacity of the liver to oxidize TCE) limit the variance in TCE metabolism under both inhalation and oral exposures.

#### 4. THE IMPACT OF CYTOCHROME P450 2E1-DEPENDENT METABOLIC VARIANCE ON A RISK-RELEVANT PHARMACOKINETIC OUTCOME IN HUMANS

##### ABSTRACT

Risk assessments include assumptions about sensitive subpopulations, such as the fraction of the general population that is sensitive and the extent that biochemical or physiological attributes influence sensitivity. Uncertainty factors (UF) account for both pharmacokinetic (PK) and pharmacodynamic (PD) components, allowing the inclusion of risk-relevant information to replace default assumptions about PK and PD variance (uncertainty). Large numbers of human organ donor samples and recent advances in methods to extrapolate *in vitro* enzyme expression and activity data to the intact human enable the investigation of the impact of PK variability on human susceptibility. The hepatotoxicity of trichloroethylene (TCE) is mediated by acid metabolites formed by cytochrome P450 2E1 (CYP2E1) oxidation, and differences in the CYP2E1 expression are hypothesized to affect susceptibility to TCE's liver injury. This study was designed specifically to examine the contribution of statistically quantified variance in enzyme content and activity on the risk of hepatotoxic injury among adult humans. We combined data sets describing 1) the microsomal protein content of human liver, 2) the CYP2E1 content of human liver microsomal protein, and 3) the *in vitro* V<sub>max</sub> for TCE oxidation by humans. The 5<sup>th</sup> and 95<sup>th</sup> percentiles of the resulting distribution (TCE oxidized per minute per gram liver) differed by approximately 6-fold. These values were converted to mg TCE oxidized/hr/kg body mass and incorporated in a human PBPK model. Simulations of 8 hr inhalation exposure to 50 ppm and oral exposure to 5 µg TCE/L in 2L drinking water showed that the amount of TCE oxidized in the liver differs by 2% or less under extreme values of

CYP2E1 expression and activity (here, selected as the 5<sup>th</sup> and 95<sup>th</sup> percentiles of the resulting distribution). This indicates that differences in enzyme expression and TCE oxidation among the central 90% of the adult human population account for approximately 2% of the difference in production of the risk-relevant PK outcome for TCE-mediated liver injury. Integration of *in vitro* metabolism information into physiological models may reduce the uncertainties associated with risk contributions of differences in enzyme expression and the UF that represent PK variability.

## **INTRODUCTION**

Traditional non-cancer risk assessments in the US EPA apply uncertainty factors to extrapolate the measures of effects between animals and humans, and among humans. These two factors (UFA and UFH, respectively), may be further subdivided into their respective pharmacodynamic (PD) and pharmacokinetic (PK) components (Bogdanffy and Jarabek, 1995; Jarabek, 1995; Bogdanffy et al., 1999). WHO (1998) and the International Programme on Chemical Safety (IPCS, 1994, 1998) have provided guidance and application of the separate consideration of PD and PK, and the US EPA has also separately quantified PD and PK variability in the UFA applied to reference concentration (RfC) values and reference dose (RfD) values, where each has been ascribed a value of one-half log ( $10^{0.5}$ , or 3.16) (U.S. EPA, 1999, 2000, 2001). In addition, PD and PK components of UFH for RfC values have also been separately considered for some substances such as methyl methacrylate (U.S. EPA, 1998). Studies with humans can be conducted to assess the pharmacodynamics or pharmacokinetics of environmental or occupational chemicals. While human clinical trials can assess the PK and PD of potential therapeutic substances, human studies with potentially toxic environmental or occupational chemicals are not usually conducted over concentration ranges known or predicted

to result in adverse effects. The limited information available from human studies with environmental chemicals provides critical (but often limited) information which can be extended by *in vitro* studies using preparations from human tissues. Care must be taken so that the *in vitro* investigations are focused on risk-relevant endpoints, and are conducted with the relevant tissues, tissue preparations, and chemical concentrations. It is critical that the concentrations used for *in vitro* studies are within the range of tissue concentrations observed or predicted *in vivo* in humans following chemical exposure. Studies with human subjects or human tissue preparations *in vitro* can identify variability in PK outcomes such as the blood concentrations of parent chemical and metabolites or the rates of metabolite production or elimination. When these PK outcomes overlap with the PK outcomes most linked to risk (verified by results from mode of action and PK studies with research animals), then additional information on the variability of these PK outcomes will advance our understanding of susceptibility, and provide information with which to replace default values for uncertainty in extrapolations of risk. Although data from multiple human subjects may seem preferable as the basis from which to determine human PK variability, those data seldom exist, and when they do the data usually offer little information on risk-relevant PK outcomes such as target tissue dosimetry. Physiologically based PK (PBPK) models allow the application of physiologic and anatomic constraints to clarify the linkage between external concentrations and target tissue concentrations (Figure 4-1) and offer a mechanism through which information obtained *ex vivo* or *in vitro* may be evaluated in proper context. Results from PBPK model simulations of relevant exposure scenarios provide a useful approach for estimation of PK variability between research animals and humans and among humans when other data are limiting. This technique offers the opportunity to extrapolate concentrations of bioactive chemical moieties in target tissues across doses and routes of

exposure. The inclusion of data derived *in vitro* through the exposure of human tissue preparations offers an advance over exposing humans to noxious agents, and several studies have demonstrated the applicability of *in vitro* findings in refining PBPK models.

While *in vitro* measurements of specific biochemical reactions from multiple human samples can yield qualitatively valuable data on human variance, they must be tied to human anatomy and physiology, and the impact of their variance evaluated under real exposure scenarios to be of quantitative value. This study was constructed on the framework for extrapolation of *in vitro* metabolic rate information and PBPK model incorporation previously suggested (Lipscomb and Kedderis, 2002).

Enzymes are protein molecules that catalyze chemical reactions (Lehninger, 1975). Over 100 years ago, the study of enzymes and their properties demonstrated that the rates of enzyme-catalyzed reactions are directly proportional to the total enzyme present in the system (Lehninger, 1975; Segel, 1975). This property of enzymes provides the basis for extrapolation of *in vitro* biotransformation data to whole animals and humans (Kedderis, 1997). Therefore data generated with subcellular fractions such as microsomes or cytosols can be extrapolated to *in vivo* based on protein content (Snawder and Lipscomb, 2000). Human liver is approximately 2.6% of body weight (Arias et al., 1982).

In addition to enzyme content or activity and organ weight, the kinetic mechanism of the enzyme (the comings and goings of substrates and products) needs to be taken into account to extrapolate *in vitro* data to whole animals or humans (Kedderis, 1997). The CYP2E1-catalyzed oxidation of TCE follows Michaelis-Menten saturation kinetics (Lipscomb et al., 1997):

$$v = (V_{\max} * [S]) / (K_M + [S]) \quad (4-1)$$

where  $v$  is the initial velocity of the reaction,  $V_{\max}$  is the maximal rate of the reaction at infinite substrate concentration,  $[S]$  is the substrate concentration, and  $K_M$  is the Michaelis constant for the reaction. The Michaelis-Menten Equation 4-1 indicates that the initial velocity of the reaction will increase hyperbolically as a function of substrate concentration. The  $V_{\max}$  is a horizontal tangent to the top (saturated) part of the curve, while the tangent to the initial linear portion of the hyperbolic curve is the initial rate of the reaction,  $V/K$ . The  $V/K$  is the pseudo-first-order rate constant for the reaction at low substrate concentrations. The point where these two tangents intersect corresponds to the  $K_M$  (Northrop, 1983). The  $K_M$  is defined as the substrate concentration that gives one-half the  $V_{\max}$ . The  $K_M$  for each substrate is an inherent property of the enzyme (Lehninger, 1975). A lower  $K_M$  for one substrate compared to a second substrate indicates that the first substrate has a more rapid initial rate ( $V/K$ ) of metabolism. The value of  $K_M$  can vary with the structure of the enzyme; for example, in the polymorphism of the CYP2D6-mediated oxidation of debrisoquine and related drugs (Gut et al., 1986).

Experimentally,  $K_M$  can vary with pH, temperature and ionic strength *in vitro*. Therefore *in vitro* kinetic measurements intended for extrapolation to intact animals and humans should be done under experimental conditions mirroring the *in vivo* situation as closely as possible (Kedderis, 1997).

The *in vitro* kinetic data can be incorporated into PBPK models after rearrangement of the  $V_{\max}$  to the appropriate units. Values of  $K_M$  have units of concentration and can be used directly if the solubility of the chemical in the *in vitro* system is known. Incorporation of the extrapolated kinetic parameters into a PBPK model for humans allows prediction of target tissue dosimetry following a variety of exposure scenarios.

We have adapted an existing PBPK model to predict the difference among humans in the risk-relevant PK outcome for the hepatotoxicity of trichloroethylene (TCE) under the conditions of human variance in the rates of TCE oxidation. We focused on the hepatotoxicity of TCE because: 1) the PK of TCE have been characterized and modeled in research animals and humans (reviewed in Fisher, 2000); 2) more than 95% of an absorbed dose of TCE is oxidized in research animals and humans (Bloemen et al., 2001); 3) CYP2E1 has been demonstrated to be the enzyme responsible for the oxidation of TCE in research animals and humans and *in vitro* preparations at low concentrations (Nakajima et al., 1988); 4) the hepatotoxicity of TCE has been demonstrated to depend on acid metabolite(s) derived from oxidative metabolites of TCE (Barton and Clewell, 2000; Bull, 2000); 5) the CYP2E1-mediated oxidation of TCE is rate limiting in the further formation of acid metabolite(s) (Ikeda et al., 1980); 6) the expression of CYP2E1 is modulated by genetic, environmental and lifestyle factors; and 7) large numbers of human liver tissue and human liver tissue preparations are currently available in contrast to preparations and tissues from other human organs. The results on the variance of the distribution of CYP2E1 in adult human liver will be especially applicable to other environmental contaminants which are also substrates for this enzyme.

The investigation was accomplished by first characterizing the variance about the CYP2E1 mediated oxidation of TCE among human samples *in vitro*, second by quantifying the variance of human hepatic CYP2E1 content, and third by extrapolating the bounds of variance of TCE oxidation among the adult human population to a human PBPK model. Two separate statistical analyses were conducted – one based on convenience and one based on technical accuracy. The amount of TCE metabolized (oxidized) in the liver was simulated as a dose surrogate for the hepatotoxicity of TCE. The goal of the present investigation was to quantify

the variability in a risk-relevant PK outcome for the hepatotoxicity of TCE, and to demonstrate the usefulness of advanced data on human biochemical individuality in quantifying the variability of risk-relevant PK outcomes for inclusion in risk assessments. Data on the distribution of CYP2E1 in the intact liver has not been used to estimate the degree of susceptibility to risk for metabolized chemicals. We hypothesized that the degree of natural variance in human hepatic levels of CYP2E1 would result in similar differences in the oxidation of TCE in the intact human.

## **METHODS**

Several sets of information describing or based on microsomal protein (MSP) were collected for assimilation, extrapolation and incorporation into a PBPK model. The objective of the extrapolation was to transition expression of apparent  $V_{max}$  from units of “pmoles TCE oxidized/min/mg MSP” to units of conventional PBPK modeling, mg/hr/kg body mass. Necessary data were compiled from multiple sources, and used to describe the various parameters, whose distributions were analyzed and combined. Table 4-1 demonstrates the relationship between those data sets and parameters. TCE is oxidized by CYP2E1, and that metabolic rate had been previously measured and presented in units of MSP (nmol/min/mg MSP). Thus, the need to express apparent  $V_{max}$  as pmol TCE oxidized/min/pmol CYP2E1. CYP2E1 is isolated in MSP, thus the need to quantify CYP2E1 in MSP (pmoles CYP2E1/mg MSP). Because MSP is one constituent of liver, the amount of MSP per gram liver tissue (mg MSP/gram liver) needed computing. These data facilitate the extrapolation of *in vitro* metabolic capacity (comprised of enzyme activity and enzyme content) to the intact liver. Units of the calculation cancel (pmol TCE oxidized/min/pmol CYP2E1) \* (pmol CYP2E1/mg MSP) \* (mg MSP/gram liver), leaving units of pmol TCE oxidized/min/gram liver. Correction for molecular

weight of TCE, 60 min/hr and assumptions about the fractional composition of body mass attributed to the liver compartment (liver = BW\*0.026) results in units of mg TCE oxidized/hr/kg.

**Human Samples and Quantification of CYP Proteins.** Both prepared MSP and intact liver tissue were obtained for this investigation from various sources (Human Cell Culture Center, Laurel, MD; International Institute for the Advancement of Medicine, Exton, PA; Vitron, Tucson, AZ; Tissue Transformation Technologies, Inc., Edison, NJ). All tissues and preparations were derived from adult human organ donors who were devoid of antibodies directed against infectious diseases. The MSP content of CYP2E1 and other CYP forms was previously investigated and reported for 40 donors (Snawder and Lipscomb, 2000). In the present analysis, 20 samples of intact tissue were obtained, and MSP prepared via the method of Guengerich (1989) (Figure 4-2). CYP2E1 content of aliquots of (post 100 x g) homogenate protein and MSP were determined by enzyme-linked immunosorbent assay (ELISA) following the method of Snawder and Lipscomb (2000).

**Distribution of CYP2E1 to Human Hepatic MSP.** Data on the CYP2E1 content from 40 samples of human hepatic MSP were available from Snawder and Lipscomb (2000), and data derived from an additional 20 samples of human hepatic MSP were combined to yield a total sample of 60 adult human organ donors for which data on the CYP2E1 content of MSP (CYP2<sub>MSP</sub>, parameter B, data set 1) were available (Lipscomb et al., 2003) (Table 4-2, described in the following section). Of this set of 60 samples of MSP (representing 60 organ donors), 15 were used to estimate the *in vitro* metabolic parameters for TCE and CYP2E1 content of MSP; 45 were subjected only to the determination of CYP2E1 in MSP (and 20 of that 45 were paired with liver homogenate to determine the MSP content of liver).

**Estimation of Proteins in Intact Liver.** In this analysis, twenty samples of intact liver tissue were assayed (Table 4-2). The total amount of protein (CYP and non-CYP; microsomal and cytosolic proteins) in intact liver ( $PRO_{Liv}$ ) was empirically determined based on the protein content of the post 100 x g liver supernatant, after correcting for volume according to Equation 4-2. It was assumed that no protein was lost during the sedimentation of nuclei and debris at 100 x g.

$$\begin{aligned} & (\text{mg protein/ml homogenate}) * (\text{ml homogenate/gram tissue}) \\ & = (\text{mg homogenate protein/gram tissue}) \end{aligned} \quad (4-2)$$

The content of CYP2E1 in total hepatic protein ( $CYP2_{Pro}$ ) and in MSP ( $CYP2_{MSP}$ ; parameter B) was determined so that a measure of the liver content of MSP ( $MSP_{Liv}$ ; parameter C) could be derived. The content of CYP2E1 in liver (pmoles CYP2E1/gram liver;  $CYP2_{Liv}$ ; parameter A) was derived empirically by combining two data sets ( $PRO_{Liv}$   $CYP_{PRO}$ ), described in Equation 4-3, and was estimated via the statistical method of moments (Analysis via Method of Moments section) and by computational statistics (Analysis via Computational Statistics section), below. For the 20 individual organ donors, the separate amounts of CYP2E1 per gram liver was empirically determined according to the following equation:

$$\begin{aligned} & (\text{pmol CYP2E1/mg homogenate protein}) * (\text{mg homogenate protein/gram tissue}) \\ & = (\text{pmol CYP2E1/gram tissue}) \end{aligned} \quad (4-3)$$

The amount of MSP per gram liver was estimated according to Equation 4-4. This is the data set ( $MSP_{Liv}$ ; parameter C, data set 2) which will be combined with information on the distribution of CYP2E1 to MSP ( $CYP2_{MSP}$ ; parameter B, data set 1) to determine the distribution of CYP2E1 to the intact liver ( $CYP_{Liv}$ ; parameter A).

$$\begin{aligned} & (\text{pmol CYP2E1/gram tissue}) / (\text{pmol CYP2E1/mg MSP}) \\ & = (\text{mg MSP/gram tissue}) \end{aligned} \quad (4-4)$$

**CYP2E1-Dependent Oxidation of TCE.** The Michaelis-Menten kinetic constants were available for 23 samples of MSP from Lipscomb et al. (1997). The metabolism of TCE to chloral hydrate, representing oxidation by CYP2E1, was quantified by measuring the formation of chloral hydrate. Apparent  $V_{max}$  was expressed as pmol TCE oxidized/min/mg MSP. From this set of 23 original samples, 15 remained, and CYP2E1 content of those microsomal protein samples was quantified by ELISA (Snawder and Lipscomb, 2000). We sought to develop a more technical description of  $V_{max}$  (the theoretical maximal initial rate of the reaction in the presence of unlimiting substrate concentration), and one which would be more readily extrapolable to the *in vivo* setting through incorporation of the information on the hepatic content of CYP2E1. To accomplish this, the  $V_{max}$  values (pmoles/min/mg MSP) available from the previously published study (Lipscomb et al., 1997) were divided by the CYP2E1 content of MSP (pmoles CYP2E1/mg MSP) to yield  $V_{max}$  values expressed as pmoles TCE oxidized/minute/pmol CYP2E1 (Table 4-3). This measure (parameter D) and its distribution are referred to as data set 3 and are described as  $TCE_{CYP2}$ .

**Statistical Analysis.** Tables 4-2 and 4-3 summarize the data employed in the statistical analyses. Probability distributions were fitted by the SAS<sup>®</sup> 8.0 Analyst routine to data describing the following variables (with mnemonic variable name): A = pmol CYP2E1/gram liver ( $CYP2_{Liv}$ ); B = pmol CYP2E1/mg MSP ( $CYP2_{MSP}$ ); C = mg MSP/gram liver ( $MSP_{Liv}$ ) = A/B. StatFit software was used to determine an optimal distribution fit to the 15 observations for parameter D, pmoles TCE oxidized, min/pmol CYP2E1 ( $TCE_{CYP2}$ ). The LogNormal distribution was selected with parameters  $\mu = 3.4812$  and  $\sigma = 0.4156$  for the imbedded normal distribution, implying a geometric mean and standard deviation of 32.5 and 1.515, and an arithmetic mean

and standard deviation of 35.4 and 15.4. This distribution was accepted via Chi-Squared, Kolmogorov-Smirnov, and Anderson-Darling statistical tests at the  $\alpha = 0.05$  (95%) confidence level.

Three sets of data were available: a set of  $n = 60$  samples, for which laboratory measurements were available on  $B = (CYP2_{MSP})$ , an  $n = 20$  subset of the 60 samples, for which several additional laboratory measurements were available ( $PRO_{Liv}$ ,  $CYP2_{Pro}$ ,  $CYP2_{MSP}$ ), and a set of  $n=15$  samples, for which one laboratory measurement was available ( $TCE_{CYP2}$ ). These three sets of available data were first analyzed separately. The additional variables ( $CYP2_{Liv}$ , and  $C = MSP_{Liv}$ ) were calculated from the measurement data.

For all variables, normal, lognormal, exponential and Weibull distributions were fit using standard statistical tests of goodness-of-fit (Kolmogorov-Smirnoff, Cramer-von Mises & Anderson-Darling) and a visual examination of quantile-quantile plots. The null hypothesis was that the distribution fit the data well, with a rejection of the null at  $p \leq 0.10$ . All these analyses were performed using SAS<sup>®</sup>. Each of the distributions was adequately approximated by a lognormal distribution, the parameters of which are the mean ( $\mu$ ) and standard deviation ( $s$ ) of the logarithms of the observations.

**Analysis via Method of Moments** – For convenience, ignoring the dependence between data set 2 and the  $n=20$  (matched subset) of data set 1, and because the consistency of goodness-of-fit of the data to the lognormal distributions (excluding data set 3:  $TCE_{CYP2}$ ; pmol TCE oxidized/min/pmol CYP2E1), we applied the statistical method of moments (addition of errors, Equation 4-5 to combine data sets 1-3 to estimate parameter E, pmol TCE oxidized/minute/gram liver. All goodness-of-fit p-values were greater than 0.15. As a convenience, the lognormal

parameter will be represented by the geometric mean ( $GM = e^{\mu}$ ) and geometric standard deviation ( $GSD = e^s$ ), respectively, in this paper. Equation 4-5 demonstrates the method used to estimate the distribution of Vmax values, where the distributions for parameters B (pmol CYP2E1/mg MSP), C (mg MSP/gram liver), and D (pmol TCE oxidized/min/pmol CYP2E1) are combined mathematically. The values at the 5<sup>th</sup> ( $X_{05}$ ) and 95<sup>th</sup> ( $X_{95}$ ) percentiles for the resulting distribution (parameter E, pmoles TCE oxidized/min/gram liver) were calculated by Equations 4-6 and 4-7, respectively.

$$\text{Lnorm}[\mu = \mu_1 + \mu_2 + \mu_3, s = \text{sq root}(s_1^2 + s_2^2 + s_3^2)] \quad (4-5)$$

where:

- $\mu_i$  = mean of logs of observations
- $s_i$  = standard deviation of logs of observations
- 1 = data set 1 - ( $\text{CYP2}_{\text{MSP}}$ )
- 2 = data set 2 - ( $\text{MSP}_{\text{Liv}}$ )
- 3 = data set 3 - ( $\text{TCE}_{\text{CYP2}}$ )

$$X_{05} = e^{[\mu - 1.645 * s]} \quad (4-6)$$

$$X_{95} = e^{[\mu + 1.645 * s]} \quad (4-7)$$

**Analysis via Computational Statistics** – We next sought to model the distribution of A = pmol CYP2E1/gram liver with greater precision by using all of the available data, including the correlation (Figure 4-3) on variables B = pmol CYP2E1/mg MSP and C = mg MSP/gram liver. Since  $A = B * C$ , these three variables are not statistically independent. Moreover, it is perhaps not obvious how or whether the 40 measurements of B that are *not* matched to measurements on A and C (observations 21-60 in Table 4-2) can be used to improve estimation of the distribution of A. However, we were able to synthesize and apply two techniques from computational statistics – mixture distribution modeling (Titterington et al., 1985) and

classification trees (Zhang and Singer, 1999; Breiman et al., 1984) – to use all of the B and C data, including the 40 unmatched measurements on B, to model the distribution of A.

The methodology for estimating the frequency distribution of A using all available measurements (i.e., using the joint distribution of A and B, as well as the derived variable C) was as follows.

1. The frequency distribution for A can be expressed using marginal and conditional probabilities as follows:

$$\begin{aligned}\Pr(A = a) &= \sum_{(b, c)} \Pr(A | B = b \ \& \ C = c) \Pr(B = b \ \& \ C = c) \\ &= \sum_{(b, c)} \Pr(A | B = b \ \& \ C = c) \Pr(B = b) \Pr(C = c | B = b)\end{aligned}$$

where the sum (or integral) is taken over all (b, c) pairs of values. Thus, A is interpreted as having a distribution that depends on the (perhaps unobserved) values of B and C.

2. The terms  $\Pr(A | B = b \ \& \ C = c)$ ,  $\Pr(B = b)$ , and  $\Pr(C = c | B = b)$  are estimated empirically from all of the available data using a classification tree estimator. Figure 4-4 shows the classification tree fit to the first 20 cases in Table 4-2, i.e., those with data on both A and B (and hence C). This tree provides an estimate of the distribution of A conditioned on the values of B and C. The fit was performed using the KnowledgeSeeker™ package (<http://www.angoss.com/ProdServ/indexH.html>.)

Interpretively, the distribution of A is modeled as a finite mixture distribution (Titterton et al., 1985) with a number of components to be estimated from the data. These components correspond to leaves in the classification tree in Figure 4-4. The conditional distribution of A depends on which component distribution a case belongs to. Figure 4-4 shows the sample means and standard deviations for four component distributions (leaves), estimated from the first 20 cases in Table 4-2. Using only these data, the estimated distribution of A would correspond to the following finite (4-component) mixture distribution:

Cluster 1: weight = 9/20, sample mean = 2029.23, sample standard deviation = 614.41  
Cluster 2: weight = 4/20, sample mean = 2416.88, sample standard deviation = 182.68  
Cluster 3: weight = 5/20, sample mean = 3093.62, sample standard deviation = 496.97

Cluster 4: weight = 2/20, sample mean = 4728.3, sample standard deviation = 389.9

Here, the four components are termed “clusters” since they correspond to sets of cases for which the distribution of A values is approximately the same (i.e., the classification tree algorithm is unable to find any statistically significant difference among them.)

3. This initial tree based on the first 20 (full-data) cases in Table 4-2 was refined by using the remaining 40 observations of B values in Table 4-2 (i.e., cases 21-60) to better estimate the fraction of all cases for which  $B < 53$  (the defining characteristic of Cluster 1). The pooled estimate from all 60 cases is that  $32/60 (= 0.53, 95\% \text{ CI} = 0.40 \text{ to } 0.66)$  of A values are drawn from Cluster 1. The revised cluster weights using all 60 observations on B are: 0.53 for Cluster 1; 0.17 for Cluster 2; 0.21 for Cluster 3; and 0.09 for Cluster 4. While the cluster-specific sample sizes are very small ( $n = 2$  for Cluster 4), this decomposition of the distribution of A into a weighted mixture of component distributions actually *decreases* the variance in estimates of the true mean (and other statistics) of A compared to using a single estimated distribution (Feller, 1968).

The methodology summarized in steps 1-3 can be further refined, e.g., by using resampling to establish robust boundaries for the classification tree splits, or by using a Bayesian posterior distribution for the fraction of cases belonging to different clusters. However, given the small number of cases ( $n = 20$ ) with full data, additional refinements of the tree estimator in Figure 4-4 with the cluster weights obtained from all 60 measurements for B are not expected to greatly improve the estimation of the distribution of A.

**Combination of Data Sets.** A program was developed in the MATLAB software (see Appendix A) to produce A, D and A\*D random variates in accordance with the distributions for A and D derived above. The distribution of A was taken from that determined by computational statistics. This program identified 100,000 random variates. Eight thousand of the generated A\*D values were selected at random and were subjected to a further analysis to find an optimal distributional fit (StatFit has a limit of 8000 values).

**PBPK Model.** Human metabolism of TCE was simulated using the PBPK model of Allen and Fisher (1993) and SimuSolv software (Dow Chemical Co., Midland, MI). The model structure consisted of four tissue compartments (liver, rapidly perfused tissues, slowly perfused tissues, and fat) and a gas exchange compartment (lung) connected by blood flows. All TCE biotransformation was assumed to take place in the liver and follow Michaelis-Menten kinetics. The liver was described as a well-stirred homogeneous compartment. Previous studies have demonstrated that more complex heterogeneous models of the liver, such as the parallel tube and dispersion models, were not better than the simple well-stirred model at predicting the *in vivo* clearance of 28 drugs from *in vitro* data (Houston and Carlile, 1997). The model was set to simulate two extreme exposure scenarios – 1) simulating a higher, but permitted, occupational exposure at the Threshold Limit Value (TLV) for TCE, which is 50 ppm in air for an 8-hour working day (ACGIH, 2001), and 2) simulating a low-dose environmental exposure via drinking water containing the maximally allowable concentration of TCE (5 µg/L) (U.S. EPA, 1997). With knowledge that the hepatic metabolism of TCE *in vivo* is limited by blood flow, the model was set to simulate a “worst case” scenario of an oral bolus dose, because this (rather than a slower oral ingestion rate) would be the more likely scenario to produce differences in the amount of TCE metabolized (AML). AML is presented in units of mg TCE metabolized over the course of the simulation per L of liver tissue. Simulations of AML (amount of TCE metabolized in the liver compartment) were evaluated, because the CYP2E1-dependent oxidation of TCE is a required step in the formation of the hepatotoxic metabolite, trichloroacetic acid (TCA), *in vivo*. Chloral hydrate, the oxidative metabolite of TCE, does not have a measurable half-life *in vivo* following its formation from TCE, but is immediately converted to

TCA and trichloroethanol. For these simulations, the model incorporated both extremes of the distribution of the  $V_{max}$  for TCE oxidation (5<sup>th</sup> and 95<sup>th</sup> percentiles).

## RESULTS

**Distribution of CYP2E1 to Human Hepatic MSP.** Analysis of 60 samples of MSP derived from individual adult human organ donors for the content of CYP2E1 (pmoles CYP2E1/mg MSP, parameter B, data set 1) indicated that the Lognormal distribution adequately represented the set of observations. The geometric mean and geometric standard deviations required to reconstruct the overall distribution and simulate the value for a percentile of interest are presented in Table 4-4. These values agree well with those reported by Shimada et al. (1994). Variance between the values at the 5<sup>th</sup> and the 95<sup>th</sup> percentiles of the distribution approximated 4-fold.

**Distribution of CYP2E1 to Intact Human Liver.** Three types of analytical procedures were used to determine the distribution of CYP2E1 to intact liver tissue (pmoles CYP2E1/gram liver, parameter A) derived from adult human organ donors. First, the most direct measure, but one for which only 20 observations are available, is depicted in equations 1 and 2 and involved the application of the ELISA technique to liver homogenate (post 100 x g) protein. The empirical distribution of the 20 observations indicates that the magnitude of variance between the observations representing approximately the 5<sup>th</sup> and approximately the 95<sup>th</sup> percentiles of the empirical distribution is approximately three-fold. These raw data indicate a mean value of 2643 and a standard deviation of 962 pmoles CYP2E1/gram liver.

Second, the application of the statistically-limited method of moments required the characterization of the two underlying distributions: 1) parameter B, pmoles CYP2E1/mg MSP,

data set 1, and 2) parameter C, mg MSP/gram liver, data set 2. Because the observations in these two sets of data were adequately fit by a lognormal distribution, the values for the geometric mean and geometric standard deviations for each data set (Table 4-4) were combined (Equation 4-4). The lognormal distribution of the liver content of MSP (parameter C) was characterized by a geometric mean of 52.9 mg MSP/gram liver and a geometric standard deviation of 1.476 (arithmetic mean and standard deviation of  $57 \pm 23$  mg MSP/gram liver). The MSP content of CYP2E1 (Parameter B) was determined in a sample set of 60, and demonstrated a lognormal distribution, with a geometric mean of 48.9 pmoles CYP2E1/mg MSP and a geometric standard deviation of 1.6. The arithmetic mean  $\pm$  standard deviation was  $54 \pm 23$  pmoles CYP2E1/mg MSP. When combined, the results indicated a geometric mean of 2587 pmoles CYP2E1/gram intact adult human liver, with a geometric standard deviation of 1.48. From analysis via Equations 4-5 and 4-6, these parameter values indicate values at the 5<sup>th</sup> and 95<sup>th</sup> percentile of the distribution to be 949 and 7053 pmoles CYP2E1/gram. These values are similar to those indicated by the direct measurement of CYP2E1 in homogenate protein, above. These data indicate that the central 90% of the population represented by these adult organ donors expresses a CYP2E1 content which varies 7.4-fold.

Finally, a specific probability distribution for the parameter A was developed, based upon the clusters derived in the Analysis via Computational Statistics section above. Recall that clusters of values for A were identified, into which values for parameter B (pmoles CYP2E1/mg MSP) were segregated. In this manner, the influence of parameter B, or its determinant qualities, on parameter A were characterized. A continuous probability distribution was not fit to the individual clusters due to the small number of observations within each cluster; instead, the distribution of A was assumed to be discrete and consist only of the observed values (4th

column, parameter A, of Table 4-2). Clusters were assumed to occur with proportional frequencies equal to the weights {0.53, 0.17, 0.21, 0.09} and to have counts of {9, 4, 5, 2} as described previously. Within a cluster, each value belonging to that cluster is assumed to occur with equal frequency. This approach provides probabilities of 0.53/9 (=0.0589) for values in cluster 1, 0.17/4 (=0.0425) for values in cluster 2, 0.21/5 (=0.0420) for values in cluster 3, and 0.09/2 (=0.0450) for values in cluster 4. Cluster statistics are presented in Figure 4-4. If we use  $x_i$  to represent the  $i^{\text{th}}$  value of parameter A, and  $p_i$  to represent the probability of the  $i^{\text{th}}$  value, then the mean of the resulting distribution is:

$$\sum_{i=1}^{20} p_i x_i = 2561.77 \quad (4-8)$$

while the variance of the distribution is

$$\sum_{i=1}^{20} p_i x_i^2 - \left( \sum_{i=1}^{20} p_i x_i \right)^2 = 865,563.40 \quad (4-9)$$

providing a standard deviation of 930.36.

Note that the mean of the raw data for parameter A (Table 4-2) is 2642.8 while the standard deviation (using Equation 4-9) is 937.21 (the sample standard deviation is 962). We see that accounting for the influence of parameter B has shifted our estimates of parameter A slightly downward, and has slightly decreased the standard deviation. This is a result of the individual probabilities being shifted slightly upward or downward from 0.05 in accordance with the distribution shown in empirical distribution. This distribution was used in the recombination of data describing parameter A with data describing parameter D, as discussed below.

***In vitro* Metabolic Rate Constant (Vmax).** The Vmax for the oxidation of TCE by CYP2E1 (pmoles TCE oxidized/min/pmol CYP2E1, parameter D, data set 3, Table 4-3) was evaluated in

a data set of 15 samples. The apparent  $V_{max}$  observed *in vitro* (pmoles TCE oxidized/min/mg MSP) was converted to the more specific units of pmol TCE oxidized/min/pmol CYP2E1 by dividing the observed  $V_{max}$  value by the content of CYP2E1 in the MSP (pmoles CYP2E1/mg MSP). The resulting set of 15 observations (pmol TCE oxidized/min/pmol CYP2E1) were fit optimally with the lognormal distribution; its parameters were  $\mu = 3.4812$  and  $\sigma = 0.4156$  for the imbedded normal distribution, implying a geometric mean and standard deviation of 32.5 and 1.515, and an arithmetic mean and standard deviation of 35.4 and 15.4. This distribution was accepted via Chi-Squared, Kolmogorov-Smirnov, and Anderson-Darling statistical tests at the  $\alpha = 0.05$  (95%) confidence level. The difference between values at the 5<sup>th</sup> and 95<sup>th</sup> percentiles of the distribution approximated 4-fold.

#### **Determining the Metabolic Capacity of Intact Tissue and Extrapolation of Units.**

MATLAB results of the simulations of 100,000 random variates of  $A \cdot D$  revealed a plot (not shown) suggestive of a lognormal distribution, and a normal distribution (not shown) of the logs of values of  $A \cdot D$ . StatFit analyzed 8000 of these variates, and indicated that the most likely distribution was the lognormal, with parameters  $\mu = 11.2748$  and  $\sigma = 0.5466$ . The lognormal distribution was accepted via Chi-Squared, Kolmogorov-Smirnov and Anderson-Darling statistical tests at the  $\alpha = 0.05$  (95%) confidence level. The parameters of the lognormal distribution indicate a geometric mean of 78,810 pmoles TCE oxidized/minute/gram liver, and a geometric standard deviation of 1.7274. Applying these values in Equations 4-6 and 4-7 results in 5<sup>th</sup> and 95<sup>th</sup> percentile values of 32,069 and 193,679 pmoles TCE oxidized/minute/gram liver, respectively. These values were corrected for molecular weight, time and fractional composition

of the body represented by the liver (liver weight = 2.6% body mass) to yield values of 6.6 and 39.7 mg/hr/kg at the 5<sup>th</sup> and 95<sup>th</sup> percentiles of the distribution, respectively.

**PBPK Model Predictions.** The PBPK model for TCE was used to simulate exposure of a 70 kg male human to 50 ppm TCE for 8 hours. This exposure scenario represents the maximum recommended exposure of an individual to TCE in the workplace. The extremes of expression of the CYP2E1-mediated oxidation of TCE in the liver used here (approximately 6-fold) resulted in a difference in TCE hepatic metabolism of approximately 2% (Table 4-5). For this simulation, the amount of TCE oxidized over the exposure period per volume of liver ( $\mu\text{g/L}$ ) was used as the dose metric most linked with hepatotoxic injury/risk. Simulation of the oral ingestion of TCE ( $5 \mu\text{g/L}$ ) in 2 L of drinking water using the 5<sup>th</sup> and 95<sup>th</sup> percentiles of the TCE oxidation rate gave similar results (Table 4-5). These data indicate that physiological processes limit the full impact of the differences in CYP2E1 activity toward TCE mediating the formation of toxic metabolites. Previous PK analyses of the effect of enzyme induction on the bioactivation of TCE and other volatile organic compounds indicated a hepatic blood flow limitation of the bioactivation process (Kedderis, 1997). The rate of blood flow delivery of these substances to the liver is much slower than the rate of bioactivation in the liver, limiting the impact of enzyme induction or interindividual variability. This study focused on the issue of whether enzymic variance alone could contribute substantially to susceptibility to hepatotoxic injury, and did not attempt to capture or examine the effect of other factors (e.g., differences in hepatic blood flow) on the PK of TCE.

## **DISCUSSION**

Advanced PK studies and PBPK modeling allow the development of the linkage between external dose and target tissue dosimetry. PBPK models can predict target tissue concentrations

associated with specific levels of response in animals or humans (LOAEL, NOAEL or BMD-derived level of response). Human PBPK models can examine the risk-relevant PK outcome of chemical exposure (i.e., tissue levels of bioactive metabolite) and predict the external exposure (i.e., mg/kg/day) required to produce this PK outcome at the same level observed in research animals at the corresponding level of toxicity. When adequate information is available to quantify the metabolism to or from the bioactive chemical form, the human PBPK model can be further refined to include data on enzyme (metabolic) variance in human tissues. Then the PBPK models can be exercised to examine not only animal to human differences in the risk-relevant PK outcome, but also the human interindividual variance in the expression of that PK outcome.

Biotransformation is a critical determinant of both PK and risk since metabolism is involved in the bioactivation and detoxication of xenobiotics. Genetic polymorphisms and enzyme induction due to environmental and lifestyle factors can affect the level of expression of xenobiotic metabolizing enzymes. Thus, genetic polymorphisms become critical to risk only when they alter PK outcomes. The refinement of human health risk assessments for chemicals metabolized by the liver to reflect data on human interindividual PK variability can be accomplished through 1) the characterization of enzyme expression in large banks of human liver samples, 2) the employment of appropriate techniques for the quantification and extrapolation of metabolic rates derived *in vitro*, and 3) the judicious application of PBPK modeling.

Numerous PK outcomes may be simulated by PBPK modeling; the identification of the risk-relevant PK outcome(s) from toxicity studies allows the study of their variability through adequately constructed PBPK models. When PK models are constructed to include metabolic rates (and rate constants) derived *in vitro*, several extrapolations are necessary, not the least of

which is the extrapolation of enzyme content (Figure 4-5). PBPK models include the apparent  $V_{max}$  expressed as mg/hr/kg body mass, while typical *in vitro* studies express  $V_{max}$  in terms of nmoles product formed/minute/mg microsomal protein. Accurate extrapolation requires initially that enzyme content be expressed per unit intact liver (i.e., pmoles CYP2E1/gram liver), and the extrapolation has usually included a numerical estimation of the MSP content of liver (i.e., 50 mg MSP/gram liver). The MSP content of intact liver has been measured and used to extrapolate *in vitro*-derived metabolism kinetic constants for use in PBPK modeling efforts in humans (Reitz et al., 1996; Lipscomb et al., 1998) and to infer measures of intrinsic clearance ( $Cl_{int}$ ) in traditional rat-based PK models (Carlile et al., 1997). In the previous PBPK based approach for TCE (Reitz et al., 1996), samples expressing extreme values for kinetic constants ( $K_m$  and  $V_{max}$ ) were chosen for extrapolation to a PBPK model. Those extrapolations were based on the hepatocellularity of intact liver tissue, and on microsomal protein content of liver, rather than the content of CYP2E1 of liver. The  $V_{max}$  value was not previously extrapolated on the basis of CYP2E1 content as no data existed at the time through which to quantify the distribution of the key metabolic enzyme within human liver. With respect to the distribution of the cytochromes P450 in one preparation of human liver (microsomes), several investigations (Lipscomb et al., 1997; Shimada et al., 1994; Iyer and Sinz, 1999) have revealed quantitative information about the content of these multiple enzyme forms in this preparation, but reveal no direct information on the type of distribution (i.e., lognormal) of the enzymes within MSP, their content or distribution to the intact liver *in situ*. In the present study, we developed measures of the liver content of microsomal protein, of which the CYP enzymes (and other important xenobiotic-metabolizing enzymes, i.e., glucuronyl transferases) are a constituent. This key piece of information is necessary to estimate the content of the enzyme(s) in the intact liver. By

combining the two data sets on 1) the MSP content of CYP (pmoles CYP/mg MSP), and 2) the liver content of MSP (mg MSP/gram liver), we derived the liver content of CYP (pmoles CYP/gram liver), and developed measures of that variance, employing a total number of 60 samples derived from adult human organ donors. The approach also included the determination and inclusion of the human interindividual variance in metabolic activity toward TCE derived in an additional set of 15 samples. This analysis allowed the variance of that critical enzyme kinetic parameter ( $V_{max}$ ) to be examined among humans, and expressed as pmoles TCE oxidized per minute per pmol CYP2E1. This parameter (pmol TCE oxidized/min/pmol CYP2E1) did vary among the human samples evaluated, not surprisingly. This may be explained, in part, by potential underlying genetic differences impacting CYP2E1 activity, differences in the presence of other CYP forms which also metabolize TCE at higher concentrations and human to human interindividual differences in the lipid composition (both qualitative and quantitative) of isolated MSP preparations. The activity of isolated enzymes represents the functional status of their respective donors. The stability of these enzymes upon isolation and storage seems not to be a major contributor to this variance. The level of detail in this expression of  $V_{max}$  allowed for a direct combination with information on the variance of CYP2E1 in intact human liver, which enabled the resulting PBPK analysis of the impact of that variance on the risk-relevant pharmacokinetic (PK) outcome, amount of TCE metabolized in the liver, among adult humans. Together, these data sets separately describing enzyme activity and enzyme content combine to describe the metabolic capacity of the liver. The resulting combined distribution for the  $V_{max}$  value demonstrated that this parameter (mg/hr/kg) differed more than 6-fold between the values at the 5<sup>th</sup> and 95<sup>th</sup> percentiles of the distribution. When these values were separately integrated into the PBPK model, resulting estimates of the amount of TCE

oxidized over the exposure period differed by only 2%. Thus, widely divergent values for apparent  $V_{max}$ , resulting from both variance in enzyme content and activity, had little effect on the *in vivo* metabolism of TCE, and will have little effect on the hepatotoxic injury following TCE exposure in humans.

The present work demonstrates a significant advantage over earlier studies in that statistically valid and robust measures of enzyme content and enzyme activity have been developed and incorporated into the PBPK-based approach. This advance allows the application of the approach to estimate population distributions of risk, when chemical dose-response parameters (e.g., slope factors) are available. With the availability of large banks of well-characterized subcellular fractions (mainly hepatic MSP) derived from the livers of human organ donors comes the opportunity to determine several measures of human biochemical individuality, which will be applicable to many environmental, occupational and therapeutic compounds. Although several investigations have failed to identify a consistent inverse relationship between post mortem cold-clamp time (the time interval between the perfusion, removal and refrigeration of liver tissue; and the freezing of the tissue or microsomal protein isolation) and microsomal enzyme activity, the assumption that the activity of these enzymes *in vitro* represents their activity *in vivo* must be recognized as such. From these samples, we can measure interindividual differences in enzyme activity and differences in enzyme content in isolated MSP. The *in vitro* metabolism of several CYP2E1 substrates, such as furan (Kedderis et al., 1993; Kedderis and Held, 1996), perchloroethylene (Reitz et al., 1996), and trichloroethylene (Lipscomb et al., 1998) have been successfully extrapolated to the *in vivo* setting through application of adequately developed and validated PBPK models. The additional validation of the extrapolation procedure for metabolic activity based on enzyme recovery data is important.

This demonstrates the applicability of the methodology to determine the interindividual differences of risk-relevant PK outcomes (i.e., the amount of metabolite formed in the liver for a bioactivated hepatotoxicant) for xenobiotics to which humans cannot be safely exposed for the generation of experimental data. It is anticipated that toxicological data can be generated in test species *in vivo* and *in vitro* to determine the metabolic species responsible for toxicity, the PK of the xenobiotic and metabolite(s), and the identity of the enzyme responsible for metabolism. With this information, an adequate test animal-based PBPK model can be extrapolated to humans, using human tissue partition coefficients and the appropriate physiological parameters. Data on human enzyme recovery could be used to develop appropriate bounds on the distribution of metabolic activity for evaluation with the PBPK model to represent predefined proportions of the population.

The successful application of this approach requires the avoidance of several pitfalls. It requires the following:

1. The metabolic process under investigation must be as directly linked to the risk-relevant PK outcome as possible. The correct identification of the critical toxic effect, against which protection is warranted, or toward which susceptibility requires evaluation. In the absence of a defined link between this effect and its most closely related and measurable or predictable PK outcome (e.g., AML), then further effort will not advance the goals of the approach.
2. The tissues/preparations included in the experiments must be viable. The reliance on human tissues of research grade can be troublesome; the comparison of *in vitro*-derived metabolic rates and rate constants, especially in humans, requires some justification that these *ex vivo* or *in vitro* systems maintain the metabolic capacity they possess *in vivo*. The isolated hepatocyte model is more closely related to the *in vivo* situation than the isolated microsomal protein preparation, but metabolic rates from both systems require extrapolation based on recovery information, to the *in vivo* situation. Reliance upon data derived from compromised *in vitro* systems can lead to under predictions of *in vivo* metabolism. The inclusion of data from compromised systems (i.e., lengthy 37° incubations of microsomal protein, the application of immortalized cell lines, etc.) must be avoided. The evaluation of metabolic activity toward recognized marker substrates and assessment of cellular viability provide some evidence of *in vitro* system stability.

3. There must be sufficient data to enable extrapolation based on protein recovery. Lack of data or uncertainty in the available data quantifying the relationship between the *in vitro* system and the *in vivo* situation greatly complicate the extrapolation procedure. Values for hepatocellularity in rats and humans, and values for microsomal protein content of rats and humans are available for use in extrapolation procedures.
4. The derivation of metabolic rate constants must be accomplished under valid experimental conditions. Rate constants must be derived under conditions where rate is proportionate to an increase in protein content, over time and with increasing substrate concentrations (for first-order reactions). The value of such data is enhanced when rate constants are tied specifically to the enzyme, rather than the subcellular fraction (e.g. pmoles/min/pmol CYP2E1 vs pmoles/min/mg MSP).
5. Data should be used to identify the pertinent enzyme; the presence of more than one enzyme complicates enzyme kinetic evaluations. Additional uncertainty is encountered in the metabolic evaluation of substrates, toward which multiple enzymes are active. Given the human interindividual variability on enzyme expression as a result of genetic, dietary and lifestyle choices, different ratios of two potentially active enzymes may be observed. In this instance, the approach to *in vitro* enzyme kinetic investigations must be robust enough to separately identify the kinetic constants applicable to each of the enzymes. Kinetic constants derived for the preparation, without regard to the pertinent enzymes can falsely indicate that the apparent  $V_{max}$  value is shifted upward due to the contribution of a low affinity form, when *in vivo* substrate concentrations would not be sufficient to drive an appreciable contribution of this enzyme to the reaction.
6. This approach relies on the availability of a “validated” PBPK model. While generalization of model structure and physiological components across chemicals is often the case, the models must include parameters demonstrated or judged to be chemical-specific. In addition to metabolic rate constants, tissue partition coefficients (PC) are highly chemical-specific, and differ for the same tissue type among species. The application of PC values derived in other species or adapted from PC values of related chemicals requires justification.
7. Finally, the approach is aimed specifically at quantifying human interindividual differences in metabolic capacity. This approach is specifically not aimed at quantifying human interindividual PK difference for TCE oxidation; it was developed to test the hypothesis that variability in metabolic capacity alters susceptibility to hepatotoxic injury from TCE exposure. The approach, here, demonstrates the applicability of the statistical bounds established for the population under investigation. In that regard, the application of a representative sample set is required. The data must support the identification of distribution type and include enough observations so that confidence can be placed in the identification of values at predetermined points of the distribution. While these are some of the general pitfalls, investigators trained in the disciplines of the individual investigatory steps will be quite familiar with many of the more technical pitfalls.

To members of the risk assessment community who are advocating the development of approaches which provide more information than just “safe exposure limits” (e.g., RfC and RfD values), the present approach may be useful. The approach is centered on the identification of the risk-relevant PK outcome through evaluation of toxicity and PK investigations, not necessarily through PBPK investigations. Under optimal conditions, the linking of PBPK modeling approaches with data describing human biochemical individuality (enzyme content and enzyme activity) will allow the quantification of the PK component of UFH. The collection of advanced measures of human biochemical individuality (e.g., differences in the liver’s content of critical xenobiotic metabolizing enzymes) will broaden the applicability of this approach to other chemicals whose PK are modulated by the same enzyme. It is conceivable that when this parameter (enzyme content and activity) modulates the production of the risk-relevant PK outcome, information about the population distribution of the parameter (i.e., hepatic content of CYP2E1) will lead to applications demonstrating the fraction of the population which will be protected by regulations which specify a given level of chemical exposure. Similarly, with carcinogenicity slope factors, risk-relevant PK outcomes can be converted directly to measures of risk, indicating the level of risk corresponding to a given level of enzyme content and activity. By converting exposure to tissue dose, and having information to link tissue dose to risk, the PBPK modeling approach may be usefully employed to develop distributions of risk, rather than simply assessing or demonstrating the health protective nature of a given exposure.

The purpose of the present study was to explore the potential advantage of including additional, specific, information on human biochemical individuality as a process to refine the human health risk assessment process. Because an ever-increasing amount of data is being developed through the analysis of tissues derived not only from surgical resections, but also from

human organ donors, these sources of tissues offer a unique potential to increase our knowledge about human biochemical individuality.

## **SUMMARY AND CONCLUSIONS**

Human interindividual PK variability is important both for chemicals with adequate human PK data and for those chemicals to which humans cannot be experimentally exposed. Because CYP2E1 activity limits (*in vitro*) the production of oxidative, hepatotoxic metabolites of TCE, we evaluated the distribution of that enzyme in liver from up to 75 adult human organ donors by applying published and accepted biochemical and statistical methods. The extrapolation of *in vitro* data captured both the variance in enzyme content and enzyme activity among adult humans.

CYP2E1 content and metabolic activity toward TCE are described by lognormal distributions. The central 90% of the human population represented by these adult organ donors differs by less than 4-fold in the hepatic content of this critical xenobiotic metabolizing enzyme; that same fraction of the population differed by approximately 6-fold with respect to the oxidation of TCE. The finding and additional information to be gained from the now-characterized distribution of CYP2E1 to intact human liver will be useful not only to the assessment of risk from TCE exposure, but also to the assessment of risks from other environmental chemicals that are also metabolized by this enzyme including chloroform, carbon tetrachloride, benzene, toluene, and styrene. Because the metabolism of TCE is limited by blood flow to the liver, divergent values of  $V_{max}$  do not result in appreciable differences in the risk-relevant PK outcome, the amount of TCE metabolized in the liver. Therefore, factors which increase the hepatic expression of CYP2E1 and/or its metabolic activity will not always result in

proportionate changes in key PK outcomes. This is because of the relatively low solubility of TCE in blood, and the relatively high capacity of the liver to metabolize TCE (due to a relatively high level of expression of the enzyme and the relatively high metabolic activity of the enzyme toward TCE), the limiting factor, *in vivo*, for TCE oxidation becomes the rate at which TCE is delivered to liver tissue by hepatic blood flow. In this situation, increases in TCE metabolic capacity, even from the 5<sup>th</sup> to the 95<sup>th</sup> percentiles of the distribution, result in only a 2% increase in the amount of TCE metabolized. With respect to the hepatotoxicity of TCE resulting from exposure scenarios similar to those employed in this analysis, these data indicate that the amount of PK variability attributed to enzymic variance among humans is approximately 2%. The approach described here is especially applicable to chemicals to which humans cannot be experimentally exposed for ethical reasons. The application of actual, not hypothesized, bounds of variance and the definition of the distribution of enzyme content and activity among humans can allow the calculation of finite levels of risk (when dependent on the PK outcome) at different chosen percentiles of the distribution of enzyme content and activity.

Several conditions must first be met for this strategy to be successful:

- The target organ, mode or mechanism of action, and metabolic species responsible for toxicity must be known.
- The target tissue-toxic chemical species dose response relationship must be known.
- The biotransforming enzyme must be known and information on the variance and type of its distribution among humans must be known.
- The kinetic mechanism of metabolism must be known and expressed per unit of enzyme.
- An adequately characterized PBPK model must be available for adaptation.

We have quantified the extent of variance in enzyme content of a critical xenobiotic metabolizing enzyme, CYP2E1, and the variance in the hepatic biotransformation of a key environmental contaminant, trichloroethylene. The parameters of the resulting lognormal distributions can be used to identify the bounds of biochemical and pharmacokinetic variance (e.g., 90% of the population), within which susceptibility can be determined and allows the replacement of hypothesized magnitudes of difference with actual measurement of such when determining the impact of enzyme variance on risk.

This manuscript identifies the conditions and types of data required, communicates and applies a logical approach, and describes the limitations of the approach in estimating the human interindividual variance of risk-relevant PK outcomes which may signify susceptibility to chemical injury. While data set 3 is unique to TCE, data set 2 will be useful in estimating the hepatic content of all enzymes contained in the microsomal fraction, when their distribution characteristics are known, and the information derived from the combination of data sets 1 and 2 are directly applicable to other environmental contaminants that are also substrates for CYP2E1.

## **REFERENCES**

- ACGIH (American Conference of Governmental Industrial Hygienists). 2001. Threshold Limit Values for Chemical Substances and Physical Agents and Biological Exposure Indices. Cincinnati, OH.
- Allen, B.C. and J.W. Fisher. 1993. Pharmacokinetic modeling of trichloroethylene and trichloroacetic acid in humans. *Risk Anal.* 13:71-86.
- Arias, I.M., H. Popper, D. Schachter and D.A. Shafritz. 1982. *The Liver: Biology and Pathobiology*. Raven Press, New York, NY.
- Barton, H.A. and H.J. Clewell, III. 2000. Evaluating the noncancer effects of trichloroethylene: Dosimetry, mode of action, and risk assessment. *Environ. Health Perspect.* 108(Supp. 2): 323-334.

- Bloemen, L.J., A.C. Monster, S. Kezic et al. 2001. Study on the cytochrome P-450- and glutathione-dependent biotransformation of trichloroethylene in humans. *Int. Arch. Occup. Environ. Health.* 74:102-108.
- Bogdanffy, M.S. and A.M Jarabek. 1995. Understanding mechanisms of inhaled toxicants: Implications for replacing default factors with chemical-specific data. *Toxicol. Lett.* 82-83:919-932.
- Bogdanffy, M.S., R. Sarangapani, D.R. Plowchalk, A.M. Jarabek and M.E. Andersen. 1999. A biologically-based risk assessment for vinyl acetate-induced cancer and noncancer inhalation toxicity. *Toxicol. Sci.* 51:19-35.
- Breiman L., J. Friedman, R. Olshen and C. Stone. 1984. *Classification and Regression Trees.* Wadsworth Publishing.
- Bull, R.J. 2000. Mode of action of liver tumor induction by trichloroethylene and its metabolites, trichloroacetate and dichloroacetate. *Environ. Health Perspect.* 108(Supp. 2):241-259.
- Carlile, D.J., K. Zomorodi and J.B. Houston. 1997. Scaling factors to relate drug metabolic clearance in hepatic microsomes, isolated hepatocytes, and the intact liver: Studies with induced livers involving diazepam. *Drug Metab. Dispos.* 25:903-911.
- Feller W. 1968. *An Introduction to Probability Theory and Its Applications, Vol. 1, 3rd ed.* Wiley, New York, NY. p. 231.
- Fisher, J.W. 2000. Physiologically based pharmacokinetic models for trichloroethylene and its oxidative metabolites. *Environ. Health Perspect.* 108, Supp. 2:265-273.
- Guengerich, F.P. 1989. Analysis and characterization of enzymes. In: *Principles and Methods of Toxicology*, A.W. Hayes, Ed. Raven Press, New York, NY. p. 777-814.
- Gut, J., T. Catin, P. Dayer, T. Kronbach, U. Zanger and U.A. Meyer. 1986. Debrisoquine/sparteine-type polymorphism of drug oxidation: Purification and characterization of two functionally different human liver cytochrome P-450 isozymes involved in impaired hydroxylation of the prototype substrate bufuralol. *J. Biol. Chem.* 261:11734-11743.
- Houston, J.B. and D.J. Carlile. 1997. Prediction of hepatic clearance from microsomes, hepatocytes, and liver slices. *Drug Metab. Rev.* 29:891-922.
- Ikeda, M., Y. Miyake, M. Ogata and S. Ohmori. 1980. Metabolism of trichloroethylene. *Biochem. Pharmacol.* 29:2983-2992.

IPCS (International Programme on Chemical Safety). 1994. Environmental Health Criteria 170. Assessing human health risks of chemicals: Derivation of guidance values for health-based exposure limits. World Health Organization, Geneva.

IPCS (International Programme on Chemical Safety). 1998. Environmental Health Criteria 204: Boron. World Health Organization, International Programme on Chemical Safety, Geneva, Switzerland. ISBN 92 4 157204 3.

Iyer, K.R. and M.W. Sinz. 1999. Characterization of phase I and phase II hepatic drug metabolism activities in a panel of human liver preparations. *Chem. Biol. Interact.* 118:151-169.

Jarabek, A.M. 1995. Interspecies extrapolation based on mechanistic determinants of chemical disposition. *Human Ecol. Risk Assess.* 1:641-662.

Kedderis, G.L. 1997. Extrapolation of *in vitro* enzyme induction data to humans *in vivo*. *Chem. Biol. Interact.* 107:109-121.

Kedderis, G.L. and S.D. Held. 1996. Prediction of furan pharmacokinetics from hepatocyte studies: Comparison of bioactivation and hepatic dosimetry in rats, mice, and humans. *Toxicol. Appl. Pharmacol.* 140:124-130.

Kedderis, G.L., M.A. Carfagna, S.D. Held, R. Batra, J.E. Murphy and M.L. Gargas. 1993. Kinetic analysis of furan biotransformation by F-344 rats *in vivo* and *in vitro*. *Toxicol. Appl. Pharmacol.* 123:274-282.

Lehninger, A.L. 1975. *Biochemistry*, 2nd ed. Worth, New York, NY. p. 183-216.

Lipscomb, J.C. and G.L. Kedderis. 2002. Incorporating human interindividual biotransformation variance in health risk assessment. *Sci. Total Environ.* 288:13-21.

Lipscomb, J.C., C.M. Garrett and J.E. Snawder. 1997. Cytochrome P450-dependent metabolism of trichloroethylene: Interindividual differences in humans. *Toxicol. Appl. Pharmacol.* 142:311-318.

Lipscomb, J.C., J.W. Fisher, P.D. Confer and J.Z. Byczkowski. 1998. *In vitro* to *in vivo* extrapolation for trichloroethylene metabolism in humans. *Toxicol. Appl. Pharmacol.* 152:376-387.

Lipscomb, J.C., L.K. Teuschler, J.C. Swartout, C.A.F. Striley and J.E. Snawder. 2003. Variance of microsomal protein and cytochrome P450 2E1 and 3A forms in adult human liver. *Toxicol. Mech. Meth.* 13:45-51.

- Nakajima, T., T. Okino, S. Okuyama, T. Kaneko, I. Yonekura and A. Sato. 1988. Ethanol-induced enhancement of trichloroethylene metabolism and hepatotoxicity: Difference from the effect of phenobarbital. *Toxicol. Appl. Pharmacol.* 94:227-237.
- Northrop, D.B. 1983. Fitting enzyme-kinetic data to V/K. *Analyt. Biochem.* 132:457-461.
- Reitz, R.H., M.L. Gargas, A.L. Mendrala and A.M. Schumann. 1996. *In vivo* and *in vitro* studies of perchloroethylene metabolism for physiologically based pharmacokinetic modeling in rats, mice and humans. *Toxicol. Appl. Pharmacol.* 136:289-306.
- Segel, I.H. 1975. *Enzyme Kinetics*. Wiley, New York, NY. p. 1-17.
- Shimada, T., H. Yamazaki, M. Mimura, Y. Inui and F.P. Guengerich. 1994. Interindividual variations in human liver cytochrome P450 enzymes involved in the oxidation of drugs, carcinogens and toxic chemicals: Studies with liver microsomes of 30 Japanese and 30 Caucasians. *J. Pharmacol. Expt. Ther.* 270:414-423.
- Snawder, J.E. and J.C. Lipscomb. 2000. Interindividual variance of cytochrome P450 forms in human hepatic microsomes: Correlation of individual forms with xenobiotic metabolism and implications in risk assessment. *Regul. Toxicol. Pharmacol.* 32:200-209.
- Titterton D.M., A.F.M. Smith and U.E. Makov. 1985. *Statistical Analysis of Finite Mixture Distributions*. Wiley, New York, NY.
- U.S. EPA. 1987. National Primary Drinking Water Regulations; Synthetic Organic Chemicals; Monitoring for Unregulated Contaminants. *Federal Register*. 52(130):25690.
- U.S. EPA. 1998. Toxicological Review of Methyl Methacrylate (80-62-6) in Support of Summary Information on the Integrated Risk Information System (IRIS). National Center for Environmental Assessment, Washington, DC. Available online at <http://www.epa.gov/iris>.
- U.S. EPA. 1999. Toxicological Review of Ethylene Glycol Monobutyl Ether (111-76-2) in Support of Summary Information on the Integrated Risk Information System (IRIS). National Center for Environmental Assessment, Washington, DC. Available online at <http://www.epa.gov/iris>.
- U.S. EPA. 2000. Toxicological Review of 1,3-Dichloropropene (542-75-6) in Support of Summary Information on the Integrated Risk Information System (IRIS). National Center for Environmental Assessment, Washington, DC. Available online at <http://www.epa.gov/iris>.
- U.S. EPA. 2001. Toxicological Review of Hexachlorocyclopentadiene (77-47-4) in Support of Summary Information on the Integrated Risk Information System (IRIS). National Center for Environmental Assessment, Washington, DC. Available online at <http://www.epa.gov/iris>.

WHO (World Health Organization). 1998. Guidelines for Drinking Water Quality, Geneva, Switzerland, 2nd ed., Addendum to Volume 2, Health Criteria and Other Supporting Information. Geneva, Switzerland. p. 15-30. ISBN 92 4 1545143.

Zhang H. and B. Singer. 1999. Recursive Partitioning in the Health Sciences. Springer, New York, NY.

**NOTICE:** The views expressed in this paper (NCEA-C-0956) are those of the individual authors and do not necessarily reflect the views and policies of the US Environmental Protection Agency (EPA). This research was supported by an interagency agreement between US EPA/NCEA and CDC/NIOSH (No. DW75851501; John C. Lipscomb, Project Officer) and through a cooperative agreement between US EPA/NCEA and Dr Gregory Kedderis (No. CR828047-01-0, John C. Lipscomb, Project Officer). The authors wish to express their gratitude to Glenn Suter and Bob Bruce (EPA, NCEA, Cincinnati) and Ulrike Bernauer (BgVV, Berlin, Germany) for insightful comments during preparation of the manuscript. Preliminary results from this investigation were presented at the annual meeting of the Society for Risk Analysis, December 2000, Arlington, VA and December 2001, Seattle, WA; at the annual meeting of the Society of Toxicology, March 2001, San Francisco, CA and March 2002, Nashville, TN; and at the Spring Toxicology Conference April 2001, Wright-Patterson Air Force Base, OH. We are sincerely grateful to organ donors and their families; these and other studies would not be possible without their generous contributions. This paper has been published in Risk Analysis:

Lipscomb, J.C., L.K. Teuschler, J. Swartout, D. Popken, T. Cox, and G.L. Kedderis. 2003. The Impact of Cytochrome P450 2E1-dependent Metabolic Variance on a Risk Relevant Pharmacokinetic Outcome in Humans. Risk Anal. 23:1221-1238.

TABLE 4-1

## Identification of Data Sets and Parameters for Statistical Evaluation

Information	Data set	Units	Parameter	Notes
CYP2E1 content of intact liver		pmol CYP2E1/gram liver	A	Directly measured via ELISA (n=20); and separately predicted statistically
CYP2E1 content of MSP	Data Set 1 (n=60)	pmol CYP2E1/mg MSP	B	Directly measured via ELISA
MSP content of intact liver	Data Set 2 (n=20)	mg MSP/gram liver	C	Derived: $C = A/B$
TCE metabolized per unit CYP2E1	Data Set 3 (n=15)	pmol TCE/min/ pmol CYP2E1	D	Original measurements from (11) corrected by CYP2E1 content from (18)
TCE metabolized per unit of intact liver		pmol TCE oxidized/minute/gram liver	E	Statistically estimated: $E = B * C * D$ ; extrapolated to $V_{max_c}$

TABLE 4-2

## Liver Enzyme Data\*

SAMPLE	mg homog. protein per gram liver	CYP2E1 per mg Homog. Protein	Parameter A = pmol CYP2E1 per gram liver	Parameter B = pmol CYP2E1 per mg MSP	Parameter C= mg MSP per gram liver = A/B
1	134	16.1	2157.4	85.5	25.2
2	101	25.6	2585.6	99.8	25.9
3	137	17.9	2452.3	83.4	29.4
4	100	15.2	1520.0	23.0	66.1
5	113	10.9	1231.7	34.0	36.2
6	151	12.2	1842.2	36.3	50.7
7	154	25.0	3850.0	76.8	50.1
8	148	12.4	1835.2	46.0	39.9
9	115	21.5	2472.5	69.0	35.8
10	137	20.9	2863.3	58.5	48.9
11	181	24.6	4452.6	54.0	82.5
12	180	27.8	5004.0	64.0	78.2
13	126	21.4	2696.4	68.0	39.7
14	124	21.9	2715.6	53.0	51.2
15	122	22.3	2720.6	46.0	59.1
16	137	24.4	3342.8	66.0	50.6
17	152	16.3	2477.6	41.0	60.4
18	130	24.1	3133.0	24.0	130.5
19	69	25.2	1738.8	42.0	41.4
20	126	14.0	1764.0	41.0	43.0
21				52.5	
22				94.0	
23				46.5	
24				90.0	
25				11.0	
26				64.0	
27				41.0	
28				64.0	
29				30.0	
30				57.5	
31				53.5	
32				55.0	
33				52.0	
34				29.0	
35				39.0	
36				39.0	
37				73.0	
38				70.0	
39				130.0	
40				34.0	
41				31.0	
42				48.0	
43				29.5	
44				19.0	
45				77.0	
46				91.0	
47				37.0	
48				74.0	

TABLE 4-2 cont.

SAMPLE	mg homog. protein per gram liver	CYP2E1 per mg Homog. Protein	Parameter A = pmol CYP2E1 per gram liver	Parameter B = pmol CYP2E1 per mg MSP	Parameter C= mg MSP per gram liver = A/B
49				44.0	
50				50.0	
51				75.0	
52				29.5	
53				69.0	
54				91.0	
55				48.0	
56				36.0	
57				41.0	
58				26.0	
59				26.0	
60				53.0	

\*Source: Lipscomb et al., 2003

TABLE 4-3

CYP2E1 Content and TCE Metabolic Activity Used to  
Produce Data Set 3, Describing Parameter D

SAMPLE	Sample number (from 17)	pmol TCE oxidized/ min/mg MSP (from 17)	pmol CYP2E1/ mg MSP (from 15)*	pmol TCE oxidized/ min/pmol CYP2E1 (Parameter D)
61	HHM 67	1113	11	101.2
62	HHM 84	1724	64	26.9
63	HHM 86	1039	44	23.6
64	HHM 88	1432	50	28.6
65	HHM 55	1422	52.5	27.1
66	HHM 60	1746	91	19.2
67	HHM 77	943	19	49.6
68	HHM 78	1627	77	21.1
69	HHM 81	1416	37	38.3
70	HHM 82	2353	74	31.8
71	HHM 89	890	30	29.7
72	HHM 144	1584	30	53.7
73	HHM 58	2078	94	22.1
74	HHM 61	2623	90	29.1
75	HHM 79	3455	91	38.0
Geometric Mean				32.5
Geometric Standard Deviation				1.538

\*Data not used in estimation of parameter B.

TABLE 4-4

Distributions of TCE Metabolism Rate Constant, Microsomal Protein  
and CYP2E1 Content of Adult Human Liver

Parameter	A	B	C	D	E
Description	CYP2 <sub>Liv</sub> <sup>a</sup> (derived)	CYP2 <sub>MSP</sub> <sup>b</sup> (data set 1)	MSP <sub>Liv</sub> <sup>c</sup> (data set 2)	TCE <sub>CYP2</sub> <sup>d</sup> (data set 3)	TCE <sub>Liv</sub> <sup>e</sup> (derived)
Distribution	Discrete	Log Normal	Log Normal	Log Normal	Log Normal
GM	2562	48.9	52.9	32.5	78,810
GSD	930	1.6	1.476	1.515	1.7274
Range	1232 - 5004	11 - 130	27 - 108	19.2 - 101.2	--
5 <sup>th</sup> Percentile	1232	22.5	27.9	16.4	32,069
95 <sup>th</sup> Percentile	4453	106	100	64.4	193,679

<sup>a</sup>pmoles CYP2E1/gram liver; data are presented as the arithmetic mean, arithmetic standard deviation and values at the 5.89<sup>th</sup> and 95.5<sup>th</sup> percentiles, n=20.

<sup>b</sup>pmoles CYP2E1/mg MSP, n = 60.

<sup>c</sup>mg MSP/gram liver, n = 20.

<sup>d</sup>V<sub>max</sub> of CYP2E1 in human liver MSP toward TCE, pmoles/min/pmol CYP2E1, n = 15

<sup>e</sup>V<sub>max</sub> as pmoles TCE oxidized/min/gram liver, derived via computational statistics

TABLE 4-5

Effect of Human Hepatic CYP2E1 Activity Distribution on the Bioactivation of TCE  
Following an Inhalation and an Oral Exposure

Oxidation Rate	Liver Metabolites (ug/L)	
	Inhalation <sup>a</sup>	Oral <sup>b</sup>
5 <sup>th</sup> Percentile (6.6 mg/hr/kg)	258.3	5.4
95 <sup>th</sup> Percentile (39.7 mg/hr/kg)	264.9	5.5
Difference	2%	2%

<sup>a</sup>Simulations of 8 hr exposure to TCE (50 ppm) by a 70 kg male human as described under Methods.

<sup>b</sup>Simulations of exposure to TCE in drinking water (5 µg/L; 2 L) over 24 hr by a 70 kg male human as described under Methods.

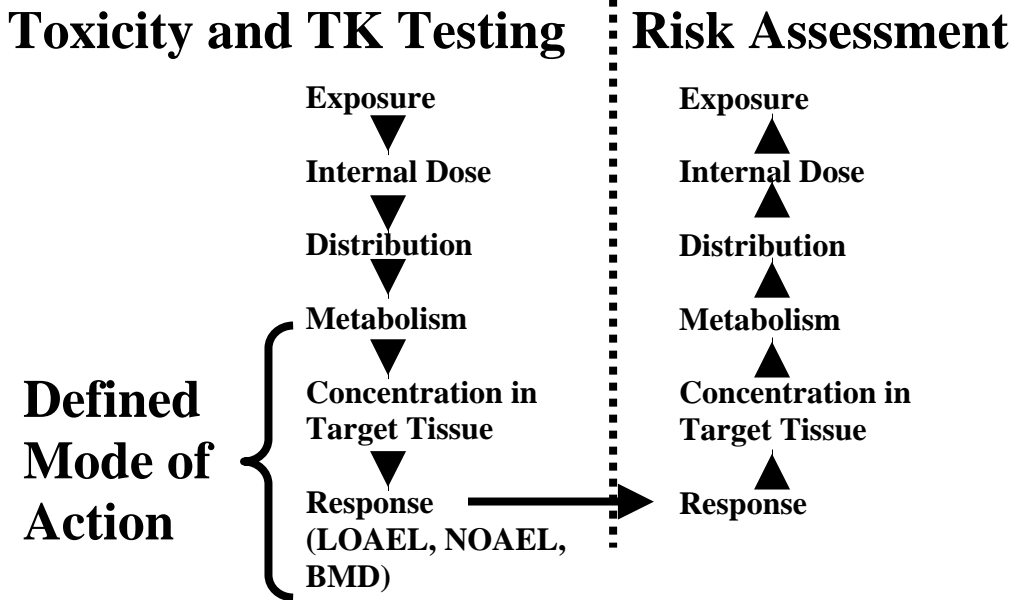


FIGURE 4-1

Application of PBPK Modeling to Link External Dose with Concentration of Toxicant in Target Organs. The approach builds upon information on mode of action, which demonstrates the relationship between tissue response, a PD phenomenon, and the PK outcome directly related to that response. PBPK models are then developed and employed to define the relationship between the external exposure and the target organ toxicant concentration, usually performed in test animal species. Once completed, and based on assumptions about the similarity in the qualitative and quantitative nature of the PD effect (mode of action) between the test species and humans, parallel PBPK models are developed for the human, and are exercised to `back-track` the toxicant from a predetermined concentration in the target tissue to the corresponding exposure concentration (external dose).

## Isolation of Microsomal Protein

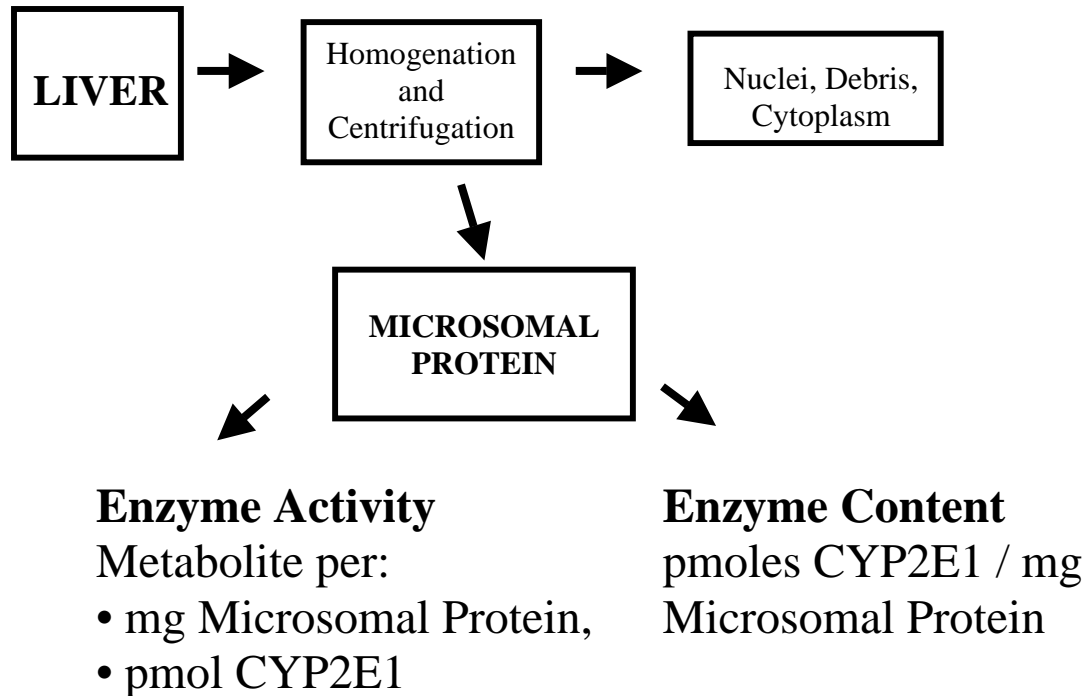


FIGURE 4-2

Relationship Between Intact Liver, Microsomal Protein and Some CYP Forms. The isolation of microsomal protein from intact liver via homogenation of tissue and differential centrifugation results in a 100,000 x g pellet which is enriched for endoplasmic reticulum content. The enrichment results in an artificial increase in the concentration of biological components associated with the endoplasmic reticulum. This isolation produces a fraction (microsomes; MSP) which is subjected to *in vitro* investigations of metabolic activity and enzyme content. However, a quantitative relationship to the intact liver is not possible without further information on the distribution of microsomal protein to the intact liver.

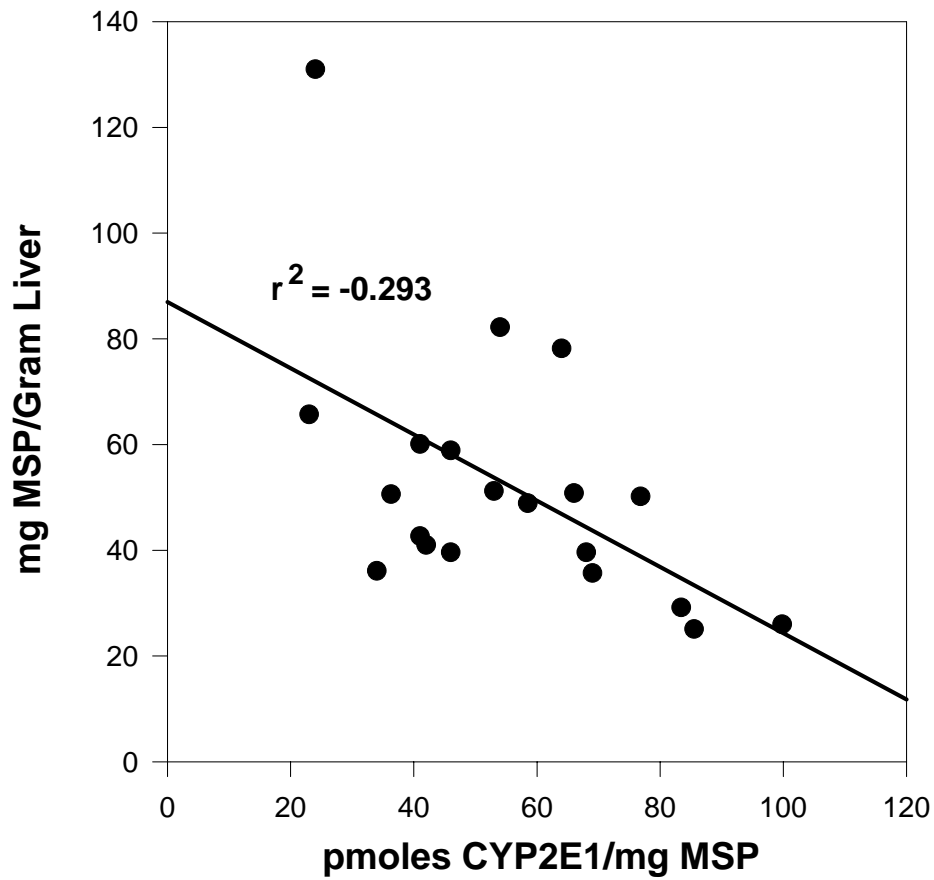


FIGURE 4-3

Correlation Between mg MSP/gram and pmol CYP2E1/mg MSP. The slight, but statistically significant, correlation between the two parameters dictated the choice of statistical methods. Data from Lipscomb et al. (2003).

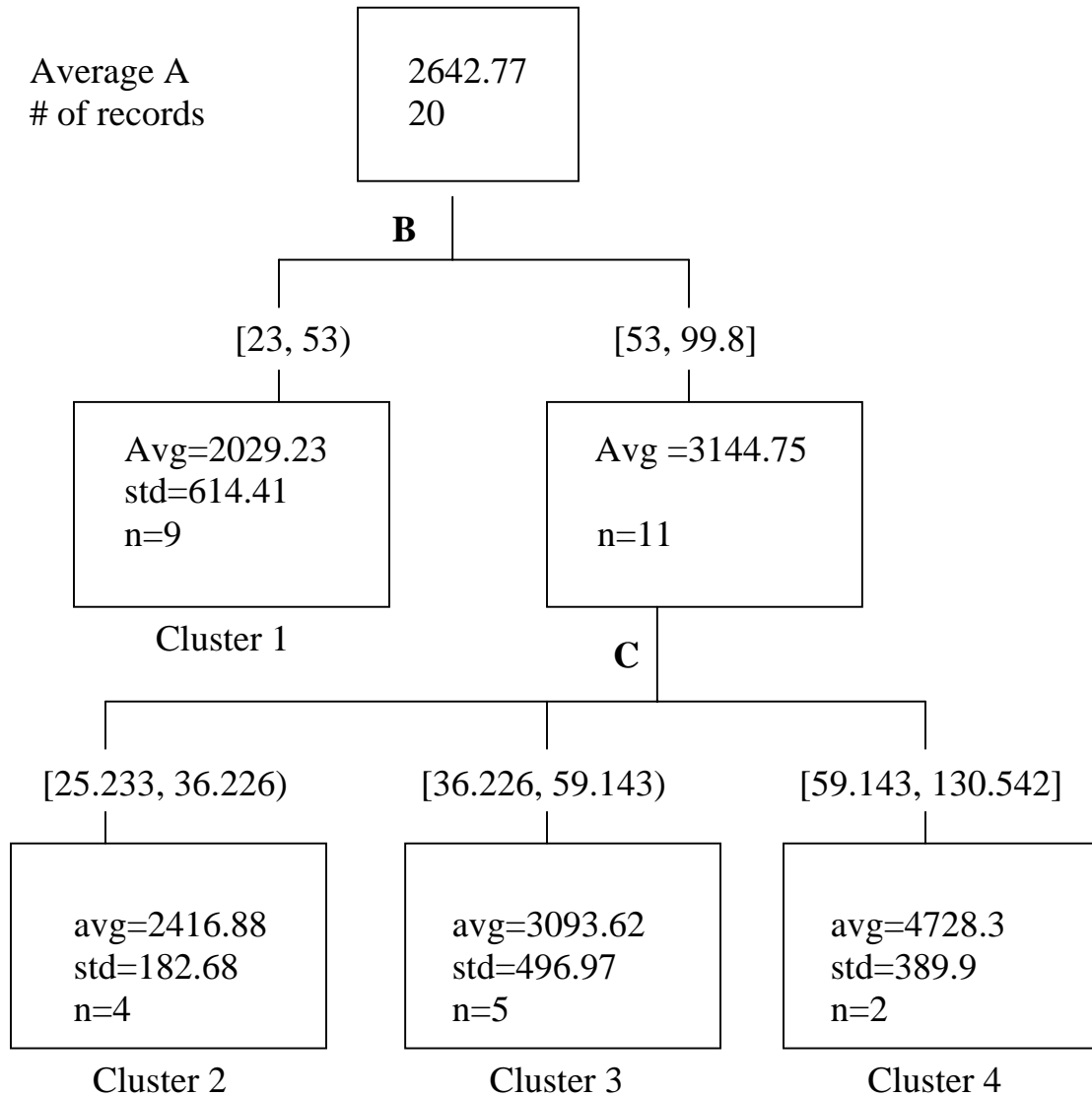


FIGURE 4-4

Classification Tree Model for the Distribution of A = pmol CYP2E1/gram Liver. The distribution of A is modeled as a finite mixture distribution with components corresponding to the leaves in the depicted classification tree. The conditional distribution of A depends on which component distribution a case belongs to. The components are bounded by breakpoints in the observed values for B and C. The sample means and sample standard deviations for the four component distributions are estimated from the first 20 cases in Table 4-2.

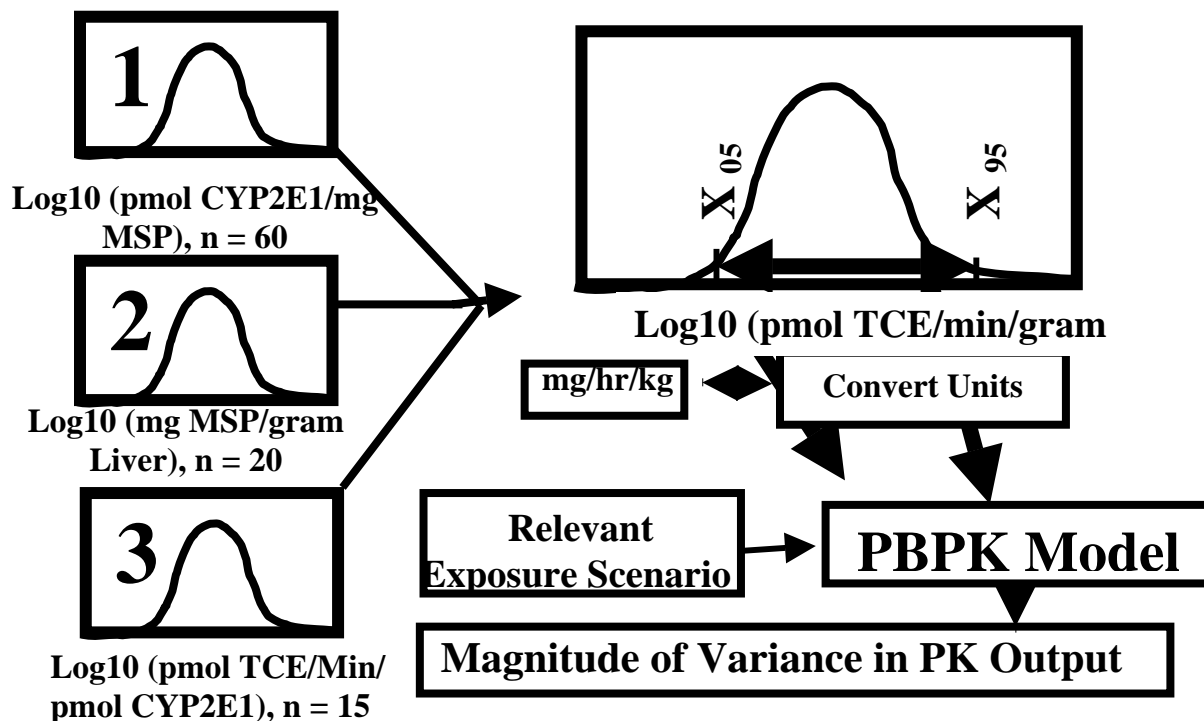


FIGURE 4-5

Extrapolation and Incorporation of *in vitro* Derived Metabolic Rates in PBPK Modeling. This figure depicts the framework for deriving appropriate *in vitro* measures and their extrapolation into a PBPK model. The model was exercised to simulate environmentally and occupationally relevant exposures.

## APPENDIX

### MATLAB Code to Generate AxD

```
numReps = 250000;
cluster{1}= [1520 1231.7 1842.2 1835.2 2720.6 2477.6 3133 1738.8 1764];
cluster{2}= [2157.4 2585.6 2452.3 2472.2];
cluster{3}= [3850 2863.3 2696.4 2715.6 3342.8];
cluster{4}= [4452.6 5004];
clusterCDF= [.53 .70 .91 1.0];
A = zeros(1,numReps);
result = zeros(1,numReps);
for i = 1:numReps
    D = exp(3.4812 + .4156*randn);
    clusterNum = min(find(rand < clusterCDF));
    clusterSize = length(cluster{clusterNum});
    clusterIndex = ceil(rand*clusterSize);
    A(i) = cluster{clusterNum}(clusterIndex);
    result(i) = A(i)*D;
end
writeArray = result';
save Dvalues.txt writeArray -ASCII
disp('A parameters')
disp([mean(A) std(A)])
disp('AxD parameters')
disp([mean(result) std(result)])
hist(result,100)
title('Empirical Distribution of A x D')
figure(2)
hist(log(result),100)
title('Empirical Distribution of ln(A x D)')
```

## **5. PHARMACOKINETIC ANALYSES TO SUPPORT AN INHALATION RfC FOR CHLOROFORM**

### **BACKGROUND**

Chloroform ( $\text{CHCl}_3$ ) is a problematic drinking water contaminant and byproduct of the disinfection (DBP) of drinking water with chlorine (Richardson, 1998; Rook, 1974). Chloroform is carcinogenic to rats and mice; and the assessment of its risk involves nonlinear concentration extrapolation because of the involvement of cytotoxicity. Cytotoxicity appears to be dependent on the formation of a reactive metabolite, phosgene, from chloroform and its interaction with cellular components. When the damage due to the formation of reactive phosgene exceeds the normal repair capacity, cytotoxicity occurs, predisposing the tissue to a carcinogenic response.

Chloroform metabolism has been assessed through various experimental designs, in several mammalian species, and with differing degrees of specificity. Studies with rodent liver preparations have indicated that cytochrome P450 2E1 (CYP2E1) is the major enzyme in metabolizing low concentrations of chloroform. Other enzymes can contribute to chloroform metabolism at higher chloroform concentrations (Testai et al., 1996); however, these higher concentrations are unlikely to be found in the tissues of humans exposed to chloroform through drinking water or by inhalation, even at occupational exposure limits (threshold limit value and time-weighted average value of 10 ppm; ACGIH, 2003).

Physiologically based pharmacokinetic (PBPK) modeling has been usefully applied to extrapolate tissue concentrations of toxicants across dose, route, and species for health risk assessment. It also allows for the interjection of realistic measures of human interindividual biochemical and physiologic variability into the determination of tissue doses of toxicants (Lipscomb and Kedderis, 2002). This report employs PBPK modeling to combine measures of

biochemical, physiologic, and anatomic variability between test animal species and humans, as well as among human life stages, to quantify the risk-relevant pharmacokinetic outcome, i.e., liver metabolism of chloroform, under inhalation exposure scenarios. The results are considered in the context of evaluating the role of species and human interindividual toxicokinetic (TK) variability in determining uncertainty factors for risk assessment (Figure 5-1).

**Purpose.** At present, the risk assessment for chloroform does not include a Reference Concentration (RfC) for inhaled chloroform. The purpose of this analysis is to provide information on tissue dosimetry (concentration of the metabolite in liver), including differences between rats and humans as well as variability among humans, to support the derivation of the uncertainty factors governing inter- and intraspecies TK for subsequent derivation of the RfC.

**Objective.** The objective of this analysis is to identify several anatomic, physiologic, and biochemical parameters associated with the distribution and metabolism of chloroform and to apply PBPK modeling in the rat and human to quantify species and human-interindividual differences in the amount of chloroform metabolized at steady state during a continuous exposure.

## **RISK ASSESSMENT APPLICATION**

This approach was developed to reduce uncertainty in the derivation of the RfC for chloroform by applying PBPK modeling to quantify species extrapolation and to provide a framework through which the impact of quantified human interindividual variability in important model parameters could be evaluated with respect to the risk-relevant internal dose metric. Animal bioassay data were evaluated via benchmark dose modeling. After identifying a no-effect intermittent exposure in mice, PBPK modeling was applied to transform the external concentration to an internal dose metric, the value of which was used as a point of departure for

## Toxicity and TK Testing

## Risk Assessment

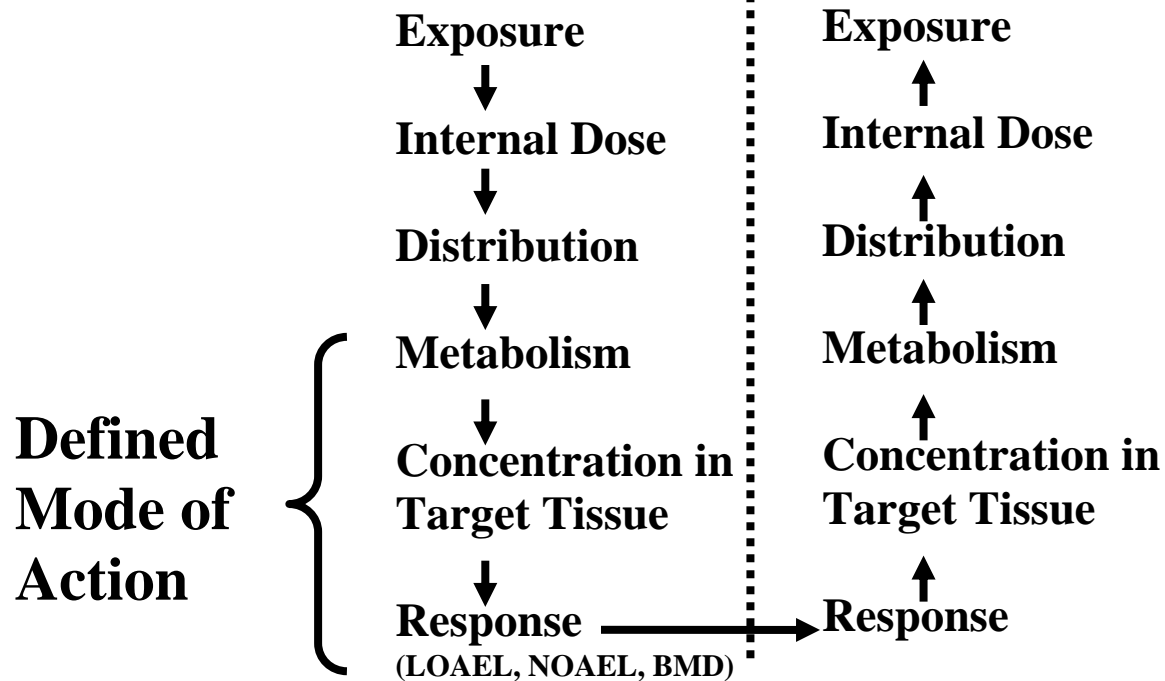


FIGURE 5-1

A Conceptual Presentation of the Application of TK Information and the TK Approach to Human Health Risk Assessment. Data from animal studies can identify the target organ or tissue, the toxicologically relevant form of the chemical (parent or metabolite), and can describe the link between metabolism and response. With this information, and information sufficient to develop TK models for the test species and the human, some linkage can be made based on knowledge or assumptions about species sensitivity to the toxicologically active form of the chemical. With this information, and these models in hand, the animal model can be exercised to simulate the appropriate dose metric under NOAEL exposure conditions, and the human model can be “run backwards” to correlate the level of the appropriate dose metric with an exposure concentration.

further modeling in humans, with specific attention devoted to assessing age-dependent and adult interindividual variability of several key physiologic and biochemical parameters. These parameters include blood:air partitioning of chloroform, hepatic blood flow (HBF), and CYP2E1-dependent bioactivation of chloroform. The results are expressed relative to external concentrations, consistent with EPA policy regarding the derivation of the Human Equivalent Concentration for inhaled substances.

### **SCOPE AND LIMITATIONS**

This analysis was constrained for several reasons. The mode of action of chloroform involves metabolism to phosgene, and chloroform metabolism (disappearance of parent chemical) was measured using a closed and recirculating system gas uptake with rat and human microsomal proteins (separately). As such the assumption is that the formation of reactive metabolites from chloroform is accurately indicated by the disappearance of parent chemical. Second, the liver was chosen as the site of toxicity by considering the prevalence of liver injury noted in animal studies and humans, and the lack of epidemiologic information indicating respiratory (nasal) toxicity in chloroform-exposed humans (results not here presented). Third, the analysis was undertaken to evaluate only two of the five non-cancer uncertainty factors, those relating to inter- and intraspecies uncertainty/variability. Further, the analysis was conducted to evaluate only the toxicokinetic component, and did not include a technical consideration of inter- and intraspecies variability in response (toxicodynamics). Any presentation of reference concentrations derived from suggested uncertainty factor values should be considered as illustrative examples. In conclusion, the present work was aimed at developing a human equivalent concentration for the inhalation exposure to chloroform and developing and

presenting results that will be useful in establishing a value for the toxicokinetic component of intraspecies uncertainty factor.

## **APPROACH**

The approach is based on toxicological information identifying the metabolism of chloroform as a causative factor of damage leading to cytotoxicity in the liver. Recently, an expert panel was convened by the International Life Sciences Institute / Health and Environmental Sciences Institute to evaluate the mode of action of chloroform (Andersen et al., 2000; ILSI, 1997). This panel concluded that the body of available evidence was sufficient to warrant confidence in oxidatively-derived chloroform metabolites as causative in tissue insult/injury, and that carcinogenicity was secondary to chloroform-induced cytotoxicity. The panel concluded that the “likely mode of action was the accumulation of reactive, oxidized metabolites, leading to cell toxicity” but was unable to distinguish between the amount of metabolite formed per unit tissue or the rate of metabolism (Andersen et al., 2000; ILSI, 1997). They recommended that critical studies of chloroform cytotoxicity should be conducted on the basis of rates or amounts of metabolite produced per volume of tissue, and that a PBPK modeling-based approach including “specific parameter (value)s related to metabolic rates, enzyme affinities and enzyme tissue distribution” be undertaken. The panel indicated that “measures of effective dose related to the rate of metabolism, or rate of formation of phosgene, would be expected a priori to be meaningful”, and that the mean daily rate of chloroform metabolism in tissue would be an appropriate dose measure. The approach taken in this document is consistent with the recommendations of the ILSI expert panel.

While some investigators have begun to address “rate” of chloroform oxidation, this investigation has relied on the accumulation of metabolite, specifically the cumulation of

metabolism over a 24-hour period, as the dose metric for evaluation. This approach is absolutely consistent with the recommendations developed by the ILSI-convened panel of experts. Here, chloroform metabolism is assessed as  $CM_{24}$ , the integrated amount of chloroform metabolized over a 24-h period, expressed in milligrams per liter (mg/L) of liver tissue. The 24-h time frame is based on two considerations: (1) chloroform is cleared from mouse liver before the end of a 24-h period beginning at the initiation of a 6-h exposure period (5 ppm), i.e., each 24-h period is independent and (2) the 24-h period is applied in humans, due to the relationship between the intent of RfC values to reflect risk/safety under continuous-exposure conditions. Determining  $CM_{24}$  under steady state conditions avoids underestimating metabolism, which may occur when extrapolating the results of an intermittent exposure to a chronic-exposure situation. For extrapolating animal effects, the  $CM_{24}$  resulting from “no-effect” exposure scenarios identified from inhalation bioassays will be used as the point of departure.

Following a practice for which precedent exists in IRIS files for other chemicals, the mode of action for chloroform has been determined and related to the formation of toxicologically active metabolites via oxidation by cytochrome P450. While other metabolites are formed, and are also reactive in nature, those metabolites formed by and following the oxidation of chloroform make up more than 90% of metabolized chloroform. Hence, this analysis will focus on the metabolic pathway catalyzed by cytochrome P450 2E1 (CYP2E1). The internal dose metric,  $CM_{24}$ , will be the basis of comparison of exposures between and among species in describing the human equivalent concentration (HEC) and selection of values for the TK component of the uncertainty factor addressing human interindividual variability/uncertainty ( $UF_H$ ) (Figure 5-2).

This analysis includes specific information on several factors that vary within the human population in order to address the human interindividual differences in chloroform TK. These factors are evaluated by quantifying their effect on the external concentrations required to derive the  $CM_{24}$  values of interest. Because CYP2E1 catalyzes the oxidation of many low molecular weight solvents and environmental contaminants, and because its expression among humans varies appreciably, this analysis includes quantitative information on CYP2E1 variance among humans. Furthermore, because delivery of chloroform to the liver tissue through HBF can be a limiting factor in its metabolism at low blood concentrations, the analysis also includes quantitative information on the variability of HBF among humans. Specific human models have been constructed to simulate the adult male, the obese adult male, the adult female, the 1-year-old and the 9-year-old child. These characteristics (quantified variability of chemical-specific metabolic capacity, and quantified variance of HBF) set the present analysis apart from its predecessors. This is the first time, to our knowledge, that these data have been combined in the analysis of tissue dosimetry in humans for conducting a human health risk assessment.

Briefly, the analysis will follow several steps. Steps 1 to 4 are depicted in Figure 5-3.

1. A PBPK model will be developed using the structure for styrene (Ramsey and Andersen, 1984; Figure 5-4) and parameter values for chloroform, including partition coefficients and metabolic parameters deemed appropriate, or developed, for rats, mice, and humans.
2. The PBPK model for mice and rats will be used to simulate  $CM_{24}$  based on the exposure conditions identified from inhalation bioassays. The lowest  $CM_{24}$  value will be used for extrapolation to humans.
3. The PBPK model for the adult male human will be parameterized to include human-specific parameters including body weight, organ volumes and flows, and metabolic parameters.

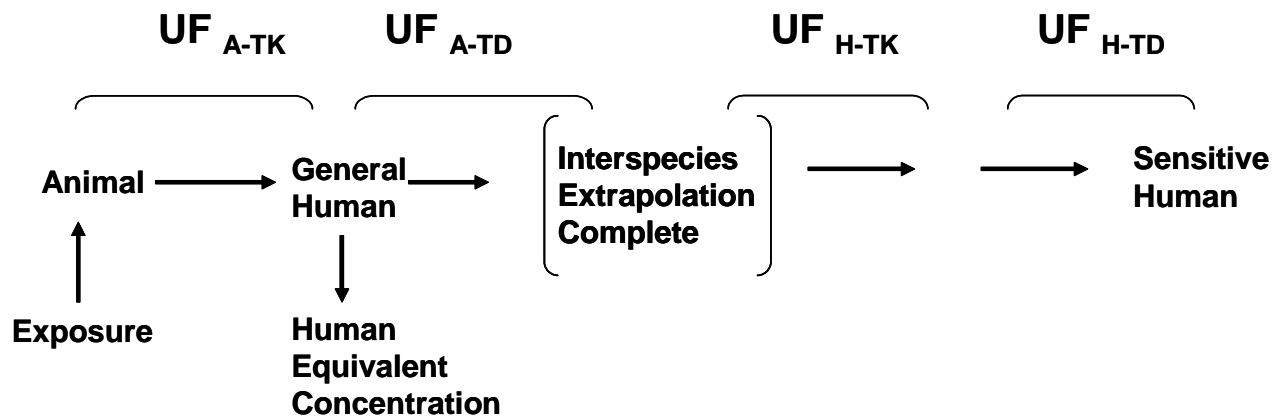


FIGURE 5-2

Subdivision of Uncertainty Factors into Toxicokinetic and Toxicodynamic Components. The International Programme on Chemical Safety (IPCS, 2001) has released draft guidance on the development of Chemical-Specific Adjustment Factors (CSAF), which demonstrates the separation of  $UF_A$  and  $UF_H$  into respective TK and TD components, allowing replacement of default values with data-derived values. With respect to animal-to-human extrapolation, this is consistent with U.S. EPA policy governing the development of HECs in the inhalation RfC methodology, which addresses species differences in toxicokinetics.

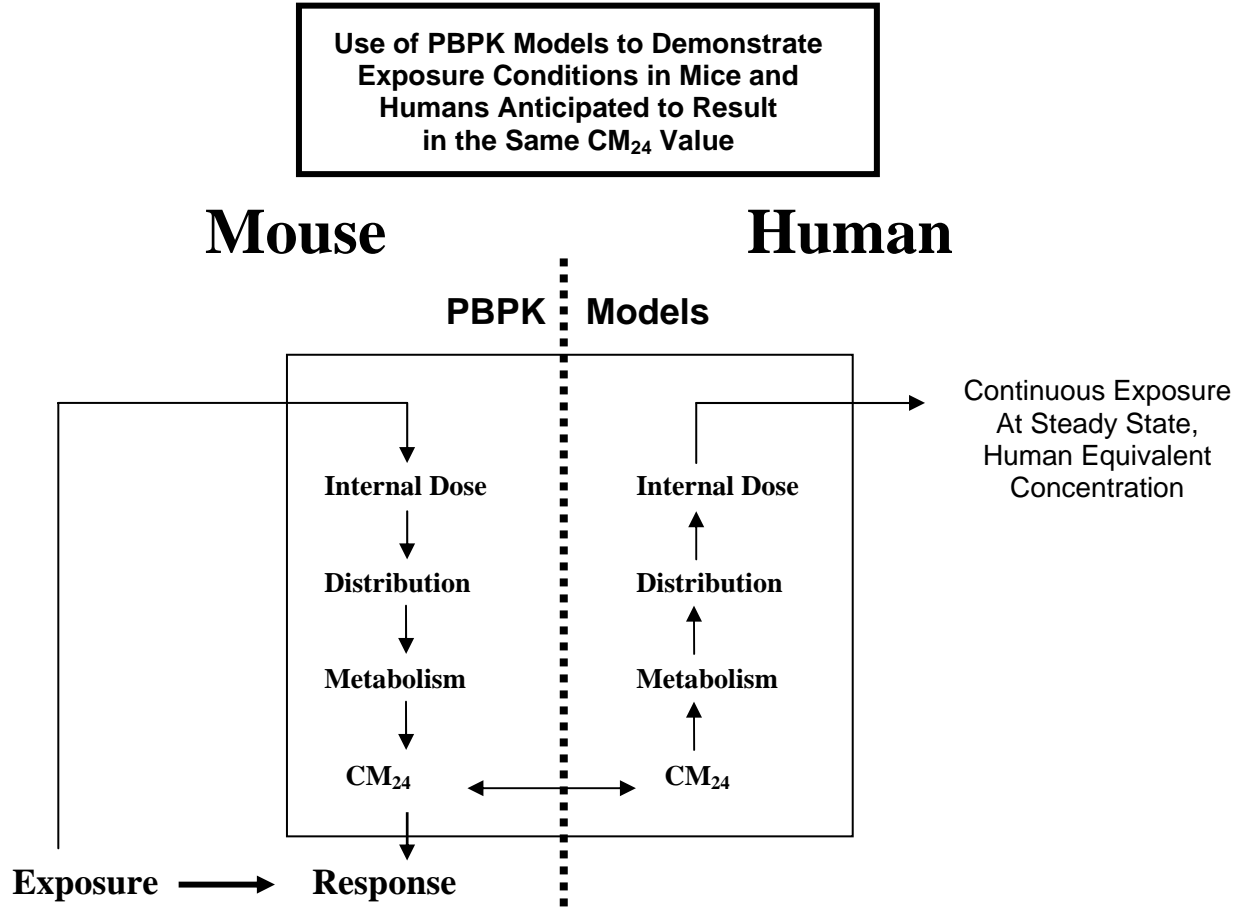


FIGURE 5-3

Application of PBPK Modeling to Extrapolate Internal Dosimetry Between Species. The development of the Human Equivalent Concentration from mouse no-effect levels was accomplished based on  $CM_{24}$ , the integrated amount of chloroform metabolized over a 24-h period, expressed per L of liver tissue. Studies with mice indicated a NOAEL exposure of 5 ppm, which was not duration-adjusted. The mouse PBPK model was exercised to reveal  $CM_{24}$  in the mouse, and the human model was exercised over a range of continuous exposure concentrations to reveal a linear relationship between  $CM_{24}$  and exposure concentration. This relationship was used to determine the human exposure condition necessary to develop the  $CM_{24}$  value obtained from simulations of the mouse exposure conditions (see Figure 5-6).

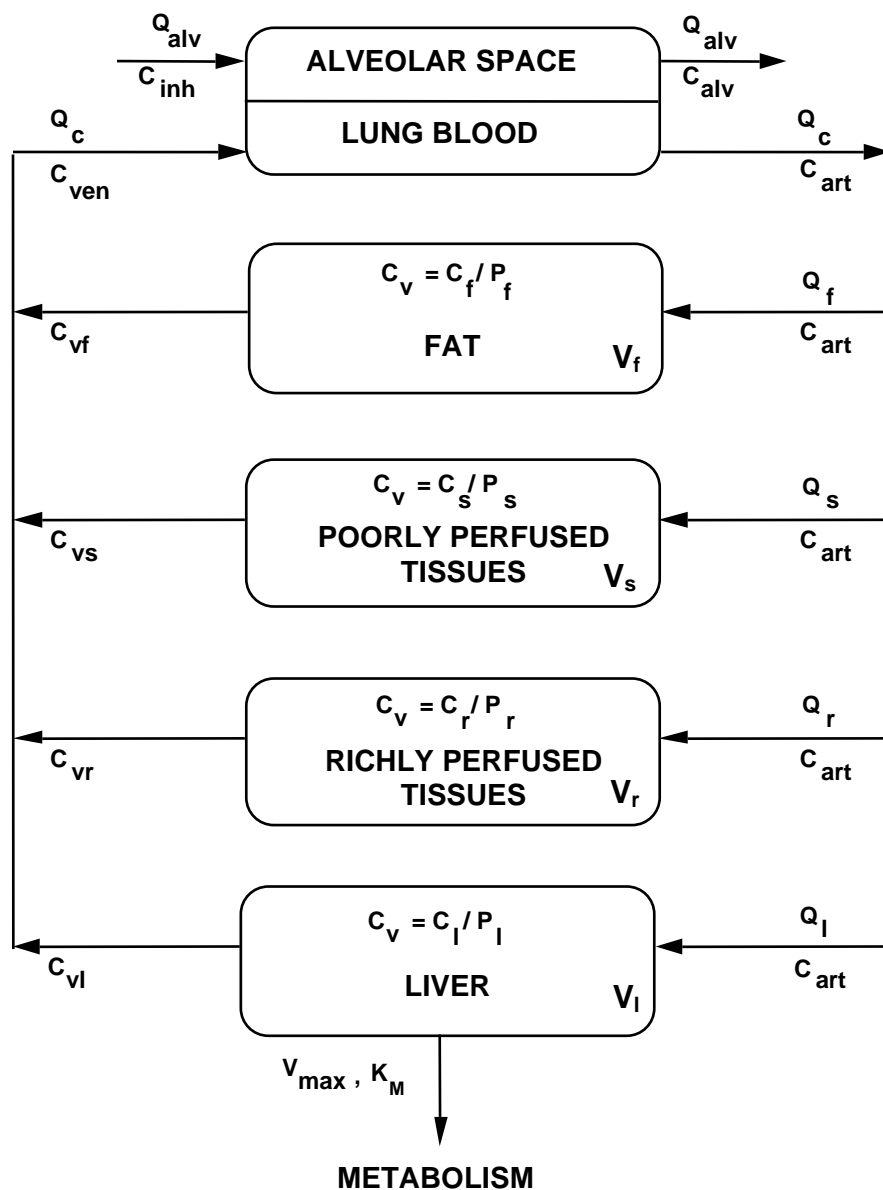


FIGURE 5-4

Five-Compartment PBPK Model. A five-compartment PBPK model was developed to address chloroform dosimetry and metabolism in rats, mice, and humans, based on structure developed and originally published for styrene (Ramsey and Andersen, 1984). This structure has been successfully applied for a range of volatile organic compounds.

4. Using values for these parameters that are representative of the median values for adult male humans, the model will be used to simulate an inhalation exposure to chloroform in inspired air. Through an iterative process, the model will determine the duration of exposure and the concentration of chloroform in inspired air required to reach the steady state that produces a value for  $CM_{24}$  equivalent to that observed in the identified animal exposure scenario. This will represent the HEC.
5. The adult male human PBPK model will be re-parameterized to reflect human interindividual differences in the  $V_{max}$  for CYP2E1-dependent chloroform metabolism, HBF, and blood:air partitioning of chloroform.
6. The adult male human PBPK model will again be used to demonstrate the effects of parameter variability on  $CM_{24}$ . Model simulations will demonstrate differences in exposure concentrations necessary to obtain a  $CM_{24}$  value equivalent to that demonstrated at exposure to (HEC/3) ppm. The adult female model will be exercised to simulate this exposure to compare  $CM_{24}$  values.
7. Finally, the human PBPK model will be re-parameterized to include the values for parameters known to differ between adults and children. Those include fractional contribution of the fat and liver compartments to body mass, metabolic parameters for chloroform, and values for tissue partition coefficients. Because discussions with the Office of Water have identified the reliance on 10 kg as a representative body mass for some risk analyses with chemicals, the model will specifically include parameters on body composition derived from reference values for that body mass. Additional analyses will address the 30 kg child. These body masses are representative of children aged 1 and 9 years, respectively.
8. The child PBPK models will be used to compare exposure concentrations necessary to reproduce the value for  $CM_{24}$  observed at the HEC in the adult human model containing median values for parameters whose values are varied.

## **APPLICATION OF PHYSIOLOGICALLY BASED PHARMACOKINETIC MODELING**

PBPK modeling will be applied to transform external concentrations to measures of internal doses for species extrapolation in derivation of the inhalation RfC. The model structure (Figure 5-4) is that of Ramsey and Andersen (1984) developed for styrene and successfully applied to numerous substances since its publication two decades ago; source code is presented as Appendix A. The derivation of the HEC follows EPA methodology on RfCs (U.S. EPA, 1994) related as differences in external exposure under the conditions of maintaining the internal dose metric between species. Here, the value of  $CM_{24}$  obtained from model predictions based on

bioassay exposure conditions is standardized between species. The human PBPK model predicts the continuous exposure, under steady state conditions, that would be required to produce that value for  $CM_{24}$ . Likewise, variability within humans is evaluated as the difference in the concentration of chloroform in inspired air required to produce the same  $CM_{24}$  value. These differences can be considered during the process of estimating the value for the TK component of  $UF_H$ .

This approach differs in several areas from the traditional use of default uncertainty factors to extrapolate animal findings to humans. Under the traditional NOAEL approach, a no- or lowest-observed-adverse-effect level is determined in animals and adjusted for duration (subchronic to chronic) to account for animal-to-human differences as well as human interindividual differences. Each of these three factors has a default value of 10. In the present approach, division of the animal-to-human uncertainty factor ( $UF_A$ ) and human interindividual uncertainty factor ( $UF_H$ ) into their respective TK and toxicodynamic (TD) components provides the structure for the inclusion of TK information on chloroform metabolism between species (rats and humans) and among humans into the model. Sufficient information describes a mode of action and its causative chemical moiety (i.e., the oxidative metabolite) toward which PBPK modeling may be aimed. Pharmacokinetic and species-specific information are sufficient to describe the development of species-specific PBPK models to allow this more comprehensive approach to be used in developing values for uncertainty factors.

The approach undertaken develops an HEC based on pharmacokinetic information pertinent to liver toxicity as the critical effect. The derivation of the HEC obviates the TK component of the animal-to-human uncertainty factor ( $UF_{A-TK}$ ). The remaining TD portion of the uncertainty factor ( $UF_{A-TD}$ ) remains, and will be addressed using a default value of 3 (half an

order of magnitude). Additional data demonstrating human interindividual differences in HBF, which is a major limiting factor in chloroform metabolism, will be incorporated in the adult PBPK model. Additional data describing metabolic variability available from measured levels of CYP2E1 in adult and child liver tissues quantitative measures of CYP2E1 activity toward chloroform and human variability in blood:air partitioning of chloroform will be used to construct models useful in addressing human interindividual variability. This representation of intraspecies differences, as well as sex- and age-dependent variability in blood flows, ventilation, body weight and compartment sizes, will be incorporated in the model to ascertain their influence on chloroform metabolism *in vivo*. This process will be used to support a value to replace the default uncertainty factor addressing the TK component of the human interindividual uncertainty factor ( $UF_{H-TK}$ ). Figure 5-1 illustrates the application of TK information and concepts in human health risk assessment. Figure 5-3 demonstrates the concept of using such information to develop the HEC for chloroform. We will develop this HEC based on  $CM_{24}$  of the most sensitive species (i.e., the mouse) as the point of departure.

PBPK modeling for the human will be conducted at steady state, based on the concept that the RfC is for a chronic, lifetime-continuous exposure. Because data demonstrate species-dependent differences in biochemical parameters (e.g., tissue partitioning and metabolism) exposure influences the time it takes to reach steady state. Model simulations of species differences in intermittent exposures will be complicated by species-dependent differences in biochemical parameters. Thus, species differences in the amount of chemical metabolized (i.e., the risk-relevant TK outcome) may be influenced by exposure duration. However, because chloroform is cleared from the mouse liver within 18 hours after the end of a 6-h, 5 ppm exposure,  $CM_{24}$  will be estimated in mice based on a single cycle of a 6-h-on/18-h-off exposure.

This model is constructed to demonstrate the  $CM_{24}$ , the 24-h integrated amount of chloroform metabolized, normalized per liter of liver tissue. It is expressed in units of concentration, mg chloroform metabolized per liter liver (mg/L). In that respect, it differs in output metric and application from models developed and employed to simulate intermittent exposures (i.e., Tan et al., 2003).

## **METHODS: PBPK MODEL STRUCTURE AND PARAMETERS**

**Model Structure.** The five-compartment structure developed by Ramsey and Andersen (1984) for styrene was employed as the template. This model structure (Figure 5-4) assumes that the concentration of chemical in blood coursing through tissues of the body comes to equilibrium with concentrations of the chemical in tissues and air during the duration of perfusion.

**Partition Coefficient Derivation.** Blood:air PC (B:A PC) and tissue:air (T:A PC) values were developed using the vial equilibration method (Sato and Nakajima, 1979), combined with gas chromatographic evaluation of chemical concentration, quantified by an external standard curve of known concentrations. This method was employed to determine T:A PC values for chloroform in blood of rats and humans, and in solid tissues from rats for this study. Because initial intentions were to rely on the rat as the most sensitive species, because of the larger tissue masses available from rats and because of the marked similarity across species in the solid-tissue:air partition coefficients (Thomas, 1975), tissue:air partition coefficients were derived using liver, kidney, muscle and adipose tissues from rats. Complete results, and a comparison of observed values to values predicted using structure-activity relationships, are contained in Appendix B. Samples of blood from rats, mice, and humans were exposed to a mixture of chloroform and five other volatile organic compounds; the concentrations of the individual organic compounds in the headspace were determined at equilibrium. This approach has been

determined to produce PC values equivalent to those obtained with single chemicals in the vial equilibration method (Beliveau et al., 2001). All studies were conducted through institutionally reviewed protocols. Human blood samples were remnant samples (unperturbed blood remaining after analytical procedures had been performed) obtained from the Division of Clinical Laboratory Services, Wright-Patterson Regional Medical Center, OH and coded to ensure anonymity of the subjects. The study protocol was reviewed and approved by the Wright-Patterson Institutional Review Board and the EPA Human Studies Coordinator. Samples were provided from 11 adult males, aged 36 to 80 years, 10 adult females aged 22 to 87 years, and 11 children aged 3 to 7 years.

PBPK models incorporate partitioning information as tissue:blood partition coefficient (T:B PC) values, which represent the ratio of chemical concentrations in tissue:blood at equilibrium. Like most PBPK models, the model structure used in this examination was based on the assumption that the duration of perfusion of tissues (organs) is sufficient for tissue and blood concentrations of parent chemical to come to equilibrium, at concentrations dictated by the T:B PC value for that tissue. Tissue:Blood PC values are determined by Equation 5-1:

$$T:A \text{ PC} / B:A \text{ PC} = T:B \text{ PC} \quad (5-1)$$

**Mice.** Partition coefficient values used to populate the mouse PBPK model were taken from Tan et al. (2003), which relied, in part, on PC values originally reported by Corley et al. (1990). These values can be found later in Table 5-7. Because they were not experimentally derived for the present investigation, they are not here demonstrated.

**Adult Rats.** The T:A PC values derived from tissues obtained from 10 adult male rats are presented in Table 5-1, and the resulting T:B PC values are presented in Table 5-2. The B:A and T:B PC values were used to parameterize the rat PBPK model for chloroform.

TABLE 5-1					
Adult Rat Blood:Air and Tissue:Air Partition Coefficient Values*					
	Blood:Air	Liver:Air	Kidney:Air	Muscle:Air	Fat:Air
Mean	17.7	17.6	14.8	16.9	351
S.D.	2.5	3.2	2.7	10.1	48

\*Ten adult male Fischer 344 rats were employed in this investigation. B:A PC and T:A PC values were derived using tissues from individual rats.

TABLE 5-2				
Adult Rat Tissue:Blood Partition Coefficient Values Derived from Paired Tissues*				
	Liver:Blood	Kidney:Blood	Muscle:Blood	Fat:Blood
Mean	1.0	0.8	1.0	19.9
S.D.	0.2	0.1	0.8	2.0

\*B:A PC and T:A PC values were derived using tissues from individual rats, and rat-specific T:B PC values developed using animal-matched samples were used in the rat PBPK model.

**Adult Humans.** Blood:Air PC values were derived for chloroform in 21 remnant blood samples from adult humans (Table 5-3). The mean value of 11.34 was combined with rat T:A PC values to compute T:B PC values for inclusion in the adult human PBPK models for chloroform. Thomas (1975) previously demonstrated that, for methylene chloride, T:A PC values across species (rat to human) are more consistent (rat:human ratios of 1.0 to 1.2) for liver, kidney, muscle, and fat, than for blood (rat:human ratio of 1.9). Therefore, the human B:A PC value was combined with adult rat T:A PC values (presented in Table 5-1) to compute T:B PC values representative of the adult human (Table 5-4). These values were used to parameterize the adult human PBPK model for chloroform.

TABLE 5-3		
Adult Human Blood:Air Partition Coefficient Values		
	B:A PC value	Range of Observations
Males, n = 11	11.9 ± 0.9 <sup>a</sup>	9.7 - 13
Females, n = 10	10.7 ± 2.1	6.9 - 13.3
Combined, n = 21	11.34 ± 1.65 <sup>b</sup>	

<sup>a</sup> Data presented as mean ± S.D. Mean values for men and women were not significantly different as determined by one-tail *t*-test assuming unequal variance ( $p = 0.063$ ); and by two-tailed *t*-test assuming unequal variance ( $p = 0.126$ ).

<sup>b</sup> Because there was no statistical difference between males and females, we chose to combine the data.

TABLE 5-4				
Tissue:Blood Partition Coefficient Values for Adult Humans*				
	Liver:Blood	Kidney:Blood	Muscle:Blood	Fat:Blood
Mean	1.6	1.3	1.5	31.0
S.D.	0.3	0.2	0.9	4.2

\*Blood from 21 adult humans and solid tissues from 10 adult male Fischer 344 rats were used in this investigation. A B:A PC value of 11.34 (the human mean) was combined with individual T:A PC values to develop 10 estimates of individual T:B PC values (via equation 5-1). Data are presented as the mean and S.D. of those 10 values.

**Children.** Remnant blood samples obtained from 7 male and 4 female pediatric patients (age 3 to 7 years) were used to determine B:A PC value for children. The B:A PC values demonstrated a mean and standard deviation of  $12.41 \pm 1.17$ . Samples of liver, kidney, muscle, and fat were taken from 8 male and 8 female rat pups on postnatal day (PND) 10 and used to determine T:A PC values (Table 5-5). This report relies on B:A PC values derived from blood from children aged 3-7 years to inform T:B PC values used in PBPK models constructed for the 1-year-old and the 9-year-old child (Table 5-6). No data describing the B:A PC values in these specific ages were available; no age-specific information on blood composition suitable to inform structure-activity-based predictions (i.e., water content, total lipid content, neutral lipid content) were available in Reference Man or its update (ICRP, 1975, 2002). The validity of this generalization is based on several pieces of information and some assumptions. Malviya and Lerman (1990) determined the blood:air PC values for halothane, sevoflurane and isoflurane (two-carbon halogen substituted anesthetics) in blood from preterm neonates, full-term neonates and adults. Their results indicated that B:A PC values increase from the neonatal period to adulthood and that the values increase less than 14% between the neonatal period (average age 39 weeks) and adulthood. Lerman et al. (1984) demonstrated B:A PC values for halothane, and isoflurane in infants at delivery, children aged 3-7 years and adults. Those results indicated B:A PC values in children aged 3-7 that were intermediate between values observed in infants and in adults. Given the magnitude of increase between children (aged 3-7 years) and adults, it seems that the B:A PC values characterized for this group are sufficient for children aged 9 years.

**Parameter Values:** For this evaluation, the model structure has been reparameterized for rats, mice, and humans and to include age-specific parameter values for humans (Table 5-7) with newly available chloroform-specific partitioning data and chloroform-specific metabolism

TABLE 5-5				
Tissue:Air PC Values in PND 10 Rat Pups				
	Liver:Air	Kidney:Air	Muscle:Air	Fat:Air
Mean	17.4	12.6	34.3	243
SD	1.3	0.9	24.7	48

TABLE 5-6				
Tissue:Blood PC Values Used for Children PBPK Model*				
	Liver:Blood	Kidney:Blood	Muscle:Blood	Fat:Blood
Mean	1.4	1.0	2.8	19.6
SD	0.1	0.1	2.0	3.9

\*Results were obtained by combining the mean B:A PC value (12.41) determined from 11 pediatric patients with T:A PC values for solid tissues presented in Table 5-5 via equation 5-1.

**TABLE 5-7**  
Age and Species Dependent Model Parameter Values

	Adult Male	Adult Female	Child, 9 yr	Child, 1 yr	Rat	Mouse
BW	70	60	30	10	0.25	0.025
KM	0.012	0.012	0.012	0.012	0.012	0.352 <sup>a</sup>
V <sub>max</sub> C — 5 <sup>th</sup> Percentile	4.306	4.306	3.595	3.304	ND	ND
V <sub>max</sub> C — Geo. Mean	8.956	8.956	7.866	7.23	5.218	22.8 <sup>a</sup>
V <sub>max</sub> C — 95 <sup>th</sup> percentile	15.56	15.56	17.212	15.82	ND	ND
QPC	15	15	15	15	14	23
QCC	15	15	15	15	14	23
VFC	0.19	0.21	0.158	0.1245	0.07	0.10
VLC	0.026	0.026	0.0268	0.03425	0.04	0.055
QLC	0.25	0.25	0.25	0.25	0.25	0.25
QFC	0.09	0.09	0.09	0.09	0.09	0.09
PB	11.34	11.34	12.41	12.41	17.7	24.1 <sup>b</sup>
PL	1.6	1.6	1.4	1.4	1.0	0.7 <sup>b</sup>
PR	1.6	1.6	1.4	1.4	1.0	0.7 <sup>b</sup>
PS	1.5	1.5	2.8	2.8	1.0	0.54 <sup>a</sup>
PF	31	31	19.6	19.6	19.9	10.04 <sup>a</sup>

<sup>a</sup> From Corley et al. (1990).

<sup>b</sup> From Tan et al. (2003), PL = PR.

ND = not determined.

PB = Blood:Air PC Value; PL = Liver:Blood PC Value; PR = PC Value for rapidly perfused tissues, derived using liver tissue; PS=PC Value for slowly perfused tissues, derived using muscle tissue; PF = Fat:Blood PC value. Values for the body composition of fat (VFC) and liver (VLC) of children were obtained from ICRP (1975).

Variability in hepatic blood flow (QLC) is presented in Table 5-8.

TABLE 5-8

Parameters and Selected Percentile Values for the Fraction of Cardiac Output  
as Hepatic Blood Flow

Distribution	Parameter and Value	Percentile		
		5 <sup>th</sup>	50 <sup>th</sup>	95 <sup>th</sup>
Normal	Mean = 0.273, Standard Deviation = 0.087	0.130	0.273	0.417
Lognormal*	Geometric Mean = 0.258, Geometric Standard Deviation = 1.411	0.147	0.259	0.456
Beta	$\alpha = 6.865$ , $\beta = 18.269$	0.141	0.267	0.427

\*Values from the lognormal distribution were included in the pharmacokinetic analysis.

information. As demonstrated in the table, the adult female differed from the adult male with respect to body weight and fraction of body weight represented by the fat compartment. In addition, a model was constructed for the obese adult male human by modifications made relating to the fat compartment.

One measure of obesity in adults is the body mass index (BMI) (CDC, 2005). The BMI is defined as BW in kg divided by the square of height in meters. The normal range of BMI in adults is 18.5 to 24.9. The CDC (2005) defines an obesity as a BMI greater than 30. This information was used to develop physiological parameters for an obese male human.

A 70 kg male with a BMI of 21.7 is defined as a “normal” individual. From the definition of BMI, the “normal” individual has a height of 1.796 meters ( $70/(1.796)^2 = 21.7$ ). Assuming that the obese individual has the same height as the “normal” individual but has a BMI of 30, the obese individual weighs 97 kg ( $97/(1.796)^2 = 30$ ). Assuming that the increase in BW in the obese individual is solely due to fat accumulation, the liver in the obese individual would weigh the same as the liver of the “normal” individual, 1.82 kg ( $VLC = 0.026 * BW$ , Table 1). In the “normal” individual, the fat compartment ( $VFC = 0.19 * BW$ , Table 1) would weigh 13.3 kg. If the additional weight (27 kg) in the 97 kg obese individual was entirely due to an increased fat compartment, then the fat compartment in the obese individual would be  $13.3 + 27 = 40.3$  kg. These calculations indicate that an obese individual would have a VLC of  $0.019 * BW$  and a VFC of  $0.415 * BW$ .

The model has been further modified to allow for the naturally occurring variance in the HBF in humans (Table 5-8). The model contains parameter values and details for the mouse that differ from some other reports. Many of the values for physiological parameters used in Corley et al. (1990), such as organ volumes and flow rates, are nonstandard. That model also included a

pathway for CYP destruction in male mice that Amman et al. (1998) showed does not occur, and which was not included in another recent chloroform PBPK model (Tan et al., 2003). Therefore, we used recommended standard mouse physiological values from Arms and Travis (1988), as had been used by Kedderis and Held (1996) for their study of furan pharmacokinetics in rats, mice, and humans. The B:A and liver:air (L:A) partition coefficients from Tan et al. (2003) were used, along with the values for fat and muscle partition coefficients from Corley et al. (1990), to calculate T:B PC values. Partition coefficients used in the models for rats and humans are based on B:A and T:A PC values determined using samples from young and mature animals/subjects for this investigation. For the mouse model, PC values for B:A, liver:air and kidney:air were taken from Tan et al. (2003) and values for fat:air and muscle:air were taken from Corley et al. (1990). Note that these values from Corley are also used in the Tan et al. work. Both Tan and Corley relied on values for  $V_{maxC}$  and  $K_m$  that were optimized by fitting to separately-developed gas uptake data. Because of the number of successful models based on or adapted from the Corley et al. (1990) model and/or its parameter values (i.e., Constan et al., 2002; Corley et al., 2000; Delic et al., 2000; Evans et al., 2002; Gearhart et al., 1993; Reitz et al., 1990), we chose to incorporate the  $V_{maxC}$  and  $K_m$  values from the Corley model, rather than from the Tan model. More recently derived PC values for blood, liver and kidney were available from the work of Tan, and those values were employed in the present work.

Paired measurements (obtained simultaneously from the same person) of cardiac output (CO) and HBF were available for 35 human subjects and databased predictions of CO were developed for an additional 234 subjects for which hepatic blood flow measurements were available (see Appendix C). Only measures of HBF determined by indocyanin green (ICG) clearance were employed. A total of 35 sets of paired (individual) observations were available in

the open literature (Caesar et al., 1961; Wiegand et al., 1960; Feruglio et al., 1964; Reemtsma et al., 1960), and an additional 24 paired data sets were graciously provided by the authors of publications in which mean values were available (Iijima et al., 2001; Sakka et al., 2001). Commercially available software (Statistical Analysis System, SAS) was applied to the above 59 individual values for HBF/CO to determine the parameters for the normal, lognormal, and beta distributions according to the method of moments. Results are presented in Table 5-8. The derivation of these values is described in detail in Appendix C. Among the 35 sets for which CO was measured, HBF and CO appeared uncorrelated.

### **METABOLIC VARIABILITY**

This section provides a brief description of the methodology employed; for a detailed description, see Appendix D. Metabolic capacity is a function of the separate contributions of enzyme expression (content) and enzyme activity. Historically, differences in enzyme content of microsomal protein (MSP) isolated from liver have been used to infer differences among humans in the liver enzyme content. However, those investigations ignored the distribution of MSP content of intact liver as an additional contributor to human interindividual variability. This investigation used ELISA-based measures of CYP2E1 in liver tissues from 60 adult human organ donors and 10 child organ donors to determine the range of variability of CYP2E1 expression (CYP2E1 content) among adults and children. An additional *in vitro* metabolism study was also performed to determine the activity of CYP2E1 toward chloroform. Valid statistical procedures were applied to determine the metabolic capacity of the human liver, incorporating measures of variability of enzyme content as well as *in vitro*-derived metabolic rate constants. Finally, metabolic capacity was extrapolated to the intact liver, and scaled by

body weight for inclusion in PBPK modeling efforts designed to assess the contribution of the variance in metabolic capacity to chloroform metabolism.

Statistical analyses determined that the distribution of CYP2E1 in adult human liver was lognormal. The values at the 5<sup>th</sup> percentile, the geometric mean, and 95<sup>th</sup> percentile of the distribution are presented in Table 5-9.

To measure of the activity of human CYP2E1 toward chloroform, 3 samples of adult human MSP were evaluated in an *in vitro* gas uptake system developed and employed by EPA/ORD/NHEERL. Although genetic polymorphisms of CYP2E1 are known, no evidence exists to support their involvement in altering the catalytic activity of the enzyme. Should such evidence be demonstrated in the future, the applicability of genetic polymorphisms to *in vivo*, as opposed to *in vitro*, chloroform metabolism must be demonstrated to substantiate their inclusion as risk-modifying factors.

With knowledge of the CYP2E1 content of the 3 MSP samples used to study chloroform metabolism, *in vitro*-derived  $V_{\max}$  values could be converted from units of mass/time/mg MSP to units of mass/time/pmol CYP2E1. The results demonstrated a specific activity of human CYP2E1 of 5.24 pmoles chloroform metabolized/minute/pmol CYP2E1. The value in rats was 5.29 pmoles chloroform metabolized/minute/pmol CYP2E1. The similarity in values among these species is not surprising, given the conservation of CYP2E1 across mammalian species. This more specific measure of enzyme activity was then combined with measures of enzyme content to produce measures of metabolic capacity ( $V_{\max}$ ), expressed per gram liver tissue, and converted to units of body weight by accounting for the fractional composition (for adults, 0.026) of body weight accounted for by liver mass. Results of the extrapolation to intact tissue are presented in Table 5-9.

TABLE 5-9			
Distribution of Chloroform Metabolic Rate Constants in Adults and Children			
Parameter	Adult	Child <sup>a</sup>	
Enzyme Content — pmoles CYP2E1/gram Liver			
5 <sup>th</sup> percentile	1232 <sup>b</sup>	1288	
Geometric mean	2562 <sup>b</sup>	2818	
95 <sup>th</sup> percentile	4453 <sup>b</sup>	6167	
Specific Activity — pmoles CHCl <sub>3</sub> /min/pmol CYP2E1	5.24	5.24 <sup>c</sup>	
Metabolic Capacity (V <sub>max</sub> ) — μg CHCl <sub>3</sub> /h/gram Liver			
5 <sup>th</sup> percentile	46.3	48.35	
Geometric mean	96.3	105.8	
95 <sup>th</sup> percentile	167.3	231.5	
Metabolic Capacity (V <sub>max</sub> ) — mg CHCl <sub>3</sub> /h <sup>d</sup>			
	Adult	9-year-old Child	1-year-old Child
5 <sup>th</sup> percentile	84.27	38.87	16.56
Geometric mean	175.27	85.06	36.24
95 <sup>th</sup>	304.49	186.13	79.29

<sup>a</sup> Child organ donors ranges 10 months to 17 yrs of age, refer to Appendix D, Table D-2.

<sup>b</sup> From Lipscomb et al. (2003).

<sup>c</sup> Measured in adult samples (Lipscomb et al., 2004).

<sup>d</sup> mg CHCl<sub>3</sub>/h = μg CHCl<sub>3</sub>/h/gram liver × (1000 μg/mg) × BW × VLC × (1000 grams/kg); difference between values derived for the 9- and 1-year-old child are based on differential contributions of liver mass to body mass (VLC = body composition of liver).

For incorporation into PBPK modeling, the above measures of  $V_{\max}$  (mg/h) were scaled by  $BW^{0.7}$ , and the parameter was redescribed as  $V_{\max}C$  by Equation 5-2. The results are demonstrated in Table 5-10.

$$V_{\max}C = V_{\max}/BW^{0.7} \quad (5-2)$$

**Simulated Exposure Conditions.** Although the mouse is considered to be the most sensitive species and  $CM_{24}$  is to be determined using a 24-h period with intermittent exposure, a comparison of chloroform metabolism among rats, mice, and adult male humans can provide valuable insight. Three sets of simulations were performed, with the goals of (1) evaluating the temporal responses of chloroform metabolism in all species, (2) characterizing species differences in chloroform metabolism to derive the HEC, and (3) characterizing human interindividual differences in chloroform metabolism that may be used to estimate the value for the TK component of the  $UF_H$ . The first two sets of simulations used the rat, the mouse, and the “general” adult human models (that developed for the adult male human and including median values for parameters whose values varied), while the third set used the adult male human PBPK model that had been parameterized to reflect age-dependent and human interindividual differences in enzyme activity, HBF, and blood:air partitioning. The first set of simulations examined the amount of time required to attain steady state, defined chloroform:liver concentrations, and defined species differences in chloroform metabolism at the same concentrations under steady state conditions. Figure 5-5 illustrates the chloroform concentration-time profile for the first 24 hours of exposure to 5 ppm chloroform in inspired air in rats, mice, and humans. Steady state in humans is not reached until approximately 7 ds of exposure (not shown). To provide an additional comparison, the rat, mouse, and general adult human models were programmed to describe  $CM_{24}$  under steady state at exposure concentrations of 0.1, 0.5,

TABLE 5-10

Derivation of  $V_{\max}C$  Values for Inclusion in PBPK Modeling for Adults, Children, and Rats

	$V_{\max}$ (mg/h)	BW (kg)	$BW^{0.7}$	$V_{\max}C$ (mg/h/kg)
Mouse	1.73	0.025	0.076	22.8 <sup>a</sup>
Rat	1.98	0.25	0.38	5.218
Adult Human, 5 <sup>th</sup> percentile	84.27	70	19.57	4.36
Adult Human, Geometric Mean	175.27			8.956
Adult Human, 95 <sup>th</sup> percentile	304.49			15.56
9-year-old Child, 5 <sup>th</sup> percentile	38.87	30	10.81	3.595
9-year-old Child, Geometric Mean	85.07			7.866
9-year-old Child, 95 <sup>th</sup> percentile	187.13			17.212
1-year-old Child, 5 <sup>th</sup> percentile	16.56	10	5.01	3.304
1-year-old Child, Geometric Mean	36.24			7.230
1-year-old Child, 95 <sup>th</sup> percentile	79.29			15.82

NOTE: For comparison, Corely et al. (1990) employed a  $V_{\max}C$  value of 15.7 mg/h/kg for humans, and 6.8 mg/h/kg for rats to model the disposition of chloroform.

<sup>a</sup> From Tan et al. (2003).

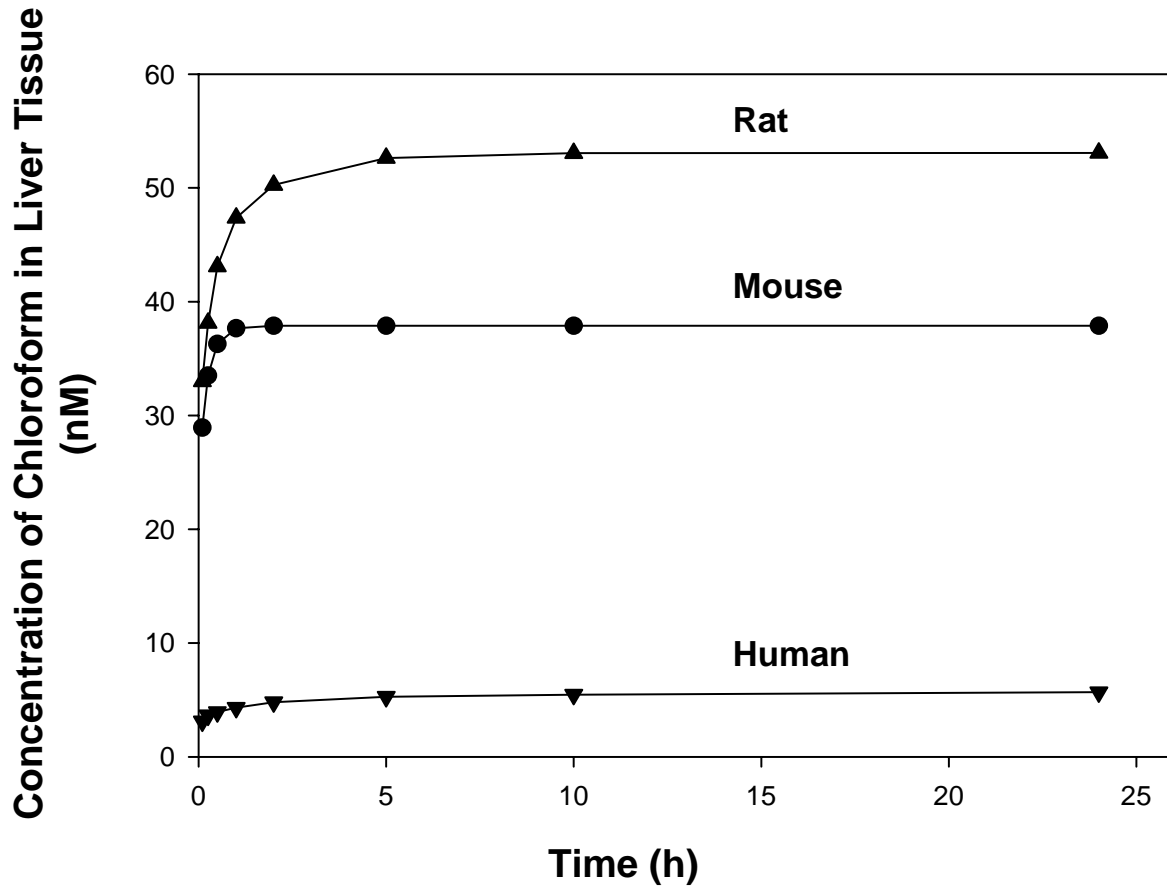


FIGURE 5-5

Achieving Steady State in Liver Tissue. Each of the models was used to simulate a continuous exposure to 5 ppm chloroform in inspired air. Results demonstrate that the concentration of chloroform in liver reaches steady state in mice more rapidly than humans or rats.

1.0, 1.5, 2, 5, 10, and 20 ppm. Once steady state for chloroform concentration in liver was attained, each of the models was used to simulate chloroform metabolism over the ensuing 24 hours to provide general information on species differences in metabolism (Figure 5-6). This simulation differs from that in which 24-h chloroform metabolism was predicted using rats and mice exposed for 6 hours as the basis for quantitative dose adjustment for risk assessment (refer to Figure 5-3). The present simulation was conducted to examine the exposure-metabolism relationship.

The second, and least extensive, set of simulations involved only the mouse model in estimating  $CM_{24}$  under an intermittent exposure. To demonstrate that chloroform concentrations do not accumulate with repeated daily 6-h exposures and that a single exposure cycle with an intermittent exposure was sufficient to estimate  $CM_{24}$  for species extrapolation, the model simulated a 6-h, 5 ppm exposure repeated daily for 7 ds. Results (not shown) demonstrated that hepatic chloroform concentrations returned to baseline within 24 hs of exposure (6 hs on exposure, 18 hs off). Therefore,  $CM_{24}$  was determined using a 6-h, 5 ppm chloroform exposure. The resulting  $CM_{24}$  value was used as a point of departure for species comparison. The concentration-metabolism relationship developed for the general adult human model (Figure 5-7) was used to identify the continuously encountered concentration resulting in the  $CM_{24}$  value observed in the 6-h, 5-ppm exposed mouse.

The third set of simulations examined changes in chloroform metabolism related to human interindividual differences in metabolic capacity, tissue:air partitioning, and HBF, as well as differences in sex- and age-related parameter values. To demonstrate age-dependent differences, three continuous exposure concentrations (0.9, 2.5, and 5 ppm) were used, and the

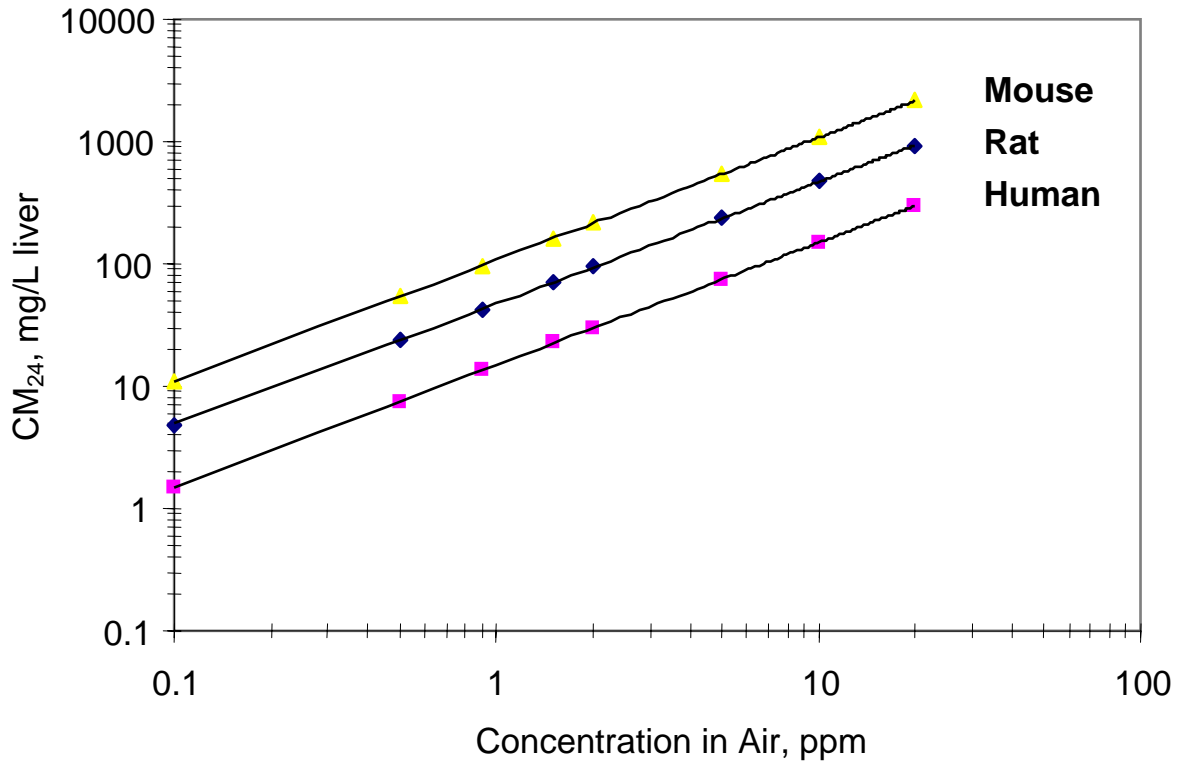


FIGURE 5-6

Relationship Between Exposure Concentration and CM<sub>24</sub> in Rats, Mice, and Humans at Steady State. These results demonstrate a marked linearity in chloroform metabolism (CM<sub>24</sub>) over the exposure range 0.1 to 20 ppm in both rats and humans under steady state, and infer species differences useful in estimating the HEC.

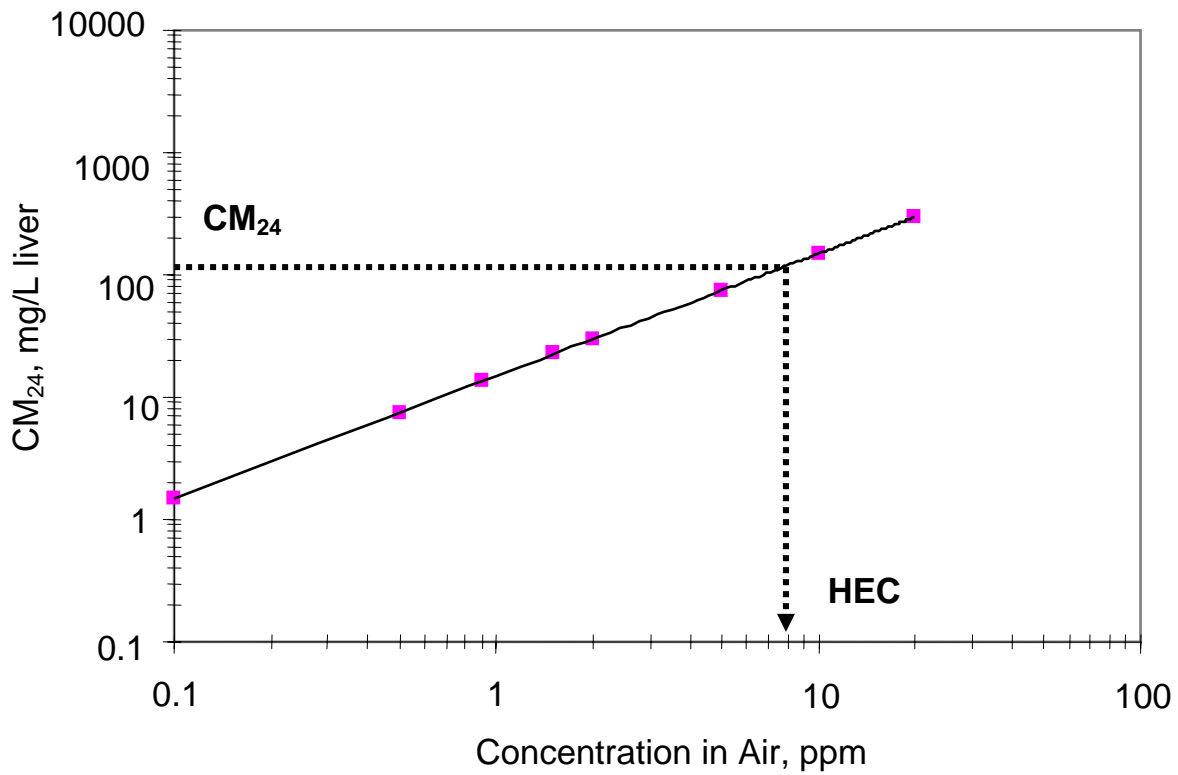


FIGURE 5-7

Derivation of the Human Equivalent Concentration (HEC). CM<sub>24</sub> resulting from the no-effects exposure (5 ppm × 6 hours) in mice was determined. Results from the human PBPK model, under a continuous exposure at steady state indicate that an equivalent exposure would be 8.1 ppm.

human model was adapted to include “general” values for each parameter, including those for children.

Demonstration of the HEC accounts for species-dependent TK differences. To account for species differences in sensitivity (the TD component of the animal-to-human uncertainty factor;  $UF_{A-TD}$ ) and because of the linear relationship between exposure and metabolism order of magnitude, e.g., 3.16. This half-order of magnitude value was applied because TK accounts for only part of the interspecies differences, and the EPA has recently retained a partial default (one-half order of magnitude,  $10E^{0.5}$ ) for residual TD differences. Because the default value for  $UF_A$  is 10, a value of 3.16 (one-half order of magnitude) was assigned to represent the TD “uncertainty” for  $UF_A$ . The  $CM_{24}$  in the general adult human model resulting from an exposure to  $HEC/3.16$  was determined and used as a benchmark against which to evaluate human interindividual differences. The adult male human model was reparameterized to include values for  $V_{max}C$ , HBF, and blood:air partitioning (with resulting changes in blood:tissue partitioning) that were representative of observed variability. The model was adapted for children of 30 kg and 10 kg body mass (aged nine and one years, respectively) by including (external concentration and  $CM_{24}$ , the HEC (rather than the  $CM_{24}$  value) was divided by one-half weight/age-related child organ volumes and enzyme content, B:A PC values (derived using remnant blood samples from children), and T:A PC values (derived from PND 10 rats). The  $CM_{24}$  resulting from exposure of the general adult to  $HEC/3.16$  was determined at steady state. Within each model, one parameter was varied at a time to demonstrate the effect of its variance on  $CM_{24}$ , and the magnitude of impact of varying each parameter was characterized by the change in external concentration resulting in the same  $CM_{24}$  value. To determine the impact of sex-dependent changes in body composition, the model for the adult human female was

exercised to simulate exposure to (HEC/3.16) ppm until steady state was reached, and CM24 was compared to that attained in the adult human male model, exercised to simulate the same exposure conditions. To examine the impact of obesity, the “general” adult human male model and the obese adult male human model were exercised to simulate steady state exposures to 0.75, 2.56 and 10 ppm chloroform.

## **RESULTS**

**Derivation of the Rodent NOAEL Values.** Four important studies (Larson et al., 1996; Templin et al., 1996, 1998; Constan et al., 2002) provide data useful in estimating a NOAEL for liver and/or kidney effects in mice. This section reviews the exposure concentrations and estimates a duration-adjusted exposure concentration for each exposure concentration to compare results among slightly differing exposure protocols and to demonstrate the use of conventional risk assessment methods in estimating an RfC value with default uncertainty factor values. However, no duration adjustment will be made in the exposure extrapolation between animals and humans, because the extrapolation will be based on an internal dose metric describing chloroform metabolism in the liver.

Constan et al. (2002) exposed female B6C3F1 mice to chloroform for 7 ds at concentrations of 0, 10, 30, and 90 ppm for different daily durations (Table 5-11). These authors concluded that duration, as well as concentration, played a critical role in toxicity. They concluded that exposures at 10 ppm for durations of approximately 6 hours or longer could lead to an increased LI, which is evidence of tissue regeneration, in the liver of B6C3F1 mice. They also applied a PBPK model for mice and humans into which they incorporated their derived values for mouse chloroform partition coefficients and the values for human chloroform tissue partition coefficients from Corley et al. (1990). The B:A PC values used in Constan et al. (2002)

TABLE 5-11

Exposure Conditions, Relative Liver Weight, and Hepatocyte Labeling Index  
from Constan et al. (2002)

Exposure		Relative liver weight <sup>a</sup>	Labeling Index
Conc., Duration	C × T		
0 ppm, 6 hours	0	4.72 ± 0.32	0.55 ± 0.27 <sup>b</sup>
0 ppm, 18 hours	0	4.45 ± 0.21	0.70 ± 0.22 <sup>c</sup>
10 ppm, 6 hours	60 ppm × h	5.54 ± 0.46 <sup>d</sup>	0.93 ± 0.32
10 ppm, 18 hours	180 ppm × h	5.55 ± 0.31 <sup>d</sup>	1.83 ± 1.05
30 ppm, 2 hours	60 ppm × h	4.93 ± 0.14	1.50 ± 1.23
30 ppm, 6 hours	180 ppm × h	5.07 ± 0.25	2.94 ± 1.95 <sup>d</sup>
30 ppm, 12 hours	360 ppm × h	5.97 ± 0.37 <sup>d</sup>	10.04 ± 3.96 <sup>d</sup>
90 ppm, 2 hours	180 ppm × h	5.16 ± 0.17 <sup>d</sup>	2.82 ± 1.10 <sup>d</sup>
90 ppm, 6 hours	540 ppm × h	6.27 ± 0.42 <sup>d</sup>	19.92 ± 4.00 <sup>d</sup>

Values are presented as mean ± S.D., n = 5 mice.

<sup>a</sup> Percentage weight gain at necropsy from preexposure body weight. Average initial body weights were 12.1 ± 1.2 grams.

<sup>b</sup> Control for the 2- and 6-h exposure groups.

<sup>c</sup> Control for the 12- and 18-h exposure groups.

<sup>d</sup> Significantly greater than respective control,  $p < 0.05$ .

were 24.3 for mice and 7.3 for humans. Their model results demonstrated that the human would have to be exposed to 110 ppm to drive chloroform metabolism at the rate per gram liver observed in the 10-ppm exposed mouse.

Templin et al. (1998) exposed BDF1 mice to chloroform 6 hs/d, 5 ds/wk via inhalation for up to 13 wks (Table 5-12). Targeted exposure concentrations were 0, 1, 5, 10, 30, and 90 ppm. Daily checks verified that chamber concentrations were within 0.5% of targeted concentrations for the 5-, 30-, and 90-ppm concentrations, and within 8% of the 1-ppm concentration. Male mice were exposed for 3, 7, or 13 wks. Female mice were exposed for 3 or 13 wks. Male mice exposed to 30 and 90 ppm were “stepped up” to the final concentration. Male mice in the 30-ppm group were exposed to 5 ppm for 2 wks, to 10 ppm for another 2 wks, then to 30 ppm beginning on wk 5. Male mice in the 90-ppm group were exposed to 5 ppm for 2 wks, to 10 ppm for the next 2 wks, to 30 ppm for wks 5 and 6, then to 90 ppm beginning on wk7. Female mice were exposed for 3 and 13 wks to 5, 30, or 90 ppm without the step-up procedure.

Templin et al. (1998) found that concentrations above 5 ppm produced histological changes in liver and kidney of male and female mice, but histological changes were not evident in liver or kidney of either males or females exposed to 5 ppm chloroform. This data set establishes 5 ppm as a NOAEL for these effects in BDF1 mice (Table 5-13).

Larson et al. (1996) examined the response of B6C3F1 mice exposed to chloroform at 0, 0.3, 2, 10, 30, and 90 ppm by inhalation. Measured chloroform average concentrations were 0.3, 1.99, 10.0, 29.6, and 88 ppm. Exposures were conducted for 6 hs/d, daily for 4 ds for 3, 6, or 13 wks; or for 6 hs/d, 5 ds/wk for 13 wks (Table 5-12). Histopathology and LI of the nasal passages, kidney, and liver were examined. In female mice, that nasal turbinate LI was significantly elevated after 4-d exposure at 10 ppm and above, after 3-wk exposure at 2 ppm and

TABLE 5-12

## Exposure Conditions and Endpoints Examined in Rodent Inhalation Bioassays

Study	Species	Concentration	Duration	Endpoint
Constan et al. (2002)	B6C3F1 mice	0, 10, 30, 90 ppm	2, 6, 12, 18 hs/d × 7 ds	LW:BW, hepatocyte LI
Templin et al. (1998)	BDF1 mice	0, 1, 5, 30, 90 ppm	6 hs/d, 5 ds/wk, 3, 7, or 13 wks	Liver and kidney histopathology
Larson et al. (1996)	B6C3F1 mice	0, 0.3, 2, 10, 30, 90 ppm	6 hs/d, 7 ds/wk, 4 ds, 3, 6 or 13 wks; 6 hs/d, 5 ds/wk, 13 wks	Nasal passages, liver, and kidney histopathology
		0, 10, 90 ppm	13 wks, 6 hs/d, 5 ds/wk	Liver and kidney LI
Templin et al. (1996)	F344 rats	0, 2, 10, 30, 90, 300 ppm	6 hs/d, 7 ds/wk, 4 ds, 3, 6 or 13 wks	Nasal passages, liver, and kidney histopathology and LI; LW:BW; KW:BW
		0, 30, 90, 300 ppm	6 hs/d, 5 ds/wk, 13 wks	

TABLE 5-13

## Endpoints and Response Levels Identified in Rodent Inhalation Bioassays

Study	Duration	NOAEL	LOAEL	Endpoint
Constan et al. (2002)	7 ds	30 ppm, 2 hs/d; 10 ppm, 18 hs/d	30 ppm, 6 hs/d	Hepatocyte LI
Templin et al. (1998)	13 wks, 5 ds/wk	90 ppm male 30 ppm female	ND male 90 ppm female	Liver LI
		5 ppm male 90 ppm female	30 ppm male ND female	Kidney LI <sup>a</sup>
		5 ppm male 30 ppm female	30 ppm male 90 ppm female	LW:BW
Larson et al. (1996)	13 wks, 7 ds/wk	30 ppm male 10 ppm female	90 ppm male 30 ppm female	Liver LI
	13 wks, 5 ds/wk	10 ppm male 10 ppm female	90 ppm female 90 ppm female	Liver LI
	13 wks, 7 ds/wk	10 ppm male	30 ppm male	Kidney LI <sup>a</sup>
	13 wks, 5 ds/wk	ND male	10 ppm male	
	13 wks, 7 ds/wk	90 ppm male 90 ppm female	ND male ND female	Nasal turbinate LI
Templin et al. (1996)	13 wks, 7 ds/wk	90 ppm male 90 ppm female	300 ppm male 300 ppm female	Liver LI
	13 wks, 5 ds/wk	90 ppm male 90 ppm female	300 ppm male 300 ppm female	Kidney LI
	13 wks, 7 ds/wk	10 ppm male 10 female	300 ppm male 30 ppm female	
	13 wks, 5 ds/wk	30 ppm male 30 ppm female	90 ppm male 90 ppm female	LW:BW and KW:BW
	13 wks, 7 ds/wk	30 ppm <sup>b</sup>	90 ppm <sup>b</sup>	
	13 wks, 7 ds/wk	2 ppm male <sup>c</sup>	10 ppm male <sup>c</sup>	Nasal ULLI
	13 wks, 5 ds/wk	10 ppm male <sup>c</sup>	30 ppm male <sup>c</sup>	

<sup>a</sup> Chloroform exposure did not induce histologic changes in kidneys of female mice.

<sup>b</sup> Reported in general without regard to sex.

<sup>c</sup> Data for females stated to be similar, but not shown.

ND = effect level not demonstrated.

above; and after 6-wk exposure only at 90 ppm; but it was not significantly elevated in any group examined after 13 wks of exposure. Nasal lesions occurred in mice exposed to 10 ppm and above; they were transient and only observable after 4 ds of exposure. These authors concluded that after 6 wks of exposure, only exposure to 30 ppm and higher produced biologically significant liver alterations in the female mice. After 7-ds/wk exposure for 13 wks, “very mild degenerative changes” were noted in the livers of mice exposed to 10 ppm. In contrast, no significant liver changes were found in the mice exposed for 13 wks to 10 ppm chloroform but only for 5 ds/wk. The authors concluded that 10 ppm was a NOAEL value for liver effects. Renal effects were not observed in female mice exposed under any of these experimental exposure regimens (Table 5-13).

Larson et al. (1996) indicated that nasal lesions and regenerative cell proliferation in males were similar to those in female mice and observed no other respiratory tract effects. The incidence of “mild” liver lesions in male mice was elevated to 30 ppm and higher over controls after 6 wks of exposure. The hepatocyte LI was significantly elevated only in male mice that were exposed to 90 ppm, at both 6 and 13 wks of exposure. Among mice exposed to 90 ppm chloroform for 13 wks, those exposed for 5 ds/wk demonstrated a significantly elevated hepatocyte LI versus controls; however, the LI in those exposed mice was significantly lower than that observed in male mice exposed to 90 ppm for 7 ds/wk. The effect of exposure duration (continuous versus 2 ds off) was also evident in the liver changes observed in female mice exposed to 30 ppm chloroform, indicating the importance of duration of exposure as a determinant of effect. Renal lesions (nephropathy) in male mice were confined to the proximal convoluted tubules (PCT) epithelial cells. After 3 wks of exposure, concentration-dependent increases in nephropathy were evident in the 30- and 90-ppm groups. Enlarged PCT epithelial

cell nuclei were observed in male mice exposed for 13 wks to chloroform at 10, 30, and 90 ppm; enlarged nuclei and scattered areas of regenerating foci were found in male mice exposed for 13 wks, 5 ds/wk. For renal effects, the 5-ds/wk, 13-wk concentration of 10 ppm represents a LOAEL; and the 2-ppm exposure represents the NOAEL (Table 5-13). The authors concluded that, for kidney effects, B6C3F1 mice were more sensitive to a 5-ds/wk regimen than a continuous regimen, indicating that a “days-off” exposure might better allow for cellular regeneration. Furthermore, Larson et al. (1996) found that the nasal lesions demonstrated in these mice occurred only at 10 ppm and higher concentrations and were transient. They concluded that the nasal response may be only a minor concern for environmentally exposed people, given the lower concentrations found in the environment.

Templin et al. (1996) examined the formation and distribution of histologic changes and LI in liver, kidney, and nasal tissues of F-344 rats exposed to chloroform vapor for up to 13 wks. Male and female rats were exposed for 6 hs/d, 7 ds/wk to chloroform at concentrations of 0, 2, 10, 30, 90, or 300 ppm. Renal effects such as scattered vacuolization, individual tubular cellular necrosis, and enlarged nuclei were observed in male rats exposed to 90 and 300 ppm for 7 ds/wk, but not in those exposed to 30 or 90 ppm for 5 ds/wk. A significantly increased LI in renal cortex was observed in male and female rats exposed to 30 ppm 7 ds/wk, but not in those exposed 5 ds/wk, for 13 wks. Livers of male rats were affected by 13 wks of chloroform exposure at the 90 and 300 ppm exposure level, but not at the lower concentrations. The LI was only elevated at the 300 ppm level. Rats exposed for 13 wks at 90 ppm demonstrated scattered vacuolated hepatocytes (6 of 15 rats) and single-to-multiple hepatocytes necrosis (9 of 15 rats). Mitotic figures and diffuse vacuolization of liver were evident in male rats exposed to 300 ppm

for 13 wks. Thus, as determined for male F-344 rats, 30 ppm is the NOAEL for male rat liver effects, and 10 ppm is the NOAEL for renal effects (Table 5-13).

In female F-344 rats exposed 13 wks to 30 ppm and above, Templin et al. (1996) observed histologic changes consisting of vacuolization, whereas comparable male rats demonstrated vacuolization and necrosis. As in the male rats, the LI in renal cortex was significantly elevated in 30-ppm exposed female rats. In the liver, areas of mild vacuolization and, infrequently, hepatocyte degeneration were observed in female rats exposed for 13 wks to 90 ppm chloroform. Centrilobular-to-midzonal degeneration was evident in 300-ppm exposed female rats. Similar to previous observations in male rats, female rats exposed to 90 ppm for 5 instead of 7 ds/wk demonstrated liver profiles that were not significantly different from control rats. Among the 13-wk exposed female rats, the hepatocyte LI was increased only in the 300-ppm exposure group. This concentration, but no other, produced increases in the LI after 3 wks of exposure. Thus, female F-344 rats appeared to demonstrate fewer of the severe consequences of chloroform exposure, even though they demonstrated a NOAEL for renal effects at 10 ppm. The NOAEL for female rat liver effects was 90 ppm (Table 5-13).

In summary, liver effects can serve as the critical effect, and NOAEL values can be developed for both the mouse and rat from studies by Templin et al. (1998) and Templin et al. (1996), respectively. Data from these studies demonstrate a 6-hs/d exposure to 5 ppm in mice as a NOAEL.

**Model Response.** The model was successfully parameterized with mouse, rat, and adult male human values for partitioning, body composition, blood flows, and metabolic rates extrapolated from *in vitro* studies with hepatic MSP (rat and human) or extrapolated from *in vivo* gas uptake studies with mice. To examine the likelihood of the rapid attainment of steady state, as measured

by the concentration of chloroform in liver tissue, each model was used to simulate a continuous exposure to 5 ppm chloroform in inspired air. Results over the initial 24 hours (see Figure 5-3) show that several hours are necessary to reach steady state, and that steady state is not achieved in a similar time frame between species.

An example of model function at a fixed, continuously encountered concentration was provided by simulating exposure to 5 ppm chloroform, which represents a concentration one-half that established as the TLV for the workplace. Results indicated that 5-ppm exposure resulted in roughly 540 mg/L (in liver) of metabolites formed over a 24-h period in the mouse and that 234 mg/L (in liver) of metabolites formed over a 24-h period in the rat. Exposure of the general adult (male) human to 5 ppm under steady-state conditions resulted in a  $CM_{24}$  of roughly 75 mg/L (in liver), about one-third that of the similarly exposed rat and nearly 14% that of the similarly exposed mouse (see Table 5-14, Figure 5-6). In comparison, simulated exposure to 16 ppm in the general adult (male) human was required to bring the  $CM_{24}$  value (238.8 mg/L) near the  $CM_{24}$  value attained in the 5-ppm exposed rat (234.39 mg/L). Exposure of the human to 36 ppm was required to attain the  $CM_{24}$  value (540 mg/L) demonstrated in the 5-ppm exposed mouse. These results demonstrate that, compared to rodents, the human converts much less of a dose of chloroform to toxic metabolites. The results presented in Table 5-14 indicate that the formation of metabolites was proportionately related to exposure concentration over the range surrounding this concentration, in adults and in children. Likewise, differences among age groups were consistent over this range.

**Chloroform Model Verification.** This report presents the application of a single model structure to characterize metabolism of chloroform in mice, rats and humans. Confidence in the model's predictive ability is increased when predictions of pharmacokinetic outcomes are similar

TABLE 5-14

## Chloroform Metabolized in Liver in Mice, Rats, and General Adult (Male) Humans

Species	CM <sub>24</sub> (mg/L)	Percent of General Adult Human
5 ppm at Steady State		
Mouse	540.4	724
Rat	234.39	314
General Adult Human	74.64	100
General 9-year-old Child	93.97	126
General 1-year-old Child	100.56	135
2.5 ppm at Steady State		
Mouse	270.18	724
Rat	117.15	314
General Adult Human	37.31	100
General 9-year-old Child	46.99	126
General 1-year-old Child	50.21	135
0.9 ppm at Steady State		
Mouse	97.29	724
Rat	42.22	314
General Adult human	13.43	100
General 9-year-old Child	16.91	126
General 1-year-old Child	17.97	134

to observed values for pharmacokinetic measurements made *in vivo* in the species studied. There are no established guidelines for acceptability, though increased emphasis should be placed on regions of the exposure-response continuum relevant to the intended use. For example, confidence in model predictions verified only by fit to observations made at exposure concentrations that are orders of magnitude above the range of exposures where the model will be used in species extrapolation will do little to instill confidence in model predictions at low concentrations. Increased confidence in model predictions can be obtained when comparisons between observed values and predicted values can be made using data more closely related to the dose metric of interest, rather than further from it. In the present application, the identified dose metric was the integrated exposure of the liver to chloroform metabolites over 24 hours, basically, an AUC measurement. Several pharmacokinetic outcomes could have been selected for efforts to verify the model. These could have included disappearance of chloroform from closed-chamber studies, exhalation of absorbed chloroform, concentration-time profiles for chloroform in circulating blood or plasma, etc. However, this effort identified and employed observations of chloroform metabolism because they are more closely related to the risk-relevant dose metric for the toxicity studies. Here, comparisons between observations of chloroform metabolism in mice (Corley et al., 1990) and adult male and female humans (Fry et al., 1972) and model predictions are made for the purpose of model verification.

Initially, it was thought that the rat would serve as the sensitive species, instead of the mouse, and thus represent the species from which human predictions would be extrapolated. For that reason, partition coefficients were determined using blood, liver, kidney, muscle, and fat from the rat as well as blood from humans; and metabolic rate constants were derived *in vitro* using liver preparations from rats and humans. Inasmuch as the approach was ultimately revised

to employ the mouse as the sensitive species, and because the human model contains tissue:blood partition coefficient values derived from rat tissue:air and human blood:air partition coefficient values, it seems only reasonable that efforts be undertaken to compare model predictions to observations of chloroform metabolism in rat, mouse and humans, where possible. Additionally, we will examine implications of the appreciable difference between the values for  $K_m$  which we derived *in vitro* and applied in the present modeling approach versus values for  $K_m$  optimized by modeling software used in previous PBPK approaches to chloroform dosimetry, including that of Corley et al. (1990). This will serve four purposes: 1) model structure will be justified, 2) the application of values for partition coefficients developed for rat tissues will be justified, 3) greater confidence can be placed in model predictions from the human model, which contain tissue partition coefficients based in part on observations made with rat tissues, and 4) sufficient confidence can be placed in the approach of extrapolating and incorporating *in vitro*-derived metabolic rate constants as accomplished in the present work.

**Comparisons to Mouse and Rat Pharmacokinetic Data.** A data set described by Corley et al. (1990) contains information obtained from rats and mice exposed to chloroform in an open-chamber study design. In that modeling approach, whole-body chloroform metabolism was simulated by developing metabolic rate constants using data describing whole-body metabolism. Metabolic rate constants ( $K_m$  and  $V_{maxC}$ ) were optimized by allowing the model software to vary them until adequate fit was observed between experimentally-collected data and model predictions. *In vivo* data on chloroform metabolism were collected from mice and rats by conducting open-chamber exposures were for six hours. Mice were exposed to 10, 89 and 399 ppm; rats were exposed to 93, 356 and 1041 ppm. These exposure concentrations are higher

than those used in the simulations here conducted for species extrapolation of dose, especially so for the rat.

Differences between the modeling approaches used (Corley et al. versus the present), especially those relating to developing model predictions of total (whole-body) chloroform in the former and application only of liver-specific metabolic capacity to predict chloroform metabolism in the latter, require specific considerations of fit between observed and predicted values for metabolism. Additionally, the source for metabolic rate constants for the rat in the two modeling approaches (Corley used model-optimized values; the present approach extrapolated *in vitro*-derived metabolic rate constants) and the tissue-specificity of the rate constants must also be considered. Chloroform metabolism is saturable, and Michaelis-Menten rate descriptions of metabolic rate are appropriate. *In vivo*, tissue concentrations of chloroform serve as substrate concentrations in the Michaelis-Menten rate equation.

The model structure and exposure scenarios simulated in our investigation are suitable to simulate open-chamber results simulated by Corley et al. (1990). Corley et al. (1990) used radio labeled chloroform to facilitate metabolite quantification; loss rates from atmosphere are not collected in the open-chamber design. The evaluation of these data offer advantage over closed-chamber data describing loss of chloroform from the finite amount available in the atmosphere, because Corley measured chloroform metabolism in rats and mice, rather than disappearance from headspace/atmosphere. This pharmacokinetic outcome (chloroform metabolized) is more closely related to the dose metric of interest (chloroform metabolite per unit liver mass;  $CM_{24}$ ) than is loss of chloroform from atmosphere. Inasmuch as Corley observed saturation of whole-body (total) chloroform metabolism between 93 and 356 ppm concentrations in the rat, and because predictions of metabolic rates under saturating exposure conditions are sensitive to

values for  $V_{maxC}$ , but insensitive to values for  $K_m$ , and because the rat is not the species used for extrapolation, fit to the rat data is not so critical as fit to the mouse data.

Corley's predicted values were 0.88 to 2.08 fold different from observed values, and these differences were more pronounced in rats and mice, each, at the lower range of concentrations evaluated. Table 5-15 demonstrates the observed amounts of chloroform metabolized from rats and mice (Corley et al., 1990), amounts of chloroform metabolized as predicted by the model developed by Corley et al. (1990) and the amounts of chloroform metabolized as predicted by the present model. As presented, the fit between Corley's predictions and the observations is not appreciably different for the mouse, but differ to some extent for the rat. However, both are adequate.

Although the species extrapolation here employed involves mice and humans, emphasis on rat model comparison is made because 1) human tissue partition coefficients are based in part on rat tissue:air partition coefficients, which are used in the rat model, and 2) both the rat and human models rely on the extrapolation of *in vitro*-derived metabolic rate constants for chloroform derived with liver preparations, and are expressed solely in terms of hepatic metabolism. Confidence developed for the adequacy of the rat model and its basis should carry over directly over directly to the human model, and should be tempered with information describing the comparison of human predictions to observations of chloroform metabolism in the human.

With respect to mice, the present model offers a slightly improved fit to the available observations for chloroform metabolism seen at the lowest concentrations. This lends confidence to its application to simulate chloroform metabolism in mice, used as the point of

TABLE 5-15

Results from Open Chamber Metabolism Studies in Rats and Mice <sup>a</sup>

Species	ppm	Total Metabolized			
		Observed	Corley -Predicted		Present - Predicted
Mouse	10	0.22 mg	0.46 mg	(2.08) <sup>b</sup>	0.37 mg (1.68) <sup>b</sup>
	89	2.14	3.99	(1.86)	3.25 (1.51)
	366	6.76	6.18	(0.91)	9.95 (1.47)
Rat	93	12.10	13.41	(1.11)	9.49 (0.78)
	356	19.40	22.74	(1.17)	11.75 (0.61)
	1041	35.03	30.79	(0.88)	11.83 (0.34)

<sup>a</sup> From Corley et al. (1990).<sup>b</sup> (Predicted:Observed)

extrapolation and the basis for quantification for species difference in chloroform metabolism that will be used to develop the HEC.

The values for model parameters employed in the Corley et al. (1990) model fit the data better, but  $K_m$  values in that study were determined by model optimization, rather than by a more direct *in vitro* evaluation, as done in the present study. Thus, it is not surprising that the model parameters employed in the Corley model result in a better “fit” to the observations than those in the present study. However, for the reasons discussed in following paragraphs, this apparent difference in model fit (for rat data, especially) should not diminish confidence in the predictive capabilities of the present model. Smith and Evans (1995) have also addressed confidence placed in model-optimized values for metabolic rate constants.

The observed difference between observations and predictions of Corley and of the present work of chloroform metabolism in the rat should not diminish confidence placed in the model, inasmuch as exposures of interest are much below 25 ppm, and because the rat does not serve as the basis for species extrapolation and HEC determination. Reasons for differences may relate to  $K_m$  values employed and the contributions of extrahepatic tissues to chloroform metabolism. While argument may be made that the observation of metabolic saturation in the present model may be a result of a lower  $K_m$  value being employed in the present model, versus the application of a model-optimized  $K_m$  value, as done in the previous (Corley) model, this seems to be poorly founded, for reasons discussed in following paragraphs.

**Model Sensitivity.** The sensitivity of the CF PBPK model to changes in selected parameter values was determined from simulations of inhalation exposure of an adult male to 2.56 ppm CF by varying the values of PB (blood:air partition coefficient for CF; unitless), QLC (hepatic blood flow; L/hr/kg),  $V_{maxc}$  (maximal rate of CF metabolism; mg/hr/kg) and  $K_M$

(Michealis constant for CF metabolism; mg/L) individually and examining the effect on  $CM_{24}$ , the integrated exposure of the liver to CF metabolites over 24 hours.

Figure 5-8 shows the effect of varying PB, the blood:air partition coefficient for CF, on  $CM_{24}$ . The PB reflects the solubility of CF in the blood that carries CF to the internal organs. As expected, the  $CM_{24}$  was low when the partition coefficient (solubility in blood) was low.  $CM_{24}$  increased nonlinearly when the value of the partition coefficient increased, reaching a plateau at a value of approximately 50 (Figure 5-8). Figure 5-9 shows the effect of changing the liver blood flow rate (QLC) on  $CM_{24}$  for CF.  $CM_{24}$  increased nonlinearly with increasing QLC. The dramatic decreases in  $CM_{24}$  were observed at QLC values below approximately 20% of cardiac output.

Figure 5-10a shows the relationship between  $V_{maxc}$ , the maximal rate of CF metabolism, and  $CM_{24}$ .  $CM_{24}$  was strongly dependent upon the rate of metabolism and rapidly increased up to a  $V_{maxc}$  value of approximately 0.5 mg/hr/kg. Figure 5-10b shows an expanded scale of the relationship between  $CM_{24}$  and  $V_{maxc}$  up to values of 2 mg/hr/kg, clearly illustrating the plateau in  $CM_{24}$  above a  $V_{maxc}$  of 0.5 mg/kg/hr. The  $CM_{24}$  values above this  $V_{maxc}$  were essentially the same, consistent with the interpretation that the rate of CF metabolism in the liver is limited by the rate of hepatic blood flow. Figure 5-10 clearly demonstrates that  $V_{maxc}$  values greater than 0.5 mg/hr/kg do not significantly increase  $CM_{24}$ . Thus, interindividual variability in  $V_{maxc}$  (a reflection of variability in enzyme content) at values greater than approximately 0.5 mg/hr/kg does not translate to interindividual variability in CF metabolism or  $CM_{24}$  (a risk-related endpoint), as has been demonstrated in the simulations of the CF PBPK model (U.S. EPA, 2004).

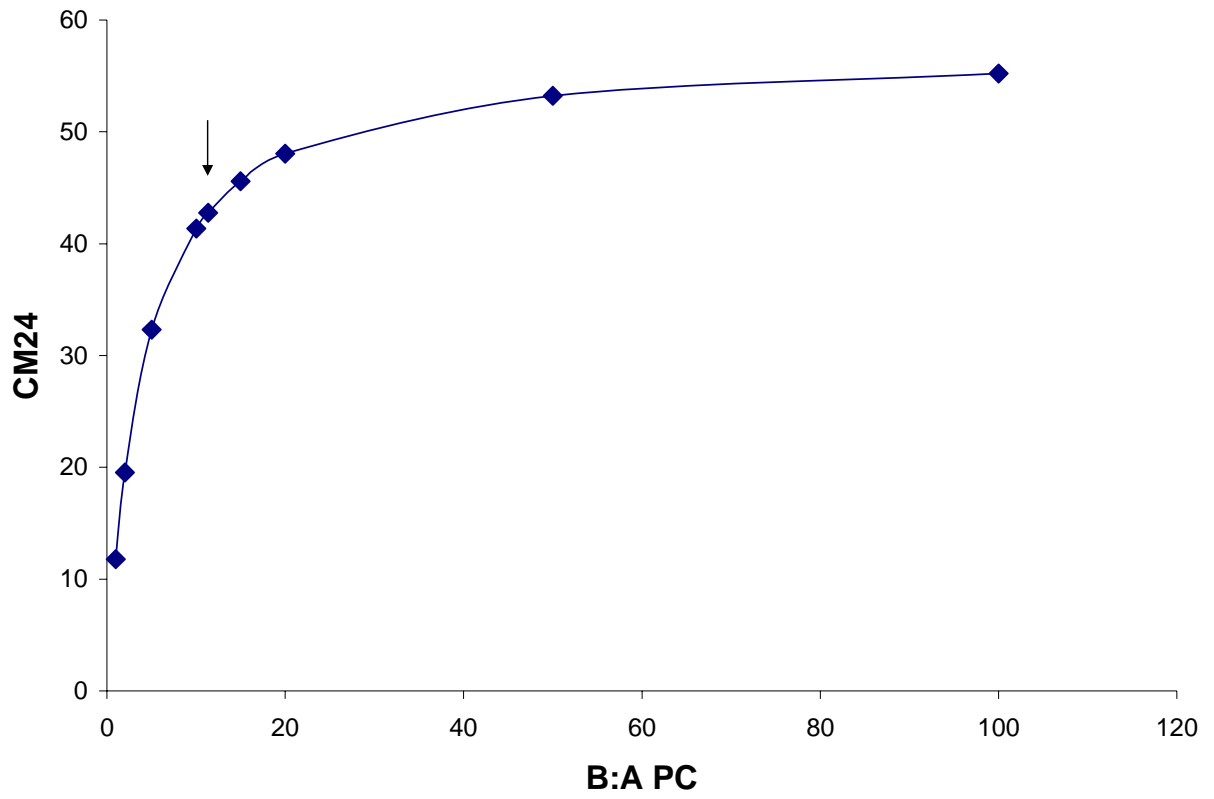


FIGURE 5-8

Relationship Between the Blood:air Partition Coefficient (B:A PC) for CF and CM<sub>24</sub>. The arrow indicates the B:A PC value used in the PBPK model.

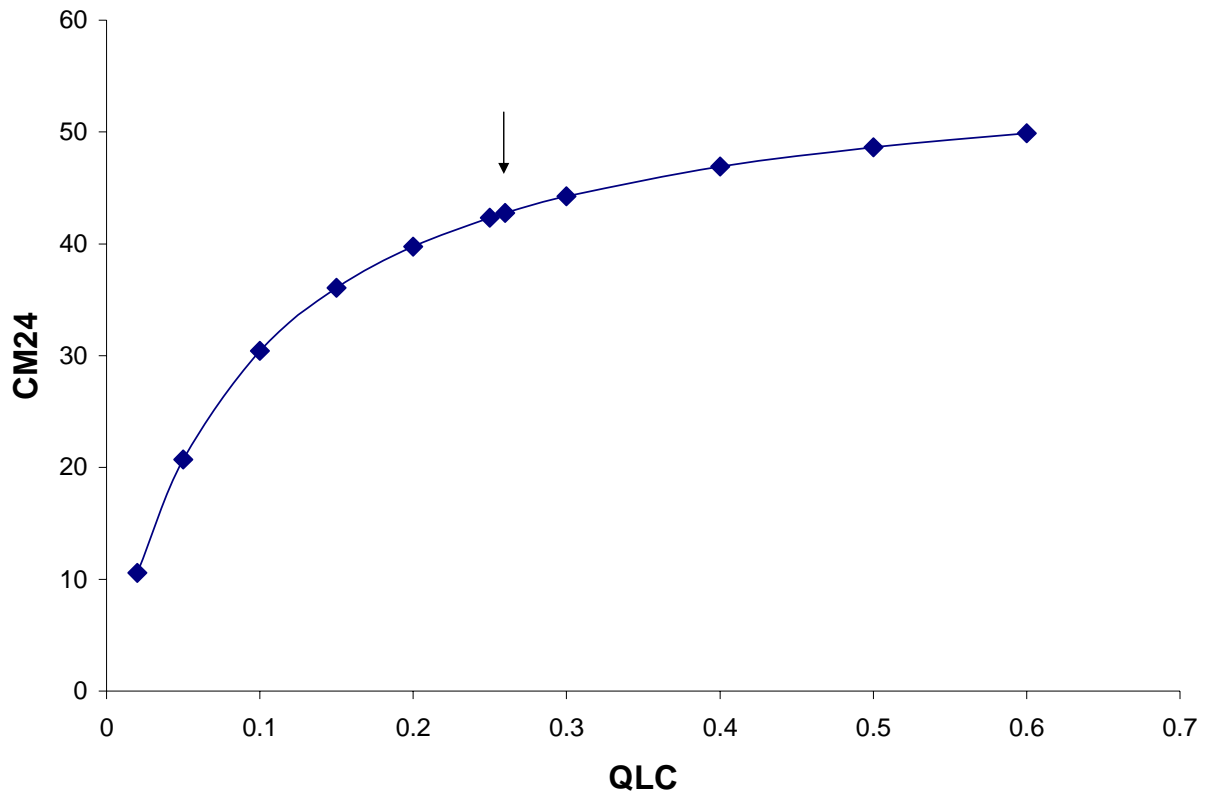


FIGURE 5-9

Relationship Between Hepatic Blood Flow (QLC) and  $CM_{24}$  for CF. The arrow indicates the QLC value used in the PBPK model.

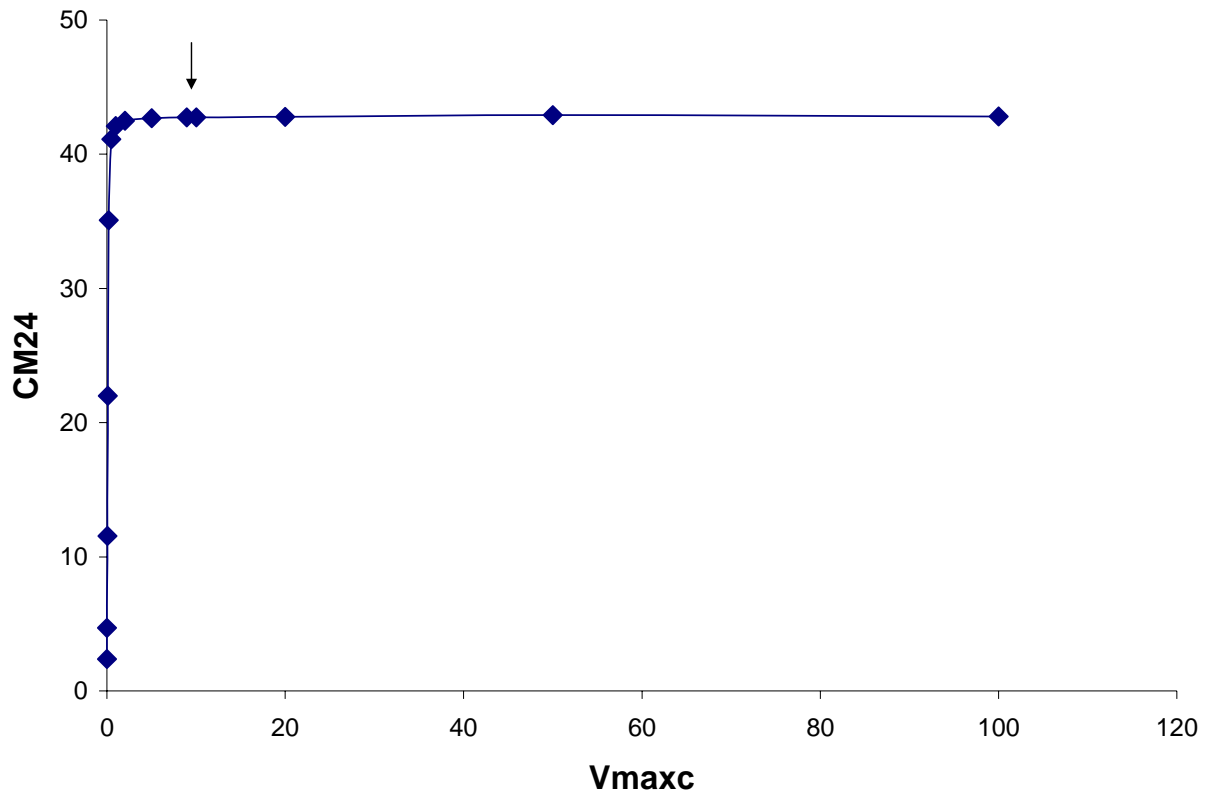


FIGURE 5-10a

Relationship Between the Maximal Rate of CF Metabolism (V<sub>maxc</sub>) and CM<sub>24</sub>. The arrow indicates the V<sub>maxc</sub> value used in the PBPK model.

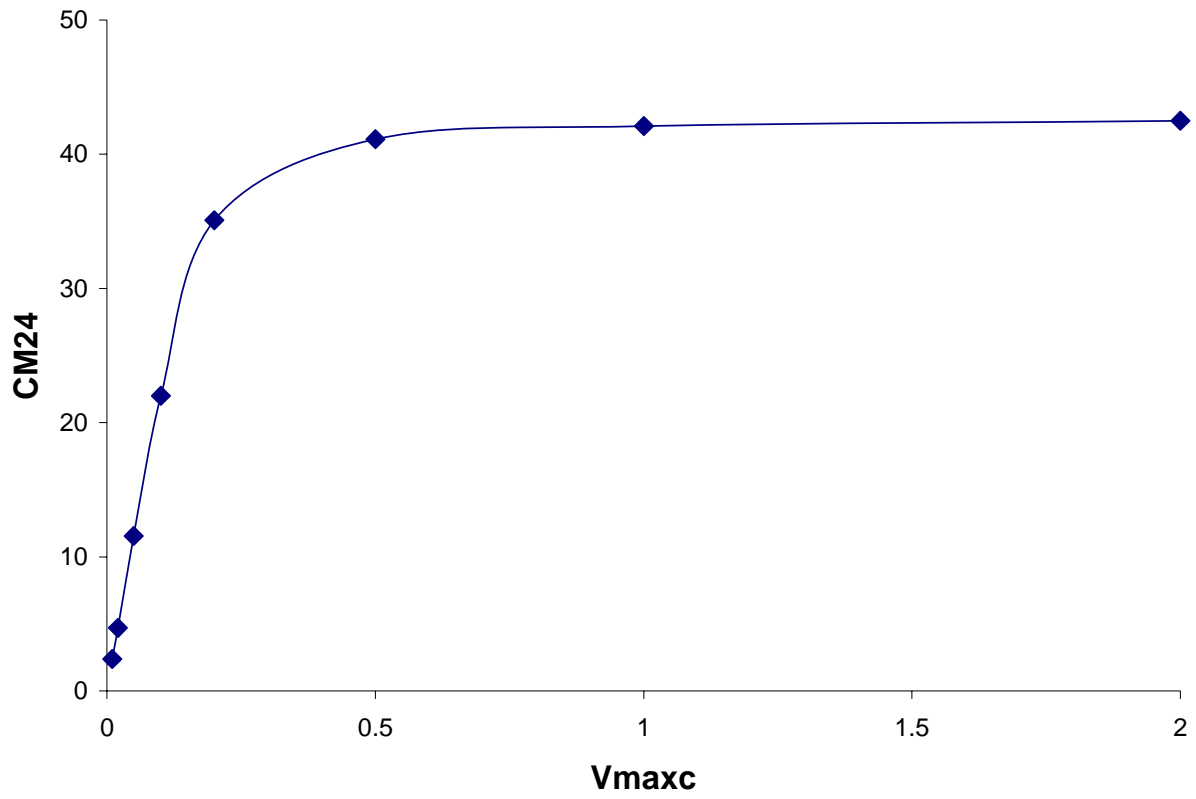


FIGURE 5-10b

Expanded Scale Showing the Relationship Between the Maximal Rate of CF Metabolism (Vmaxc) and CM<sub>24</sub>

Figures 5-11a and 5-11b show the effect of varying  $K_M$ , the Michaelis constant for CF metabolism, on  $CM_{24}$ . The  $K_M$  is defined as the CF concentration that gives one-half the maximal rate ( $V_{maxc}$ ) of CF metabolism. The  $K_M$  is a complex kinetic constant that contains terms for both the binding and catalytic oxidation of CF by CYP2E1. Changes in  $K_M$  will affect the initial rate ( $V/K$ ) of CF metabolism, with smaller  $K_M$  values yielding higher initial rates and hence larger  $CM_{24}$  values (Figure 5-11). As  $K_M$  increases, the initial rate of CF metabolism decreases, resulting in lower values of  $CM_{24}$  (Figure 5-11).

**Comparisons to Human Pharmacokinetic Data.** Corley et al. (1990) also reported findings from Fry et al. (1972), in which the cumulative amount of chloroform metabolized 8 hours following oral dosing was evaluated in human subjects. Fry et al. (1972) dosed human volunteers with 500 mg chloroform in olive oil encased in a gelatin capsule and measured pulmonary exhalation of  $^{13}C$ -labeled chloroform and carbon dioxide, and unchanged chloroform in urine. Subjects 1-5 were males with an average body weight of 70 kg (range 61.8-80 kg), and data from these subjects were pooled for a single representative example. For this group of five individuals, 1) average dose (mg/kg) was calculated, 2) average fraction of dose accounted for by pulmonary excretion of unmetabolized chloroform from average dose was determined, 3) average fraction of dose metabolized was determined by subtracting the fraction excreted unchanged in expired air from 1.0 to yield the average fraction of dose metabolized, and 4) the average fraction of dose metabolized was multiplied by the average dose to yield the average amount of chloroform metabolized, expressed as mg/kg. Subjects 6-8 were females with body weights 62.7, 59 and 58 kg, respectively. The PBPK model for the adult female was reparameterized to reflect these body weights and the amount of chloroform metabolized was calculated as above. Original data for body weight, total dose, and fraction of dose exhaled

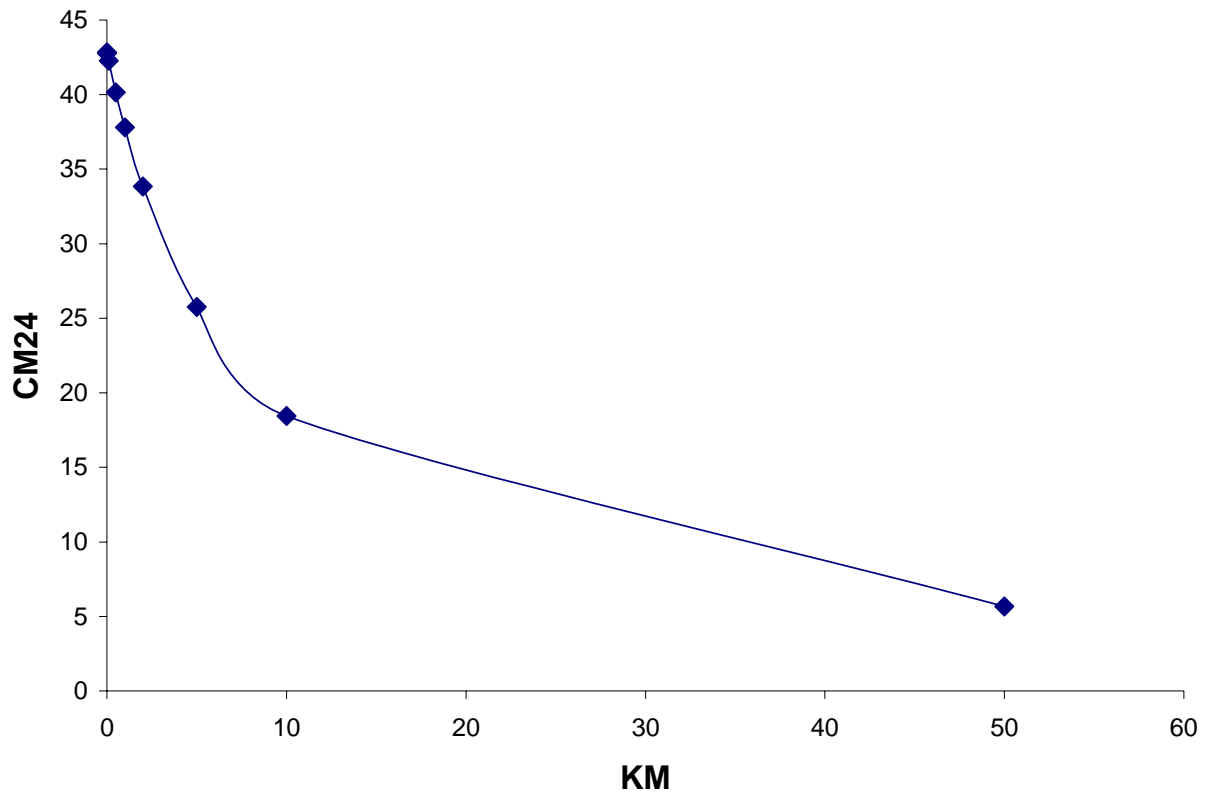


FIGURE 5-11a

Relationship Between the Michaelis Constant ( $K_M$ ) for CF Metabolism and  $CM_{24}$

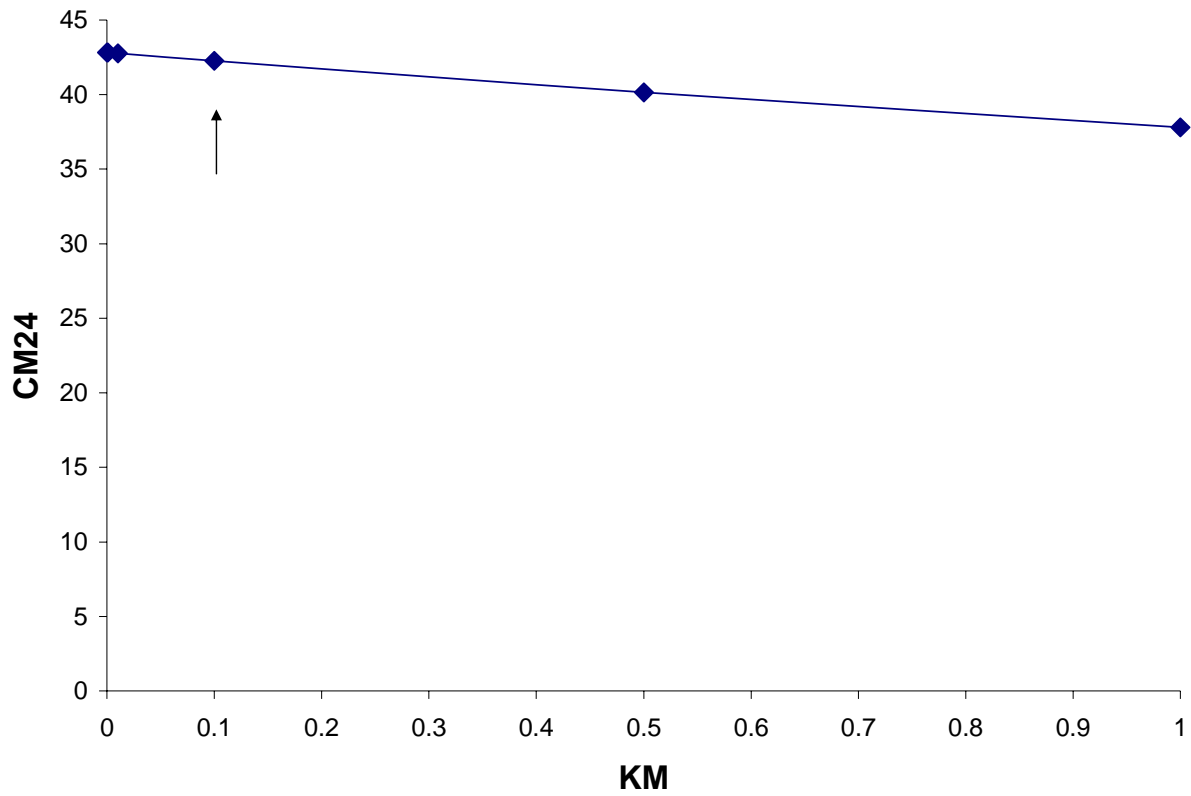


FIGURE 5-11b

Expanded Scale of the Relationship Between the Michaelis Constant ( $K_M$ ) for CF Metabolism and  $CM_{24}$ . The arrow indicates the  $K_M$  value used in the PBPK model.

unchanged are reported by Fry et al. (1972). Corley et al. (1990) reported the comparison of their prediction of chloroform metabolized to observations of Fry et al. (1972) for Subject 9, a 65-kg male receiving a dose of 1000 mg (15.4 mg/kg); for mean values from the group of five males; and for mean values from the group of three 500 mg-dosed females.

These comparisons were used to develop confidence in the original publication by Corley et al., and represent the best available data through which to develop comparisons of model predictions of chloroform metabolism in humans. Results presented in Tables 5-16 and 5-17 demonstrate a reasonable fit between observed amounts of chloroform metabolized and predictions, whether from the model developed previously by Corley and coworkers or the presently developed model, though predictions for the single 65 kg male are not as good as for the group. Based on the magnitude of the difference between observations and predictions, the comparison of predictors developed by the model here presented and the observations made by Fry et al. (1972) instills confidence in the predictive ability of the human models developed. These results, in the face of 5- to 15-fold different values for  $K_m$  and results presented in Figures 5-11a and 5-11b, underscore the relative insensitivity of this model to values for  $K_m$  and should belay concerns about the impact of  $K_m$  values as a sensitive model parameter when predicting cumulated amounts of chloroform metabolized (e.g.,  $CM_{24}$ ).

**Choice of Values for  $K_m$ .** The modeling of chemicals whose metabolism is limited by hepatic blood flow is somewhat complicated. In this endeavor, cumulated amounts of metabolite formed may not track closely with rates of metabolism. The present modeling endeavor has been scrutinized concerning the appreciable difference between the  $K_m$  values employed here and  $K_m$  values employed in previously published PBPK models for chloroform. Present values for  $K_m$  (0.012 mg/L) were extrapolated from *in vitro* investigations of subcellular preparations from

TABLE 5-16				
Results from Studies with Male Humans				
Human Male	Oral dose	Total Metabolized		
		Observed	Corley - Predicted	Present - Predicted
70kg BW (avg, n=5)	7.14 mg/kg	268.8 mg	305.9 (1.14)	328.4 (1.22)
65 kg BW (one individual)	15.4 mg/kg	317.2 mg	501.8 (1.58)	495.6 (1.56)

<sup>a</sup> Metabolite formation calculated from observations reported to 8 hours post-exposure (Fry et al., 1972).

<sup>b</sup> (Predicted:Observed)

TABLE 5-17			
Results from Studies with Female Humans <sup>a</sup>			
Subject	BW (kg)	Oral Dose (mg/kg)	CF Metabolized (mg)
Subject 6	62.7	7.975	317.8
Subject 7	59.0	8.475	312.6
Subject 8	58.0	8.621	311.1
Corley et al (1990) Average <sup>b</sup>	60.0	8.357	295.8
Fry et al (1972) Average <sup>b</sup>	60.0	8.357	324.0 <sup>c</sup>

<sup>a</sup> Experiment described by Fry et al. (1972).

<sup>b</sup> Reported in Table 10 of Corley et al. (1990).

<sup>c</sup> Actual measurement of excreted CO<sub>2</sub> by Fry et al. (1972).

human liver (see Appendix D), whereas the publication of Corley et al. (1990) developed and employed a model-optimized  $K_m$  values ranging from 0.3 to 0.5 mg/L.

In a criticism of developing point estimates for values used for metabolic rate constants in PBPK modeling efforts, Smith and Evans (1995) undertook a systematic evaluation of chloroform PBPK modeling approaches to simulating open chamber, closed chamber and iv chloroform data sets. These authors employed the model structure of Corley et al. (1990), but like our present work, they opted not to include a term describing metabolic inhibition in mice. This is based on findings of Gearhart et al. (1993) in which liver samples obtained from male mice exposed to chloroform were subsequently subjected to *in vitro* analysis and demonstrated no loss of cytochrome P450-dependent activity.

Using maximum likelihood techniques, Smith and Evans (1995) demonstrated that a range of  $K_m$  values, extending downward from values of approximately 2 mg/L even to negative values, were capable of simulating chloroform metabolism equally well. These authors indicate that this is possible because “when metabolism is blood-flow limited, any model of metabolism with rate constants capable of metabolizing 100% or more of delivered substrate will describe the data equally well.” Using several data sets, including that from Corely et al. (1990), Smith and Evans (1995) demonstrated that  $K_m$  values approximating 0.05 mg/L fell well within the 95<sup>th</sup> percent confidence limits for  $K_m$  developed from simulations of gas uptake data originally reported by Gargas et al. (1986). For gas uptake data derived in mice, there was no appreciable difference in fit when  $K_m$  values were varied from approximately 0.05 to 0.9 mg/L. Thus the values for  $K_m$  employed in the present investigation fall well within the range of values determined plausible and demonstrated to effectively simulate chloroform metabolism. While optimized point estimates used in other modeling efforts may be higher than those presently

employed, there is no reason to suspect that the approximately forty-fold lower value for  $K_m$  employed here for rats and humans should serve as a basis upon which to lower confidence in model predictions. We have here demonstrated a high degree of similarity in our model predictions to observed data, particularly for mice and humans.

**Human Equivalent Concentration.** To adjust the animal no-response exposure metrics to an anticipated human NOAEL, this analysis was focused on developing a  $CM_{24}$  value in the general human that correlated with  $CM_{24}$  in the animal models for each test species. This was done by developing and exercising PBPK models for each species. Figure 5-3 illustrates the process and Figure 5-7 shows the results. The exposure scenario chosen was the 6-h, 5-ppm exposure in the mouse. It was not duration-adjusted, because exposure adjustment was based on an internal dose metric,  $CM_{24}$ . The relationship between  $CM_{24}$  and exposure concentration (Figure 5-6) demonstrated near perfect linearity for a continuous exposure to concentrations between 0.1 and 20 ppm in mice, rats, and humans. Some degree of similarity in the internal dose metric in rats and mice occurs when the internal dose metric is developed from the respective duration adjusted NOAEL values (see Table 5-18). Of note is that a difference of 6-fold in external NOAEL values corresponds with a difference of 2.6-fold when evaluated for the internal dose metric.

TABLE 5-18			
Derivation of the Human Equivalent Concentration from Liver Effects Observed in Mice and Rats			
Species	NOAEL	$CM_{24}$ (mg/L liver over 24 hours)	Human Equivalent Concentration
Mouse <sup>a</sup>	5 ppm	136	8.1 ppm
Rat <sup>b</sup>	30 ppm	355	≈ 25 ppm

<sup>a</sup>Templin et al. (1998).

<sup>b</sup>Templin et al. (1996).

This difference suggests that mice are “more sensitive” than rats for both TK and TD reasons. The HEC developed from studies with mice is 8.1 ppm, and the HEC developed from studies with rats is approximately 25 ppm.

**Human Variability.** Because the mode of action for chloroform involves hepatic metabolism and because the metabolism of chloroform is known to be limited by its delivery to the liver via HBF, studies were designed to simulate the effect of biologically plausible variability in metabolism and blood flow. In the adult, 9-year-old child, and 1-year-old child simulations, metabolic capacity ( $V_{\max}C$ ) and blood flow to the liver (QLC, fraction of CO) were varied according to the values determined for the 5<sup>th</sup> and 95<sup>th</sup> percentiles of each distribution.

**Deriving  $CM_{24}$  at Which to Determine Human Variability.** The following calculation was performed to reduce the mouse internal dose metric to account for potentially greater sensitivity (a pharmacodynamics consideration) in humans. Standard EPA practice has been to allow a one-half order of magnitude ( $10E^{0.5} = 3.16$ ) uncertainty factor to account for species TK or TD differences. With the aid of pharmacokinetic information, or only B:A PC values, it is possible to effectively reduce the mouse TK component to 1 and adjust the animal NOAEL by 3.16 to account for PD differences. Thus, the HEC of 8.1 ppm was divided by 3.16 to yield a concentration of 2.56 ppm. From the relationship described by the general human model for inspired concentration and  $CM_{24}$ , 2.54 ppm corresponds to a  $CM_{24}$  value of 42.75 mg/L. This value was established as a benchmark, and the various human models were used to determine the concentration of chloroform in inspired air that was necessary to produce this  $CM_{24}$  value.

**Human Variability: Metabolic Capacity and Age.** The results of the simulation experiments using actual values for the percentiles of the distribution for chloroform metabolism in human adults and children indicated that variability in this parameter had little effect on overall

chloroform metabolism within a given age group. The results presented in Table 5-19 demonstrate the exposure concentrations, under the influence of varying metabolic capacities, required to produce a  $CM_{24}$  value of 42.75 mg/L of liver, the value predicted in the general human model under an exposure to 2.56 ppm. In the general adult model, changes in  $V_{max}C$ , corresponding to values at the 5<sup>th</sup> and 95<sup>th</sup> percentile of the distribution did not require that exposure concentrations be adjusted more than 0.5% to bring  $CM_{24}$  values back to the value observed when  $V_{max}C$  represented the median value. This lack of impact of  $V_{max}C$  variability on  $CM_{24}$  values was also observed in the 9-year-old and 1-year-old child.

Among age groups, an equivalent  $CM_{24}$  value (42.75 mg/L) was reached at 2.56 ppm in the general adult, at 2.07 ppm in the general 9-year-old child, and at 1.99 ppm in the general 1-year-old child. With concentrations in inspired air equivalent between adults and children,  $CM_{24}$  values in children were nearly 35% higher than  $CM_{24}$  values in the adult (Table 5-14).

**Human Variability: Hepatic Blood Flow.** Data from multiple human studies were used in evaluating variability in the fraction of CO directed to the liver, HBF/CO. The PBPK model for the human was varied to include different rates of hepatic perfusion. Because the liver represents a richly perfused tissue, blood flow to the liver (QLC) was balanced against flow to other richly perfused tissues (QRC). From the available 59 measures of HBF (as a fraction of CO), statistical analysis was unable to differentiate a goodness of fit between the lognormal distribution type and the beta distribution type. Additionally, the base model was parameterized to include HBF as 0.25 of CO; the geometric mean for HBF was 0.259 from the lognormal distribution and 0.267 from the beta distribution. Therefore, the examination of the impact of blood flow will not produce 42.75 mg/L as the central point for  $CM_{24}$ . Instead, that point will be slightly different because the model was reparameterized to include distribution-specific measures of central

TABLE 5-19

The Impact of CYP2E1-Dependent Metabolic Parameters on Chloroform Metabolism Among Selected Segments of the Human Population

Subject Group	CM <sub>24</sub>	ppm	Magnitude of difference (ppm)*
Adult — 5 <sup>th</sup> percentile	42.75 mg/L	2.56	0.002
General adult		2.56	1.0
Adult — 95 <sup>th</sup> percentile		2.56	-0.001
9-year-old — 5 <sup>th</sup> percentile		2.07	0.003
General 9-year-old		2.07	1.0
9-year-old — 95 <sup>th</sup> percentile		2.07	-0.001
1-year-old — 5 <sup>th</sup> percentile		1.99	0.003
General 1-year-old		1.99	1.0
1-year-old — 95 <sup>th</sup> percentile		1.99	-0.001

\*The model output was used to predict the exposure concentration required to produce a CM<sub>24</sub> value of 42.75 mg/L. Difference in this exposure concentration within an age group is presented. A higher metabolic capacity (95<sup>th</sup> percentile) requires lowering the exposure concentration slightly (0.1%) to produce an equivalent CM<sub>24</sub> value. Individuals with lower metabolic capacity (V<sub>max</sub>C value) can tolerate slightly higher (0.3% higher) concentrations while maintaining the same CM<sub>24</sub> value.

tendency. Table 5-20 demonstrates the impact of variance in HBF on chloroform metabolism among adult humans. For this simulation, metabolic capacity was held constant at the geometric mean value of 8.956 mg/h-kg for  $V_{\max}C$ . Chloroform was present in inhaled air at 2.56 ppm.

These results indicate that the difference in  $CM_{24}$  values between the mean of the general distribution for HBF and the  $CM_{24}$  in individuals at the 95% percentile for the distribution is less than 17%. Thus, while HBF plays a deterministic role in regulating chloroform metabolism, the bounds of the rather wide, but naturally occurring, variance in HBS (a physiologic limitation) restrict its impact (quantified as the difference in external exposure concentrations (2.56 versus 2.19 ppm) producing the same  $CM_{24}$  value) to less than 17% among adults. Differences in Table 5-20 that were in the negative range were not considered, because a negative difference in  $CM_{24}$  would confer a reduction in risk.

**Human Variability: Blood:Air PC Value.** In experiments to support this study, the range of B:A PC values observed in actual samples of adult blood was 6.6 to 13.3. The model was parameterized to simulate the conditions of  $V_{\max}C$  and HBF representing the values at the mean for their respective distributions. Observed maximal and minimal values for blood:air partitioning were used to recompute the liver:blood PC (L:B PC) value. It was observed that incorporating the lowest observed B:A PC value (6.6) resulted in a  $CM_{24}$  value of 37.62, a decrease of 12.7%. On the other hand, increasing the B:A PC value to the maximally observed value (13.3) resulted in a slight increase in  $CM_{24}$  value (to 44.46, or 104% of the previous value).

**Combined Variability in the Adult.** To estimate the combined impact of increased blood flow in conjunction with increased metabolic capacity and high blood:air partitioning, the model was populated with values corresponding to those at the 95<sup>th</sup> percentiles of the distribution for HBF from the lognormal (0.456), with the  $V_{\max}C$  value representing that at the 95<sup>th</sup> percentile of the

TABLE 5-20			
Effect of Variance in Hepatic Blood Flow on Chloroform Metabolism Among Adult Humans			
HBF (% of CO)	Chloroform (ppm)	CM <sub>24</sub>	Magnitude of Difference in CM <sub>24</sub>
Lognormal distribution			
0.147	2.56	35.79	-0.163
0.259		42.75	1.0
0.456		49.95	1.12*

\*With respect to external concentrations producing an equivalent CM<sub>24</sub> value in humans, maximal difference was noted in the lognormal distribution values, between the HBF values at the geometric mean and the 95<sup>th</sup> percentile of the distribution. Model results describing the relationship between CM<sub>24</sub> and external chloroform concentrations indicate that an exposure to 2.19 ppm in this segment of the population (HBF = 0.456 CO) would be required to produce a CM<sub>24</sub> value of 42.75 mg/L (see Figure 5-12).

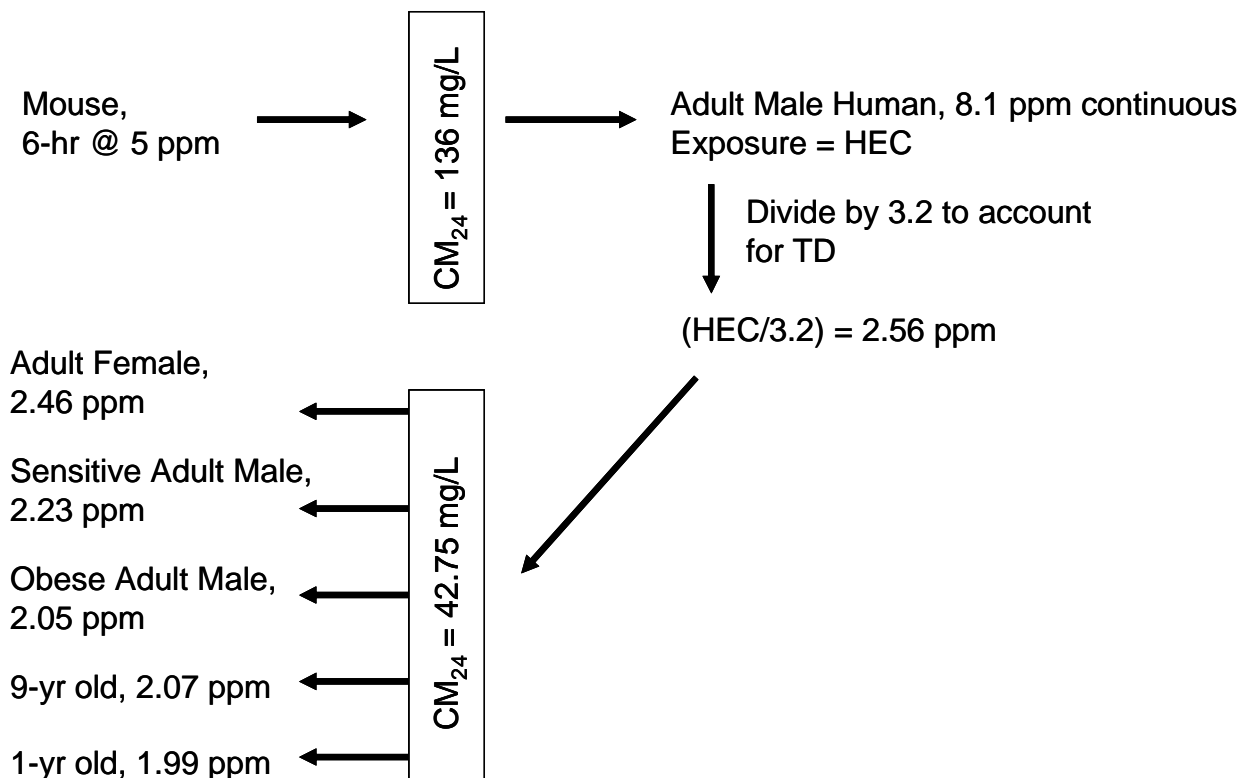


FIGURE 5-12

Application of Toxicokinetic Analysis to Address Animal-to-Human and Human Interindividual Differences for Chloroform Metabolism and Risk Assessment.  $CM_{24}$  was used as the basis to adjust concentration between and among species. With  $CM_{24}$  set to 136 mg/L from mouse studies, the HEC is 8.1 ppm, and dividing that concentration by 3.16 to account for TD differences between test animals and humans results in a concentration of 2.56 ppm, for a continuous exposure at steady state (in male humans)  $CM_{24}$  value of 42.75 mg/L. The  $CM_{24}$  value in adult females exposed to 2.56 ppm was 44.50.

The lower portion of the figure depicts the process used to ascertain the impact that measured differences in blood flow to the liver and metabolic activity of CYP2E1 toward chloroform, as well as age-dependent parameter values, have on the development of  $CM_{24}$ . These differences, as best expressed for risk assessment purposes, are expressed in units of exposure concentration (ppm). Those concentration differences may be considered in developing a quantitative value for the TK portion of UFH. This analysis demonstrated that differences in age (adults versus children), differences in CYP2E1 content/activity, and differences in HBF (as the difference between the geometric mean value and the value at the 95<sup>th</sup> percentile of the distribution) result in differences of up to 1.3-fold (2.56 ppm/1.99 ppm) in this measure. No data are available to describe the magnitude of TD variability among humans.

distribution (15.56 mg/h-kg), and with a B:A PC value of 13.3 (and resulting L:B PC value of 1.3) and used to simulate an exposure to 2.56 ppm. The results indicated that  $CM_{24}$  increased by approximately 15% (to 49.19 mg/L) above the  $CM_{24}$  value observed in the general adult human population. Under these conditions (high HBF, high metabolic capacity, high B:A PC value), exposure to 2.23 ppm would result in a  $CM_{24}$  value of 42.75 mg/L.

**Obesity in Adult Males.** The adult male PBPK model was reparameterized to reflect a state of obesity as defined by CDC. The model was exercised to determine  $CM_{24}$  at steady state under exposures to 0.75, 2.56 and 10 ppm. At those concentrations,  $CM_{24}$  values of 15.662, 53.458 and 208.8 mg/L were observed, respectively. Because of the near linearity of the relationship between external concentrations and  $CM_{24}$ , linear regression was employed to determine what external concentration equated to a  $CM_{24}$  value of 42.75 mg/L. Results indicated that the obese adult male exposed to 2.05 ppm at steady state would be expected to attain the targeted value for  $CM_{24}$ .

**Summary of Results.** These results demonstrate the successful application of PBPK modeling of chloroform metabolism in multiple species. The mouse appears to be more sensitive than the rat, and the model employed  $CM_{24}$  to equalize concentrations of chloroform in inspired air between mice and humans and between rats and humans. The HEC, developed from results with mice, is 8.1 ppm. A downward adjustment by a factor of 3.16 was performed to account for TD sensitivity of humans compared with rats. The resulting concentration of chloroform was 2.56 ppm. The  $CM_{24}$  value (42.75 mg/L of liver) corresponding to this concentration in the adult model was used to simulate human interindividual differences in  $CM_{24}$  under the conditions of varying age, HBF, and chloroform metabolic capacity. Results indicated that children were somewhat more sensitive to  $CM_{24}$  production at concentrations equivalent to those in adults.

CM<sub>24</sub> values equivalent to those in the 2.56-ppm exposed adult were reached at 2.07 ppm in the 9-year-old child and at 1.99 ppm in the 1-year-old child — a differential sensitivity of 1.28-fold (i.e., 2.56 ppm/1.99 ppm). The impact of variation in HBF among adults, assessed by comparing the concentrations of chloroform required to produce equivalent CM<sub>24</sub> values was 1.17-fold whether HBF was set at the geometric mean or at the 95<sup>th</sup> percentile of the distribution (2.56 ppm and 2.19 ppm, respectively). While the impact of blood flow on chloroform metabolism is not surprising, it does represent the initial quantitative demonstration of biologically defensible values for variability in liver blood flow, and its impact on bioactivation, as assessed via PBPK modeling. The sensitivity of CM<sub>24</sub> to changes in HBF is roughly 0.75, meaning that quite less than a 1:1 relationship exists between blood flow and chloroform metabolism, implicating the additional impact of other factors on chloroform metabolism. Changes in liver blood flow had a more appreciable impact on chloroform metabolism than changes in metabolic capacity (V<sub>max</sub>C) when assessed within an age group. Within an age group, changes in the V<sub>max</sub>C parameter had less than 1% influence on CM<sub>24</sub>, when the difference was quantified between the CM<sub>24</sub> values at the geometric mean and at the 95<sup>th</sup> percentile for metabolic capacity. The impact of combining high HBF with high metabolic capacity and high blood:air partitioning in the adult resulted in a 1.15-fold difference (2.23 versus 2.56 ppm) in the external concentrations required to produce a CM<sub>24</sub> value of 42.75 mg/L of liver.

## **DISCUSSION**

These results indicate that chloroform is absorbed by rats, mice, and humans and that substantial hepatic metabolism occurs. Because the metabolites of chloroform are responsible for its mode of action, this analysis focused on the metabolism of chloroform in the liver. In spite of nasal epithelium being a rather sensitive tissue in rodents exposed to chloroform by

inhalation, a 13-wk inhalation study identified the liver as the critical target of toxicity and a 6-h, 5-ppm exposure was identified as the mouse no-effect level. Similarly, the rat no-effect level was identified as a 6-h, 30-ppm exposure in a 13-wk inhalation study. The apparent lack of sensitivity of human nasal tissues to inhaled chloroform was also taken into consideration. Thus, the PBPK models employed were structured to quantify liver metabolism of chloroform in order to enable comparisons of sensitivity across species and within segments of the human population. Units of comparison were those of the integrated amount of chloroform metabolized over 24 hours, identified as  $CM_{24}$ . The use of  $CM_{24}$  allows a direct comparison of liver concentrations across species and within the human species, as opposed to simply comparing the amounts metabolized.

Because this analysis was constructed to support the derivation of an RfC value based on liver effects, indicative of risk from lifetime exposure,  $CM_{24}$  was determined using intermittent exposures in the mouse (replicating the response-related exposure), and the human model was then run until steady state was reached. Thus, human  $CM_{24}$  values were demonstrated under steady state during continuous exposure. Differences between rats, mice, and humans exposed to the same conditions demonstrate that rats and mice absorb and metabolize chloroform more efficiently than equally exposed humans. Furthermore, rats appear to be less sensitive to chloroform, based on no-effect levels expressed as external concentrations. However, this differential sensitivity is not based solely on differences in chloroform absorption and metabolism. The no-effect level in rats (30 ppm) is 6-fold higher than that observed in mice (5 ppm), and the  $CM_{24}$  values at the no-effect level are roughly 3-fold higher in the rat versus the mouse, as well — indicating the existence of species differences in response to metabolite production. Thus, issues of sensitivity among species (rats, mice, and humans) should include

specific consideration of internal dose metrics best linked with the mode of action, rather than consideration solely of external exposure measurements. This is why dosimetric analyses of  $CM_{24}$  were performed in mice, rats, and humans via PBPK modeling. The  $CM_{24}$  value of 136 mg/L (derived in mice) was chosen as the value for the dose metric upon which to base species extrapolation, and derive the HEC (Figure 5-7). Through an iterative analysis, the human PBPK model indicated that under internal steady-state the continuously-encountered external exposure concentration resulting in a  $CM_{24}$  value of 136 mg/L in the human was 8.1 ppm. Consistent with U.S. EPA guidance, this HEC was divided by a factor of 3 to account for remaining uncertainty (i.e., toxicodynamics, etc) in the animal to human extrapolation step. Because of the near-linearity observed in the relationship between external concentrations and internal doses ( $CM_{24}$ ) in this range of concentrations, the same species-adjusted concentration (e.g., 2.56 ppm, Figures 5-7 and 5-12) would have resulted had the remaining factor of 3 been used to downwardly adjust the internal dose metric (a process not covered by U.S. EPA guidance).

Delic et al. (2000) also performed a PBPK model-based analysis of chloroform metabolism in mice and humans. However, the focus of that investigation was for intermittent, occupational exposures, rather than continuous exposures representative of environmental exposures. Another difference is that that investigation compared of *rates of metabolism* among species (Delic et al., 2000) versus *integrated amount of metabolites* formed under the conditions of continuous exposure and at steady state in the human. Furthermore, the results of Delic et al. (2000) are based on a human model that includes values for organ volumes, blood flows, partition coefficients, and metabolic rate constants that differ from those employed in our investigation. Interestingly, the  $K_M$  value used in the human model by Corley et al. (1990) — which served as the basis for Delic's human model — was derived as the mean value of

optimized KM values from rats and mice, while the KM value employed in the present work was extrapolated from *in vitro* experiments conducted specifically for this purpose using samples of human hepatic microsomal protein (Lipscomb et al., 2004). Delic et al. (2000) reported that a peak metabolic rate of 391 nmol/h/gram liver was observed (at 3.7 hs into the 6-h exposure) in mice exposed to 10 ppm, but that this metabolic rate was not observed in humans until the exposure concentration reached 130 ppm — 13-fold higher. While credible, using such a comparison of species differences in dose metrics instantaneously determined under conditions that were not representative of environmental conditions is ill-advised.

In contrast to the interpretations of Delic et al. (2000), our results based on the integrated amount of metabolite formed between species indicate a difference at this (mouse 6-h) exposure concentration of approximately 3-fold between mice and humans who are subjected to a continuous exposure. Our results may differ from those of Delic et al. (2000) for several reasons, including differences in modeling approaches and in values for model parameters, such as for tissue partitioning and metabolism. In contrast to results from rodents, adequate human data on chloroform disposition in humans that could be used to verify the present human PBPK model and its predictions of chloroform metabolism do not exist. An attempt was made to find information against which to compare the model predictions of human interindividual TK variability — specifically data that relate directly to hepatic chloroform metabolism following inhalation exposure. However, even in studies which sound relevant, complications and limitations of study design, evaluation, and the level of detail in reporting limit their value in verifying our results.

The PBPK modeling approach to chloroform dosimetry has been undertaken by several groups (Corley et al., 1990, 2000; Xu and Weisel, 2004). In developing and evaluating these

models, the respective authors cite no data sets involving humans except that of Fry et al. (1972) that would be useful as comparators for estimations of human interindividual differences in chloroform metabolism. Corley et al. (1990) developed PBPK models for chloroform disposition in rats, mice, and humans and used the human data available (Fry et al., 1972) against which model predictions were compared. A comparison of the present model predictions to those data are in Tables 5-15 and 5-16. Corley et al. (1990) also examined human interindividual differences in hepatic microsomal metabolism of chloroform, but reported metabolism at only one substrate concentration. They also reported the value as velocity over substrate concentration ( $V/S$ ), a measure that is not informative of human differences in metabolism kinetic constants that are required as parameter values in models designed to evaluate the impact of metabolic variance on tissue dosimetry. Furthermore, Corley et al. (1990) made no mention of human chloroform data obtained from an inhalation exposure. More recently, Corley et al. (2000) developed a PBPK model to assess the dermal absorption of chloroform in human. Multiple subjects were exposed via the dermal route, but the only measures of exposure were obtained in exhaled breath. The sampling strategy, combined with model structure and parameterization, hinder the application of these data to assess human interindividual variability in chloroform metabolism. Of the multiple studies cited by Corley et al. (2000), none reported data from humans in which study design and individual human characteristics were sufficient to aid in the understanding of chloroform metabolism.

On a number of occasions, Weisel and colleagues have undertaken and reported results of modeling investigations designed to determine chloroform uptake by humans. In a recent investigation (Xu and Weisel, 2004), human subjects were exposed to chloroform vapor via the dermal and inhalation routes, and samples of expired breath were analyzed to ascertain route-

dependent fractional uptake of chloroform. However, these results (concentrations of chloroform in expired air) are not useful benchmarks against which to compare the metabolism of chloroform, as we report. In conclusion, no data were located describing chloroform disposition in humans against which the predictions of the model developed in the present study could be verified.

Our present work quantifies species differences in chloroform metabolism and has applied it to rodent no-effect exposure values in order to demonstrate values for the HEC for application in the derivation of chloroform's RfC. We have used data from mice to demonstrate an HEC of 8.1 ppm. Confidence in this species extrapolation is increased, given the ability of the model to adequately simulate chloroform metabolism in both test species and humans.

An additional analysis of the impact that human interindividual variance exerts on the risk-relevant TK outcome,  $CM_{24}$ , was also performed. This was accomplished first by quantifying the extent to which adult humans vary in the fraction of CO delivered to the liver. To avoid the introduction of operator-based confounding factors that may occur in ultrasound studies as well as the natural variability in bifurcation of the hepatic vasculature, we employed only data derived from studies that developed ICG-based measures of HBF in the supine position among fasted adults. Because ICG is a dye effectively cleared by the liver, measures of ICG can be used to determine total HBF from the hepatic artery, splanchnic vein, and hepatic portal vein. Data on a total of 59 subjects were available, either from values published in the open literature or as individual data graciously provided by investigators who had published mean values from that sample of subjects.

A second measure of human variance was quantified as the extent to which cytochrome P450 2E1 (CYP2E1) content and activity toward chloroform (two separate measures) varied

among adults. The variance of CYP2E1 content among samples of liver from child organ donors was also determined. Because the metabolic activity of CYP2E1 is not a function of age (as is content), the activity of adult CYP2E1 was also employed in analysis of children via PBPK modeling.

The influence of age was estimated by incorporating values for body composition (i.e., VLC, volume of the liver compartment) developed for adults and children of different ages, incorporating values for tissue partitions developed for adult humans and for children, using adult and child blood as well as solid tissues from adult and young rats, and by incorporating age-dependent variations in the hepatic content and activity of CYP2E1. The impact of body weight and fat compartment size was investigated by developing models for adult females, adult males and for obese adult males. Finally, for adults, variability in HBF was incorporated into the model developed for the 70 kg adult male. These modifications represent a natural, but not heretofore accomplished, extension of PBPK modeling to address biochemical, as well as physiologic, variation among humans.

Varying chloroform metabolic capacity between the geometric mean and 95<sup>th</sup> percentile for the adult population resulted in less than 1% change in chloroform metabolism. Biologically plausible changes in CYP2E1 content and/or activity toward chloroform did not change  $CM_{24}$ . On the other hand, increasing HBF from the geometric mean (approximately 26% of CO) to the value at the 95<sup>th</sup> percentile of the distribution in adults (approximately 45% of CO) resulted in a 17% increase in  $CM_{24}$ . No data on variability of HBF were available for children. Chloroform metabolism ( $CM_{24}$ ) in the 9- and 1-year-old child at the geometric mean for  $V_{max}C$  was 126 and 135% of the value at the geometric mean for  $V_{max}C$  in the adult population. Increasing  $V_{max}C$  to values at the 95<sup>th</sup> percentile of the distributions for the 9- and 1-year-old child resulted in less

than a 1% increase in  $CM_{24}$ . These results within age groups indicate that differences in CYP2E1 content and activity toward chloroform, which may reach approximately 2-fold ( $V_{max}C$  when extrapolated from *in vitro* data), have little or no effect on the risk-relevant measure,  $CM_{24}$ , in intact humans. This is consistent with findings of the impact of CYP2E1 variability and its influence on the metabolism of trichloroethylene (Lipscomb et al., 2003) and is a function of blood flow delivery to the liver as the rate-limiting step in metabolism. On the other hand, consistent with blood flow as the rate-limiting step in metabolism, differences in HBF result in alterations of  $CM_{24}$ , but the sensitivity of  $CM_{24}$  to HBF is only about 75%.

In a previous investigation of PK differences among adults and between adults and children, Pelekis et al. (2001) used predicted values for chloroform partition coefficients in adult and child tissues, based on age-dependent differences in lipid and water content of tissues. In that analysis, the concentration of parent chloroform, but not its metabolism or metabolites, was addressed following a simulated 30-d exposure. Those adult-child differences in the concentration of parent compound in tissues (i.e., liver, muscle, fat, blood) were less than 10, but were consistently higher in the child. Although our present analysis was not designed to capture tissue concentrations of parent compound, this difference is consistent with our demonstration that the child converts a higher dose of chloroform to toxic metabolites than the adult.

To investigate the impact of sex- and obesity-related changes in body composition, related to the fat compartment, models were additionally constructed for the adult female and the obese adult male. Results indicated an approximate 4% difference between  $CM_{24}$  values attained in adult males and adult females; and an approximate 25% difference in  $CM_{24}$  values attained in the obese adult male compared to the 70 kg adult male.

Recently, Tan et al. (2003) published the results of modeling efforts designed to link chloroform metabolism with hepatocyte repair and regeneration. Data on hepatocyte LI originally published by Constan et al. (2002) were used as the basis for their model development and its evaluation. Their pharmacodynamic model employed a PBPK model to transition an external (i.e., inhaled) concentration to a measure of chloroform metabolism (rate per cubic centimeter of liver) during an intermittent exposure regimen. The Tan et al. (2003) model was based on the female B6C3F1 mouse and employed the base model of Corley et al. (1990), with the exception that the parameters governing the inhibition of CYP2E1-dependent metabolism by chloroform metabolites were not included, as Tan et al. indicated that they were not necessary. Corley's model was based on the structure developed by Ramsey and Andersen (1984) for styrene. Tan et al. (2003) developed B:A, L:A, and kidney:air (K:A) PC values for this sex and strain of mouse using Sato and Nakajima's vial equilibration technique (Sato and Nakajima, 1979). B:A, L:A, and K:A PC values were 24.1, 16.9, and 12.2, respectively, and resulted in L:B and K:B PC values of 0.7 and 0.5, respectively. The PBPK model was used, after fitting to *in vivo* chloroform gas uptake data for female B6C3F1 mice, to optimize  $V_{\max}C$ , which the model predicted to be 10.06 mg/h-kg. The PD model was constructed to define "virtual damage" by linking chloroform exposure to cytolethality. Virtual damage was not directly correlated with any measured endpoint, and the rate of damage formation was proportional to the rate of chloroform metabolism per volume of tissue. The parameter,  $R_{\text{met}}$ , was defined as the rate of chloroform metabolism per volume tissue, and was expressed in units of  $\text{mg/h-cm}^3$ . The model was constructed around the premise that a liver-derived factor circulating in blood (a signal kinetic factor) serves as a stimulus to existing hepatocytes to divide and replace dead cells and that a saturable rate exists for repair of cytotoxic damage from oxidative metabolites of

chloroform. The authors indicated that, “The rate of damage repair, the form of the linkage between damage and cellular death rate, and the signal kinetics that drive regenerative proliferation constitute a structural alternative to an empirical correlation between a target tissue dose surrogate and the toxicological endpoint.” Results demonstrated a good fit between model predictions of hepatocyte LI (from Constan et al., 2002) and model predictions for 2-, 6-, 12-, and 18-h exposures to 10, 30, and 90 ppm. In their publication (Tan et al., 2003), Figure 4 demonstrates that a 12 h/d exposure to 10 ppm for 7 consecutive days produced a hepatocyte LI roughly equivalent to the control (nonexposed) hepatocyte LI of  $0.7 \pm 0.2$  %.

Uncertainty factors can be revised from default values or obviated by TK evaluations. Three levels of specificity can be used to develop RfC values. The first is the application of default methodologies to external concentrations. The second is the application of TK evaluations to develop the HEC, and the application of the default value for  $UF_H$ . The third method is to employ available information (here TK information) to both develop the HEC and describe the value of the TK component of  $UF_H$ . Each of these approaches would result in appreciably different values for the RfC for chloroform.

In the first case, the application of default methodology to external concentrations employs duration adjustment. The no-effect exposure of 5 ppm  $\times$  6 hours, 5 ds/wk is adjusted to yield a duration-adjusted concentration of 0.9 ppm, to which default values of  $UF_A$  (10) and  $UF_H$  (10) are applied, resulting in a concentration of 0.009 ppm adjusted for inter and intra species uncertainty (i.e., 0.9 ppm/100).

The application of TK information, whether only for species extrapolation or for the additional extrapolation within humans, results in appreciably different values. The second approach would quantify TK variability between species to develop the HEC and apply the

default value for  $UF_H$  to develop the RfC. This approach develops and applies species differences in the translation of external concentrations to the internal dose metric in order to extrapolate a no-effect mouse exposure to an HEC (inhalation) of 8.1 ppm. Applying default values for  $UF_{A-TD}$  (3) and for  $UF_H$  (10), would result in a concentration of 0.27 ppm adjusted for inter and intra species uncertainty (i.e.,  $8.1 \text{ ppm}/[3 \times 10]$ ).

Finally, TK information may be used to develop the HEC and to quantify human interindividual variability, yielding a “data-derived” value for  $UF_{H-TK}$ . In this approach, the HEC is adjusted downward by one-half order of magnitude to adjust for the increased TD sensitivity of the human compared to animals, resulting in a concentration of 2.56 ppm. Consistent with the application of TK evaluation to adjust for external exposures, the internal dosimeter,  $CM_{24}$ , was again employed to address human interindividual variability. Analogous to addressing species differences, the TK evaluation precedes the application of TD uncertainty factors within the human species. When evaluations were conducted at steady state and PBPK models for adults and children were varied to include values for HBF, blood:air partitioning of chloroform, metabolic rate constants and body composition, the largest difference in external concentrations was observed between the 70 kg adult male model and the model for the 1-year-old child. When standardized on a  $CM_{24}$  value of 42.75 mg/L, the magnitude of that difference (expressed in terms of the external concentration) was 1.3 (i.e.,  $2.56 \text{ ppm}/1.99 \text{ ppm}$ ). This difference exceeded the difference between the 70 kg adult male human and the adult female (1.04); the adult human concomitantly “sensitized” for B:A PC value, HBF, and metabolic capacity (i.e.,  $2.56 \text{ ppm}/2.23 \text{ ppm} = 1.15$ -fold); and the obese adult male (1.25). The difference between these external exposure conditions (maximally observed difference of  $2.56 \text{ ppm}/1.99 \text{ ppm} = 1.3$ ) should be included in discussions of the value to be ascribed to  $UF_{H-TK}$ . In the absence of data directing the

selection of the value for  $UF_{H-TD}$ , the  $UF_{H-TD}$  should remain at the default value of one-half order of magnitude (3.16). With enough confidence in the present evaluation of human interindividual TK variability (child:adult = 1.3-fold), quantitative reliance in these results may support replacement of the default uncertainty factor value. Following the development of the HEC (inhalation) of 8.1 ppm, a default value of 3 for  $UF_{A-TD}$ , the data-derived value of 1.3 for  $UF_{H-TK}$  and a default value of 3 for  $UF_{H-TD}$  could be applied in the development of an RfC value.

## CONCLUSIONS

PBPK modeling was successfully applied to convert external exposure concentrations to internal measures of chloroform metabolites in the mouse, rat, and human. These models were used to transition no-effect values from toxicity studies with rats and mice into HECs, based on an internal dose metric quantifying chloroform metabolism in each species/model. Humans convert less of a dose of chloroform to metabolites than do either rats or mice.

Separate human models were constructed to represent the adult, the 9-year-old and the 1-year-old child. Models were populated with age-specific organ volumes and partition coefficients. CYP2E1 content of liver was determined for adults and children. Chloroform metabolic rate constants were derived *in vitro*, extrapolated to the intact organ, scaled by  $BW^{0.7}$ , and incorporated into the PBPK models. Laboratory studies demonstrated variability of the blood:air partitioning of chloroform into human blood. Variability of HBF among adults was determined from previously published results. Under no conditions was the difference between chloroform metabolism under mean conditions in the adult human and under conditions representing extreme values (or values at the 95<sup>th</sup> percentile for a distribution) elevated more than 25%. Among the factors assessed within the adult human the impact on variability in

chloroform metabolism was greatest:  $\text{HBF} > \text{B:A PC value} > V_{\text{max}}$ . Children converted as much as 30% more of a dose of chloroform to metabolites than adults.

This report demonstrates the feasibility of using PBPK modeling as a platform to integrate anatomic variance (i.e., relative organ volumes), and physiologic variance (i.e., HBF) with biochemical variance (e.g., in CYP2E1 content, enzyme kinetic parameters, and blood:air partitioning) to assess their separate impact on the formation of a risk-relevant pharmacokinetic outcome. These results indicate the potential application of this approach to quantitatively assess human interindividual variability at the level of the risk-relevant pharmacokinetics outcome, which for chloroform is the amount of chloroform oxidized in the liver. This is significant because other conditions (e.g., diseases) can alter basic physiology and biochemistry in humans, and these results demonstrate the applicability of PBPK modeling to translate those changes into harbingers of susceptibility, when they, themselves, can be quantified.

The present report follows Agency RfC guidance in the sequence of extrapolating animal internal dosimetry to a human equivalent concentration (i.e., the external concentration resulting in the same internal dose), then continuing on with application of the toxicodynamic uncertainty factor. A more technically correct procedure may have been to have downwardly adjusted the animal internal dose ( $\text{CM}_{24}$ ) by a default factor of 3 for animal to human differences in response (toxicodynamics), then employed the PBPK model to predict an external concentration resulting in a value for the internal dose that could be used as the starting point for application of the human interindividual variability uncertainty factor (UFH). This is an important point. When the relationship between external concentration and internal dosimetry is non-linear in the range of the animal point of departure, this issue becomes critical. However, because the system here

studied demonstrates marked linearity in this range, the results will be the same, whether the downward adjustment for TD is applied to the external concentration or the internal dose.

## REFERENCES

ACGIH (American Conference of Governmental Industrial Hygienists). 2003. Threshold Limit Values for Chemical Substances and Physical Agents and Biological Exposure Indices. American Conference of Governmental Industrial Hygienists, Cincinnati, OH.

Amman, P., C.L. Laethem and G.L. Kedderis. 1998. Chloroform-induced cytolethality in freshly isolated male B6C3F1 mouse and F-344 rat hepatocytes. *Toxicol. Appl. Pharmacol.* 149:217-25.

Andersen, M.E., M.E. Meek, G.A. Boorman et al. 2000. Lessons learned in Applying the U.S. EPA proposed cancer guidelines to specific compounds. *Toxicol. Sci.* 53:159-172.

Arms, A.D. and C.C. Travis. 1988. Reference physiological parameters in pharmacokinetic modeling. U.S. Environmental Protection Agency, Washington, D.C. EPA/600/6-88/004.

Beliveau, M., G. Charest-Tardif and K. Krishnan. 2001. Blood:air partition coefficients of individual and mixtures of trihalomethanes. *Chemosphere.* 44:377-381.

Caesar, J., S. Shaldon, L. Chiandussi, L. Guevara and S. Sherlock. 1961. The use of indocyanin green in the measurement of hepatic blood flow and as a test of hepatic function. *Clin. Sci.* 21:43-57.

CDC (Centers for Disease Control and Prevention). 2005. BMI - Body Mass Index: BMI for Adults. Centers for Disease Control and Prevention. Available at <http://www.cdc.gov/nccdphp/dnpa/bmi/bmi-adult.htm>.

Constan, A.A., B.A. Wong, J.I. Everitt and B.E. Butterworth. 2002. Chloroform inhalation exposure conditions necessary to initiate liver toxicity in female B6C3F1 mice. *Toxicol. Sci.* 66:201-208.

Corley, R.A., A.L. Mendrala, F.A. Smith et al. 1990. Development of a physiologically based pharmacokinetic model for chloroform. *Toxicol. Appl. Pharmacol.* 103:512-527.

Corley, R.A., S.M. Gordon and L.A. Wallace. 2000. Physiologically based pharmacokinetic modeling of the temperature-dependent dermal absorption of chloroform by humans following bath water exposure. *Toxicol. Sci.* 53:13-23.

Delic, J.I., P.D. Lilly, A.J. MacDonald and G.D. Loizou. 2000. The utility of PBPK in the safety assessment of chloroform and carbon tetrachloride. *Reg. Toxicol. Pharmacol.* 32:144-155.

- Evans, M.V., W.K. Boyes, J.E. Simmons, D.K. Litton and M.R. Easterling. 2002. A comparison of Haber's rule at different ages using a physiologically based pharmacokinetic (PBPK) model for chloroform in rats. *Toxicology*. 176:11-23.
- Feruglio, F.S., F. Greco, L. Cesano, D. Indovina, G. Sardi and L. Chiandussi. 1964. Effect of drug infusion on the systemic and Splanchnic circulation: I. Bradykinin infusion in normal subjects. *Clin. Sci.* 26:487-491.
- Fry, B.J., R. Taylor and D.E. Hathaway. 1972. Pulmonary elimination of chloroform and its metabolite in man. *Arch. Int. Pharmacodyn.* 196:98-111.
- Gargas, M.L., M.E. Andersen and H.J. Clewell III. 1986. A physiologically based simulation approach for determining metabolic constants from gas uptake data. *Toxicol. Appl. Pharmacol.* 86:341-352.
- Gearhart, J.M., C. Sekel and A. Vinegar. 1993. *In vivo* metabolism of chloroform in B6C3F1 mice determined by the method of gas uptake: The effects of body temperature on tissue partition coefficients and metabolism. *Toxicol. Appl. Pharmacol.* 119:258-266.
- ICRP (International Commission on Radiological Protection). 1975. Task Force on Reference Man, Vol 25.
- ICRP (International Commission on Radiological Protection). 2002. Basic Anatomical and Physiological Data for Use in Radiological Protection: Reference Values. ICRP Publication 89. J. Valentin, Ed. Pergamon Press, New York, NY. ISBN 0080442668.
- Iijima, T., F. Ohishi, T. Tataru and Y. Iwao. 2001. Effect of continuous infusion of prostaglandin E1 on hepatic blood flow. *J. Clin. Anesth.* 13:250-254.
- ILSI (International Life Sciences Institute). 1997. An Evaluation of EPA's Proposed Guidelines for Carcinogen Risk Assessment Using Chloroform and Dichloroacetate as Case Studies. Report of ILSI HESI Expert Panel. International Life Sciences Institute, Washington, DC.
- IPCS (International Programme on Chemical Safety). 2001. Guidance Document for the Use of Data in Development of Chemical-Specific Adjustment Factors (CSAFs) for Interspecies Differences and Human Variability in Dose/Concentration-Response Assessment. World Health Organization, Geneva. Available at [http://www.who.int/pcs/harmon\\_site/harmonize/index.htm](http://www.who.int/pcs/harmon_site/harmonize/index.htm).
- Kedderis, G.L. and S.D. Held. 1996. Prediction of furan pharmacokinetics from hepatocyte studies: Comparison of bioactivation and hepatic dosimetry in rats, mice, and humans. *Toxicol. Appl. Pharmacol.* 140:124-30.
- Larson, J.L., M.V. Templin, D.C. Wolf et al. 1996. A 90-day chloroform inhalation study in female and male B6C3F1 mice: implications for cancer risk assessment. *Fundam. Appl. Toxicol.* 30:118-37.
- Lerman, J., G.A. Gregory, M.M. Willis and E.I. Eger Jr. 1984. Age and solubility of volatile anesthetics in blood. *Anesthesiology*. 61(2):139-143.

- Lipscomb, J.C. and G.L. Kedderis. 2002. Incorporating human interindividual biotransformation variance in health risk assessment. *Sci. Total Environ.* 288:13-21.
- Lipscomb, J.C., L.K. Teuschler, J. Swartout, D. Popken, T. Cox and G.L. Kedderis. 2003. The impact of cytochrome p450 2e1-dependent metabolic variance on a risk relevant pharmacokinetic outcome in humans. *Risk Anal.* 23:1221-1238.
- Lipscomb, J.C., H. Barton, R. Tornero-Velez et al. 2004. The metabolic rate constants and specific activity of human and rat hepatic cytochrome P450 2E1 toward chloroform. *J. Toxicol. Environ. Health.* 67:537-553.
- Malviya, S. and J. Lerman. 1990. The blood/gas solubilities of sevoflurane, isoflurane, halothane, and serum constituent concentrations in neonates and adults. *Anesthesiology.* 72(5):793-796.
- Pelekis, M., L.A. Gephart and S.E. Lerman. 2001. Physiological-model-based derivation of the adult and child pharmacokinetic intraspecies uncertainty factors for volatile organic compounds. *Reg. Toxicol. Pharmacol.* 33:12-20.
- Ramsey, J.C. and M.E. Andersen. 1984. A physiologically based description of the inhalation pharmacokinetics of styrene in rats and humans. *Toxicol. Appl. Pharmacol.* 73:159-175.
- Reemtsma, K., G.C. Hottinger, A. DeGraff, Jr. and O. Creech. 1960. The estimation of hepatic blood flow using indocyanin green. *Surg. Gynecol. Obstet.* 110:353-356.
- Reitz, R.H., A.L. Mendrala, R.A. Corley et al. 1990. Estimating the risk of liver cancer associated with human exposure to chloroform using physiologically based pharmacokinetic modeling. *Toxicol. Appl. Pharmacol.* 105:443-459.
- Richardson, S.D. 1998. Identification of drinking water disinfection by-products. In: *The Encyclopedia of Environmental Analysis & Remediation*, Vol. 3, R.A. Meyers, Ed. John Wiley, New York, NY. p. 1398-1421.
- Rook, J.J. 1974. Formation of haloforms during chlorination of natural waters. *Water Treat. Exam.* 23:234-243.
- Sakka, S.G., K. Reinhart, K. Wegscheider and A. Meier-Hellmann. 2001. Variability of splanchnic blood flow in patients with sepsis. *Intensive Care Med.* 27:1281-1287.
- Sato, A. and T. Nakajima. 1979. A vial-equilibration method to evaluate the drug-metabolizing enzyme activity for volatile hydrocarbons. *Toxicol. Appl. Pharmacol.* 47:41-46.
- Smith, A.G. and J.S. Evans. 1995. Uncertainty in fitted estimates of apparent *in vivo* metabolic constants for chloroform. *Fundam. Appl. Toxicol.* 25:29-44.
- Tan, Y.-M., B.E. Butterworth, M.L. Gargas, and R.B. Conolly. 2003. Biologically motivated computational modeling of chloroform cytotoxicity and regenerative cellular proliferation. *Toxicol. Sci.* 75:192-200.

Templin, M.V., J.L. Larson, B.E. Butterworth et al. 1996. A 90-day chloroform inhalation study in F-344 rats: Profile of toxicity and relevance to cancer studies. *Fund. Appl. Toxicol.* 32:109-125.

Templin, M.V., A.A. Constan, D.C. Wolf, B.A. Wong, and B.E. Butterworth. 1998. Patterns of chloroform-induced regenerative cell proliferation in BDF1 mice correlate with organ specificity and dose-response of tumor formation. *Carcinogenesis.* 19:187-193.

Testai, E., V. de Curtis, S. Gemma, L. Fabrizi, P. Gervasi, and L. Vittozzi. 1996. The role of different cytochrome P-450 isoforms in *in vitro* chloroform metabolism. *J. Biochem. Toxicol.* 11:305-312.

Thomas, V. (V. Fiserova-Bergerova). 1975. Biological-Mathematical Modeling of Chronic Toxicity. U.S. Air Force, Aerospace Medical Research Laboratory, Aerospace Medical Division, Wright-Patterson AFB, Ohio, AMRL-TR-75-5.

U.S. EPA. 1994. Methods for Derivation of Inhalation Reference Concentrations and Application of Inhalation Dosimetry. Office of Research and Development. October. EPA/600/8-90/066F.

Weigand, B.D., S.G. Ketterer, and E. Rapaport. 1960. The use of indocyanin green for the evaluation of hepatic function and blood flow in man. *Am. J. Dig. Dis.* 5:427-436.

Xu X and C.P. Weisel. 2004. Human respiratory uptake of chloroform and haloketones during showering. *J Expo Anal Environ Epidemiol.* 2004:1-11. Available at: <http://www.nature.com/cgi-taf/DynaPage.taf?file=/jea/journal/vaop/ncurrent/full/7500374a.html&filetype=pdf>.

**NOTICE:** This chapter has been subjected to internal and external peer review in accord with EPA/ORD policy. The authors wish to thank Hugh Barton, Justin Teegarden and Jeff Gearhart for review comments. The work has been further improved through insightful comments from Harvey Clewell, Michael Gargas, Janusz Byczkowski, Dick Bull, Moiz Mumtaz and Gary Ginsberg.

## APPENDIX A

### COMPUTER CODE FOR THE CHLOROFORM PBPK MODEL

The PBPK model for chloroform was coded in acslXtreme software (Aegis Technologies, Huntsville, AL), versions 1.3.2 and 1.3.19. The parameter values used for chloroform are shown in Table Y. The code for the chloroform PBPK model follows below. The ! separates comments from computer code.

```
PROGRAM volatiles
! PBPK model for volatile organic chemicals
! 6/24/03 GLK based on furan 5/11/94
INITIAL
CONSTANT QPC = 14. !alveolar ventilation rate (L/hr/kg)
CONSTANT QCC = 14. !CARDIAC OUTPUT (L/HR/KG)
CONSTANT QLC = 0.25 !FRACTIONAL BLOOD FLOW TO LIVER
CONSTANT QFC = 0.09 !FRACTIONAL BLOOD FLOW TO FAT
CONSTANT BW = 0.25 !BODY WEIGHT (KG)
CONSTANT VLC = 0.04 !FRACTION LIVER TISSUE
CONSTANT VFC = 0.07 !FRACTION FAT TISSUE
CONSTANT BVC = 0.06 !FRACTION BLOOD VOL
CONSTANT VABC = 0.35 !FRACTION ARTERIAL BLOOD VOL
CONSTANT VVBC = 0.65 !FRACTION VENOUS BLOOD VOL
CONSTANT PL = 0.90 !LIVER/BLOOD PARTITION COEFF
CONSTANT PF = 9.72 !FAT/BLOOD PARTITION COEFF
CONSTANT PS = 0.64 !SLOWLY PERFUSED/BLOOD PART COEFF
CONSTANT PR = 0.90 !RICHLY PERFUSED/BLOOD PART COEFF
CONSTANT PB = 6.59 !BLOOD/AIR PARTITION COEFF
CONSTANT MW = 68.07 !FURAN MOLECULAR WEIGHT (G/MOL)
CONSTANT VMAXC = 4.86 !MAXIMAL VELOCITY (MG/HR/KG)
CONSTANT KM = 0.136 !MICHAELIS-MENTEN CONSTANT (MG/L)
CONSTANT ODOSE = 0. !ORAL DOSE (MG/KG)
CONSTANT KA = 2.0 !ORAL UPTAKE RATE (/HR)
CONSTANT IVDOSE = 0. !IV DOSE (MG/KG)
CONSTANT CONC = 0. !INHALED CONC (PPM)
! TIMING COMMANDS
CONSTANT TSTOP = 6. !LENGTH OF EXPT (HR)
CONSTANT TCHNG = 4. !LENGTH OF EXPOSURE (HR)
CONSTANT TINF = 0.002 !LENGTH OF IV INFUSION (HR)
CONSTANT POINTS = 500 !NUMBER OF POINTS IN PLOT
CINT = TSTOP/POINTS !COMMUNICATION INTERVAL
!SCALED PARAMETERS
QC = QCC*BW**0.74
QP = QPC*BW**0.74
QL = QLC*QC
QF = QFC*QC
```

```

QS = 0.24*QC - QF
QR = 0.76*QC - QL
VL = VLC*BW
VF = VFC*BW
VS = 0.82*BW - VF
VR = 0.09*BW - VL
BV = BVC*BW
VAB = BV*VABC
VVB = BV*VVBC
VMAX = VMAXC*BW**0.7
DOSE = ODOSE*BW
IVR = IVDOSE*BW/TINF
END !OF INITIAL
DYNAMIC
IALG = 2 !GEAR METHOD FOR STIFF SYSTEMS
DERIVATIVE
!CI = CONC IN INHALED AIR (MG/L)
CIZONE = RSW(T.GT.TCHNG,0.,1.)
CI = CIZONE*CONC*MW/24450
!AI = AMOUNT INHALED (MG)
RAI = QP*CI
AI = INTEG(RAI,0.)
!MR = AMOUNT REMAINING IN STOMACH (MG)
RMR = -KA*MR
MR = DOSE*EXP(-KA*T)
!CA = CONC IN SYSTEMIC ARTERIAL BLOOD (MG/L)
CA = (QC*CV + QP*CI)/(QC + (QP/PB))
AUCB = INTEG(CA,0.)
!AX = AMOUNT EXHALED (MG)
CX = CA/PB
CXPPM = (0.7*CX + 0.3*CI)*24450./MW
RAX = QP*CX
AX = INTEG(RAX,0.)
!AS = AMOUNT IN SLOWLY PERFUSED TISSUES (MG)
RAS = QS*(CA - CVS)
AS = INTEG(RAS,0.)
CVS = AS/(VS*PS)
CS = AS/VS
!AMOUNT IN RAPIDLY PERFUSED TISSUES (MG)
RAR = QR*(CA - CVR)
AR = INTEG(RAR,0.)
CVR = AR/(VR*PR)
CR = AR/VR
!AF = AMOUNT IN FAT (MG)
RAF = QF*(CA-CVF)
AF = INTEG(RAF,0.)

```

```

CVF = AF/(VF*PF)
CF = AF/VF
!AL = AMOUNT IN LIVER (MG)
RAL = QL*(CA - CVL) - RAM1 + RAO
AL = INTEG(RAL,0.)
CVL = AL/(VL*PL)
CL = AL/VL
AUCL = INTEG(CL,0.)
!AM1 = AMOUNT METABOLIZED, P450 SATURABLE PATHWAY (MG)
RAM1 = (VMAX*CVL)/(KM + CVL)
RAM1M = RAM1*1000./MW
AM1 = INTEG(RAM1,0.)
CAM1 = AM1/VL
DM = CAM1*1000./MW
!AO = TOTAL MASS INPUT FROM STOMACH (MG)
RAO = KA*MR
AO = DOSE - MR
!IV = IV INFUSION RATE (MG/HR)
IV = IVR*(1. - STEP(TINF))
!CV = MIXED VENOUS BLOOD CONC (MG/L)
CV = (QF*CVF + QL*CVL + QS*CVS + QR*CVR + IV)/QC
!TMASS = MASS BALANCE (MG)
TMASS = AF + AL + AS + AR + AM1 + AX + MR
TERMT(T.GE.TSTOP)
END !OF DERIVATIVE
END !OF DYNAMIC
END !OF PROGRAM

```

## APPENDIX B

### DERIVATION OF CHLOROFORM PARTITION COEFFICIENTS

#### TISSUE PARTITION COEFFICIENTS

Partition coefficients (PC) is a unitless number which describes the partitioning of a substance between two dissimilar media. The solubility of chemical substances in tissues and the body is a primary driver of tissue concentrations of the chemical upon exposure from an environmental medium. In PBPK modeling, the T:B PC and B:A PC values are included in the file of anatomic, physiologic, and biochemical parameters used to develop the model. The derivation first requires the characterization of B:A PC and T:A PC values; T:B PC values are then computed by Equation B-1.

$$\text{T:A PC value} / \text{B:A PC value} = \text{T:B PC value} \quad (\text{B-1})$$

Some more recent PBPK models employ PC values derived using only human tissues. However, the availability of solid tissues from humans, and their application in determining these PC values is the exception, rather than the rule. Many models employ PC values determined using tissues from rats only, given the similarity of tissue types and composition among mammalian species. However, it is rather well accepted that differences, especially in the B:A PC, exist between rats and humans. For chloroform's B:A PC value, previous investigations demonstrated this species-dependent variability. Gargas et al. (1989) presented values of 20.8 and 6.85 for adult male F-344 rats and humans, respectively; Beliveau et al. (2001) reported a B:A PC value of 21.3 for adult male F-344 rats; Batterman et al. (2002) reported a B:A PC value of 10.7 for human blood. In 1990, Corley et al. published a PBPK model for chloroform in humans, which was based on PC values derived for rats and humans. Rat PC values were determined specifically for the study, and PC values for human tissues were

obtained from Steward et al. (1973). In that publication, previously available published findings were condensed and reported for several solvents and anesthetic agents. Steward's report indicates a B:A PC value of 7.43 in humans. This paper also reported PC values for chloroform in human blood, liver, kidney, muscle, and brain tissue based on original observations and in fat based on predictions based on partitioning into olive oil. For comparison, the PC values employed by Corley et al. (1990) are repeated in Table B-1. Because of the availability of these data, chloroform was also included in a suite of chemicals, for which PC values in rat blood and tissues and human blood has also recently been re-investigated (reported in the following sections).

TABLE B-1					
Rat and Human Blood:Air and Tissue:Blood Partition Coefficient Values as reported in Corley et al. (1990)					
	Blood:Air	Liver:Air	Kidney:Air	Muscle:Air	Fat:Air
Rat <sup>a</sup>	20.8	21.1	11.0	13.9	203
Human <sup>b</sup>	7.43	17.0	11.0	12.0	280
	Blood:Air	Liver:Blood	Kidney:Blood	Muscle:Blood	Fat:Blood
Rat	20.8	1.01	0.53	0.67	9.75
Human	7.43	2.28	1.48	1.61	37.68

<sup>a</sup> Generated by and reported in Corley et al. (1990).

<sup>b</sup> From values collected in Steward et al. (1973), reported in Corley et al. (1990).

The availability of laboratory resources or tissues and the need for more automation has also driven the development of quantitative structure-activity methods. Several approaches have been developed, some of which are tailored to fit the characteristics of specific classes of chemicals. These methods have been employed to predict T:A PC values, based on the

physicochemical properties of the chemical (i.e., octanol-water partition coefficient and water solubility) and tissue-specific characteristics (i.e., lipid and water content).

## **DETERMINATION OF VALUES**

Blood:Air and T:A PC values were developed using the vial equilibration method (Sato and Nakajima, 1979), combined with gas chromatographic evaluation of chemical concentration, quantified by an external standard curve of known concentrations. Chloroform and five other volatile organic compounds were exposed in a mixture, and their concentrations in headspace were determined at equilibrium. This approach has been determined to produce PC values that are the same as those obtained using single chemical exposures. All studies were conducted through institutionally reviewed protocols. Human samples were remnant samples obtained from the Division of Clinical Laboratory Services, Wright-Patterson Regional Medical Center, OH and coded to ensure anonymity of the subjects. Study protocol was reviewed and approved by the Wright-Patterson Institutional Review Board and the EPA Human Studies Coordinator. Samples were provided from 11 adult males, aged 36 to 80 years, and 10 adult females aged 22 to 87 years.

## **PREDICTION OF PC VALUES**

Blood:air and tissue:air PC values were predicted according to Equation A-2.

$$P_{B:A} \text{ or } P_{T:A} = [P_{O:W} \times P_{W:A}(V_{nlB})] + [P_{W:A} \times V_{wB}] \quad (B-2)$$

where,  $P_{B:A}$  is the B:A PC value,  $P_{T:A}$  is the T:A PC value,  $P_{O:W}$  is the octanol:water partition coefficient,  $P_{W:A}$  is the water:air partition coefficient,  $V_{nlB}$  is the volume fraction of neutral lipids in blood, and  $V_{wB}$  is the volume fraction of water in blood.  $P_{O:W}$  and  $P_{W:A}$  were predicted by the freeware, KOWWIN and HenryWIN, respectively (U.S. EPA, 2003). The fractional

content of water in blood was available (ICRP, 1975) and the fat content of blood as reported (ICRP, 1975) was employed for the value for VnlB (Table B-2).

TABLE B-2					
Fractional Fat and Water Content of Adult Human Tissues (ICRP, 1975)					
	Blood	Liver	Kidney	Muscle	Fat
Water	0.806	0.71	0.76	0.79	0.15
Fat	0.0065	0.069	0.05	0.022 (male) 0.029 (female)	0.80

Several data sets of PC values for chloroform were available for this investigation. We have combined those data and predictions from QSAR approaches to develop and compare T:B PC values for chloroform. They are based on (1) B:A and T:A PC values derived using rat tissues, (2) B:A PC values derived using human blood and T:A PC values using solid tissues from rats, (3) QSAR predictions of B:A and T:A PC values using information characterizing the fat and water content of human tissues, and (4) a hybrid approach which employs QSAR predictions of B:A and T:A PC values for human tissues, but scaled to account for the differences between the observed human B:A PC value and the predicted human B:A PC value. The results of these are presented in Tables B-3 through B-7.

The final approach (Table B-8) to estimating T:B PC values combined observed human B:A values with predictions of B:A and T:A values to refine estimates of T:A PC values is based on the ratio of observed:predicted values for chloroform's B:A PC value in human blood. The predicted B:A PC value was 3.94, and the observed value was 11.34 — 2.88-fold higher than predicted. Thus, the predicted T:A PC values for humans were multiplied by 2.88 and combined with the human mean B:A PC value of 11.34 to estimate human T:B PC values. Table B-9

TABLE B-3

Blood:Air and Tissue:Air Partition Coefficient Values Derived from Studies with Rat Tissues

Rat	Blood:Air	Liver:Air	Kidney:Air	Muscle:Air	Fat:Air
1	17	17.2	16.8	10.9	365
2	17.5	17.4	17.6	10.7	352
3	15.2	17.8	21.1	10.1	346
4	20.3	18.3	16.9	32.5	405
5	12.3	13.6	8.7	38.1	229
6	18.5	25.7	14.8	9.5	327
7	17.4	16.3	14	13.8	365
8	18.4	15.6	16.3	17.7	378
9	20.7	16.2	15	12	350
10	20	18.2	16	13.5	379
Mean	17.7	17.6	14.8	16.9	351
S.D.	2.5	3.2	2.7	10.1	48

Ten adult male Fischer 344 rats were used in this investigation. B:A PC and T:A PC values were derived using tissues from individual rats (USAF, 2005).

NOTE: Tissues from rat 4 demonstrates a generally higher B:A PC and T:A PC values than other rats, this is also true to some extent for tissues from rat 5. Chloroform PC values were determined in a cocktail approach, and this same pattern is observed for other chemicals in this exposure suite, including benzene, methyl ethyl ketone, trichloroethylene, and perchloroethylene (not shown). Because this pattern is demonstrated for multiple tissues (brain not shown) from the same rats and for multiple chemicals, this indicates that the data are not spurious.

TABLE B-4				
Tissue:Blood Partition Coefficient Values Derived from Studies with Rat Tissues				
Rat	Liver:Blood	Kidney:Blood	Muscle:Blood	Fat:Blood
1	1.01	0.99	0.64	21.5
2	0.99	1.01	0.61	20.1
3	1.17	0.80	0.66	23.9
4	0.90	0.83	1.60	19.9
5	1.11	0.71	3.10	18.6
6	1.39	0.80	0.51	17.7
7	0.94	0.80	0.79	20.9
8	0.85	0.89	0.96	20.5
9	0.78	0.72	0.58	16.9
10	0.91	0.8	0.68	19.0
Mean	1.0	0.8	1.0	19.9
S.D.	0.2	0.1	0.8	2.0

Ten adult male Fischer 344 rats were employed in this investigation. B:A PC and T:A PC values were derived using tissues from individual rats, and rat-specific T:B PC values were developed (USAF, 2005).

TABLE B-5		
Blood:Air Partition Coefficient Values Derived from Studies with Adult Human Blood		
	B:A PC value	Range of Observations
Males, n = 11	11.9 ± 0.9	9.7-13
Females, n = 10	10.7 ± 2.1	6.9-13.3
Combined, n = 21	11.34 ± 1.65	6.9-13.3

Data presented as mean ± S.D. Mean values for men and women were not significantly different as determined by one-tail *t*-test assuming unequal variance ( $p = 0.063$ ) (USAF, 2005).

TABLE B-6				
Tissue:Blood Partition Coefficient Values Derived by Combining Mean Human B:A PC Values With Individual Rat T:A PC Values				
Rat	Liver:Blood	Kidney:Blood	Muscle:Blood	Fat:Blood
1	1.52	1.48	0.96	32.2
2	1.53	1.55	0.94	31.0
3	1.57	1.07	0.89	32.1
4	1.61	1.49	2.86	35.7
5	1.20	0.77	3.36	20.2
6	2.27	1.31	0.84	28.8
7	1.44	1.23	1.22	32.1
8	1.37	1.44	1.56	33.3
9	1.43	1.32	1.06	30.8
10	1.60	1.41	1.19	33.4
Mean	1.6	1.3	1.5	31.0
S.D.	0.3	0.2	0.9	4.2

Blood from 21 adult humans and solid tissues from 10 adult male Fischer 344 rats were used in this investigation. A B:A PC value of 11.34 (human mean) was combined with individual T:A PC values to develop estimates of individual T:B PC values (USAF, 2005).

TABLE B-7				
Predictions of Human Blood:Air, Tissue:Air, and Tissue:Blood Partition Coefficient Values				
Blood:Air	Liver:Air	Kidney:Air	Muscle:Air male)*	Fat:Air
3.94	12.38	9.98	6.27	110.15
	Liver:Blood	Kidney:Blood	Muscle:Blood	Fat:Blood
	3.14	2.53	1.59	27.95

\*The muscle:air PC and Muscle:blood PC values for females were 7.23 and 1.83, respectively.

TABLE B-8				
Human Tissue:Air and Tissue:Blood Partition Coefficient Values Based on Adjusted Predictions of Tissue:Air PC Values				
Blood:Air*	Liver:Air	Kidney:Air	Muscle:Air (male)	Fat:Air
11.34	35.63	28.72	18.05	317
	Liver:Blood	Kidney:Blood	Muscle:Blood	Fat:Blood
	3.14	2.53	1.59	27.95

\*Mean value for human B:A PC, observed in humans.

TABLE B-9					
Comparison of B:A and T:B PC Values for Mature Individuals					
Method	Blood: Air	Liver: Blood	Kidney: Blood	Muscle: Blood	Fat: Blood
1. Rat Only (this study)	17.7	1.0	0.8	1.0	19.9
Rat (Corley et al., 1990)	20.8	1.01	0.53	0.67	9.75
2. Human B:A, Rat T:A (this study)	11.34	1.6	1.4	1.2	33.4
3. Predicted	3.94	3.14	2.53	1.59	27.95
4. Adjusted	(to) 11.34	3.14	2.53	1.59	27.95
Human only (Stewart et al., 1973)	7.43	2.28	1.48	1.61	37.68

Methods 3 and 4 yield the same values for T:B PC value because Method 4 adjusts each solid tissue T:A PC value to account for differences between the observed and predicted value for the B:A PC. The difference between values derived in these methods is the B:A PC value. In addition, Gargas et al. (1989) demonstrated B:A PC values of 6.85 and 20.8 in blood from humans and rats, respectively, for chloroform.

presents a comparison of available PC values for chloroform, including (1) empirically derived T:A PC values in rat tissues, (2) T:A PC values from rat tissues combined with B:A values from humans, (3) values determined by estimating partitioning into lipid and water in combination with information on the water and lipid composition of tissues, and (4) a hybrid approach using observed values for B:A PC values to adjust those predicted from oil and water partitioning.

### **ESTIMATION OF PC VALUES IN CHILDREN**

For this investigation, B:A PC values for chloroform were collected in remnant samples of children's blood. Because age-specific values for tissue lipid and water content were available (ICRP, 1975), predictions of T:A PC values for solid tissues were developed using adult- and child-relevant lipid and water contents (Table B-10). When data described a range of fat or water content, the median of the range was employed. ICRP (1975) presented no data for the water content of child kidney, so the water content of adult kidney was included. The ratio of these values was used to adjust the T:A PC values for adult human tissues reported by Steward et al. (1973) to values reflective of child T:A PC values (Table B-11). These T:A PC values were combined with child-specific B:A PC values to develop T:B PC values for inclusion in the model (Tables B-12 and B-13).

Pelekis et al. (2001) also used the tissue contents of water, neutral lipids, and phospholipids to estimate T:A PC values and to derive T:B PC values for the hypothetical 10 kg child, the median body weight between 1 and 2 years of age. Water and lipid content was obtained from literature summarized in Pelekis et al. (1995).

### **DERIVATION OF PC VALUES IN PND RAT PUPS**

Individual blood and tissue samples were obtained from 10 male and 10 female PND 10 rat pups. B:A and T:A PC values were derived for each tissue sample individually, and T:A and

TABLE B-10				
Fractional Fat and Water Content of Children's Tissues (ICRP, 1975)				
	Liver	Kidney	Muscle	Fat
Water	0.799	0.76 <sup>a</sup>	0.785 <sup>b</sup>	0.475
Fat	0.036	0.0273	0.02	0.555

<sup>a</sup> Value from adult kidney.

<sup>b</sup> Value at 4 to 7 months of age.

TABLE B-11				
Predicted T:A PC Values in Humans				
	Liver:Air	Kidney:Air	Muscle:Air	Fat:Air
Adult	12.38	9.98	6.27	110.15
Child	8.23	6.87	5.98	77.95
Adult:Child Ratio	0.66	0.66	0.66	0.66
Observed Adult value	17.0	11.0	12.0	280
Adjusted Child Value	11.30	7.31	7.98	186
Child-Specific Blood:Air and Tissue:Blood PC Values				
Blood:Air	Liver:Blood	Kidney:Blood	Muscle:Blood	Fat:Blood
12.41	0.91	0.59	0.64	15.0

TABLE B-12			
Child-Specific Blood:Air and Tissue:Blood PC Values			
Blood:Air*	Liver:Blood	Muscle:Blood	Fat:Blood
14.9	5.79	4.79	86.4

\*B:A PC value was predicted by the PBPK model employed.

TABLE B-13

Adult-Specific Blood:Air and Tissue:Blood PC Values<sup>a</sup>

Blood:Air <sup>b</sup>	Liver:Blood	Muscle:Blood	Fat:Blood
7.43	3.0 (H)	3.69 (H)	77.0 (H)
	2.8 (L)	2.56 (L)	23.6 (L)

<sup>a</sup> T:B PC Values presented as high (H) and low (L) values predicted from extreme values for water and lipid content.

<sup>b</sup> B:A PC value was predicted by the PBPK model employed.

B:A values from each pup were paired to generate individual-specific values for T:B PCs. Table B-14 presents mean and ranges for chloroform B:A and T:B PC values for PND 10 rats.

TABLE B-14					
Blood:Air and Tissue:Blood PC Values in PND 10 Rat Pups					
	Blood:Air	Liver:Blood	Kidney:Blood	Muscle:Blood	Fat:Blood
Mean	13.3	1.31	0.95	2.54	18.27
SD	0.84	0.13	0.09	1.61	3.44
Min	12.2	1.03	0.81	1.24	10.96
Max	15.0	1.53	1.05	7.95	23.7

(USAF, 2005)

### DERIVATION OF BLOOD:AIR PC VALUES IN CHILDREN

Remnant blood samples obtained from pediatric patients were used to determine B:A PC value for children. The B:A PC values derived using samples from 7 males and 4 females (aged 3 to 7 years) demonstrated a mean and standard deviation of  $12.41 \pm 1.17$ .

### REFERENCES

- Batterman, S., L. Zhang, S. Wang and A. Franzblau. 2002. Partition coefficients for the trihalomethanes among blood, urine, water, milk and air. *Sci. Total Environ.* 284:237247.
- Beliveau M., G. Charest-Tardif and K. Krishnan. 2001. Blood:air partition coefficients of individual and mixtures of trihalomethanes. *Chemosphere.* 44:377-381.
- Corley, R.A., A.L. Mendrala, F.A. Smith et al. 1990. Development of a physiologically based pharmacokinetic model for chloroform. *Toxicol. Appl. Pharmacol.* 103:512-527.
- Gargas, M.L., R.J. Burgess, D.E. Voisard, G.H. Cason and M.E. Andersen. 1989. Partition coefficients of low-molecular weight volatile chemicals in various liquids and tissues. *Toxicol. Appl. Pharmacol.* 98:87-99.
- ICRP (International Commission on Radiological Protection). 1975. Task Force on Reference Man, Vol. 25.
- Pelekis, M., P. Poulin and K. Krishnan. 1995. An approach for incorporating tissue composition data into physiologically based pharmacokinetic models. *Toxicol. Ind. Health.* 11:511-522.

Pelekis M., L.A. Gephart and S.E. Lerman. 2001. Physiological-model-based derivation of the adult and child pharmacokinetic intraspecies uncertainty factors for volatile organic compounds. *Reg. Toxicol. Pharmacol.* 33:12-20.

Sato A. and T. Nakajima. 1979. A vial-equilibration method to evaluate the drug-metabolizing enzyme activity for volatile hydrocarbons. *Toxicol. Appl. Pharmacol.* 47:41-46.

Steward, A., P.R. Allot, A.L. Cowles and W.W. Mapleson. 1973. Solubility coefficients for inhaled anesthetics for water, oil, and biological media. *Brit. J. Anaesth.* 45:282-293.

USAF (United States Air Force). 2005. Determination of Partition Coefficients for a Mixture of Volatile Organic Compounds in Rats and Humans at Different Life Stages. Air Force Research Laboratory Human Effectiveness Directorate, Applied Biotechnology Branch, Wright-Patterson AFB, OH. AFRL-HE-WP-TR-2005-0012.

U.S. EPA. 2003. Estimation Program Interface (EPI) Suite. Available at: <http://www.epa.gov/oppt/exposure/docs/episuite.htm>.

**NOTE:** Data in Tables B-3, B-4, B-5, B-6 and B-14 were developed through IAG No. DW-57-93960601-0 with the U.S. Air Force, Air Force Research Laboratory/HEST, Wright-Patterson AFB Ohio (USAF, 2005). Results in this report may vary from those in the Air Force Technical report in that the latter were derived from a more full sample set.

## APPENDIX C

### VARIABILITY OF HEPATIC BLOOD FLOW IN ADULT HUMANS

#### BACKGROUND

Many xenobiotics have characteristics that limit their *in vivo* rates of metabolism by the rate at which they are delivered to the liver. Pharmacokinetic modelers have investigated this phenomenon, termed it “flow-limited metabolism,” and have demonstrated that several xenobiotics important both industrially and as ubiquitous environmental contaminants fall into this category. Flow-limited metabolism can be easily conceptualized as the condition in which the metabolic capacity of the liver exceeds the capacity for delivery to the liver via hepatic blood flow (HBF). This may be based on factors including (1) low concentration of the xenobiotic in the environmental medium, (2) poor solubility of the xenobiotic in blood, (3) poor ability of the xenobiotic to leave the blood and enter the liver, or (4) a very high capacity of the liver to metabolize the xenobiotic. Regardless, for xenobiotics whose metabolism is flow-limited, blood flow to the liver is rate-limiting, and warrants further consideration, especially when examining PK differences among humans.

As a biologically active organ responsible for the bulk of xenobiotic metabolism, the liver requires adequate delivery of oxygen and nutrients. The liver is unique among organs, in that it receives both arterial and venous blood in-flow. The hepatic artery (HA) branches and perfuses the liver with oxygen-rich blood. The hepatic portal vein (PV) courses along the intestine and stomach, thence supplies the liver with blood rich in absorbed nutrients. Recognized variance in the branching of the hepatic artery occurs among humans, and abnormalities of this vasculature complicate, and may preclude, organ transplantation. The liver is drained by out-flow through the hepatic vein (HV). The conservation of mass indicates that measures of HBF may either

measure the rate of delivery through the hepatic artery and portal vein or the rate of return to the systemic circulation (hepatic vein).

The goal of this investigation was to quantify human interindividual differences in HBF, quantified as fraction of cardiac output (CO). The available scientific literature was searched and queries to the authors of several key original investigations revealed a marked interest in cooperation and the availability of several important data sets containing individual-specific measures of CO and HBF. Because of the dependence of HBF on CO, PBPK models have been structured to incorporate HBF as a fraction of CO. To reduce uncertainties in this measurement, only studies reporting both CO and HBF in a pair-wise fashion were considered for inclusion.

Multiple techniques have been applied to measure HBF, but few published studies report both HBF and CO. HBF has been measured by xenon computer-aided tomography, by echo and Doppler ultrasound, by pulsed-dye elimination, and by indocyanin green (ICG) clearance. Noninvasive (e.g., ultrasound) measurements involve significant input by the operator in carefully aiming the device, including assumptions about HA bifurcations. Specific investigations have identified inter-observed differences in U.S. investigations as a significant source of variability in measurements of HBF. The same may apply to CAT scans. Therefore, we decided to focus only on measurements taken from dyes, including ICG. An additional benefit with this decision is that dye elimination measures both HA and PV deliveries. Routinely, dye content is simultaneously measured from a peripheral site and from a catheter placed into the HV. Difference in dye concentration is adjusted by the hepatic extraction efficiency to yield a measure of HBF in units L/min. Because of the uncertainties in measuring and reporting of HBF via Doppler measurements, these were not included. This investigation relied only on HBF measured through the clearance of the dye, ICG. The application of HBF

measurements determined via ICG clearance allowed the measurement of total HBF, both arterial and venous. The underlying data from six reported investigations were available.

## **DATA AND EVALUATION**

The oft-cited publication by Brown et al. (1997) indicates a reliance on the review article by Williams and Leggett (1989) as the basis for derivation of a representative value for the fraction of CO directed to the liver. In order to be as technically accurate as possible, the eight sources of original data in which ICG was used as a measure of HBF, cited in Williams and Leggett (1989) were evaluated. Because they did not present individual data and there is a low probability of gaining such information (based on publication date), four of these studies were not used in the present estimation of variability of HBF. In addition, two more recent publications were located, and data from those studies were provided by the study authors. Whereas the older data sets often did not contain measures of CO or CI, Williams and Leggett apparently adjusted CI by fixed values or proportions of fixed values scaled to BSA, rather than by age-adjusted measures of CI. It should be noted that age plays a critical role in determining cardiac index. Because several of these data sets did not contain measures of CO or CI, CI was estimated with information on subject age, by interpolating the age-adjusted CI (in units of L/min/m<sup>2</sup> body surface) from the graph presented in Guyton (1986, Figure 23-2), and multiplying the interpolated CI by the body surface area presented in the original studies. Guyton's figure demonstrates a greater than proportionate decline in CI from a value of approximately 3.6 L/min/m<sup>2</sup> at age of 35 to a value approximating 2.3 L/min/m<sup>2</sup> at an age of 90.

From this method, it was demonstrated that the mean value for the fraction of CO as HBF from nine samples from Caesar et al. (1961) (Table C-1, "Controls" [n = 4] and "Miscellaneous"

TABLE C-1

Hepatic Blood Flow (HBF) and Fraction of Cardiac Output as HBF (CO as HBF),  
Estimated from Data of Caesar et al. (1961)

Patient	Sex	Age (years)	BSA (m <sup>2</sup> )	EHBF (mL/min)	CO* (mL/min)	CO as HBF
Control 3	M	50	1.63	1210	2863	0.259
Control 4	F	45	1.56	1470	2991	0.315
Control 6	M	52	1.80	1970	2789	0.392
Control 8	M	56	2.00	1190	2716	0.219
Misc. 33	M	60	1.68	1500	2679	0.333
Misc. 34	F	48	1.50	1390	2899	0.320
Misc. 35	M	55	1.76	1420	2753	0.293
Misc. 36	M	51	1.72	2000	2881	0.404
Misc. 37	F	31	1.28	950	3487	0.213
Mean						0.305
S.D.						0.068
C.V.						0.223

\*Estimate of age-specific CI read from Guyton (1986, Figure 23-2), multiplied by BSA. Body weight was not reported.

cases [n = 5]) were not significantly different, and so they were pooled to give a sample of n = 9, with a value of  $0.305 \pm 0.067$  (mean  $\pm$  S.D.).

Individual values for the fraction of CO directed to the liver (HBF/CO) were determined from 35 paired of observations of CO and HBF based on measurements of ICG clearance. A total of 35 sets of paired (individual) observations were available in the open literature (Caesar et al., 1961; Wiegand et al., 1960; Feruglio et al., 1964; Reemtsma et al., 1960) (Tables C-2 through C-4) and an additional 24 paired data sets were graciously provided by the authors of more recent publications in which mean values were available (Iijima et al., 2001; Sakka et al., 2001) (Tables C-5 and C-6).

TABLE C-2						
Hepatic Blood Flow (HBF) and Fraction of Cardiac Output as HBF (CO as HBF), Estimated From Data of Wiegand et al. (1960)						
Patient	Sex	Age (years)	BSA (m <sup>2</sup> )	EHBF <sup>a</sup> (ml/min)	CO <sup>b</sup> (ml/min)	CO as HBF
15	M	41	1.84	881	5639	0.156
16	M	17	1.96	1741	7733	0.225
17	F	16	1.67	1338	6510	0.206
18	M	17	1.65	1508	6628	0.227
19	M	39	2.10	1655	7247	0.228
20	F	36	1.56	827	6742	0.123
21	F	29	1.92	778	5067	0.154
22	M	14	1.74	1732	6694	0.259
23	F	57	1.54	921	5143	0.179
Mean						0.195
S.D.						0.045
C.V.						0.231

<sup>a</sup> Estimated hepatic blood flow, converted from reported units of mL/min/m<sup>2</sup> to mL/min by multiplying by the stated BSA.

<sup>b</sup> Estimate of age-specific CI interpolated from Guyton (1986, Figure 23-2), multiplied by BSA to obtain CO in units of mL/min. Body weight was not reported.

TABLE C-3

Hepatic Blood Flow (HBF) and Fraction of Cardiac Output as HBF (CO as HBF), as Reported by Feruglio et al. (1964), "Before" Condition

Case	Sex	Age (years)	HBF (mL/min)	CO (mL/min)	CO as HBF
1	F	42	855	4380	0.181
2	M	48	1260	6970	0.346
3	M	41	1390	4020	0.145
4	F	32	1480	4200	0.318
5	M	18	910	6260	0.184
6	M	39	1005	3160	0.218
7	M	29	1180	6400	0.317
8	M	36	1265	5800	0.251
9	F	38	1200	5100	0.195
10	M	43	1460	4600	0.352
11	M	60	1520	6040	0.235
Mean					0.249
S.D.					0.073
C.V.					0.293

NOTE: BSA not reported.

TABLE C-4

Hepatic Blood Flow (HBF) and Fraction of Cardiac Output as HBF (CO as HBF),  
Derived from HBF and Patient Characteristics Presented by Reemtsma et al.  
(1960, Table III, constant infusion data)

Control Subject	Sex	Age (years)	Weight (kg)	BSA <sup>a</sup> (m <sup>2</sup> )	HBF (mL/min)	CO (mL/min)	CO as HBF <sup>b</sup>
js	F	14	40	1.28	1100	5410	0.230
wl	M	26	72	1.82	2400	6299	0.381
er	M	36	89	2.03	2200	6786	0.324
dh	M	42	61.3	1.67	1800	5233	0.344
jd	M	50	70	1.79	1700	5261	0.323
tk	M	56	65.9	1.74	1000	4895	0.204
Mean					1700	5647	0.297
S.D.					566	730	0.074
C.V.					0.332	0.129	0.252

<sup>a</sup> Body Surface area not reported; determined by the formula to convert weight (in kg) to BSA in m<sup>2</sup> (ICRP, 1975, p. 17).  $BSA = [(4*W) + 7]/(W + 90)$ . Costeff (1966 — in ICRP, p. 243) evaluated the accuracy of this formula over the weight range 1.5-100 kg and demonstrated that the root mean square departure from the formulas is 12% or less.

<sup>b</sup> CO not reported, estimated by estimating age-specific CI (from Guyton, 1986, Figure 23-2) and multiplying by BSA. Note for later: %CO as HBF was lower, but NSD in cirrhotics, at  $0.237 \pm 0.101$ .

TABLE C-5

Hepatic Blood Flow (HBF) and Cardiac Output (CO) Data Which Served as the Basis for Results Presented in Iijima et al. (2001)

Case	Sex	Age (years)	Weight (kg)	HBF (mL/min)	CO (mL/min)	CO as HBF
1	M	53	67.5	1148	3070	0.374
2	M	58	44	1122	3290	0.341
3	M	50	62	2773	6700	0.414
4	M	36	59	1616	4290	0.377
5	F	47	47	1601	5020	0.319
6	M	64	51	1271	5690	0.223
7	F	74	55	1170	4510	0.259
8	F	48	49	868	5160	0.168
9	M	53	67.5	2030	6010	0.338
10	M	58	44	1547	6450	0.240
11	M	49	62	952	3740	0.255
12	M	35	59	1214	3980	0.305
13	F	48	49	871	4350	0.200
14	F	47	47	2736	6100	0.449
15	M	64	54	1652	5510	0.300
16	F	74	55	914	3720	0.246
Mean				1468	4849	0.301
S.D.				601	1146	0.079
C.V.				0.409	0.236	0.263

NOTE: BSA not reported.

Individual data describing patient characteristics, CO and HBF were graciously provided by Dr. Takehiko Iijima.

TABLE C-6

Hepatic Blood Flow (HBF) and Cardiac Output (CO) Data Which Served as the Basis for Results Presented in Sakka et al. (2001)

Case	Sex	Age (years)	Weight (kg)	BSA (m <sup>2</sup> )	HBF (mL/min)	CO (mL/min)	CO as HBF
1	F	70	110	2.17	89	10770	0.082
2	F	55	85	1.96	176	8460	0.208
3	M	46	60	1.69	331	8150	0.405
4	F	39	40	1.36	376	9020	0.417
5	M	51	95	2.15	222	9890	0.224
6	F	74	85	1.92	169	7090	0.239
7	F	74	70	1.80	128	6420	0.199
8	M	77	60	1.58	315	6550	0.480
Mean					226	8294	0.282
S.D.					104	1570	0.136
C.V.					0.460	0.189	0.483

NOTE: Individual data describing patient characteristics, CO and HBF were graciously provided by Dr. Samir Sakka. HBF measurements were based on subject-specific hepatic extraction ratios.

Iijima et al. (2001) graciously provided the original subject-specific data from their study, and a statistical analysis (one-tailed *t*-test, Excel) demonstrating that the mean values for CO, HBF, and %CO as HBF were not different between males and females in this study. Therefore all samples were pooled for further analysis (Table C-5). Consistent with other data sets, these data also demonstrated that values for CO, HBF, and %CO as HBF were slightly lower in females than in males.

### SUMMARY

All of the above studies were conducted on overnight-fasted subjects, who were evaluated in the morning in the supine position. This similarity among studies reduced the impact which feeding state, posture, and exercise status may have on the direction of blood flow to the liver. Commercially available software (Statistical Analysis System, SAS) was applied to the above 59 individual values for HBF/CO to determine the parameters for the normal, lognormal, and beta distributions according to the method of moments. Results are presented in Table C-7.

Distribution	Parameter and Value	Percentile		
		5 <sup>th</sup>	50 <sup>th</sup>	95 <sup>th</sup>
Normal	Mean = 0.273, Standard Deviation = 0.087	0.130	0.273	0.417
Log Normal	Geometric Mean = 0.258, Geometric Standard Deviation = 1.411	0.147	0.259	0.456
Beta	$\alpha = 6.865, \beta = 18.269$	0.141	0.267	0.427

## REFERENCES

- Brown, R.P., M.D. Delp, S.L. Lindstedt, L.R. Rhomberg and R.P. Beliles. 1997. Physiological parameter values for physiologically based pharmacokinetic models. *Toxicol. Ind. Health.* 13:407-484.
- Caesar, J., S. Shaldon, L. Chiandussi, L. Guevara and S. Sherlock. 1961. The use of indocyanin green in the measurement of hepatic blood flow and as a test of hepatic function. *Clin. Sci.* 21:43-57.
- Costeff, H. 1966. A simple empirical formula for calculating approximate surface area in children. *Arch. Dis. Child.* 41(220):681-683.
- Feruglio, F.S., F. Greco, L. Cesano, D. Indovina, G. Sardi and L. Chiandussi. 1964. Effect of drug infusion on the systemic and Splanchnic circulation: I. Bradykinin infusion in normal subjects. *Clin. Sci.* 26:487-491.
- Guyton, A.C. 1986. *Textbook of Medical Physiology.* W.B. Saunders, Philadelphia, PA.
- Iijima T., F. Ohishi, T. Tataru and Y. Iwao. 2001. Effect of continuous infusion of prostaglandin E1 on hepatic blood flow. *J. Clin. Anesth.* 13:250-254.
- Reemtsma, K., G.C. Hottinger, A. DeGraff, Jr. and O. Creech. 1960. The estimation of hepatic blood flow using indocyanin green. *Surg. Gynecol. Obstet.* 110:353-356.
- Sakka, S.G., K. Reinhart, K. Wegscheider and A. Meier-Hellmann. 2001. Variability of splanchnic blood flow in patients with sepsis. *Intensive Care Med.* 27:1281-1287.
- Weigand, B.D., S.G. Ketterer and E. Rapaport. 1960. The use of indocyanin green for the evaluation of hepatic function and blood flow in man. *Am. J. Dig. Dis.* 5:427-436.
- Williams, L.R. and R.W. Leggett. 1989. Reference values for resting blood flow to organs of man. *Clin. Phys. Physiol. Meas.* 10:187-217.

## APPENDIX D

### EXTRAPOLATION OF *IN VITRO* DERIVED CHLOROFORM METABOLIC RATE CONSTANTS AND VARIABILITY FOR PBPK MODELING

This section demonstrates the extrapolation of the rate constant,  $V_{\max}$ , from its units of *in vitro* measurement (i.e., pmol product/minute/pmol CYP2E1) to units (e.g., mg/h/liver) which can be scaled according to body weight and incorporated into PBPK model code, using adult-specific information and based on a fractional liver mass of 2.6% of body weight and a 70 kg adult (with a resulting liver mass of 1820 grams). This approach requires several conditions, including that the responsible enzyme has been identified, its content in the metabolic preparation (here, microsomal protein) is known, and that the concentration of the enzyme in intact liver is known (Lipscomb and Kedderis, 2002). The last point may also be addressed by measuring the content of the enzyme in liver homogenate and correcting for volume (not shown).

The first condition necessary for extrapolation is that the content of the responsible enzyme be known in the preparation used in metabolism studies and in the intact liver. This was accomplished via the Enzyme-Linked ImmunoSorbent Assay (ELISA; Snawder and Lipscomb, 2000) using antibody against CYP2E1, the enzyme responsible for chloroform metabolism.

Samples of human hepatic MSP were screened for CYP2E1 content and three samples expressing roughly 80 to 100 pmoles CYP2E1/mg MSP were selected for use in chloroform metabolism studies (Lipscomb et al., 2004). From that study, the specific activity of human CYP2E1 was determined to be 5.24 pmoles chloroform oxidized/minute/pmole CYP2E1. The specific activity of CYP2E1 expressed in samples of Fischer 344 rat liver microsomal protein was demonstrated to be quite similar, at 5.29 pmoles chloroform oxidized/minute/pmole CYP2E1. Because there are no data demonstrating an influence of age on metabolic activity,

when expressed as product per unit enzyme, the specific activity determined in samples of adult MSP was also employed for the child.

### **EXTRAPOLATION OF $V_{MAX}$ IN ADULTS**

The concentration of CYP2E1 was determined in homogenate prepared from samples of liver from 20 different adult organ donors (Lipscomb et al., 2003b) and was volumetrically extrapolated to the intact liver (pmoles CYP2E1/gram liver). CYP2E1 content was also determined in MSP (pmoles CYP2E1/mg MSP) derived from those homogenates. A mathematical combination of these data sets was accomplished to determine the concentration of MSP in intact liver for these 20 adult organ donors (Equation D-1).

$$(\text{pmol CYP2E1/gram tissue})/(\text{pmol CYP2E1/mg MSP}) = (\text{mg MSP/gram tissue}) \quad (\text{D-1})$$

Because an additional 40 samples of adult human MSP had also been analyzed for CYP2E1 content (Snawder and Lipscomb, 2000), their values were combined with the values from the 20 samples to yield a samples set of  $n = 60$ . Statistical analysis indicated a slight negative correlation between the CYP2E1 content of MSP and the MSP content of intact liver, in the set of 20 paired analyses (Lipscomb et al., 2003b), and so a more rigorous statistical analysis was performed to estimate the distribution type, parameters, and values at given percentiles of the distribution for the concentration of CYP2E1 in adult human liver (Lipscomb et al., 2003a).

To extrapolate the *in vitro* derived value for the apparent  $V_{max}$  for the reaction, the specific activity (in units of pmoles chloroform oxidized/minute/pmole CYP2E1) was incorporated with the content of CYP2E1 in intact liver (in units of pmoles CYP2E1/gram liver tissue) via Equation D-2. The resulting extrapolated rates were then corrected for units of time and molecular weight to yield rate values in units of mg/h/liver. Because each body contains

only one liver, the resulting extrapolated maximal metabolic rate ( $V_{\max}$ , in units of mg/h) was scaled by body weight (in units of kg) to the 0.7 power.

$$\begin{aligned} & (\text{product formed/min/pmol CYP}) \times (\text{pmol CYP/gram liver}) \times (\text{grams/liver}) \\ & = \text{product formed/min/liver} \end{aligned} \quad (\text{D-2})$$

To determine these values at multiple points in the distribution of CYP2E1 content, the amount of CYP2E1 in intact liver was determined at the geometric mean, and at the 5<sup>th</sup> and 95<sup>th</sup> percentiles of the (lognormal) distribution, by multiplying the concentration (pmoles CYP2E1/gram liver) by the mass of the liver (1820 grams). The geometric mean value for CYP2E1 content is 2562 pmoles CYP2E1/gram liver, or 2562 nmoles CYP2E1/kg liver.

If liver = 2.6% BW, if BW = 70 kg, then liver weight (mass) = 1.82 kg.

1.82 Kg  $\times$  2562 nmoles CYP2E1/kg liver = 4662.84 nmoles CYP2E1/liver.

These values were then combined with the specific activity toward chloroform, as follows.

The specific activity (apparent  $V_{\max}$ ) for CYP2E1 toward chloroform is 5.24 pmoles  $\text{CHCl}_3$ /min/pmol CYP2E1, and information in Table D-1 is used to extrapolate this measure to units representative of the intact liver.

5.24 nmoles  $\text{CHCl}_3$   $\times$  4662.84 nmoles CYP2E1/liver = 24433 nmoles  $\text{CHCl}_3$ /min/liver.

24433 nmoles  $\text{CHCl}_3$ /min/liver  $\times$  60 mins/h = 1465997 nmoles  $\text{CHCl}_3$ /h/liver.

1465997 nmoles  $\times$  119.4 ng/nmole  $\text{CHCl}_3$  = 175,040,029 ng  $\text{CHCl}_3$ /h/liver

The extrapolated  $V_{\max}$  value is 175 mg/h/liver.

TABLE D-1	
Information Used to Extrapolate <i>In Vitro</i> Derived $V_{\max}$ Value to the Intact Liver	
Specific Activity	5.24 pmoles $\text{CHCl}_3$ /min/pmole CYP2E1
CYP2E1 Concentration	2562 pmoles CYP2E1/gram liver
Body Mass	70 kg
Liver Mass	0.026 $\times$ 70 kg BW = 1820 grams liver
CYP2E1 Amount	4662840 pmoles CYP2E1/liver
Units of Time	60 minutes/h
Formula Weight	119.4 g $\text{CHCl}_3$ /mole

Equation 5-2 demonstrates the  $V_{\max}$  scaling procedure, necessary to incorporate metabolic rate constants into PBPK models. In this procedure, 175 mg/h is divided by  $BW^{0.7}$  (or,  $70^{0.7} = 19.57$  kg) to yield a  $V_{\max}C$  value of 8.9 mg/h/kg. In comparison, other PBPK models developed for chloroform have used 7 (Delic et al., 2000) or 15.7 mg/h/kg (Corley et al., 1990), and Allen et al. (1996) indicated that a reasonable range for the mean  $V_{\max}C$  was 11 to 35 mg/h, scaled to a 1-kg animal.

### EXTRAPOLATION OF $V_{\max}$ FOR CHILDREN

The extrapolation of metabolic rate in children followed the procedure as for the adult. Data in Tables D-2 and D-3 describe the sample of available children's tissues and the enzyme content of those tissues. Table D-4 presents the results of a statistical analysis to determine the parameters of the distribution of CYP2E1 to intact liver tissue from these donors.

Donor	Age (yrs)	Sex	Race	Source	Case No.
1	7	M	Not stated	HCCC	430
2	13	F	Caucasian	Vitron	646
3	<10	Not stated	Not stated	Vitron	559
4	6	F	Caucasian	Vitron	549
5	2	F	Caucasian	Vitron	550
6	12	F	Black	Vitron	565
7	9	M	Caucasian	Vitron	538
8	11 months	M	Hispanic	Vitron	635
9	8	M	Black	Vitron	555
10	17	M	Not Stated	HCCC	356

HCCC = Human Cell Culture Center Laurel, MD.

Vitron = Vitron, Inc., Tucson, AZ.

TABLE D-3

Determination of Cytochrome P450 Enzyme in Liver Tissue of 10 Child Organ Donors

Donor	Parameter				
	Mg Homog. Protein/ Gram Liver	Pmoles CYP2E1/ mg Homog. Protein	Pmoles CYP2E1/ gram liver	Pmoles CYP2E1/mg MSP	Mg MSP/gram Liver
1	122	22	2691	58	46.4
2	234	16	3745	33	113.5
3	289	32	9250	53	174.5
4	190	13	2431	35	69.5
5	302	23	6936	31	223.7
6	249	23	5747	49	117.3
7	172	22	3787	40	94.7
8	193	19	3663	62	59.1
9	205	19	3891	36	108.1
10	408	16	6529	31	210.6
Mean	236		4470 (GM)	42.8	
SD	81		1.5393 (GSD)	11.7	

55 ± 15% of total homogenate protein is MSP in children.

GM = Geometric Mean, GSD = Geometric Standard Deviation.

TABLE D-4		
Distribution of CYP2E1 to Adults and Children		
Parameter	Adult	Child <sup>a</sup>
Enzyme Content — pmoles CYP2E1/gram Liver		
5 <sup>th</sup> percentile	1232 <sup>b</sup>	1288
Geometric mean	2562 <sup>b</sup>	2818
95 <sup>th</sup> percentile	4453 <sup>b</sup>	6167
Specific Activity — pmoles CHCl <sub>3</sub> /min/pmol CYP2E1	5.24	5.24 <sup>c</sup>
Metabolic Capacity — μg CHCl <sub>3</sub> /h/gram Liver		
5 <sup>th</sup> percentile	46.3	48.35
Geometric mean	96.3	105.8
95 <sup>th</sup> percentile	167.3	231.5

<sup>a</sup> Values apply to the 9-year-old and the 1-year-old child, but are further adjusted by a liver mass of 804 grams and 342.5 grams in the 9- and 1-year-old child, respectively.

<sup>b</sup> From Lipscomb et al. (2003a).

<sup>c</sup> Measured in adult samples (Lipscomb et al., 2004).

Metabolic capacity was converted from units of  $\mu\text{g/h/gram liver}$ , to  $\text{mg/h}$ , based on a liver mass of 342.5 grams in the 1-year-old child ( $10 \text{ kg body mass} \times 0.03425 \text{ body mass as liver}$ ) and a liver mass of 804 grams in the 9-year-old child ( $30 \text{ kg body mass} \times 0.0268 \text{ body mass as liver}$ ). Resulting  $V_{\text{max}}$  values at the geometric mean were 36.24  $\text{mg/h}$  and 85.06  $\text{mg/h}$  for the 1-year-old and 9-year-old child, respectively. When scaled by  $\text{BW}^{0.7}$ , the resulting  $V_{\text{max}}C$  values were 7.23 and 7.87  $\text{mg/h/kg}$  for the 1-year-old and 9-year-old child, respectively.

### **EXTRAPOLATION OF $K_M$ VALUES FOR ADULT HUMANS**

The PBPK model developed for chloroform employs a  $K_m$  value of 0.012  $\text{mg/L}$ . In the PBPK model,  $K_m$  is expressed in venous blood at equilibrium with liver tissue (CVL), and the derivation and extrapolation of  $K_m$  value is consistent with the concept that  $K_m$  is best described in the aqueous compartment of the liver. The  $K_m$  value for chloroform oxidation in humans was derived from *in vitro* measures as demonstrated below.

Lipscomb et al (2004) reported values for three separate human microsome samples in which  $K_m$  values were reported as concentrations in the aqueous suspension, rather than concentration in headspace. This was accomplished in the original study by determining the  $K_m$  value in headspace and correcting by the gas:microsomal suspension partition coefficient measured for that study. The  $K_m$  values were 0.256, 0.113 and 0.090  $\mu\text{M}$ , and averaged 0.153  $\mu\text{M}$  in suspension. That value was corrected for the formula weight of chloroform (119.4  $\mu\text{g}/\mu\text{mol}$ ), yielding an average concentration of 18.27  $\mu\text{g/L}$ . That value represents the concentration of chloroform in solution driving reaction rates at half of their theoretical maximal initial rates. To extrapolate this value into units useful in PBPK modeling, it was necessary to express concentration in venous blood at equilibrium with liver, rather than in liver itself. The concentration in the *in vitro* suspension was assumed to adequately represent the concentration in

liver resulting in half-maximal rates of metabolism, and was adjusted to reflect the concentration of chloroform in blood at equilibrium with liver. This was accomplished by dividing 18.27 µg/L by the liver:blood partition coefficient value used in the model (PL=1.6). This resulted in a value of 11.4 µg/L, which was incorporated in the model as 0.012 mg/L.

## REFERENCES

Allen, B.C., T.R. Covington and H.J. Clewell. 1996. Investigation of the impact of pharmacokinetic variability and uncertainty on risks predicted with a pharmacokinetic model for chloroform. *Toxicology*. 111:289-303.

Corley, R.A., A.L. Mendrala, F.A. Smith et al. 1990. Development of a physiologically based pharmacokinetic model for chloroform. *Toxicol. Appl. Pharmacol.* 103:512-527.

Delic, J.I., P.D. Lilly, A.J. MacDonald and G.D. Loizou. 2000. The utility of PBPK in the safety assessment of chloroform and carbon tetrachloride. *Reg. Toxicol. Pharmacol.* 32:144-155.

Lipscomb, J.C. and G.L. Kedderis. 2002. Incorporating human interindividual biotransformation variance in health risk assessment. *Sci. Total. Environ.* 288:13-21.

Lipscomb, J.C., L.K. Teuschler, J. Swartout, D. Popken, T. Cox and G.L. Kedderis. 2003a. The impact of cytochrome P450 2E1-dependent metabolic variance on a risk relevant pharmacokinetic outcome in humans. *Risk Anal.* 23:1221-1238.

Lipscomb, J.C., L.K. Teuschler, J.C. Swartout, C.A.F. Striley and J.E. Snawder. 2003b. Variance of microsomal protein and cytochrome P450 2E1 and 3A forms in adult human liver. *Toxicol. Mech. Methods.* 13:45-51.

Lipscomb, J.C., H. Barton, R. Tornero-Velez et al. 2004. The metabolic rate constants and specific activity of human and rat hepatic cytochrome P450 2E1 toward chloroform. *J. Toxicol. Environ. Health.* 67:537-553.

Snawder, J.E. and J.C. Lipscomb. 2000. Interindividual variance of cytochrome P450 forms in human hepatic microsomes: Correlation of individual forms with xenobiotic metabolism and implications for risk assessment. *Reg. Toxicol. Pharmacol.* 32:200-209.